

STRUCTURAL COMPETENCY AND ENVIRONMENTAL SOUNDNESS OF THE  
RECYCLED BASE MATERIALS IN NORTH TEXAS

By

MOHAMMAD FAYSAL

Presented to the Faculty of the Graduate School of  
The University of Texas at Arlington in Partial Fulfillment  
of the Requirements  
for the Degree of

DOCTOR OF PHILOSOPHY

THE UNIVERSITY OF TEXAS AT ARLINGTON

May 2017

Copyright © by Mohammad Faysal 2017

All Rights Reserved

## ACKNOWLEDGEMENTS

I would like to express my sincere gratitude to my advising professor, Dr. Sahadat Hossain, for his contributions to my education and to the accomplishment of this work. His continuous guidance and constructive comments have helped me become a better researcher, and this work would not have been possible without his guidance, constant inspiration, and advice. I would also like to convey my appreciation to Dr. Laureano R. Hoyos, Dr. Xinbao Yu, and Dr. Chien-Pai Han for serving on my dissertation defense committee. Dr. Hoyos' valuable input and Dr. Han's guidance with the statistical modelling work are very much appreciated.

Sincere thanks go to the Texas Department of Transportation for their financial support throughout this project and to Mr. Al-Aramoon and Mr. Boon Thian for their help with lab testing.

Without the cooperation and assistance of my colleagues and friends, especially Masrur Mahedi, Saif Bin Salah, Dr. Sadik Khan, and Dr. Sonia Samir, this work would have been much more difficult, if not impossible.

This work is dedicated to my family in appreciation for their encouragement and continuous help and moral support; especially to my mother, for being an immense source of inspiration. I would also like to thank the Almighty for giving me the strength and patience to overcome every difficulty throughout this life.

March 2, 2017

Abstract

STRUCTURAL COMPETENCY AND ENVIRONMENTAL SOUNDNESS OF THE RECYCLED  
BASE MATERIALS IN NORTH TEXAS

Mohammad Faysal

The University of Texas at Arlington, 2017

Supervising Professor: MD. Sahadat Hossain

Aggregates, which are derived from natural resources, are the most important raw materials used in pavement construction; however, depletion of the natural resources, increasing labor costs, and environmental concerns have led us to look for alternatives. Recycled materials, such as recycled crushed concrete aggregate (RCCA) and reclaimed asphalt pavement (RAP), can be used as an alternative to natural aggregates and can be obtained from construction of newer structures and demolition of existing structures, such as buildings, bridges, pavement, etc. Recycled materials can reduce the cost, depletion of natural resources, and construction debris. The properties of recycled materials are source-dependent, which limit their utility to a great extent. Considering these factors, this experimental program was designed to evaluate the strength, stiffness, durability, and environmental impacts of using recycled materials in the pavement base.

Different combinations of recycled crushed concrete aggregates (RCCA) and reclaimed asphalt pavement (RAP) aggregates, under cement-treated or untreated conditions, were utilized to evaluate the applicability of these available materials to a flexible pavement base layer. It was found that RAP materials are relatively weaker than the RCCA materials due to the asphalt coating on its surface, but RAP materials can be mixed with RCCA to increase strength. According to this

study, RAP can be mixed with RCCA up to a ratio of 50/50, but it must be treated with 4% to 6% cement to fulfill the compressive strength requirement of 300 psi specified in the Texas Department of Transportation's guidelines. The effect of the asphalt content on the strength and stiffness was also determined with the inclusion of additional asphalt to the RAP materials. Durability tests were performed with wetting and drying cycles on the weakest combinations of RCCA and RAP materials. These materials were found to be durable even after 30 wetting and drying cycles. Environmental tests were administered, such as pH, total and volatile dissolved solids, total and volatile suspended solids, turbidity, and chemical oxygen demand (COD). Test results were compared with the requirements of various environmental protection agencies and indicated that the recycled base materials are an environmentally-sound alternative to virgin aggregates and can be used in pavement bases or sub-base layers.

The most important stiffness parameter used in pavement design is resilient modulus; however, the resilient modulus test is too complicated and costly to perform on a regular basis. The unconfined compressive strength test is easier to administer. In this study, a multiple linear regression model was developed to determine the resilient modulus value from the parameters obtained from the unconfined compressive strength tests. It is believed that the statistical model can be useful in determining the stiffness parameter of cement-treated base materials.

## Table of Contents

Chapter 1 Introduction .....	1
1.1 Background .....	1
1.2 Problem Statement .....	2
1.3 Objective and Scope .....	3
1.4 Dissertation Outline .....	4
Chapter 2 Literature Review .....	5
2.1 Introduction .....	5
2.2 Recycled Materials in Pavement Construction .....	5
2.3 Recycled Crushed Concrete Aggregate (RCCA) .....	6
2.4 Reclaimed Asphalt Pavement (RAP) .....	6
2.4.1 Use of RAP in USA .....	7
2.4.2 Properties of RAP .....	7
2.5 Pavement Structure .....	8
2.5.1 Surface Course .....	9
2.5.2 Base Course .....	9
2.5.3 Sub-Base Course .....	9
2.6 Pavement Design Criteria .....	10
2.6.1 Imparted Load on Pavement .....	10
2.6.2 Strength and Stiffness of Subgrade .....	11
2.7 Design of Flexible Pavement .....	11
2.8 Design of Rigid Pavement .....	12

2.9	Cement-Treated Bases.....	20
2.10	Design Considerations of RAP and RCCA Materials .....	20
2.10.1	Cement-Treated RAP and RCCA.....	21
2.10.2	Unconfined Compressive Strength of Cement-Treated RAP.....	21
2.10.3	Resilient Modulus and Permanent Deformation.....	29
2.11	Factors Affecting Strength of Base Materials .....	33
2.11.1	Size and Shape of Aggregate .....	34
2.11.2	Compaction .....	35
2.11.3	Dry Density .....	35
2.11.4	Aggregate Gradation .....	36
2.11.5	Moisture Content .....	36
2.11.6	Stress Condition .....	37
2.11.7	Characteristics of Materials .....	37
2.12	Resilient Modulus ( $M_r$ ) of treated Rap and RCCA Materials .....	39
2.13	Development of Correlation among UCS, Layer Coefficient and $M_r$ .....	43
2.14	Split Tensile Strength (STS) .....	50
	Chapter 3 Methodolgy .....	51
3.1	Introduction .....	51
3.2	Sample Collection .....	51
3.3	Experimental Program .....	53
3.4	Aggregate Gradation.....	58

3.5	Laboratory Compaction Characteristics and Moisture Density Relationships..	59
3.6	Specific Gravity .....	60
3.7	Specimen Preparation .....	60
3.8	Unconfined Compression Test .....	62
3.9	Split Tensile Strength (STS) Test .....	64
3.10	Resilient Modulus ( $M_r$ ) Tests.....	65
3.10.1	Specimen Preparation for Testing.....	65
3.10.2	Resilient Modulus Testing Equipment .....	66
3.10.3	Data Analysis of Resilient Modulus Tests .....	68
3.11	Leaching Tests.....	69
3.11.1	pH Test .....	69
3.11.2	Total Suspended and Dissolved Solids (TSS & TDS).....	70
3.11.3	Turbidity.....	70
3.11.4	Chemical Oxygen Demand (COD) .....	71
3.12	Durability Tests .....	72
Chapter 4 Results and Analysis.....		75
4.1	Introduction .....	75
4.2	Particle Size Distribution .....	75
4.3	Asphalt Content in RAP .....	77
4.4	Moisture-Density Tests .....	77
4.5	Specimen Preparation .....	81

4.6	Unconfined Compressive Strength Test Results .....	81
4.7	Elastic Modulus (EM) .....	86
4.8	Effect of Different Cement and RAP Contents.....	91
4.8.1	Combined Effects of Cement and RAP Content on UCS.....	91
4.9	Resilient Modulus Test Results .....	99
4.10	Effect of Cement Content on $M_r$ .....	109
4.11	Effects of Stress Conditions on $M_r$ .....	109
4.12	Effect of RAP content on $M_r$ .....	110
4.13	Statistical Analysis of Resilient Modulus Test Results .....	110
4.14	Statistical Modelling of $M_r$ , UCS, and EM Values .....	113
4.15	Prediction Models .....	114
4.16	Asphalt Content .....	121
4.17	Effect of Asphalt Content .....	121
4.17.1	Particle Size Distribution.....	123
4.17.2	Strength Tests .....	124
4.17.3	Resilient Modulus .....	132
4.17.4	Test Results Analysis .....	136
4.18	Effects of Wet and Dry Cycles .....	138
4.18.1	Resilient Modulus Test Results .....	140
4.19	Environmental Tests .....	145
4.19.1	Chemical Oxygen Demand (COD) .....	145

4.19.2	Total Suspended Solids (TSS) .....	147
4.19.3	Total Dissolved Solids (TDS) .....	149
4.19.4	Turbidity .....	151
4.19.5	pH .....	153
4.20	Summary .....	155
Chapter 5 Regression Model .....		156
5.1	Introduction .....	156
5.2	Parameters Selection for MLR Model .....	157
5.3	Multiple Linear Regression Analysis .....	158
5.3.1	Correlation Analysis .....	158
5.3.2	Development of Preliminary Model .....	164
5.3.3	Verification of Preliminary Model .....	166
5.4	MLR Model Form .....	166
5.4.2	Transformation of Variables and Check for MLR Assumptions .....	172
5.4.3	Final Model Selection .....	177
5.4.4	Transformation of Variables for Final Model .....	180
5.4.5	Simplification of Final Model .....	186
5.5	Comparison of Actual Test Data with Model Predicted Data .....	192
5.6	Development of Design Chart .....	193
Chapter 6 Conclusion and Future Recommendations .....		199
6.1	Introduction .....	199

6.2	Summary and Conclusions .....	199
6.3	Recommendations for Future Study .....	202
	Appendix A Statistical Modelling.....	204
	Reference.....	220
	Biographical Information.....	233

## List of Figures

Figure 2.1 Usage and potential of various RAP percentages in the intermediate layer (NCDOT 2007).....	7
Figure 2.2 Typical pavement structure (Ordonez, 2006).....	10
Figure 2.3 Flexible pavement design chart (AASHTO, 2003) .....	14
Figure 2.4 Chart for the determination of subgrade reaction (AASHTO, 2003) .....	15
Figure 2.5 Chart for modifying modulus of subgrade reaction due to rigid foundation (AASHTO, 2003).....	16
Figure 2.6 Chart for estimating the relative damage to rigid pavements (AASHTO, 2003) .....	17
Figure 2.7 Correction of effective modulus of subgrade reaction (AASHTO, 2003) .....	18
Figure 2.8 Design chart for rigid pavements (AASHTO, 2003) .....	18
Figure 2.9 Design chart for the rigid pavements (AASHTO, 2003) .....	19
Figure 2.10 Effects of mixing variables on the compressive strength of CTAB test mixtures (a) Recycled concrete (RC) mixtures, and (b) Crushed limestone (CL) Mixtures (Lim and Zollinger, 2003) .....	25
Figure 2.11 Increase in compressive strength with time (Croney and Croney, 1997) ....	26
Figure 2.12 28 days of compressive strength vs. maximum dry density of the mixtures (Croney and Croney, 1997) .....	27
Figure 2.13 Compressive strength prediction of CTAB mixtures (a) recycled concrete (RC) mixtures and (b) crushed limestone mixtures (CL) (Croney and Croney, 1997).....	28
Figure 2.14 Response of specimen during cyclic axial loading (Buchanan, 2007) .....	30
Figure 2.15 Compaction of aggregate shape: form (shape), angularity, and texture (Masad et al., 2003) .....	34
Figure 2.16 Repeatability of resilient modulus test results of untreated aggregates (Potturi, 2006).....	41

Figure 2.17 Repeatability of resilient modulus test results of cement treated aggregates (Potturi, 2006) .....	42
Figure 2.18 Influence of moisture content on resilient modulus value for fine grained soil where solid lines represent values measured by Virginia Department of Transportation, and dotted lines represent values measured by outside vendor (Hossain and Kim, 2013) .....	47
Figure 2.19 Strength comparison between static and proctor compacted samples for Phase II (Hossain and Kim, 2013) .....	48
Figure 2.20 Correlation between resilient modulus and initial tangent of modulus obtained from unconfined compression tests .....	49
Figure 2.21 Correlation between resilient modulus and unconfined compression tests (Hossain and Kim, 2013) .....	49
Figure 3.1 Sample collection (Big City Crushed Concrete, Dallas, Texas) .....	52
Figure 3.2 RAP sample collection from TxDOT stockpile, Ellis County .....	53
Figure 3.3 RAP sample collection from TxDOT stockpile, Rockwall County .....	54
Figure 3.4 Sample preparation for UCS and resilient modulus test .....	61
Figure 3.5 Preservation of samples in humidity room for curing .....	62
Figure 3.6 Universal testing machine (UTM) .....	63
Figure 3.7 Positioned specimen in a testing machine for split tensile strength test .....	64
Figure 3.8 Failed specimen .....	65
Figure 3.9 Resilient modulus testing machine.....	67
Figure 3.10 Dual channel pH/ion/conductivity meter .....	70
Figure 3.11 2100P Turbidimeter.....	71
Figure 3.12 COD reactor .....	72
Figure 3.13 Specimens subjected to wetting.....	73
Figure 3.14 Specimens subjected to drying .....	74
Figure 4.1 Particle size distribution of recycled base materials.....	76

Figure 4.2 OMC and MDD determination of (a) 100% RCCA 1, (b) 100% RCCA 2, (c) 100% RCCA 3, and (d) 100% RAP 1 materials for 0, 2, 4, & 6% cement content.....	78
Figure 4.3 OMC and MDD determination of (a) 10% RAP 1-90% RCCA 1, (b) 30% RAP 1-70% RCCA 1, (c) 50% RAP 1-50% RCCA 1, (d) 70% RAP 1-30% RCCA 1 Materials for 0, 2, 4, & 6% cement content.....	79
Figure 4.4 OMC and MDD determination of (a) 100% RCCA 2, (b) 10% RAP 2-90% RCCA 2, (c) 30% RAP 2-70% RCCA 2, (d) 50% RAP 2-50% RCCA 2 Materials for 4, & 6% cement content .....	80
Figure 4.5 OMC and MDD determination of (a) 100% RCCA 3 (b) 50% RAP 3 +50% RCCA 3 Materials for 0, 2, 4, & 6% cement content .....	81
Figure 4.6 Unconfined compressive strength comparison .....	83
Figure 4.7 Comparison of UCS for RCCA and RAP mixes from Source 01 .....	84
Figure 4.8 Comparison of UCS of different combinations of materials mixes from Source 03.....	85
Figure 4.9 Comparison of UCS for 50% RAP + 50% RCCA combination .....	86
Figure 4.10 Stress-strain curves (Mahedi 2016) .....	87
Figure 4.11 Statistical correlation between elastic modulus (EM) and unconfined compressive strength (UCS).....	89
Figure 4.12 Comparison of EM for different combinations of materials .....	89
Figure 4.13 Comparison of EM for different combinations of materials at different cement contents .....	90
Figure 4.14 Comparison of resilient modulus test results for 100% RCCA 1 combination .....	100
Figure 4.15 Comparison of resilient modulus test results for 10% RAP 1 + 90% RCCA 1 combination.....	101

Figure 4.16 Comparison of resilient modulus test results for 30% RAP 1 + 70% RCCA 1 combination.....	102
Figure 4.17 Comparison of resilient modulus test results for 70% RAP 1 + 30% RCCA 1 combination.....	103
Figure 4.18 Comparison of resilient modulus test results for 100% RCCA 2 combination .....	104
Figure 4.19 Comparison of resilient modulus test results for 10% RAP 2 + 90% RCCA 2 combination.....	104
Figure 4.20 Comparison of resilient modulus test results for 100% RCCA 3 combination .....	105
Figure 4.21 Comparison of resilient modulus test results for 50% RAP 3 + 50% RCCA 3 combination.....	106
Figure 4.22 Resilient modulus value comparison (Source 1) (4% Cement).....	107
Figure 4.23 Resilient modulus value comparison (Source 2) (4% Cement).....	107
Figure 4.24 Resilient modulus value comparison (Source 1) (6% Cement).....	108
Figure 4.25 Resilient modulus value comparison (Source 2) (6% Cement).....	108
Figure 4.26 Two-parameter model ( $k-\theta$ ) for different RAP 1-RCCA 1 (Source 1) combinations stabilized at (a) 6 %, (b) 4%, (c) 2% and (d) 0% cement content. ....	117
Figure 4.27 Two-parameter model ( $k-\theta$ ) for different RAP 2-RCCA 2 (Source 2) combinations stabilized at (a) 6 % and (b) 4% cement content .....	119
Figure 4.28 Two-parameter model ( $k-\theta$ ) for fitting resilient modulus of (a) 100 % RCCA 3 and (b) 50-50% RCCA 3 – RAP 3 from Source 3.....	121
Figure 4.29 Particle size analysis of RAP materials containing different asphalt contents .....	123
Figure 4.30 Decrease in UCS with the inclusion of RAP.....	127
Figure 4.31 Decrease in UCS with additional asphalt on RAP.....	127

Figure 4.32 Comparison of split tensile strength .....	131
Figure 4.33 Comparison between SCS/UCS at different cement contents.....	132
Figure 4.34 Comparison of resilient modulus ( $M_r$ ) at different combinations .....	134
Figure 4.35 Changes in resilient modulus at different asphalt contents.....	136
Figure 4.36 Graphical plot of $k-\theta$ or $2p$ models developed for (a) Control samples (CS) and (b) Test samples (TS) of MIX 4 materials.....	141
Figure 4.37 Graphical plot of $k-\theta$ or $2p$ models developed for (a) Control samples (CS) and (b) Test samples (TS) of MIX 6 materials.....	142
Figure 4.38 Chemical Oxygen Demand (COD) test results (a) 100% RCCA 3, and (b) 50% RAP 3 + 50% RCCA 3 .....	146
Figure 4.39 Change in chemical oxygen demand (COD) with wetting-drying cycles....	147
Figure 4.40 Total suspended solids (TSS) test results (a) 100% RCCA 3, and (b) 50% RAP 3 + 50% RCCA 3 .....	148
Figure 4.41 Change in total suspended solids (TSS) with wetting-drying cycles.....	149
Figure 4.42 Total dissolved solids (TDS) test results (a) 100% RCCA 3, and (b) 50% RAP 3 + 50% RCCA 3 .....	150
Figure 4.43 Change in total dissolved solids (TDS) with wetting-drying cycles .....	151
Figure 4.44 Turbidity test results (a) 100% RCCA 3, and (b) 50% RAP 3 + 50% RCCA 3 .....	152
Figure 4.45 Change in turbidity with wetting-drying cycles .....	153
Figure 4.46 Turbidity test results (a) 100% RCCA 3, and (b) 50% RAP 3 + 50% RCCA 3 .....	154
Figure 4.47 Change in pH with wetting-drying cycles .....	155
Figure 5.1 MLR model development using R Studio .....	157
Figure 5.2 The correlation of resilient modulus ( $M_r$ ) with bulk stress (BS) (units are in psi) .....	159

Figure 5.3 The correlation of resilient modulus ( $M_r$ ) (psi) with cement content (CC)....	159
Figure 5.4 The correlation of resilient modulus ( $M_r$ ) (psi) with unconfined compressive strength (UCS).....	160
Figure 5.5 The correlation of resilient modulus ( $M_r$ ) (psi) with elastic modulus (EM) (psi).....	160
Figure 5.6 The correlation between bulk stress (BS) (psi) and cement content (CC)...	161
Figure 5.7 The correlation between bulk stress (BS) (psi) and unconfined compressive strength (UCS) (psi).....	162
Figure 5.8 The correlation between bulk stress (BS) (psi) and elastic modulus (EM) (psi).....	162
Figure 5.9 The correlation between bulk stress (BS) (psi) and elastic modulus (EM) (psi).....	163
Figure 5.10 The correlation between unconfined compressive strength (UCS) (psi) and elastic modulus (EM) (psi).....	163
Figure 5.11 Residuals vs bulk stress (BS) (psi) plot.....	167
Figure 5.12 Residuals vs cement content (CC) (%) plot.....	167
Figure 5.13 Residuals vs unconfined compressive strength (UCS) (psi).....	168
Figure 5.14 Residuals vs elastic modulus (EM) (psi).....	168
Figure 5.15 Residuals vs fitted ( $\hat{y}$ ) value plot.....	169
Figure 5.16 Normal probability plot.....	170
Figure 5.17 Box-Cox plot for transformation of response variable ( $\lambda = 0.545$ ).....	172
Figure 5.18 Residual vs fitted plot.....	173
Figure 5.19 Residual vs theoretical quantiles plot after transformation.....	174
Figure 5.20 Leverage plot of transformed model.....	175
Figure 5.21 Value of $R^2$ for different subsets of variables.....	179
Figure 5.22 Value of $R^2$ for different subsets of variables.....	179

Figure 5.23 Box-Cox plot to obtain transformation of dependent variable .....	181
Figure 5.24 Residuals vs bulk stress (BS) (psi) plot.....	182
Figure 5.25 Residuals vs unconfined compressive strength (UCS) (psi) plot .....	182
Figure 5.26 Residuals vs elastic modulus (EM) (psi) plot .....	183
Figure 5.27 Residuals vs fitted value plot.....	183
Figure 5.28 Normal probability plot for transformed model. ....	184
Figure 5.29 Residuals vs bulk stress (BS) (psi) plot.....	187
Figure 5.30 Residuals vs unconfined compressive strength (UCS) (psi) plot .....	188
Figure 5.31 Residuals vs elastic modulus (EM) (psi) plot .....	188
Figure 5.32 Residuals vs fitted value plot.....	189
Figure 5.33 Normal probability plot for transformed model .....	189
Figure 5.34 Model validation using test data .....	193
Figure 5.35 Design chart ( $\sigma_c = 10$ psi, $\sigma_d = 10$ psi, $\theta = 40$ psi).....	194
Figure 5.36 Design chart ( $\sigma_c = 5$ psi, $\sigma_d = 15$ psi, $\theta = 30$ psi).....	195
Figure 5.37 Design chart ( $\sigma_c = 5$ psi, $\sigma_d = 10$ psi, $\theta = 25$ psi).....	196
Figure 5.38 Design chart ( $\sigma_c = 3$ psi, $\sigma_d = 9$ psi, $\theta = 18$ psi).....	197
Figure 5.39 Design chart ( $\sigma_c = 3$ psi, $\sigma_d = 6$ psi, $\theta = 15$ psi).....	198

## List of Tables

Table 2.1 Properties of RAP materials (Potturi, 2006) .....	8
Table 2.2 Compressive strength of the CTAB Test Mixtures at Different Curing Times (Lim and Zollinger 2003) .....	22
Table 2.3 Test Variables and Application Levels for the CTAB Test Mix Design (Lim and Zollinger, 2003) .....	23
Table 2.4 Complete Factorial of Test Mixtures for each Aggregate Type (Lim and Zollinger, 2003) .....	23
Table 2.5 Optimum Moisture Content (OMC) and Maximum Dry Density ( $\gamma_{d-max}$ ) of Different Mixtures .....	24
Table 2.6 Required Soil Properties for Base Materials (TxDOT Item 247) .....	38
Table 2.7 Results Summary of Structural Layer Coefficients Obtained from Different Studies .....	40
Table 2.8 Resilient Modulus of Untreated and Cement-Treated Aggregates (Potturi, 2006) .....	44
Table 3.1 Material Identification .....	52
Table 3.2 Experimental Program for Structural Competency .....	55
Table 3.3 Environmental Impact Assessment .....	56
Table 3.4 Experimental Program for Resilient Modulus ( $M_r$ ) test at Different Wet and Dry Cycles (Source 3 materials) .....	57
Table 3.5 Experimental Program for Environmental Tests .....	58
Table 3.6 Compaction Energy of Different Laboratory Compaction Procedures .....	59
Table 3.7 Resilient Modulus Test Sequences and Stress Values for Base and Subbase Materials (AASHTO T307-99) .....	68
Table 4.1 Material Properties .....	76
Table 4.2 Asphalt Content Test Results .....	77

Table 4.3 Material Combination ID .....	84
Table 4.4 T-Test Results for Effect of Cement Content on UCS (Source 1) .....	93
Table 4.5 T-Test Results for Effect of Cement Content on UCS (Source 2) .....	94
Table 4.6 T-Test Results for Effect of Cement Content on UCS (Source 3) .....	95
Table 4.7 T-Test Results for Effect of RAP Content on UCS (Source 1) .....	96
Table 4.8 T-Test Results for Effect of RAP Content on UCS (Source 2) .....	97
Table 4.9 T-Test Results for Effect of RAP Content on UCS (Source 3) .....	98
Table 4.10 T-test Results for Effect of RAP Content (Source 3) .....	112
Table 4.11 T-Test Results for Effect of Cement Content (Source 3) .....	113
Table 4.12 Statistical Parameters Obtained from Prediction Model for RCCA and RAP Materials Obtained from Source 1 (0% and 2% cement content) .....	115
Table 4.13 Statistical Parameters Obtained from Prediction Model for RCCA and RAP Materials Obtained from Source 1 (0% and 2% cement content) .....	116
Table 4.14 Statistical Parameters Obtained from Prediction Model for RCCA and RAP Materials Obtained from Source 2 .....	118
Table 4.15 Statistical Parameters Obtained from Prediction Model for RCCA and RAP Materials Obtained from Source 3 .....	120
Table 4.16 RAP Materials Containing Different Asphalt Contents .....	122
Table 4.17 Notation for Different Mixes .....	122
Table 4.18 Particle Size Distribution Results Description .....	124
Table 4.19 Unconfined Compressive Strength Results for 50% RAP 3a + 50% RCCA 3 (Asphalt 4.4%) .....	125
Table 4.20 Unconfined Compressive Strength Results for 50% RAP 3b + 50% RCCA 3 (Asphalt 6.5%) .....	125
Table 4.21 Unconfined Compressive Strength Results for 50% RAP 3c + 50% RCCA 3 (Asphalt 8.4%) .....	126

Table 4.22 Split Tensile Strength for 100% RCCA 3.....	128
Table 4.23 Split Tensile Strength for 50% RAP 3a + 50% RCCA 3 (4.4% Asphalt) .....	129
Table 4.24 Split Tensile Strength for 50% RAP 3b + 50% RCCA 3 (6.5% Asphalt) .....	130
Table 4.25 Model Parameters .....	135
Table 4.26 Experimental Program for Resilient Modulus ( $M_r$ ) Tests .....	138
Table 4.27 Environmental Tests Program .....	139
Table 4.28 Model Parameters for MIX 4.....	143
Table 4.29 Model Parameters for MIX 6.....	143
Table 4.30 Model Parameters for MIX 6.....	144
Table 5.1 Correlation: $M_r$ , BS, CC, UCS, EM .....	164
Table 5.2 ANOVA Summary .....	165
Table 5.3 Regression Parameters .....	165
Table 5.4 Variance Inflation Factor (VIF).....	171
Table 5.5 Parameter Estimates of the Initial Transformed Model .....	176
Table 5.6 Summary of best Subset Selection Method .....	178
Table 5.7 Estimation of Parameters of Final Model.....	186
Table 5.8 Estimation of Parameters of Final Model.....	191

## Chapter 1

### Introduction

#### 1.1 Background

The annual consumption of aggregate materials for construction of new infrastructure and pavements is 1.5 billion tons in the USA (USGS 2005). By 2020, it is estimated that more than 2.5 billion tons will be consumed due to the rapid increase of construction of different types of infrastructures (USDOT 2004). Natural resources of aggregates are depleted and increased demand has raised the costs of repair and rehabilitation. The recycled crushed concrete aggregate (RCCA) materials are obtained from the construction and demolition of concrete structures and are expected to amount to 123 million tons per year (USDOT 2004).

Reclaimed asphalt pavement (RAP) is a granular material containing a mixture of bitumen and aggregate that is removed or reprocessed as part of pavement reconstruction and resurfacing. To maintain the functionality and to impede the loss of structural reliability, asphalt concrete pavements often need to be rehabilitated by milling the upper distressed layer, which generates a huge amount of asphalt pavement as a by-product. According to the National Asphalt Pavement Association (NAPA), in 2013, approximately 350.7 million tons of plant mix asphalt were produced in the United States of America, and the total reported RAP generation was around 76.1 million tons (Annual Asphalt Pavement Industry Survey on Recycled Materials and Warm-Mix Asphalt Usage: 2009–2013). This huge quantity of RAP that is generated each year makes it necessary to investigate the further use of RAP in pavement construction (FDOT, October 2012), which will provide savings in costs and significant reductions in the use of virgin aggregates. In recent years, a large portion of RAP has been recycled in hot mix and cold mix processes (NAPA 2013), but huge quantities remain unutilized, especially in Texas. The use of RAP as a base material would provide a viable, cost-effective option for utilizing this huge portion of unused RAP. Since the early 1990s, researchers have investigated the mechanical properties of RAP (Kolias 1996). Kolias investigated the compressive strength, tensile strength, and modulus of elasticity of different RAP

mixes with unbound granular materials, and have recommended further research on RAP mixes stabilized with cement. Later on, a substantial amount of research was performed on the mechanical properties of different cement-treated RAP mixes (Taha, et al., 2002; Guthrie, et al., 2007; and Grilli, et al., 2013). L. Hoyos investigated the effects of including fiber in the mix, and evaluated different engineering properties, such as hydraulic conductivity, leachate, and shear modulus (Hoyos et al., 2011). Research has included fracture resistance and rutting potential (Research Report, FDOT, May 2007); resilient modulus response (Puppala et al., 2011); splitting tensile strength (Brand, 2012); field evaluation (Nazarian et al., 2011); flexural strength and unrestrained shrinkage (Euch Khay, et al., 2014); and dynamic modulus (Jones et al., 2014).

## 1.2 Problem Statement

In spite of numerous studies, until now, behavioral characteristics of RAP have not been fully understood. RAP properties are highly source-dependent, and the necessity of further research is undeniable. Recycled materials are weaker than virgin aggregates (Taha 2000). For this reason, these materials might need to be stabilized using fly ash, foamed asphalt, or cement to fulfill the minimum strength requirement. Behavioral responses and potential uses of RAP has yet to be investigated if it is mixed with other recycled materials such as RCCA. Literatures on different recycled materials such as recycled concrete material, (Lim and Zollinger 2003). The design guideline prepared by the American Association for State Highway and Transportation Officials (AASHTO 2003) is for natural aggregates and intended for universal use; however, there are no specific design guidelines for recycled materials, such as RCCA and RAP. The inadequacy of information available on this subject provided the impetus for this experimental study on the evaluation of cement-stabilized RAP mixed with recycled materials such as RCCA.

Unconfined compressive strength (UCS) testing, split tensile strength testing, and resilient modulus ( $M_r$ ) testing were performed to characterize the strength and stiffness response of different cement-stabilized RAP and RCCA mixes under the funded project of the Texas

Department of Transportation (TxDOT). RAP and RCCA crushed concrete base materials were mixed in different proportions, with or without cement content, and tested to determine their strength and resilient modulus ( $M_r$ ). An experimental program was designed and conducted to test and determine the optimum moisture content (OMC), maximum dry density (MDD), unconfined compressive strength (UCS), split tensile strength (STS), and resilient modulus ( $M_r$ ) properties of the mixes of RAP and RCCA base materials in different compositions and with varying dosage levels of Portland cement (Type I/II).

### 1.3 Objective and Scope

The main objective was to develop correlations between the structural layer coefficient  $a_2$  and the various strength and stiffness parameters, such as unconfined compressive strength (UCS) and resilient modulus (RM) of untreated and cement-treated RCCA, RAP, and RAP- RCCA aggregate mixes, as the base material for flexible pavement. The objectives were as follows:

1. Determination of unconfined compressive strength (UCS) and resilient modulus (RM) of untreated and cement-treated recycled base material;
2. Determination of the effectiveness of recycled materials subjected to axial cyclic loading in the base layer of flexible pavement;
3. Determination of the optimum cement content for different combinations of recycled base materials;
4. Determination of the optimum combination of different recycled materials in the mixes based on the strength and stiffness parameters;
5. Comparison of the  $M_r$  and UCS values of the different combinations of recycled materials;
6. Evaluation of environmental effects of using recycled materials as a pavement base layer;
7. Evaluation of durability of different combinations of RAP and RCCA materials at different cement content;

8. Development of statistical correlations between the  $M_r$  and UCS, and the  $M_r$ , UCS, and elastic modulus (EM) so that the resilient modulus ( $M_r$ ) can be determined from faster, easier, and less expensive tests, such as the unconfined compressive strength (UCS) test;
9. Determination of structural coefficient  $a_2$ , using the equation provided by AASHTO; and
10. Development of the correlation among structural coefficient  $a_2$ , UCS, and  $M_r$ .

#### 1.4 Dissertation Outline

The dissertation manuscript has been divided into six chapters:

- Chapter 1 provides the background, a problem statement, an objective, and the scope of this study.
- Chapter 2 presents a literature review on previous studies conducted on recycled materials, available design guidelines, and environmental tests. It also provides a glimpse of the correlation between resilient modulus ( $M_r$ ) and other strength properties, such as unconfined compressive strength (UCS), and elastic modulus (EM).
- Chapter 3 describes the experimental program; several test procedures, such as optimum moisture content (OMC); maximum dry density (MDD); unconfined compressive strength (UCS); elastic modulus (EM); resilient modulus ( $M_r$ ); split tensile strength (STS); wetting-drying tests; and different types of environmental tests.
- Chapter 4 presents test results, analysis, and discussions of the results.
- Chapter 5 provides a description of the multiple linear regression analysis procedure and development of a statistical model to determine the value of resilient modulus ( $M_r$ ), using unconfined compressive strength, elastic modulus, and bulk stress.
- Chapter 6 provides the summary and conclusions of the current study and includes recommendations for future research.

## Chapter 2

### Literature Review

#### 2.1 Introduction

The use of recycled materials has become very popular in pavement construction. These materials are cost effective, and are treated with cement and fibers to improve their performance, longevity, and engineering properties. This chapter gives an overview of the recycled base materials, pavement design criteria, and various models that are recommended to determine the strength parameters of pavement materials. The literature reviewed in this chapter was collected from different journals, design guidelines, and other research projects. A brief description of recycled pavement materials and pavement structures will be depicted, followed by brief descriptions of the pavement design methods. The characteristics and properties of cement-treated base materials will be reviewed, and the various factors that affect the strength parameters will be described. The models suggested by different guidelines and research works to determine the value of strength parameters will be introduced, and will be followed by different correlations between unconfined compressive strength and structural coefficients, as well as between unconfined compressive strength and resilient modulus of materials.

#### 2.2 Recycled Materials in Pavement Construction

Most infrastructure, such as buildings, roads, and bridges were constructed during the 1950s and 1960s, and have deteriorated to the point that they need to be repaired and/or replaced (Wilburn and Goonan, 1998). Repair, rehabilitation, and new construction of these infrastructures has led to an increase in waste production. According to the study conducted by Padgett and Stanley in 1996, approximately 4.5 billion tons of non-hazardous solid waste is produced each year and disposed of in landfills, resulting in the depletion of landfill space and an increase in the cost of disposal. At the same time, an increase in demand and the depletion of resources limits the use of natural aggregates, such as crushed stone and gravel, etc. Recycled aggregates are a

viable alternative to natural limestone (Potturi 2006), and the use of recycled materials, such as recycled crushed concrete aggregates (RCCA) and reclaimed asphalt pavement (RAP) have the potential to reduce construction costs and prevent the rapid decrease in natural resources.

### 2.3 Recycled Crushed Concrete Aggregate (RCCA)

Construction of new structures and demolition of existing structures such as buildings, airfield runways, and roads generate waste materials such as concrete, masonry, and bituminous road materials (Sherwood, 1995). These waste materials have the potential for use as recycled construction materials, resulting in the conservation of natural resources and reduction in the amount of energy used in production. The American Concrete Pavement Association estimates that approximately 322 kilometers of concrete pavement are recycled each year, and approximately 5,440 metric tons of crushed concrete can be reclaimed from 1.6 km of concrete pavement of an average thickness. This translates into 2.6 million metric tons of reclaimed concrete being recycled annually in the United States (FHWA, 1997). The recycled crushed concrete aggregate has higher water absorption, lower specific gravity, higher thermal coefficient of expansion, and higher LA abrasion loss than conventional aggregate (Won, 2001).

### 2.4 Reclaimed Asphalt Pavement (RAP)

The US produced approximately 500 million tons of new asphalt pavement material in 2007, which included 40 million tons of recycled asphalt pavement material. The removed or reprocessed pavement material, containing asphalt and aggregate, is called reclaimed asphalt pavement (RAP). According to the Environmental Protection Agency (EPA), 80% of the removed pavement materials are recycled each year. The recycling rate of reclaimed materials is higher than that for aluminum cans, plastic bottles, and glass bottles. Approximately 100 million tons of asphalt pavement material was recycled in 2011 (FHWA, 2011); the rate is even higher than the recycling rate of industrial waste products.

### 2.4.1 Use of RAP in USA

According to the survey conducted by the North Carolina Department of Transportation (NCDOT) in 2007, the majority of state transportation departments allow the use of RAP in HMA mixtures. The average national usage rate was 12% in 2007. Only ten state transportation departments use as high as 29% of RAP in the intermediate layer, although 35 of them could do so (Figure 2.1). Another survey conducted by the Materials Engineering and Research Office of the Ministry of Transportation of Ontario, Canada, (MTO) found that, in the United States, for base and binder courses, the RAP percentage ranged from 20%- 50% for medium-to-low traffic roadways. Tests were conducted to evaluate the environmental soundness of these materials.

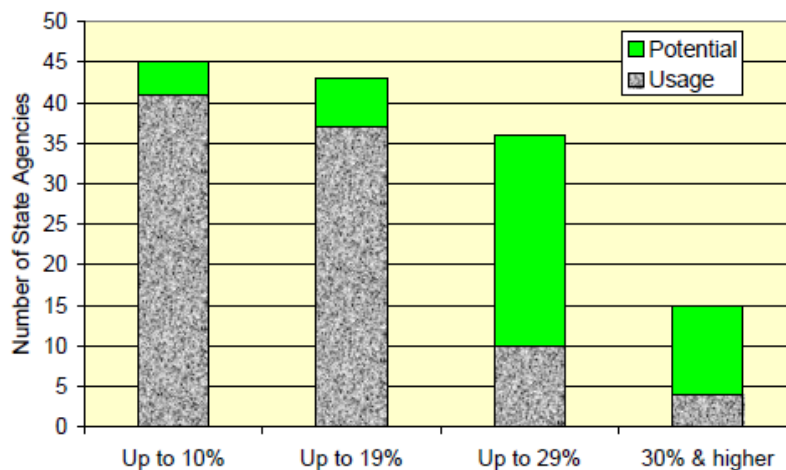


Figure 2.1 Usage and potential of various RAP percentages in the intermediate layer (NCDOT 2007)

### 2.4.2 Properties of RAP

In the following table, the physical and mechanical properties of the RAP are indicated. The typical unit weight of RAP ranges from 120 to 140 lb. /ft<sup>3</sup> and the moisture content varies from 5 to 8%. Typically, RAP materials contain about 3 to 7% of hardened asphalt content. The ignition oven method specified in AASHTO T 308 was used to determine the asphalt content in 15 state

departments of transportation, and the solvent extraction method was used by 9 state departments of transportation. Hardening of asphalt content might have occurred because of oxidation, thixotropic effect, etc. California Bearing Ratio (CBR) ranges from 20 to 25 (Table 2.1).

Table 2.1 Properties of RAP materials (Potturi, 2006)

<b>Property</b>	<b>Typical Range</b>
Unit Weight	120 to 140 pcf
Moisture Content	5 to 8%
Asphalt Content	3 to 7%
Asphalt Penetration	10 to 80 at 25°C
Absolute Viscosity	4000 to 25000 poise at 60°C
Compacted Unit Weight	100 to 125 pcf
California Bearing Ratio (CBR)	20 to 25% for 100% RAP

## 2.5 Pavement Structure

A typical pavement structure consists of several layers of different materials which receive load from the upper layers and distribute them to the lower layers. The purpose of the upper layers is to reduce the stress level to the subgrade. Classification of pavement is done by using its load distribution pattern. There are three types of pavements: rigid pavement, flexible pavement, and composite pavement. Flexible pavement generally consists of a prepared or stabilized subgrade, base or sub-base course, and surface course. Flexible pavement has higher deflection at the edges and lower deflection at the center. Rigid pavement consists of a prepared subgrade, base or sub-base course, and a pavement slab. A pavement slab is usually a concrete slab which settles

uniformly under loading. Composite pavement is a combination of both rigid pavement and flexible pavement. A rigid section is overlain by flexible pavement and includes hot mix asphalt (HMA), open graded friction course, or rubberized asphalt (Potturi, 2006). This flexible overlay works as a thermal and moisture blanket and reduces the deflection and wearing of the rigid pavement layer.

#### 2.5.1 *Surface Course*

The surface course is the top layer of the pavement, which is constructed on top of the base course and stays in contact with the traffic wheel load. For this reason, it has to resist the high traffic load and rutting, and provide drainage control and a smooth riding surface.

#### 2.5.2 *Base Course*

This is the layer above the sub-base course (if there is any); otherwise, it is directly on top of the subgrade and immediately below the surface to provide structural support. This layer consists of crushed virgin aggregate, crushed limestone, recycled crushed concrete aggregate, and recycled asphalt pavement (RAP) treated with Portland cement, lime, or other binder materials. The base material is selected in accordance with the specification. Using the recycled material significantly reduces the cost by decreasing the thickness of the layer. The performance of the base layer is dependent upon finding the optimum cement content.

#### 2.5.3 *Sub-Base Course*

This layer is usually beneath the base layer to support the surface and base course. It consists of a compacted layer of granular material, with or without treatment of stabilizer. It prevents the fines from the subgrade from moving into the base layer. The material quality of the subgrade is usually lower than the base layer, as it requires less strength. If the strength of the base layer is high enough to sustain the wheel load, then the sub-base layer is not needed.

The stress induced by the wheel load reduces with depth, especially in the flexible pavement top layer, and is a stronger layer than the materials of the bottom layers. While designing a pavement, it is important to consider the load induced by the traffic and the types of materials to be used to ensure the most economic and sustainable design. A typical cross section of a pavement structure is shown in Figure 2.2.

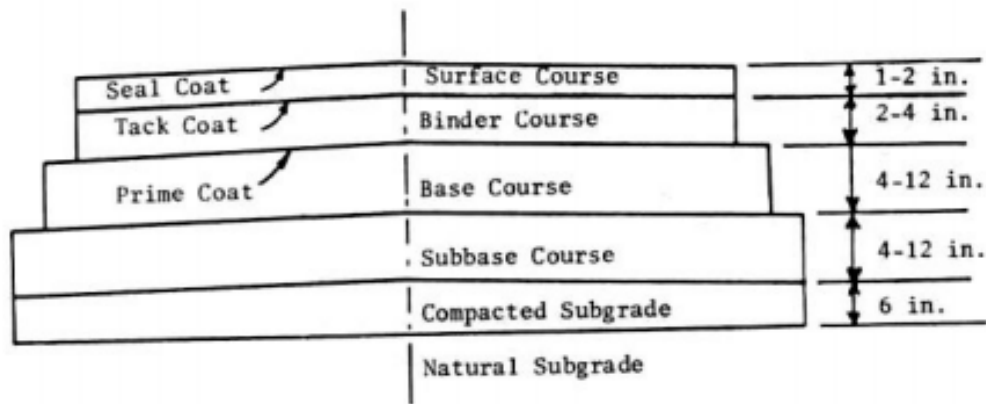


Figure 2.2 Typical pavement structure (Ordonez, 2006)

## 2.6 Pavement Design Criteria

A major component of pavement design is the thickness of the pavement layer. To determine the thickness of the pavement layer, the criteria are the imparted load on pavement and the strength and stiffness of the subgrade.

### 2.6.1 Imparted Load on Pavement

Equivalent single axle load (ESAL) is used to estimate the imposed load on the pavement, using a fourth power formula. The concept of ESAL was developed by the American Association of State Highway and Transportation Officials (AASHTO). The ESAL reference axle load is an 18 kip single axle with two tires, and it typically varies with the type of truck. The amount of traffic is predicted over a design or analysis period and then converted into an equivalent number of 18 kip single-axle loads and totaled over the design period. Consider that an 18-wheeler with tow tandem

axles and one single axle exerts ESAL equivalent to 2.44. Different trucks have different wheel load conditions, which can be found in any pavement design guide book.

### 2.6.2 *Strength and Stiffness of Subgrade*

The strength and resilient values of the subgrade soil are the most important parameters in pavement design. In the past, CBR, R-value, soil support value (SSV), and triaxial strength parameters were used as pavement design parameters. These parameters simulate the static load condition, and the failure load does not represent the actual dynamic traffic load condition of real life pavement. Soil failure does not occur in the field on a regular basis. AASHTO 2003 recommended using resilient modulus ( $M_r$ ) of soil or subgrade and base materials. The  $M_r$  value represents the dynamic modulus of soil and also considers the plastic deformation of the soil.

The parameters required for the design of a pavement structure are design variables, performance criteria, material properties, structural characteristics, and reinforcement variables. Design variables are performance period, traffic, reliability, and environmental effects. Performance criteria include serviceability, allowable rutting, aggregate loss, etc. Structural characteristics are known as drainage load transfer and detachment between the pavement surface and subgrade. Material properties are resilient modulus, effective subgrade modulus, and modulus of rupture of Portland Cement Composites (PCC). Reinforcement variables include different types of joints in concrete slabs of rigid pavements.

## 2.7 Design of Flexible Pavement

For design of flexible pavement, the two basic parameters required are the thicknesses of the different layers and estimated traffic volume. A brief description of the AASHTO 2003 guidelines for the design of the flexible pavement is given below.

Characterization of a pavement structure is done by using the structural number (SN) of the pavement, which is determined by using the design chart for flexible pavement. The input

parameters required for the design chart are the total estimated traffic passes of 18 kip ESAL load applications ( $W_{18}$ ), reliability factor ( $R$ ), design serviceability loss ( $\Delta PSI$ ), effective road bed soil resilient modulus ( $M_r$ ) in combination with soil support and the standard deviation ( $S_0$ ). The design chart for the determination of SN is shown in Figure 2.3. Once the structural number is determined, it is converted into the layer thickness, which is determined by the following equation:

$$SN = a_1 \times D_1 + a_2 \times D_2 \times m_2 + a_3 \times D_3 \times m_3$$

Where,

$a_1, a_2, a_3$  = layer coefficients for the surface, base, and sub-base,

$D_1, D_2, D_3$  = thicknesses of the surface, base, and sub-base,

$m_2, m_3$  = drainage coefficients for the base and sub-base courses

The value of the SN required is smaller than the value obtained from the equation above. Layer coefficients should be determined using resilient modulus ( $M_r$ ) values. The value of SN will vary and be larger than the design SN. It is important to select a reasonable SN value, considering the economy of the construction and maintenance constraints.

## 2.8 Design of Rigid Pavement

The design guidelines for rigid pavements were also developed by the AASHTO. Rigid pavement typically consists of a concrete slab, base, sub-base, and subgrade. A brief description of AASHTO's rigid pavement design guidelines are given below.

The value of the resilient modulus is usually converted to the modulus of the subgrade reaction ( $k$ ), which is used for rigid pavement design. The design charts are shown in Figure 2.3 to Figure 2.9. Required parameters to determine the value of  $k$  are resilient modulus ( $M_r$ ) psi, subbase thickness,  $D_{sb}$  (inches), depth of subgrade to rigid foundation,  $D_{sg}$  (ft.), and the elastic modulus ESB (psi). The estimation of relative damage to rigid foundations is shown in Figure 2.6.

A factor, LS, is introduced to reduce the subgrade reaction, considering the loss of support by foundation erosion or differential vertical soil movements. The design variables are the same as for flexible pavement design. The correction factor chart is shown in Figure 2.7. After the determination of the subgrade reaction ( $k$ ), the concrete slab thickness is determined by using the charts shown in Figure 2.8 and Figure 2.9. There are a few other parameters, such as concrete elastic modulus ( $E_c$ ), modulus of rupture of concrete ( $S_c$ ), load transfer coefficient ( $j$ ), and the drainage coefficient ( $C_d$ ) which are required for the design of the rigid pavements.

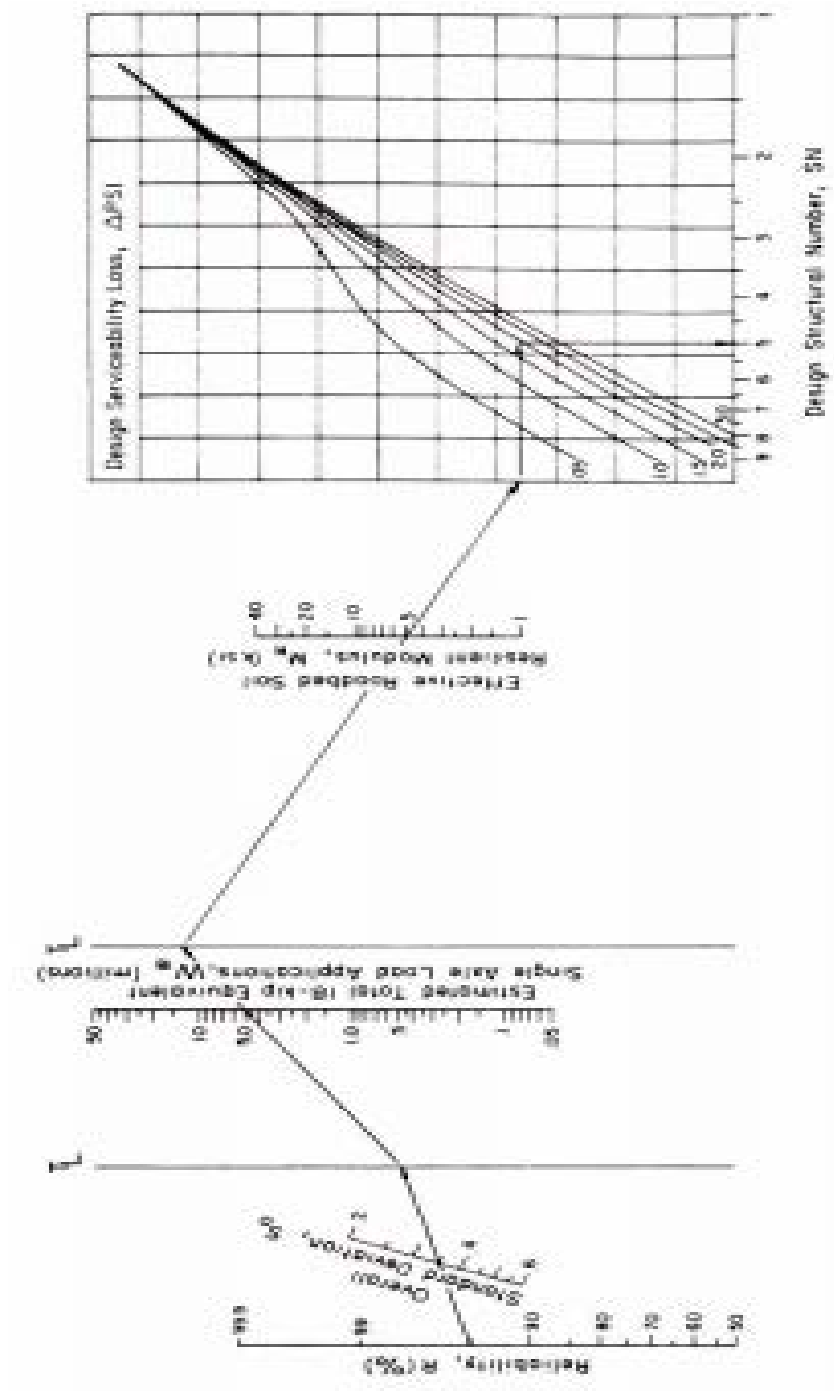


Figure 2.3 Flexible pavement design chart (AASHTO, 2003)

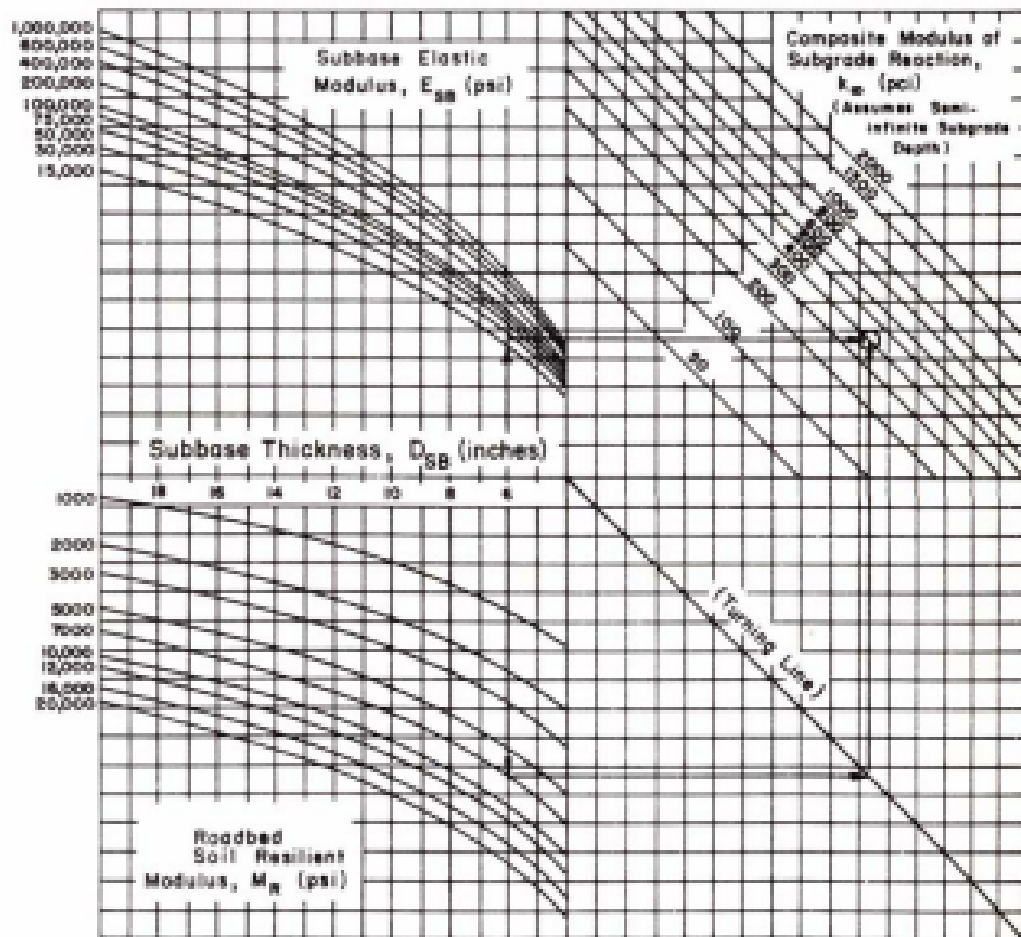


Figure 2.4 Chart for the determination of subgrade reaction (AASHTO, 2003)

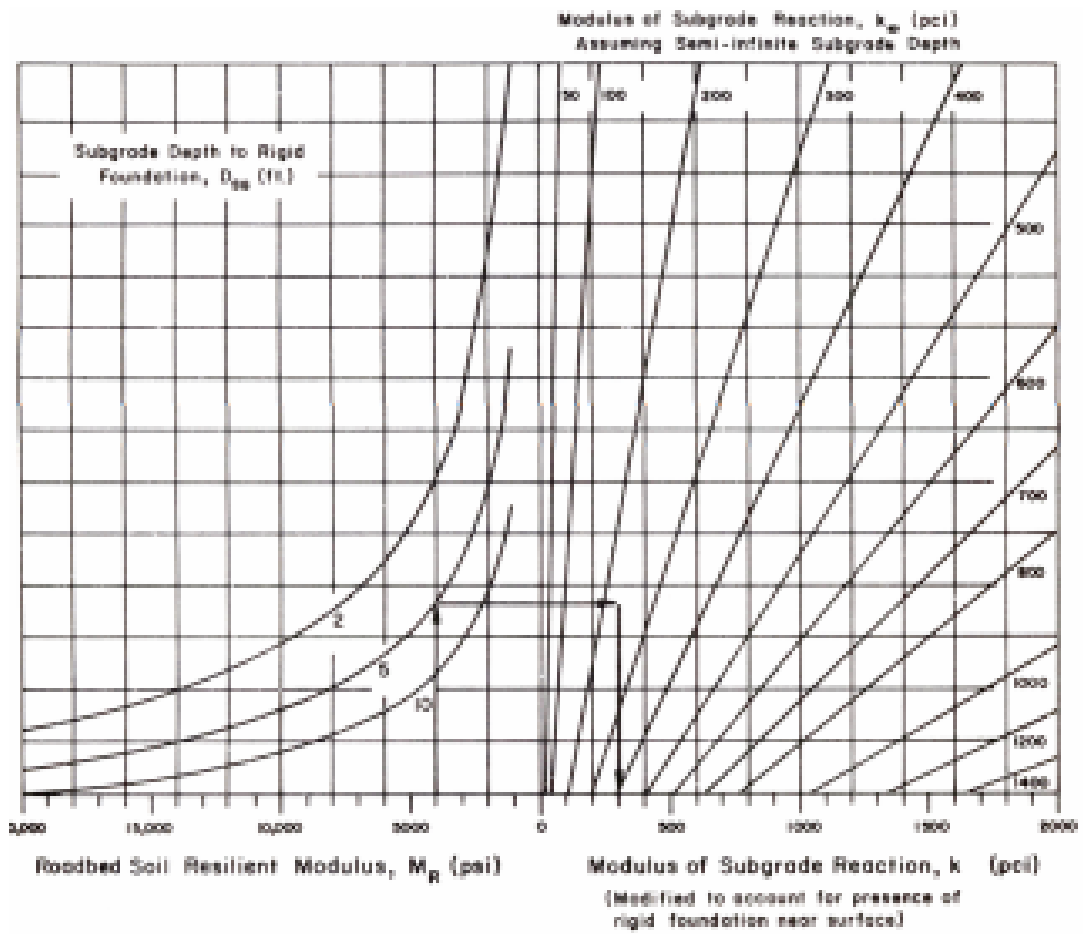


Figure 2.5 Chart for modifying modulus of subgrade reaction due to rigid foundation (AASHTO, 2003)

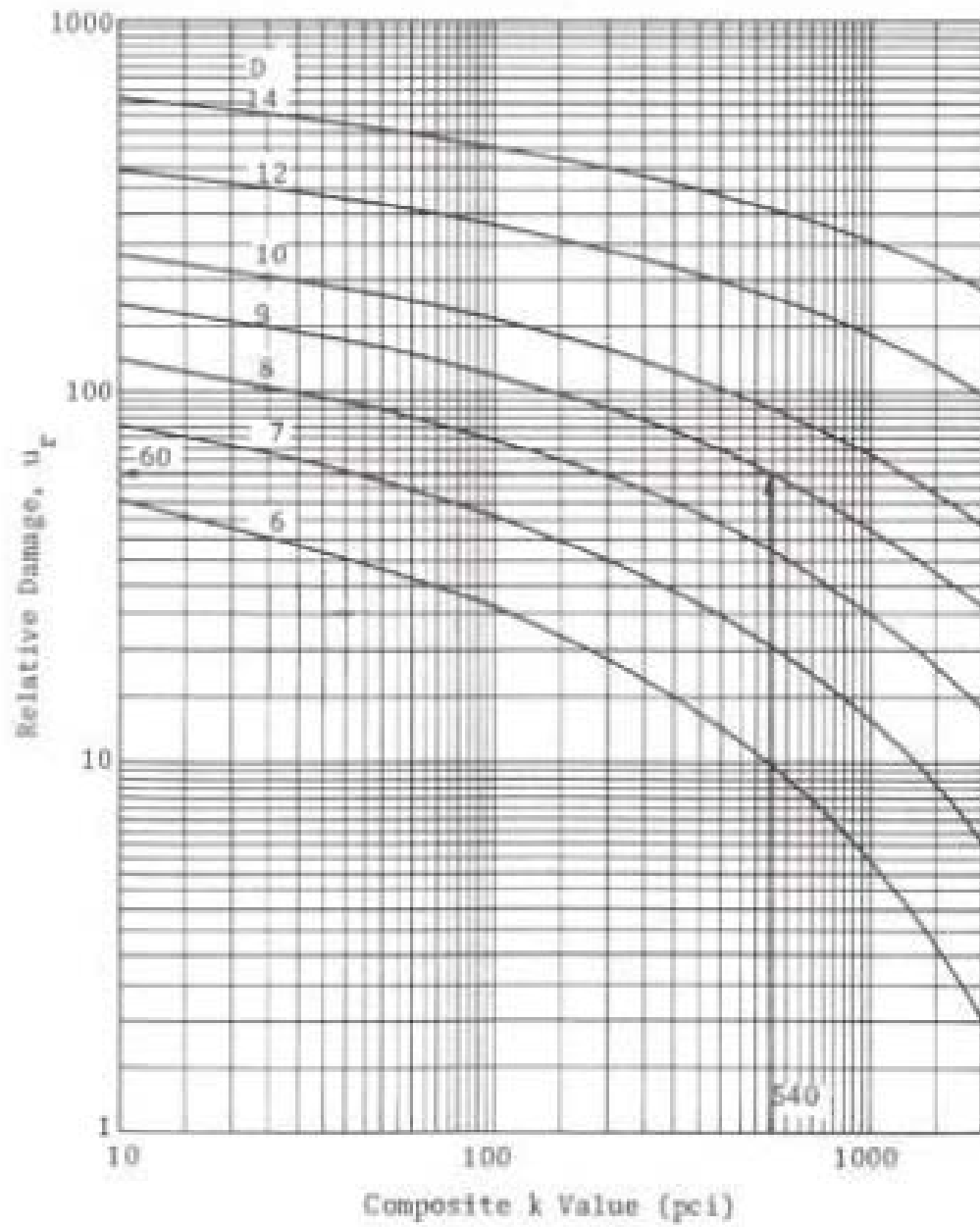


Figure 2.6 Chart for estimating the relative damage to rigid pavements (AASHTO, 2003)

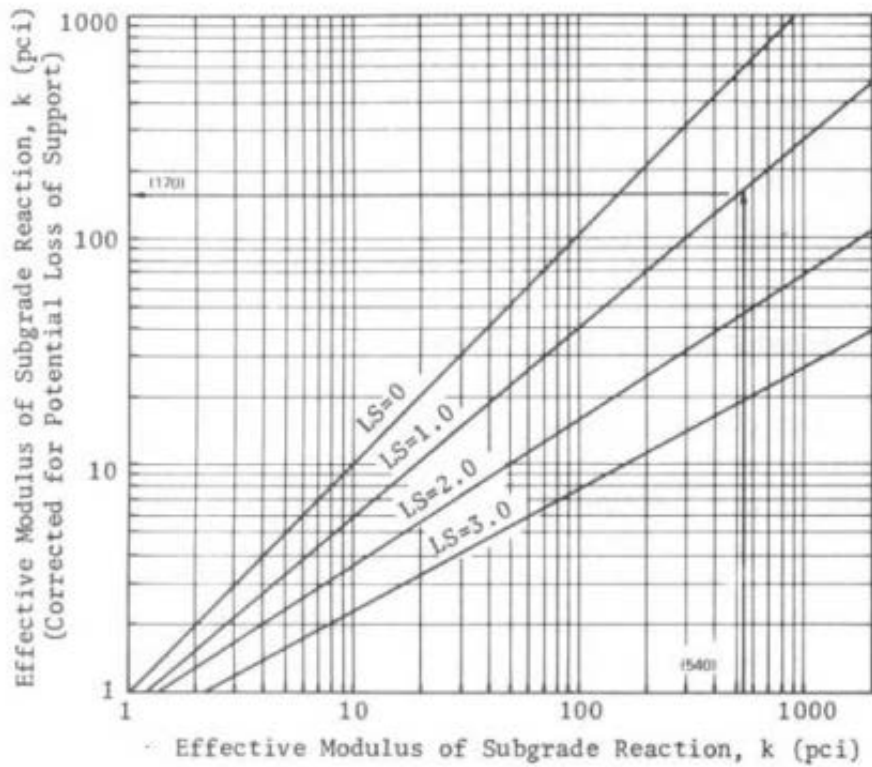


Figure 2.7 Correction of effective modulus of subgrade reaction (AASHTO, 2003)

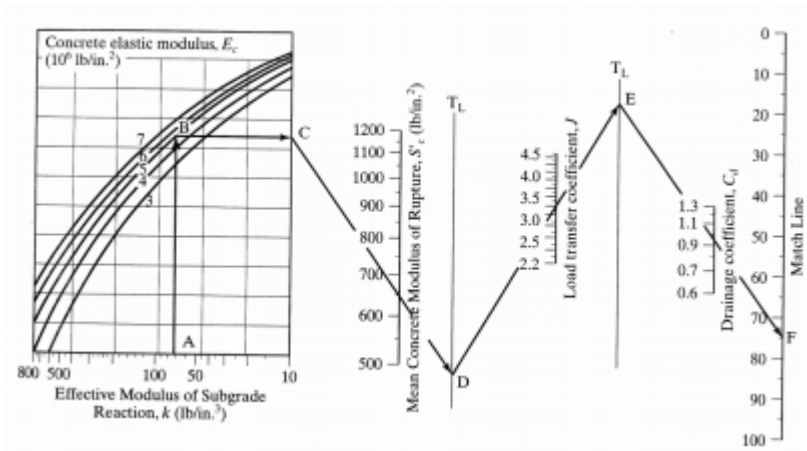


Figure 2.8 Design chart for rigid pavements (AASHTO, 2003)

It is clear from all of the design charts presented above that the resilient modulus ( $M_r$ ) is the most important design parameter for pavement design. It is therefore necessary to determine the resilient modulus value for any type of base material mixture.

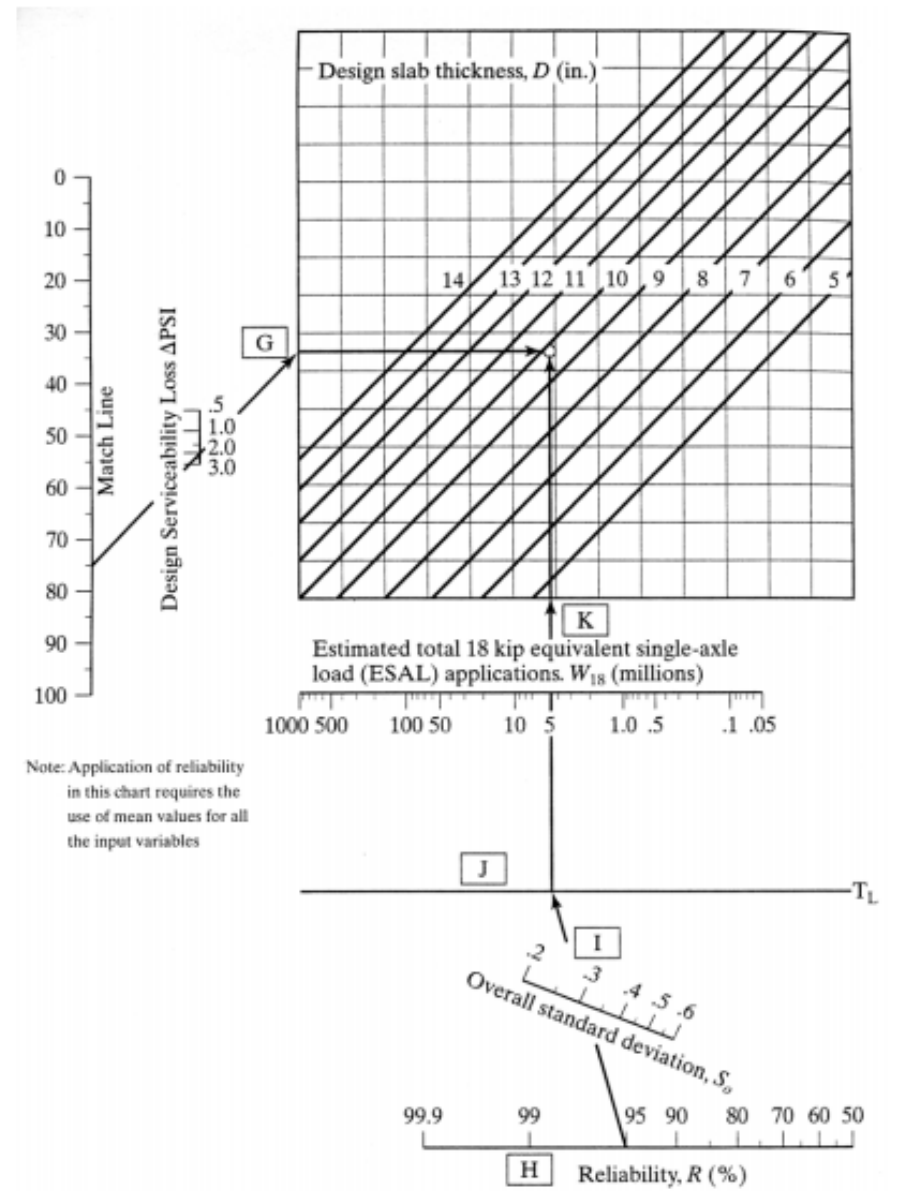


Figure 2.9 Design chart for the rigid pavements (AASHTO, 2003)

## 2.9 Cement-Treated Bases

A cement-treated aggregate base (CTAB) is defined as a mixture of aggregate materials, Portland cement, and water that hardens after compaction and cures to form a durable paving material (Rodway, 1979). It is the most-used base for both rigid and flexible pavements. CTAB usually contains coarse aggregates with higher cement content, which results in higher strength and stiffness. It acts as a slab under the application of load. The performance of CTAB depends largely on the elastic modulus and strength of the material. These properties are useful for developing design procedures based on the stress-strain relationship and fatigue characteristics parameters (George, 2004). The unconfined compression test is used largely to determine the unconfined compressive strength (UCS) of the CTAB, as it is the simplest of all methods. Compressive strength is a useful mix design parameter for CTAB. Recycled asphalt pavement (RAP) is mixed with virgin aggregate, crushed limestone or crushed concrete, and treated with cement for use as a flexible base material. To obtain the required strength in the field, the optimum cement content and quantity of water should be determined in the laboratory (Croney and Croney, 1997). In previous studies, empirical relationships were developed between the compressive strength and flexural or tensile strength of the CTAB materials to be used in the structural design of the pavement layers.

## 2.10 Design Considerations of RAP and RCCA Materials

Current design guidelines were developed based on strength, rather than on the long-term performance of the pavement. As a result, transportation departments of different states are using a higher cement content to achieve high strength values. This high strength of relatively stiff cement-treated aggregate base layers may guarantee the strength and resilient modulus, but not necessarily the long-term pavement performance (Guthrie, 2002). Roadways which contain base layers treated with high cement content are subject to rutting, shrinkage cracks, fatigue cracks, and transverse cracks, which may not cause structural deficiency, but allow water to penetrate the

pavement layers and reduce the quality of the pavement. Tensile cracking occurs at the bottom of the pavement layers, and rutting is the result of the accumulation of the pavement deformation. In recent studies, these problems, such as rutting, fatigue cracking, etc. were addressed by using fiber reinforcement with the RAP material (Potturi, 2006). Fiber-reinforced, cement-treated base materials have improved tensile strength, which reduces the propagation of cracks and the associated cracking in the pavement surface layer.

#### *2.10.1 Cement-Treated RAP and RCCA*

Recycled asphalt pavement (RAP) consists of asphalt and aggregates which are generated by cold milling of the removed hot mix asphalt (HMA) pavement. Usually, it is used as a replacement of the aggregate base course and processed to meet the requirements of the specific gradation. Recycled crushed concrete aggregates (RCCA) are produced by crushing the concrete to meet the specific particle size requirement. Its properties are different from the aggregate, as cement is attached to the surface of the natural aggregate. Both RAP and RCCA are of interest to researchers, as they could be a cost-saving alternative to the virgin aggregate. RAP and RCCA materials must meet the minimum design criteria provided by the AASHTO guidelines and state transportation departments. The addition of cement to base materials improves the strength and stiffness, i.e., resilient modulus, but does not ensure the proper performance and durability of the pavements against problems such as rutting and cracking.

#### *2.10.2 Unconfined Compressive Strength of Cement-Treated RAP*

Unconfined compression tests have been used to determine the unconfined compressive strength of the cement-treated RAP or crushed concrete. The UCS test is the most-used test to evaluate the strength of cement-treated recycled base materials. The study conducted by Croney and Croney in 1997 reported that a cement-treated base gains 70% of its strength in the first seven days. The compressive strength of a cement-treated base aggregate increases with age (Lim and

Zollinger, 2003) (Table 2.2). Two types of aggregate base materials, i.e., crushed limestone and recycled crushed concrete, were used by Lim and Zollinger in their experiment.

Table 2.2 Compressive strength of the CTAB Test Mixtures at Different Curing Times (Lim and Zollinger 2003)

Aggregate	Mix ID	Compressive strength (psi)			
		1 day	3 days	7 days	28 days
<b>Recycled Concrete (RC)</b>	1	257.8	243.8	397.4	603.7
	2	195	282.2	455	646.6
	3	257.7	286.3	454.5	550.8
	4	208.2	400.2	398.8	527.4
	5	290.3	534.6	759.8	1070.3
	6	345.1	647.3	886.6	1220.5
	7	289.1	---	797	963
	8	395.9	676.5	819.6	908.6
<b>Crushed Limestone (CL)</b>	1	378.9	524.3	630.6	1012.1
	2	318.1	490	519.7	556.9
	3	472.2	598.7	508.3	908.5
	4	278.7	543.8	461.4	734.2
	5	630.7	1083.8	1221.1	1709.5
	6	606.8	988	1224	1319.3
	7	648	1224.3	1501.7	1556.5
	8	550.5	921.7	1190.4	1292.8

Recycled crushed concrete materials were used for the experiment. Materials were obtained from road base construction sites in Harris County, Texas. Particle sizes varied from 2 in. to No. #200 sieve, meeting the specification requirements of the Texas Department of Transportation (TxDOT) Item 276, Portland Cement Treated Base. Test variables consisted of coarse aggregates, content of fines, and content of cement, as shown in the table below, in which

(-) and (+) signs indicate low and high application levels of cement (Lim and Zollinger, 2003). In the Table 2.4, the total number of test mixtures of each aggregate is shown.

Table 2.3 Test Variables and Application Levels for the CTAB Test Mix Design (Lim and Zollinger, 2003)

Test Variables	Designation	Application Levels	
		Low (-)	High (+)
Content of Coarse Aggregates	A	48%	58%
Content of Fines	F	5%	10%
Cement Content	C	4%	8%

Table 2.4 Complete Factorial of Test Mixtures for each Aggregate Type (Lim and Zollinger, 2003)

Mix ID	Test Variables and Application Levels		
	A	F	C
1	--	--	--
2	+	--	--
3	--	+	--
4	+	+	--
5	--	--	+
6	+	--	+
7	--	+	+
8	+	+	+

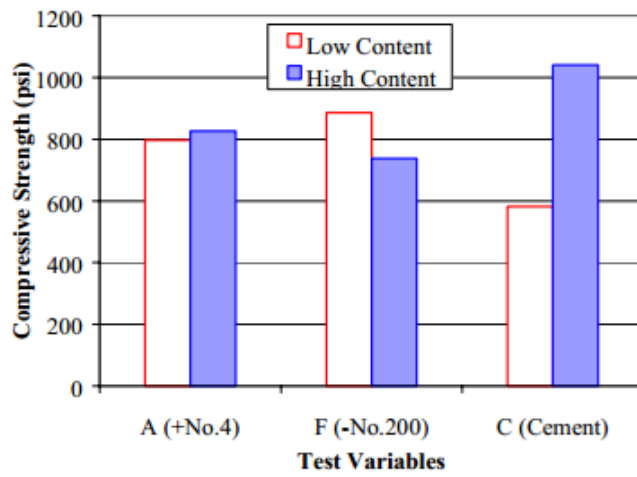
The moisture content of the mold was determined from the optimum moisture content (OMC) of the corresponding mixtures. The optimum moisture content (OMC) test results are shown in Table 2.5. The strength gained by the recycled crushed concrete was 30% lower than the strength gained by the crushed limestone material. This might have occurred due to the higher

water demand of the coarse recycled concrete material and higher water-to-cement ratio of the corresponding mixtures (Lim and Zollinger, 2003). The minimum seven-day strength requirement of most specifications ranges between 350 to 500 psi (Lim and Zollinger, 2003).

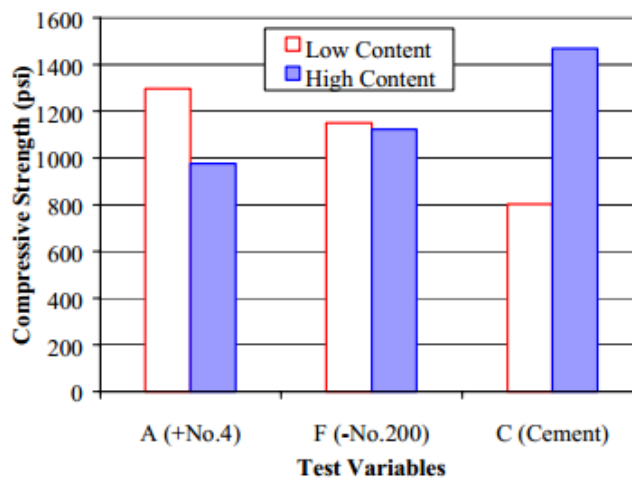
Table 2.5 Optimum Moisture Content (OMC) and Maximum Dry Density ( $\gamma_{d-max}$ ) of Different Mixtures

Mix ID	Recycled Concrete (RC)			Crushed Limestone (CL)		
	OMC (%)	$\gamma_{d-max}$ (g/cm <sup>3</sup> )	$\gamma_{d-max}$ (lb./ft <sup>3</sup> )	OMC (%)	$\gamma_{d-max}$ (g/cm <sup>3</sup> )	$\gamma_{d-max}$ (lb./ft <sup>3</sup> )
1	10.7	2.151	134.3	7.2	2.33	145.5
2	11.2	2.142	133.7	6.4	2.319	144.8
3	10.7	2.151	134.3	7.1	2.321	144.9
4	11.1	2.138	133.5	6.7	2.318	144.7
5	10.8	2.153	134.4	7.3	2.328	145.3
6	11.1	2.145	133.9	6.7	2.316	144.6
7	10.8	2.147	134.0	7.3	2.32	144.8
8	11.3	2.141	133.7	6.8	2.316	144.6

The effects of the different mixing variables, signifying the influence of cement content on the development of strength of the mixes, is shown in Figure 2.10.



(a)



(b)

Figure 2.10 Effects of mixing variables on the compressive strength of CTAB test mixtures (a) Recycled concrete (RC) mixtures, and (b) Crushed limestone (CL) Mixtures (Lim and Zollinger, 2003)

According to the studies of Croney and Croney in 1997, it takes about seven days to achieve 70% of the 28-day compressive strength, as shown in the following Figure 2.11.

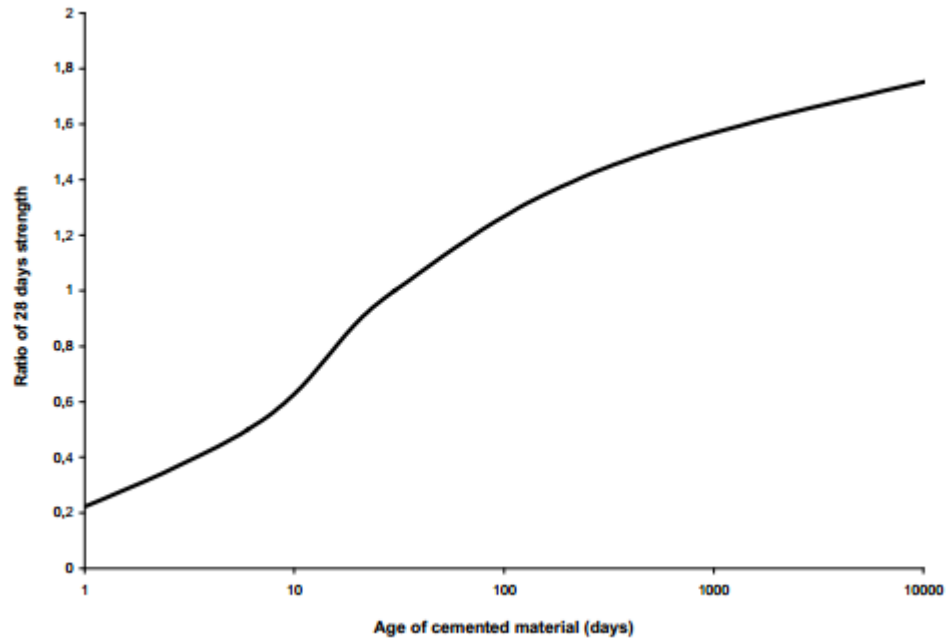


Figure 2.11 Increase in compressive strength with time (Croney and Croney, 1997)

Figure 2.12, depicts a correlation between dry density and unconfined compressive strength. However, the correlation is weak because the development of strength depends on many factors, not only a single decisive factor (Croney and Croney, 1997). The equation provided by ACI to determine the strength of the concrete is shown below:

$$f_c(t) = f_c(28) \cdot \frac{t}{a + b \cdot t}$$

Here,

$f_c(t)$  = compressive strength at time  $t$

$f_c(28)$  = Reference 28 days compressive strength

a, b = experimental coefficients (a = 0.4 and b = 0.85)

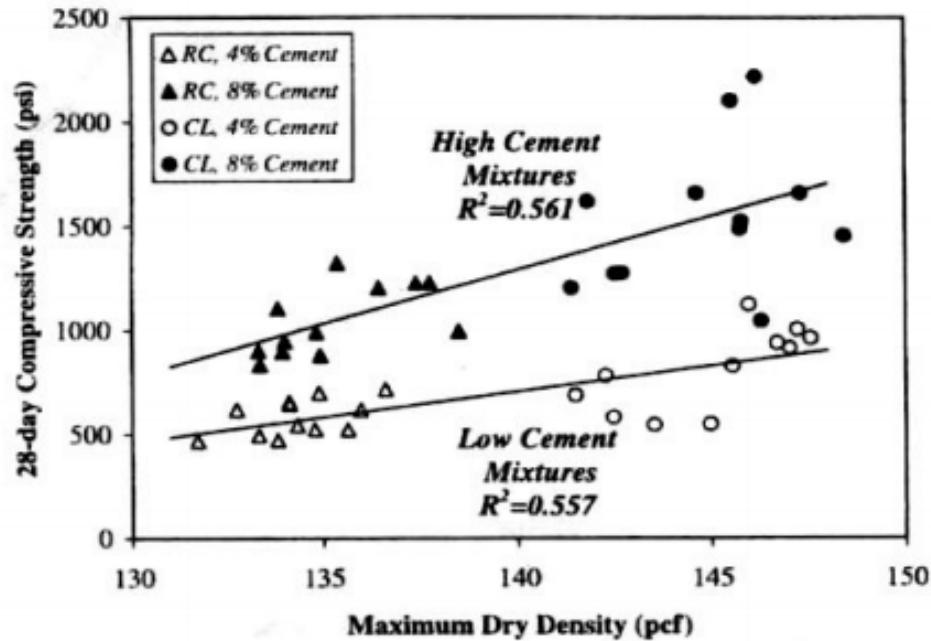
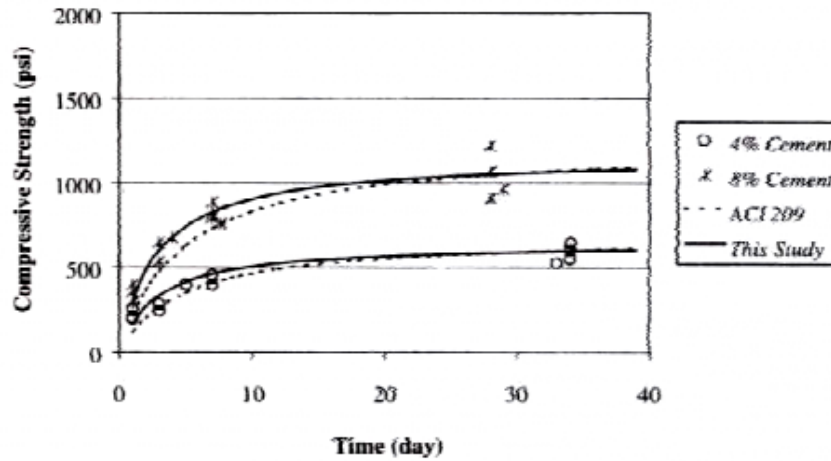


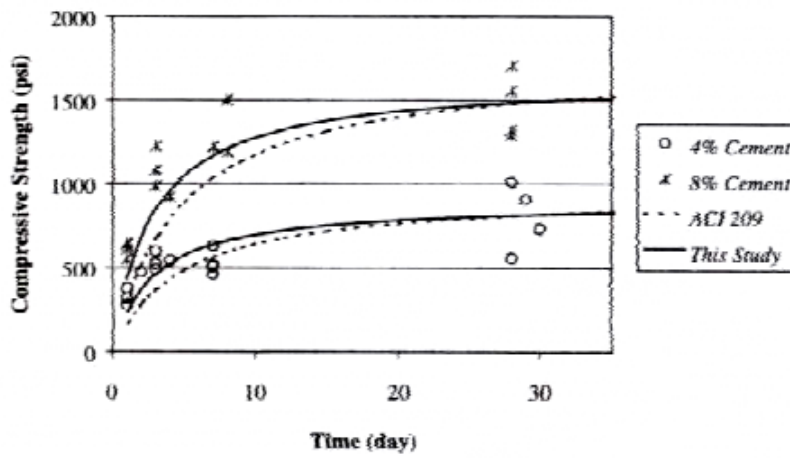
Figure 2.12 28 days of compressive strength vs. maximum dry density of the mixtures (Croney and Croney, 1997)

Using the CTAB test data, the ACI model was calibrated, and the new set of coefficients was  $a = 2.5$  and  $b = 0.9$ . These coefficients are expected to be applicable for any CTAB mixture, regardless of aggregate type and mixture proportions (Lim and Zollinger, 2003). In Figure 2.13, compressive strength predictions of the CTAB test mixture specimens are shown for the groups of as low as 4% to as high as 8% cement content (Lim and Zollinger, 2003). His estimated model and the ACI model predictions were close to each other; although at the early stages, the ACI model gave a conservative estimation of the strength of the CTAB mixtures. The elastic modulus of the CTAB mixtures was identified from the test by using the stress-strain relationship of the mixtures.

Ordonez (2006) investigated the effects of cement content on the strength of RAP base materials. Samples were prepared at different cement contents, such as 0, 2, and 4%.



(a)



(b)

Figure 2.13 Compressive strength prediction of CTAB mixtures (a) recycled concrete (RC) mixtures and (b) crushed limestone mixtures (CL) (Croney and Croney, 1997)

All of the prepared specimens were tested after seven days of curing. The use of cement increased the unconfined compressive strength significantly. When the cement content increased from 0 to 4%, the strength increased to about five times more than that of untreated specimens.

### 2.10.3 Resilient Modulus and Permanent Deformation

The two important parameters that determine the pavement performance are resilient modulus and pavement deformation or rutting. The most commonly employed method for determining these properties is repeated load triaxial tests, administered according to the guideline of AASHTO T 307-99.

Actual response of the pavement layers to traffic loading on pavement layers is determined using resilient modulus of pavement materials (Mahedi, 2016).

Resilient modulus is defined as the ratio of the repeated deviator axial stress to the resilient or recoverable strain and can be expressed as:

$$M_r = \frac{\sigma_d}{\epsilon_r}$$

Here,  $M_r$  = resilient modulus,

$\sigma_d$  = repeated deviator stress ( $\sigma_1 - \sigma_3$ ), and

$\epsilon_r$  = recoverable or resilient axial strain in the direction of principal stress

Resilient strain is the amount of deformation that may be recoverable by the exclusion of applied stress. Buchanan (2007) presented the stress-strain response of loading and unloading cycles of a typical triaxial test.

Permanent deformation is usually characterized by assuming that the permanent strain is proportional to the resilient strain (Huang, 2007). It is expressed as:

$$\epsilon_p(N) = \mu \epsilon_r N^{-\alpha}$$

Where,  $\epsilon_p(N)$  = plastic or permanent strain due to single load application such as the Nth application,

$\epsilon_r$  = resilient or recoverable strain at the 200th repetition,

N = number of load applications,

$\mu$  and  $\alpha$  = permanent deformation parameters.

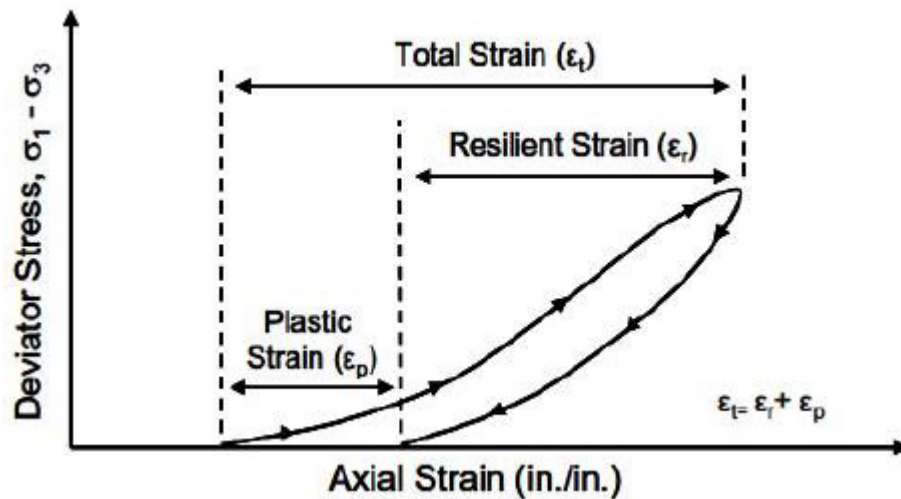


Figure 2.14 Response of specimen during cyclic axial loading (Buchanan, 2007)

According to AASHTO pavement design guidelines (1993), the value of resilient modulus  $M_r$  should be used for material characterization. It recommends the use of correlation between structural coefficients and resilient modulus. In a few studies, it was found that the results obtained from different laboratory tests for modulus were different from the back-calculated moduli. This might have occurred due to the cracks in the pavement structure (Dawson et al., 2000).

The stress dependency of base materials is usually determined by using the K- $\theta$  model. The nonlinear characteristics of pavement materials are described by K- $\theta$  model. The model is expressed as:

$$M_r = K_1 \theta^{k_2}$$

Where,

$K_1$  and  $K_2$  = material constants and

$$\theta = \text{bulk stress} = (\sigma_1 + \sigma_2 + \sigma_3) = (3 \sigma_3 + \sigma_d)$$

One of the limitations of this model is that it does not predict the volumetric strain. The following improved  $M_r$  model was suggested by Uzan (1985):

$$M_r = K_3 \theta^{K_4} \sigma_d^{k_5}$$

Where,

$K_3$ ,  $K_4$ ,  $K_5$  are material constants evaluated by a multiple regression analysis from a set of repeated load  $M_r$  tests with  $\sigma_d$  as the deviator stress.

This model is recommended by the Mechanistic Empirical Pavement Design Guide (MEPDG). Octahedral stress ( $\tau_d$ ) replaces the deviator stress ( $\sigma_d$ ), and the model is expressed as:

$$M_r = K_6 P_a \left[ \frac{\theta}{P_a} \right]^{K_7} \left[ \frac{\tau_{oct}}{P_a} \right]^{K_8}$$

Where,

$K_6$ ,  $K_7$ , and  $K_8$  are material constants.

$P_a$  = atmospheric pressure e.g. 14.7 psi (normalizing stress)

This model is recommended by MEPDG to calculate k values, which are used as analysis input. The variable octahedral shear stress  $\tau_{oct}$  is expressed as:

$$\tau_{oct} = \frac{1}{9} [(\sigma_1 - \sigma_2)^2 + (\sigma_2 - \sigma_3)^2 + (\sigma_3 - \sigma_1)^2]$$

If the tests are performed under isotropic confining pressure, the equation above can be simplified as:

$$\tau_{oct} = \frac{\sqrt{2}}{3} \sigma_d$$

When,  $\sigma_2 = \sigma_3$  and  $\sigma_d = \sigma_1 - \sigma_3$

The typical stiffness values range from 100 to 300 MPa, based on the type of granular materials that are used in some design methods (Dawson et al., 2000). There are two other relationships between  $K_1$  and  $K_2$  suggested by (Chen et al., 1995), which are expressed as:

$$\log K_1 = 4.7308 - 2.5179 K_2, \text{ (AASHTO T294-92I), and}$$

$$\log K_1 = 4.19 - 1.7304 K_2, \text{ (AASHTO T294-92I)}$$

Rada and Witczak (1981) reported that the relationship between  $K_1$ - $K_2$  varies for different materials. They investigated the possibility of developing the equation of  $M_r$  from the physical properties of the material. They used six types of aggregates. Each of these was blended at different gradations. Each gradation was compacted with three different compaction methods to establish the moisture-density relationship. It was observed that there is a possible relationship between physical properties and the  $M_r$  values of the materials. The largest variation was observed for crushed stone, but the mean values for all granular materials were  $K_1=9240$  and  $K_2 = 0.52$ .

The relationship is the same as Chen's et al., (1995) which is semi-logarithmic and can be expressed as:

$$\log K_1 = 4.66 - 1.82 K_2$$

Another finding of their study was that the effect of saturation on  $K_1$  is more significant than  $K_2$ . The value of  $K_1$  and moduli reduces with increasing moisture content. The value of bulk stress ( $\theta$ ), degree of saturation ( $S_r$ ), and maximum dry density are major parameters that influence resilient modulus.

### 2.11 Factors Affecting Strength of Base Materials

The most important factors that affect the structural integrity of flexible sections are controlled by several parameters. These are used in structural design programs like FPS19 or Texas Triaxial. The parameters are layer thickness, traffic volume, etc. Layers thicknesses are selected based on the criteria that the stresses at the contact point of HMA and the base, and the base and the sub-base or subgrade should be within limits to reduce the amount of cracking and rutting. For a certain traffic volume and the applied load, if the surface, base, and subgrade are of higher thicknesses, the stress will be lesser on the layers (Gautam et al., 2009). There are various factors that affect the resilient modulus of base materials, such as material type, sample preparation method, stress state, the condition of the samples, and the strain sensitivity of the materials (George and Uddin, 1994).

To improve the quality of untreated local materials, the thickness of the surface layer and stiffness of the subgrade must be considered. Strategies that can be followed to use the local materials are (Gautam et al. 2009):

- Increase the thickness of the layer if local materials are going to be used;
- If the thickness remains the same, then strengthen the surface and subgrade layer;
- Use a high quality base material;

- Local materials can be mixed with a high quality base material.

The strength of the base material can be improved by using an additive, such as cement, lime, etc., but an extremely strong mix is highly undesirable, as it creates potential cracking, and a weak mix will reduce the pavement performance. The optimum moisture content (OMC) and maximum dry density (MDD) are affected by the addition of the chemicals, so it is necessary to consider the change in the behavior of the material after adding these chemicals.

### 2.11.1 Size and Shape of Aggregate

Angularity, form, and surface texture are the three independent shape properties of aggregate (Barrett, 1990). They are characterized by the geometric properties of aggregates (Naidu and Adishesu, 2011). The sharpness or roundness of the aggregate corners designates the angularity of the particles. Form describes the ratio of the dimension of aggregates, and texture refers to the small scale asperities, i.e., the surface roughness of particles. Rough particles, such as gravel, have higher resilient modulus than crushed limestone (Lekarp et al. 2000). In other studies, it was learned that rounded and sub-rounded gravel have lower resilient modulus and load-spreading capability than the crushed aggregate with an angular-to-sub-angular shape (Gautam et al. 2009). Another study (Barksdale and Itani, 1989) concluded that flaky particles are more susceptible to rutting than other types of coarse aggregates.

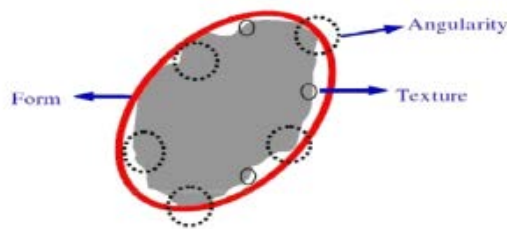


Figure 2.15 Compaction of aggregate shape: form (shape), angularity, and texture (Masad et al., 2003)

### 2.11.2 *Compaction*

Degree of compaction, degree of saturation, moisture content during compaction, and method of compaction are the factors that affect the resilient modulus of base material (Nazarian et al. 1996). Resilient modulus of base materials compacted on the wet-side of the optimum moisture content yield lower resilient modulus. Soils compacted to the maximum dry density for a certain degree of saturation result in a higher resilient modulus (Thompson and Barrenburg, 1989). The degree of saturation is a major parameter that affects the resilient modulus of the specimen. If the prepared sample is kept at a normal temperature before testing, there is a significant increase in the resilient modulus due to the thixotropic effect (Gautam et al., 2009).

### 2.11.3 *Dry Density*

Higher density results in higher resilient modulus only if the value of mean normal stress is kept low (Barksdale and Itani, 1989). The effect of density become less prominent if the stress level is higher. If the density of the sample mixture is higher than the optimum, it does not affect the value of the resilient modulus.

Rada and Witczak (1981) reported that the resilient modulus increases with an increase in density of the sample specimen, but the increment is relatively smaller than the changes that occur due to the variations in moisture and stress level.

In another study, Barksdale (1972) found that a few granular materials, if compacted at 95% of the maximum density, yielded 185% more permanent axial strain under repetitive loading.

Allen (1977) found that plastic strain reduced by 22% for gravel and 85% for crushed limestone when the method of compaction was changed from standard proctor to modified proctor. The density of rounded aggregates was higher, in the same compaction effort, than that of the angular aggregates. For this reason, the effect of density is not as profound on the rounded aggregates as it is on angular aggregates. If the amount of fine particles is higher in the aggregate,

the effect on change in density decreases. Fines contents are the particles which pass through a No. 200 sieve. It has a significant effect on the resilient modulus of base materials, which are subjected to repeated load triaxial testing, but no general trend has been determined for all types of aggregates (Dawson et al., 2000). When the amount of fines increases from 0 to 10%, the resilient modulus value decreases about 60% (Barksdale and Itani, 1989). Another study conducted by Hicks and Monismith (1971) reported that the effect of fine particles on the resilient modulus value of fully crushed gravel was much more prominent than for the partially crushed gravel.

The effect of fines content is more prominent on sand-gravel mixtures than on granular material. If the amount of fines increases up to 18%, it might influence the resilient response of the material (Dawson et al., 2000).

#### *2.11.4 Aggregate Gradation*

Thom and Brown (1988) reported that uniformly-graded aggregates showed higher resilient modulus than well-graded aggregates, which affects the permanent deformation. Resilient modulus increases with the increase in coarse particles. Permanent deformation is more affected by the gradation of the particle than it is by the compaction level.

#### *2.11.5 Moisture Content*

The amount of moisture present in untreated granular material has a profound effect on the resilient modulus of the material. Resilient modulus decreases with an increased amount of moisture (Lekarp et al., 2000).

A study, conducted by Thompson and Naumann (1993) on crushed aggregates from the AASHTO road test at different moisture contents, concluded that the permanent deformation of a sample increases with soaking of the prepared specimen. This might have occurred because of the development of transient pore pressures in the soaked samples.

Dawson et al., 2000 reported that if the moisture content of the mixes increases from the dry side to the optimum moisture content, then the permanent deformation increases as Poisson's ratio under repetitive loading. The non-linearity of the unbound material does not totally depend on the moisture content of the specimen, although the value of the resilient modulus increases if the moisture content increases from below the optimum moisture content level to the peak. If the moisture increases beyond the optimum level, the resilient modulus decreases, which might be because of the development of the positive pore pressure under repeated applied loads.

#### *2.11.6 Stress Condition*

In static failure tests, there is a sudden failure of the sample; for repeated loaded tests, the sample fails gradually (Lekarp, et al., 1997). This gradual failure condition is more representative of the actual failure condition of pavement under traffic load. Ultimate shear strength and stress levels that cause sudden failure are of no interest for analysis of material behavior when the increase in permanent strain is incremental (Gautam, 2000).

The resilient modulus of materials increases with an increase in confining pressure (Lekarp, et al., 2000). Smith and Nair (1973) suggested that the resilient modulus increases by 50% when the principal stresses are twice of the initial value.

The deviator stress is much less influential on the resilient modulus than the confining stress (Nazarian et al., 1996). The accumulation of axial permanent strain is related to deviator stress and is inversely related to confining stress (Gautam, 2000).

#### *2.11.7 Characteristics of Materials*

The base materials used in Texas must meet the specification requirements of the TxDOT Item 247; otherwise, they will be considered out-of-specification materials. The main requirements are soil gradation, liquid limit (LL), plasticity index (PI), and compressive strength. The requirements are included in Table 2.6.

Table 2.6 Required Soil Properties for Base Materials (TxDOT Item 247)

Property	Test Method	Grade 1	Grade 2	Grade 3	Grade 4
<b>Master Gradation sieve size (% retained)</b>	Tex-110-E				As shown on the plans
<b>2.5 in.</b>		-	0	0	
<b>1.75 in.</b>		0	0-10	0-10	
<b>1 in.</b>		10-35	-	-	
<b>3/8 in.</b>		30-50	-	-	
<b>No. 4</b>		45-65	45-75	45-75	
<b>No. 40</b>		70-85	60-85	50-85	
<b>Liquid Limit (% max)</b>	Tex-104-E	35	40	40	As shown on the plans
<b>Plasticity index, max</b>	Tex-106-E	10	12	12	As shown on the plans
<b>Plasticity index, min.</b>		As shown on the plans			
<b>Wet ball mill, % max</b>	Tex-116-E	40	45	-	As shown on the plans
<b>Wet ball max. Increase passing the No. 40 sieve</b>		20	20	-	
<b>Classification</b>	Tex-117-E	1	1.1-2.3	-	As shown on the plans
<b>Min. compressive strength, psi</b> <b>Lateral pressure 0 psi</b> <b>Lateral pressure 15 psi</b>		45 175	35 175	- -	As shown on the plans

## 2.12 Resilient Modulus ( $M_r$ ) of treated Rap and RCCA Materials

In a study by Taha et al., (2002), the compaction level and unconfined compression strength of the mixtures of RAP and virgin aggregates were determined at different cement contents. The laboratory test results of UCS determined the value of the resilient modulus by using a correlation between UCS and  $M_r$ . Based on the equation given in the AASHTO 1993, the values of the structural coefficient were determined, using the obtained resilient modulus values.

In a separate study by Gnanendran and Woodburn (2003), resilient modulus, CBR, and UCS tests were conducted on cement, lime, and fly ash-stabilized RAP materials. The resilient moduli, strength and CBR values increased with an increase in the amount of cement content or with each chemical treatment.

In 1194, Janoo et al., of the New Hampshire Department of Transportation (NHDOT), conducted an experiment on RAP materials collected from the selected test section by NHDOT at Concord off Interstate 89. The resilient modulus of different layers was then determined from the falling weight deflectometer (FWD) and other tests, and was subsequently used in the AASHTO 1993 design guideline for design of pavement. The results of the studies discussed above are summarized in Table 2.7.

Table 2.7 Results Summary of Structural Layer Coefficients Obtained from Different Studies

Reference	Type of Recycled Material Tested	Tests Conducted	Stress levels	Resilient Modulus	$a_2$
Lofti and Wiczak	Cement-Treated Dense Graded Aggregate, which included Limestone	Resilient Modulus ( $M_r$ )	0.28 to 2.28 MPa of bulk stress	1260 MPa (4.5% cement)	0.27
Janoo et al. 1994	Reclaimed Stabilized Base	Back Calculation from Layer Modulus (FWD)	N/A	N/A	0.15-0.19
Janoo et al. 1994	Reclaimed Stabilized Base	CBR	N/A	N/A	0.13
Taha et al. (2002)	Cement Stabilized RAP Aggregates	Unconfined Compressive Strength Tests	N/A	3726 MPa (7% cement)	0.13
Gnanendran and Woodburn (2003)	Cement Stabilized RAP Aggregates	Resilient Modulus ( $M_r$ ), CBR and UCS tests	0 to 140 kPa	310 to 590 MPa (0% to 3% cement)	N/A

Potturi (2006) investigated the effect of stabilization on the resilient modulus of RAP base materials, and covered the designs of both rigid and flexible pavements. RAP materials used in this experiment met the requirements of TxDOT's design guidelines. The AASHTO T307-99 guideline was followed to perform the resilient modulus testing of RAP specimens. To ensure repeatability and reliability of the test, three identical specimens were tested to determine standard deviation and coefficients of variation. Tests were done on RAP materials with cement contents, of 0, 2, 4, and 6%. The standard deviation ranged from 1.8 to 5.2 MPa for untreated aggregates and 4.7 to 30 MPa for cement-treated aggregate materials. The results are presented in the following figures:

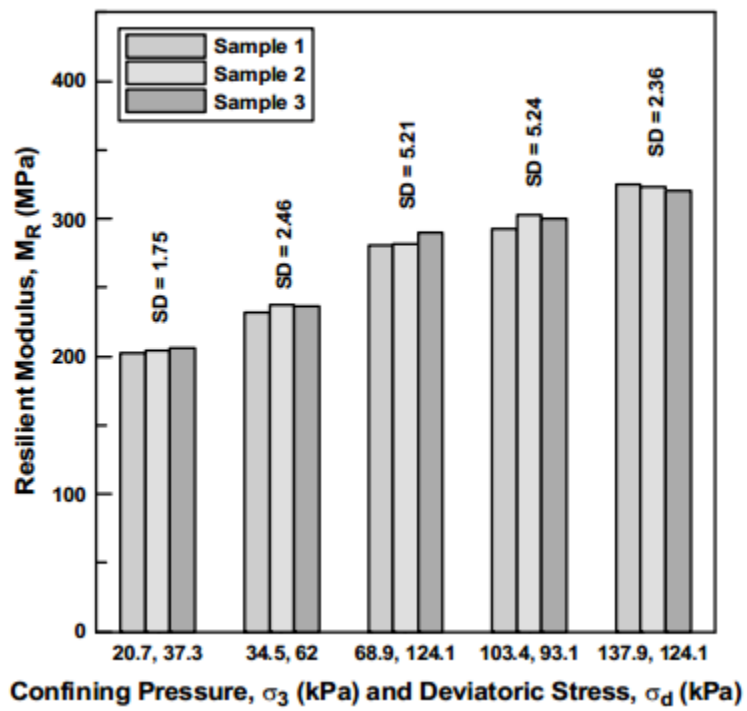


Figure 2.16 Repeatability of resilient modulus test results of untreated aggregates (Potturi, 2006)

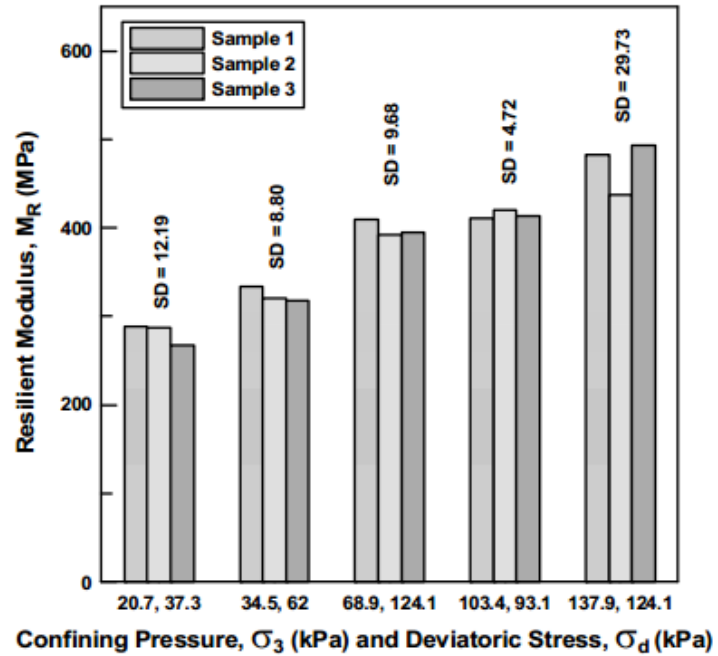


Figure 2.17 Repeatability of resilient modulus test results of cement treated aggregates (Potturi, 2006)

The value of  $M_r$  increased with an increase in deviator stresses, but the increment rate was moderate for higher confining stresses. This might have occurred because of the initial stiffening of the specimen under higher confinements which prevented additional stiffening of the specimen under higher deviator stresses. It might also be explained that, as in higher confinements, the specimen was much stronger and did not respond to the deviator stress. The resilient modulus increased with an increase in cement content, such as for a confining pressure of 137.9 kPa; the cement content increased from 0 to 2%, and the value of  $M_r$  increased by 32%.

The value of resilient modulus ( $M_r$ ) determined from the tests was used to determine the value of structural coefficients  $a_2$ , from the following the AASHTO 2003 equation,

$$a_2 = 0.249 \times \log M_r - 0.977$$

Where,  $a_2$  = Structural layer coefficient, and  $M_r$  = Resilient modulus (psi)

According to Janoo et al., 1994, the value of the structural coefficient  $a_2$  ranged from 0.13 to 0.24, which showed an increased rate with cement content and confining pressure. In the study of Potturi (2006), the structural coefficient ranged from 0.13 to 0.22.

### 2.13 Development of Correlation among UCS, Layer Coefficient and $M_r$

Resilient modulus ( $M_r$ ) is considered the most important parameter for pavement design. However, the cost, time, complications, and sampling resolutions required to get correct results from resilient modulus testing are cumbersome. For this reason it is necessary to develop a correlation between unconfined compressive strength (UCS) and resilient modulus ( $M_r$ ) to use in pavement design. Hossain (2008) reported that the quick shear test described in AASHTO T307 correlated well with resilient modulus of fine grained soil used as subgrade material.

A finite element analysis was done on the fine clay soil by Sukumaran et al., 2002. Finite element software ABAQUS was used to model the theoretical analysis of the unconfined compressive strength, CBR value, and the resilient modulus. The stress vs. displacement plot using the stress-strain input was the most accurate. The model determined the value of the resilient modulus from the unconfined compressive strength more accurately than the CBR values.

Table 2.8 Resilient Modulus of Untreated and Cement-Treated Aggregates (Potturi, 2006)

<b>Notation</b>	<b>Confining Pressure (kPa)</b>	<b>Average Resilient Moduli (MPa)</b>	<b>Structural Coefficient, <math>a_2</math></b>
Untreated	20.7	199	0.13
	34.7	235	0.15
	68.9	274	0.17
	103.4	300	0.18
	134.7	321	0.19
Treated	20.7	231	0.15
	34.7	265	0.16
	68.9	332	0.19
	103.4	360	0.20
	134.7	400	0.21

Several studies suggest different correlations between UCS and  $M_r$ , as the UCS test is less expensive and more time efficient than the resilient modulus test. A correlation between UCS and  $M_r$  tests was suggested by Lee et al., (1997) for fine cohesive soils. According to the AASHTO classification, three types of Indiana clayey soils, such as A-4, A-6, and A-7-6 were tested in this experiment under 3 psi confining stress and 6 psi deviator stress. The unconfined compression

test results at 1% strain ( $S_{u1\%}$ ) showed trends similar to those of the resilient modulus  $M_r$  at various moisture contents. The relationship developed between  $M_r$  and  $S_{u1\%}$  are as follows:

$$M_r = 695.4 * (S_{u1\%}) - 5.93 * (S_{u1\%})^2 \quad 2.1r$$

The regression coefficients was as high as  $R^2 = 0.97$

In another experiment, Thompson and Robnett (1976), developed and reported correlations between resilient modulus and soil properties of Illinois soil. The soil properties considered in this study were degree of saturation, unconfined compressive strength, and the initial tangent modulus of the stress-strain curve. A correlation was developed between the initial tangent modulus and the resilient modulus, as follows:

$$\text{Resilient modulus (ksi)} = 3.49 + 1.9 * \text{Initial tangent modulus}$$

The value of typical errors ranged between 1.5 to 3.5 ksi. Other than the initial tangent modulus, the degree of saturation was found to be one of the most important parameters which can be used to determine the resilient modulus of the soil.

Hossain and Kim (2013) suggested a possible correlation between resilient modulus and unconfined compressive strength of Virginia soils. They used the variations in degree of saturation, i.e., moisture content, as an affecting parameter for resilient modulus of soils. They divided the experiment into two phases: Phase I, to develop the correlation between resilient modulus and unconfined compressive strength; and Phase II, to predict the accuracy of the developed model. Resilient modulus tests were done according to the guidelines of AASHTO T307-99 (resilient modulus). Samples were compacted at optimum moisture content (OMC) and maximum dry density (MDD), using a static compactor. Resilient modulus values were determined from the test results by using the ratio of the deviator stress to the recoverable axial strain, and these values were put in the MEPDG-recommended constitutive model to determine the value of regression coefficients k-values. To understand the effect of moisture content on the resilient modulus of the

soils, the samples were mixed and compacted at OMC level, 20% above and below the OMC level. The variations of the resilient modulus of the soil samples with moisture content helped to select the values of unconfined compressive strength at certain moisture contents. In Phase II, all of the samples were tested at OMC. The values of stresses were calculated and used to calculate the resilient modulus of the subgrade and for comparison with the resilient modulus lab test results. Therefore, this data could be used for the MEPDG level 2 and level 3 design analyses, as well as the AASHTO 2003 design guidelines. The confining stress of 2 psi and the deviator stress of 6 psi were used for calculations. The data obtained from both the resilient modulus and the quick shear test results were analyzed and used for developing the relationship between the two sets of data. Each of the three samples was compacted to OMC level in Phase I. The effect of degree of saturation on the resilient modulus was investigated for each sample. The correlations between the resilient modulus and the degree of saturation were strong, and showed the decreasing trend of resilient modulus towards a higher degree of saturation, as shown in Figure 2.18.

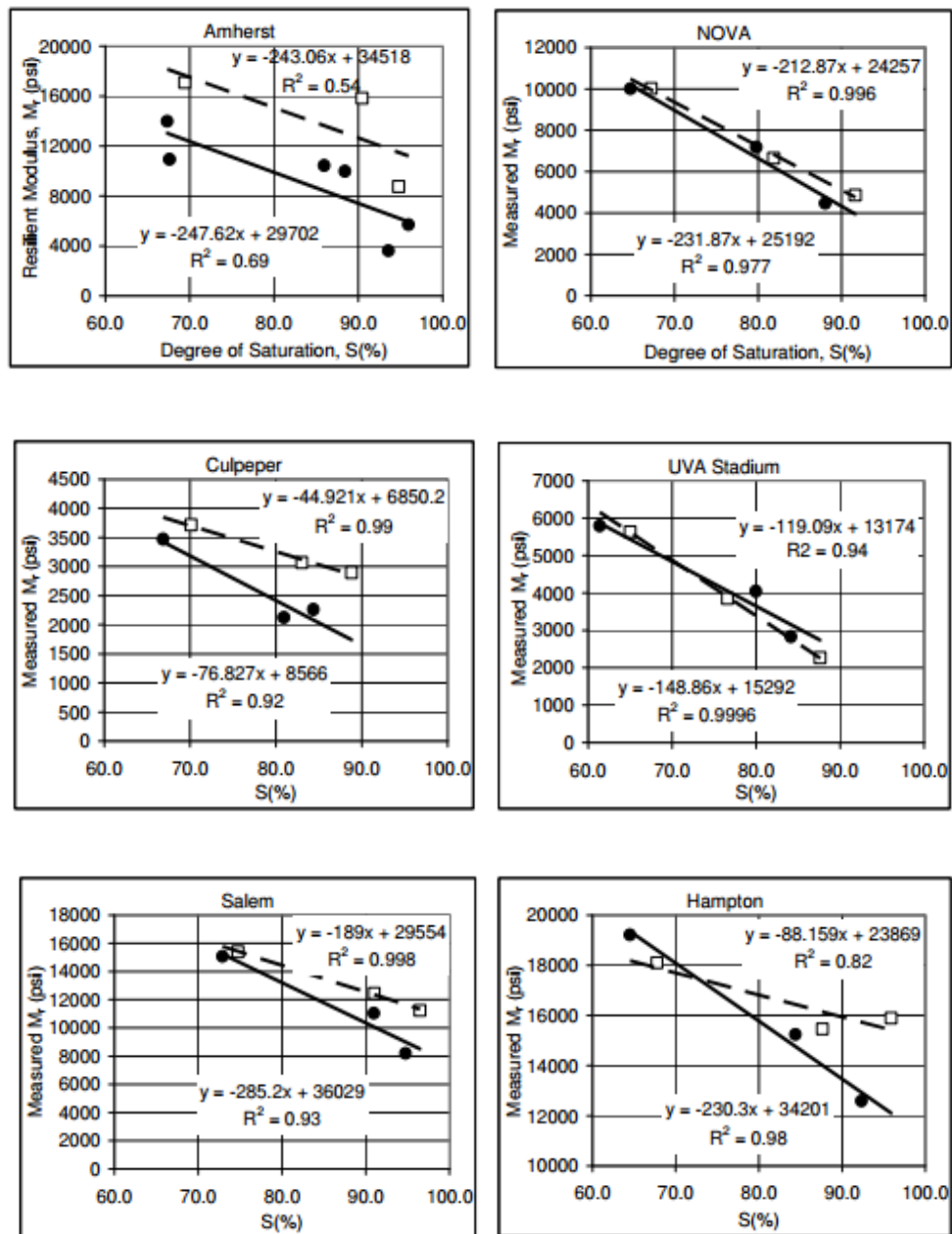


Figure 2.18 Influence of moisture content on resilient modulus value for fine grained soil where solid lines represent values measured by Virginia Department of Transportation, and dotted lines represent values measured by outside vendor (Hossain and Kim, 2013)

Unconfined compressive strength decreases with an increase in moisture content, following the same trend as the resilient modulus. The samples were prepared using both the Hampton and Harvard compaction methods. It was found that the larger Hampton samples showed less strength than the relatively small Harvard samples, which might have occurred because the small specimen had a small number of faults. The data of both the proctor and static samples were compared during Phase II, and the degree of saturation was used as a common parameter to interpolate the strength values. Comparisons between the proctor and static-compacted samples for Phase II are shown in .

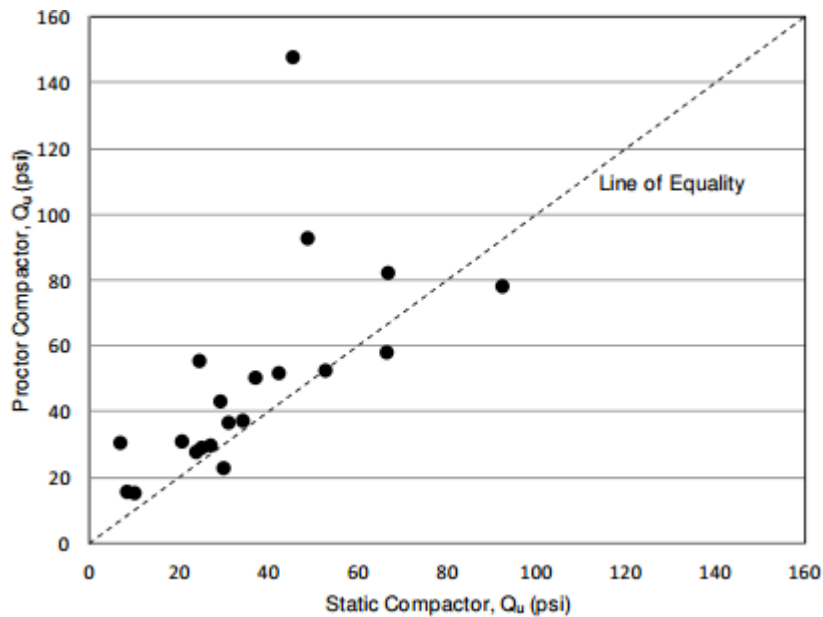


Figure 2.19 Strength comparison between static and proctor compacted samples for Phase II  
(Hossain and Kim, 2013)

To correlate both UCS and resilient modulus values, tests were performed on the identical or replicated samples which had been prepared at similar moisture contents. Resilient modulus and stress at 0.1 percent strain showed strong correlation, so a model was developed using the initial tangent modulus, which was obtained from unconfined compression tests of soil samples.

Another model was developed for the Phase II study, which correlated the resilient modulus and unconfined compressive strength. The values of unconfined compression strength were interpolated to match the degree of saturation of the resilient modulus samples. The developed predictive model is shown in Figure 2.20 and Figure 2.21. The value of regression coefficient in the model depicted earlier is low because of the influence of the degree of saturation and compaction method used to prepare the samples.

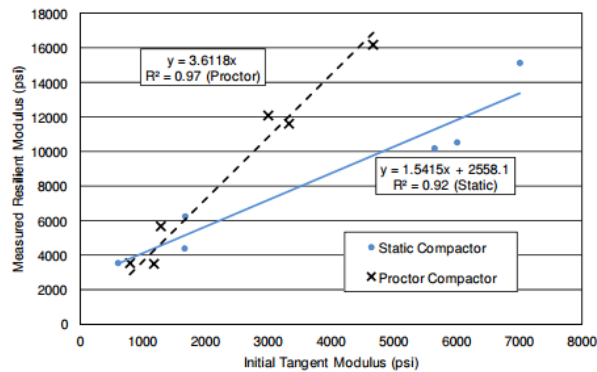


Figure 2.20 Correlation between resilient modulus and initial tangent of modulus obtained from unconfined compression tests

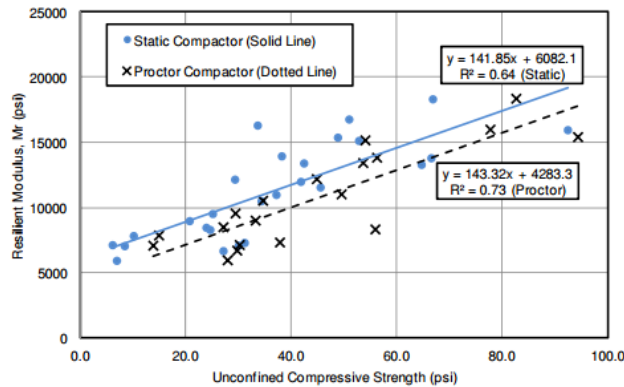


Figure 2.21 Correlation between resilient modulus and unconfined compression tests (Hossain and Kim, 2013)

#### 2.14 Split Tensile Strength (STS)

A cylindrical specimen was loaded with compressive loads that acted parallel to and along the vertical diametrical plane to determine tensile strength. The compressive load was applied through a one-inch wide stainless steel loading strip (Anagnos and Kennedy, 1998). Splitting tensile strength is a function of mix proportions and compaction efforts, similar to compressive strength (Ghafoori et al. 1995). Splitting tensile strength tests were then conducted, following Tex-421-A test procedures. The loading configuration developed uniform loading on the specimen and eventually failed the specimen by splitting or rupturing along the vertical diameter. The tensile strength at the center of the specimen was determined by using the equation as follows:

$$STS = 2P / (\pi DL)$$

Where, P = applied load, D = diameter of the specimen, and L = length of the specimen.

The STS test results can be used to estimate tensile strain at failure, Poisson's ratio, and modulus of elasticity. These relationships require integration of various mathematical functions.

## Chapter 3

### Methodology

#### 3.1 Introduction

This experimental program was developed and conducted to determine the structural competency and environmental soundness of recycled base materials under treated or untreated conditions. Unconfined compressive strength (UCS), elastic modulus (EM), and resilient modulus ( $M_r$ ) were determined for different combinations of RCCA and RAP materials at different cement contents, and were compared to achieve the strength and stiffness required by various guidelines. Multiple linear regression analysis was used to develop a design chart to determine the value of the resilient modulus and the structural layer coefficient, only using the value of UCS. Tests to determine the pH, total suspended solids (TSS), total dissolved solids (TDS), turbidity, and chemical oxygen demand (COD) were conducted to evaluate the environmental impacts of these materials. The test methods, specifications, and testing equipment are described in the following sections.

#### 3.2 Sample Collection

Recycled crushed concrete aggregate (RCCA) was collected from stockpiles of Big City Crushed Concrete located on Goodnight Lane, Dallas, Texas which is one of the TxDOT-approved recycled aggregate stockpile facilities. Reclaimed asphalt pavement (RAP) was collected from the TxDOT-specified stockpiles situated in Dallas County, Ellis County, and Rockwall County, Texas (Figure 3.1, Figure 3.2, and Figure 3.3).

Table 3.1 Material Identification

Stockpile Name	Number of Source	Material ID
Big City Crushed Concrete	1	RCCA 1
	2	RCCA 2
	3	RCCA 3
Dallas County	1	RAP 1
Ellis County	2	RAP 2
Rockwall County	3	RAP 3



Figure 3.1 Sample collection (Big City Crushed Concrete, Dallas, Texas)



(a)



(b)



(c)



(d)

Figure 3.2 RAP sample collection from TxDOT stockpile, Ellis County

### 3.3 Experimental Program

The experimental program undertaken in this research aimed at assessing the structural adequacy of combinations of recycled crushed concrete aggregate (RCCA) and reclaimed asphalt pavement (RAP) materials in flexible pavement base construction. The RCCA and RAP materials used for this research contained particle sizes ranging from 1 inch (25 mm) to No. 200 (75  $\mu$ m). Structural competency of the material was determined by using different strength and stiffness tests, such as the unconfined compression (UCS) and resilient modulus ( $M_r$ ). Different

combinations of RAP and RCCA materials were tested for structural competency under untreated or cement-treated conditions, as shown in Table 3.2.



(a)



(b)



(c)



(d)

Figure 3.3 RAP sample collection from TxDOT stockpile, Rockwall County

Table 3.2 Experimental Program for Structural Competency

Combinations of Materials	Sources	Cement Content (%)	OMC & MDD	Unconfined Compression Test	Resilient Modulus Test
70% RAP+ 30% RCCA	1	0,2,4,6	√	√	√
	2	0,2,4,6	N/A	N/A	N/A
50% RAP+ 50% RCCA	1	0,2,4,6	√	√	√
	2	4,6	√	√	√
	3	0,2,4,6	√	√	√
30% RAP+ 70% RCCA	1	0,2,4,6	√	√	√
	2	0,2,4,6	√	√	√
	3	0,2,4,6	√	√	√
10% RAP+ 90% RCCA	1	0,2,4,6	√	√	√
	2	0,2,4,6	√	√	√
	3	0,2,4,6	√	√	√
RCCA 100%	1	0,2,4,6	√	√	√
	2	0,2,4,6	√	√	√
	3	0,2,4,6	√	√	√
RAP 100%	1	0,2,4,6	√	√	√
	2	0,2,4,6	N/A	N/A	N/A

Environmental tests include pH, total suspended solids (TSS), total dissolved solids (TDS), turbidity, and chemical oxygen demand (COD). All tests were conducted on the leachate samples collected after soaking the prepared specimens in deionized water for 24 hours to determine the amount of filterable and non-filterable matter washed out from the specimens. Suspended and dissolved solids might depict the deterioration of the specimen. For this study, 100% RCCA and 50-50% RAP-RCCA mixes were utilized. If more than 50% RAP material is mixed with RCCA, it does not meet the strength and stiffness criteria required by TxDOT and the American Association of State Highway and Transportation Officials (AASHTO) guidelines (Faysal et al. 2016). Both of the material combinations were stabilized at cement dosages of 0, 2, 4, and 6%.

Portland Type I/II type cement was used to treat the base materials. A tabular presentation of this experimental program is given in Table 3.3. Repeatability of the tests was ensured by performing the same test on three identical specimens for each type of mix.

Table 3.3 Environmental Impact Assessment

Combinations of Materials	Sources	Cement Content (%)	Leachate Tests				
			pH	TSS	TDS	Turbidity	COD
50% RAP+ 50% RCCA	3	0,2,4,6	√	√	√	√	√
RCCA 100%	3	0,2,4,6	√	√	√	√	√

The durability of different combinations of RAP and RCCA materials was evaluated by applying a number of wetting-drying cycles. The experimental program undertaken regarding the durability tests are included in Table 3.4. 50% RAP 3 mixed with 50% RCCA 3 at 4% and 6% cement contents were named MIX 4 and MIX6. Durability tests included wetting-drying (WD)

cycles followed by the resilient modulus ( $M_r$ ) test on the prepared specimens (Saif et al. 2017). Leachate samples were collected after the end of the 0<sup>th</sup>, 4<sup>th</sup>, 8<sup>th</sup>, 16<sup>th</sup>, and 30<sup>th</sup> cycle. The total suspended solids (TSS), total dissolved solids (TDS), chemical oxygen demand (COD), turbidity, and pH tests were conducted on the leachate samples. The experimental program for environmental tests is included in Table 3.5.

Table 3.4 Experimental Program for Resilient Modulus ( $M_r$ ) test at Different Wet and Dry Cycles  
(Source 3 materials)

Material	Cement Content (%)	Mix ID	Tests	Test Samples					Control Samples				
				Wetting-drying (WD) cycles					Curing (days)				
				0	4	8	16	30	7	15	25	40	70
50% RAP	4%	MIX 4	$M_r$	√	√	√	√	√	√	√	√	√	√
3 + 50% RCCA 3	6%	MIX 6	$M_r$	√	√	√	√	√	√	√	√	√	√

Table 3.5 Experimental Program for Environmental Tests

Material	Cement content (%)	Mix ID	Environmental Tests	Test Samples				
				Wetting-drying (WD) cycles				
				0	4	8	16	30
50% RCCA + 50% RAP	4	MIX 4	COD	√	√	√	√	√
			TDS	√	√	√	√	√
			TSS	√	√	√	√	√
			Turbidity	√	√	√	√	√
			pH	√	√	√	√	√
50% RCCA + 50% RAP	6	MIX 6	COD	√	√	√	√	√
			TDS	√	√	√	√	√
			TSS	√	√	√	√	√
			Turbidity	√	√	√	√	√
			pH	√	√	√	√	√

### 3.4 Aggregate Gradation

Particle size distribution of those greater than No. 200 (0.075mm) sieve was determined by sieve analysis. The sieve analysis was conducted by following the guideline of Tex 110E Standard Test Method for particle size analysis of soil/particles. If less than 1% materials by weight passed through the No. 200 sieve, then a hydrometer analysis is required. In this case, the amount

of percent passing through the No. 200 sieve was less than 1%, so a hydrometer analysis was not necessary. The amount of material retained in each sieve was weighed, and the percent passing through the sieve was calculated. The material retained in each sieve was divided by the weight of the total sample and then subtracted from the total percentage of material. The percent of material passing through each sieve was plotted against the sieve size on semi-log graph paper.

### 3.5 Laboratory Compaction Characteristics and Moisture Density Relationships

The maximum dry density and optimum moisture content were determined per TxDOT's Tex0-113-E Laboratory Compaction Characteristics and Moisture-Density Relationship test procedure. The compaction effort for TxDOT is greater than for the standard proctor method, but less than for the modified proctor compaction tests. The differences in the compaction energy are included in Table 3.6.

Table 3.6 Compaction Energy of Different Laboratory Compaction Procedures

Method	Compaction Energy (ft-lb/in <sup>3</sup> )	Reference
Standard Proctor	7.18	ASTM D-698 A
Modified Proctor	32.41	ASTM D-1557
TxDOT	13.25	TEX-113-E

The compaction test was performed by using a mold that was 6 inches wide and 8 inches high, and a 10-lb. hammer, dropping from a height of 18 inches, which applied 50 blows to each of the four layers. The compaction was done on at least four samples at different moisture contents. Moisture content was determined after the samples were compacted and dry density was determined. After that, the moisture vs dry-density curve was plotted to determine the corresponding optimum moisture content and maximum dry density from the peak of the curve.

### 3.6 Specific Gravity

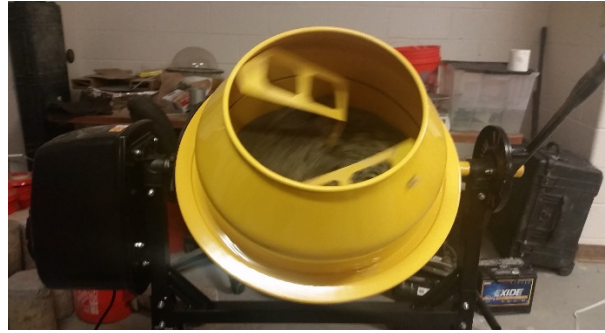
Specific gravity is the ratio of the mass of a given volume of solids or liquids to the mass of an equal volume of water at a specified temperature. The specific gravity test was conducted by using the Tex-108-E guideline for the materials passing a No. 40 sieve.

### 3.7 Specimen Preparation

The specimens were prepared at optimum moisture content (OMC) and compacted at maximum dry density (MDD). Sample preparation steps are included in Figure 3.4.



(a)



(b)



(d)



(e)



(f)



(g)



(h)



(i)

Figure 3.4 Sample preparation for UCS and resilient modulus test



Figure 3.5 Preservation of samples in humidity room for curing

### 3.8 Unconfined Compression Test

The unconfined compression tests were conducted in accordance with the Tex-120-E TxDOT specification. Specimens were prepared as described in the previous section, in accordance with TxDOT's specification. The 6-inch diameter and 8-inch high samples were cured for seven days in a moist room at 70° F. After curing, the samples were placed on the platform of

a Universal Testing Machine (UTM) and loaded at a constant rate. The strain rate applied was  $2.0 \pm 0.3\%$  to maintain a constant deformation rate on the specimen. The setup of the UTM is shown in the following figure.



Figure 3.6 Universal testing machine (UTM)

Compressive strength is determined by the maximum axial load at which the sample fails. This strength usually depends on the interlocking and cohesion of the particles.

Three samples were tested to maintain the repeatability for each combination, at 0%, 2%, 4% and 6% cement dosages. The UCS test is one of the simplest and most important tests used to determine the modulus of elasticity, but it is not the representative of the performance of base materials under tensile stress (Ordonez 2006). It is useful, however, in evaluating the changes in stiffness of various combinations of RCCA & RAP materials at cement contents of 0%, 2%, 4% and 6%.

### 3.9 Split Tensile Strength (STS) Test

The split tensile strength (STS) test determines the tensile strength of cylindrical concrete specimens. This test was conducted by following the ASTM C496 - 11, and Tex-421-A guidelines. It consists of a diametrical compressive force applied along the length of a cylindrical concrete specimen, at a rate that is within a prescribed range until failure occurs (ASTM C496 - 11). For a particular combination of RCCA and RAP materials at a fixed cement content, three identical cylindrical specimens of 150 mm (6 inches) x 300 mm (12 inches) were prepared and cured according to AASHTO T 307-99 guidelines. After seven days of curing at 76°F in a moist room, following Tex-421-A test procedures (Figure 3.7 and Figure 3.8), splitting tensile strength tests were conducted. A loading rate of 100 psi/min was applied until failure of the specimen, and the maximum applied load was recorded as tensile strength (ASTM C496 – 11; and Tex-421-A).



Figure 3.7 Positioned specimen in a testing machine for split tensile strength test



Figure 3.8 Failed specimen

### 3.10 Resilient Modulus ( $M_r$ ) Tests

Resilient modulus ( $M_r$ ) is a key parameter for pavement layer thickness design. This test was conducted using the AASHTO T 307-99 guidelines (AASHTO 2003).

#### 3.10.1 Specimen Preparation for Testing

To prepare the specimens, crushed concrete aggregates (RCCA) and RAP materials were obtained from different sources and were used individually or in mixes at different percentages. The materials were tested for resilient modulus, with or without stabilization, using cement. Repeatability of the tests was ensured by replicating three specimens for each RCCA, RAP, and cement combination. All of the specimens were 6 inches in diameter and 12 inches in height.

All of the specimens were subjected to compaction at optimum moisture content to achieve the maximum dry density from the moisture-density test results. Samples were compacted at 6 lifts, with each lift having a height of 2 inches and being subjected to 50 blows. The height of each lift was controlled by the automatic compactor itself. The maximum size of the particle was limited to 1.2 inch, which was one-fifth of the maximum diameter of the mold. The density of the

compacted specimens was within +/-5% of the maximum dry density, signifying the attainment of satisfactory compaction.

The procedure stated above was used to prepare the specimens of RCCA, RAP, and different combinations of these materials with or without stabilization. The test specimens were extracted from the mold by using the extruder, and were then wrapped with plastic to avoid any disturbance and stored in the moist room for curing for seven days. The moist room had a controlled relative humidity of about 100% and a constant temperature of 70° F during the curing period of seven days. After seven days, the specimens were tested for their resilient modulus.

### *3.10.2 Resilient Modulus Testing Equipment*

The resilient modulus of the compacted specimens was determined by using the automated system, which meets the AASHTO T307-99 requirements. The system consists of two major components: a fully automated unit, and a computerized data acquisition system. The automatic unit consists of two LOADTRAC units, one Cyclic-RM unit, a load frame, an actuator, a triaxial cell, two linear variable displacement transducers (LVDT), and an electro-pneumatic air pressure controlling unit.

The cyclic load was applied by using a cyclic-RM unit with Haversine pulse. The load pulse was applied for 0.1s, and the rest period was 0.9s. The actuator consists of a load cell, the capacity of which is 1000 lbf and applies up to 40 psi stress on 6 inches diameter and 12 inch high cylindrical specimens. Confining pressure was applied by an electro-pneumatic air pressure regulator. This regulator can increase air pressure automatically in the triaxial chamber. The axial deformation of the sample was measured from the outside, using two LVDTs attached to the piston rod at equal distance and opposite to each other.

RM6 software was installed to give initial inputs and data acquisition during the test. As the sample became stiffer with time during the test, the system controller maintained the load and

corrected it to meet accurate values. The equipment setup used to perform the resilient modulus tests is shown in Figure 3.9. Confining pressure was applied by controlled air pressure. Two types of loading sequences are specified in AASHTO T307-99, subgrade soil and base materials, to simulate traffic conditions in pavement foundations. The amount of applied stress is higher for granular-base or sub-base material than for subgrade soil. The first loading sequence is preconditioning, which consists of 500 to 1000 cycles. In this study, 500 cycles were selected for preconditioning. After preconditioning, the total load is applied in 15 load sequences, with each load sequence containing 100 cycles, in accordance with the AASHTO T307-99 code. This test was conducted on all of the treated and untreated combinations of RCCA and RAP materials.

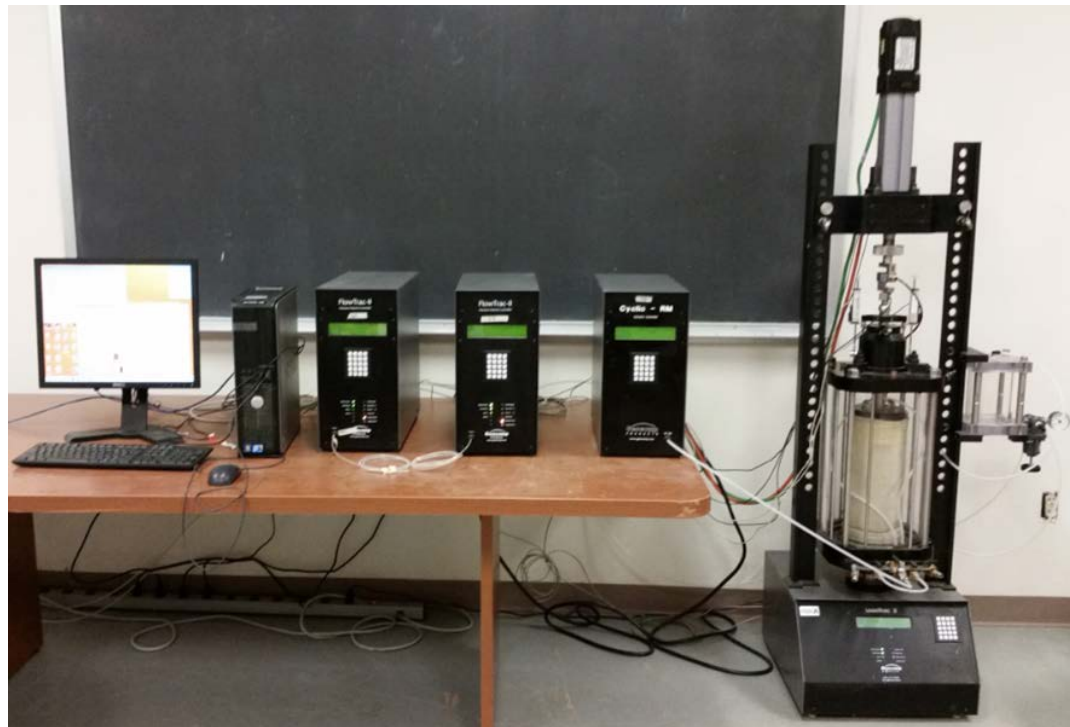


Figure 3.9 Resilient modulus testing machine

The test sequences for resilient modulus testing, according to AASHTO T307-99, are listed in Table 3.7.

Table 3.7 Resilient Modulus Test Sequences and Stress Values for Base and Subbase Materials  
(AASHTO T307-99)

Sequence No.	Confining Pressure (psi)	Max. Axial Stress (psi)	No. of Cycles
Pre-conditioning	15	15	500-1000
1	3	3	100
2	3	6	100
3	3	9	100
4	5	5	100
5	5	10	100
6	5	15	100
7	10	10	100
8	10	20	100
9	10	30	100
10	15	10	100
11	15	15	100
12	15	30	100
13	20	15	100
14	20	20	100
15	20	40	100

### 3.10.3 Data Analysis of Resilient Modulus Tests

The resilient moduli of each load sequence under different confining and deviator stresses was calculated in accordance with the AASHTO T307-99 code. The RM6 software automatically generated the resilient modulus vs bulk stress graph and the test result chart. Each value of  $M_r$  is the average of the last five cycles. The displacement results obtained from two LVDTs were averaged and divided by the specimen height to determine the accumulated strain of each reading. The difference between the maximum axial strain and the last axial strain in the 200 axial strains of each load cycle is the resilient strain of this load cycle (Li 2011). Axial stress is determined by dividing the load by the area of the specimen. Cyclic stress is the difference between the maximum axial stress and minimum axial stress in 200 readings for each load application. Resilient modulus of each load cycle is calculated by dividing the cyclic stress by the resilient strain. According to AASHTO test procedure requirements, the obtained resilient modulus

data was used to develop prediction models. One of them was the “k- $\theta$  model” proposed by Moosazedh and Witczak (1981).

$$M_r = k_1 \theta^{k_2}$$

Where  $k_1$  and  $k_2$  are model parameters and  $\theta$  is the bulk stress expressed as a combination of confining ( $\sigma_c$ ) and deviator stresses ( $\sigma_d$ ) in the form  $3\sigma_c + \sigma_d$ . The other model that was used in this study is the improved three-parameter model.

$$M_r = k_3 \sigma_c^{k_4} \sigma_d^{k_5}$$

Where  $k_3$ ,  $k_4$  and  $k_5$  are model parameters. Statistical analysis was conducted to examine the accuracy of these models.

### 3.11 Leaching Tests

Leachate tests were conducted on selected combinations of RCCA and RAP materials untreated or treated with cement. Leachate tests included pH, total dissolved and suspended solids, turbidity, and chemical oxygen demand.

#### 3.11.1 pH Test

The pH test measures acidity, and was conducted in accordance with ASTM D1287. The value of pH ranges between 0 to 14, and 7 is considered as the neutral value. A value less than 7 is considered acidic, and higher than 7 is considered alkaline. The value of pH was measured by using a dual channel pH conductivity meter device, depicted in Figure 3.10. The pH test was conducted by inserting the probe into the leachate sample that had been collected after soaking in water for 24 hours.



Figure 3.10 Dual channel pH/ion/conductivity meter

### 3.11.2 Total Suspended and Dissolved Solids (TSS & TDS)

Dissolved and suspended solids tests were conducted according to the ASTM D 5907-03 specification, Standard Test Method for Filterable and Non-Filterable Materials. Glass fiber filter paper was used to remove the suspended solids by passing the water sample through the filter. Suspended solids were retained on the filter paper, whereas filtrates were passed through the filter paper.

### 3.11.3 Turbidity

Turbidity was measured, using a 2100P Turbidimeter (Figure 3.11). The number of particles present in water represents turbidity. It is measured by passing a light through the sample.



Figure 3.11 2100P Turbidimeter

#### 3.11.4 Chemical Oxygen Demand (COD)

According to the ASTM D 1252 specification, a test method was conducted to determine the amount of oxygen that was consumed by the impurities in the water. A transmittance vs concentration of COD was calibrated, and calibration curve was produced. Then the samples were poured into COD vials and heated for two hours, as a digester period, in the COD reactor (Carlos 2006) (Figure 3.12).



Figure 3.12 COD reactor

Then the vials were removed from the digester and cooled to room temperature for about 20 minutes. The vials were then inserted into the digital reactor, and the value of transmittance and absorbance readings were taken from the device.

### 3.12 Durability Tests

Wetting-drying cycles were applied to the prepared specimens in accordance with the test plan indicated in Table 3.4 and by following the procedure described in a study conducted by Khoury and Zaman in 2002. RCCA and RAP materials mixed in 50%-50% proportions and stabilized with 4% (MIX 4) and 6% (MIX 6) cement content were used for this purpose (Saif et al. 2017). For each of the material combinations, three “control samples” and three “test samples” were prepared, cured for 7 days, and then tested for resilient modulus according to AASHTO T 307-99 test procedures. Specimens were then subjected to wetting-drying (W-D) cycles. Each W-

D cycle consisted of drying the sample in the oven (71°C/160°F) for 24 hours, followed by submerging it in potable water for 24 hours. In this study, the number of wetting-drying cycles considered were 0, 4, 8, 16, and 30. Resilient modulus ( $M_r$ ) tests were conducted on the specimens after completion of the specified number of wetting and drying cycles. The control samples were cured by following the conventional process in a moist room. After curing for 15, 25, 40, and 70 days, which matched with the end time of the specific number of wet-dry cycles, the samples were tested again for  $M_r$ . In this study, each sample was subjected to multiple resilient modulus tests after specific times. This approach was considered reasonable since resilient modulus tests involve very low levels of strain (Khoury and Zaman, 2007).



(a)



(b)

Figure 3.13 Specimens subjected to wetting



Figure 3.14 Specimens subjected to drying

## Chapter 4

### Results and Analysis

#### 4.1 Introduction

Particle size distribution, optimum moisture content and maximum dry density, unconfined compressive strength, and resilient modulus test results are included in this section. These test results are compared with respect to the amount of RAP materials added into the mix, cement content, etc.

#### 4.2 Particle Size Distribution

The quantitative determination of the distribution of the particle sizes in the aggregates was determined by using the sieve analysis method, as per the Tex-110E specification. Sieve sizes used for the analysis were in accordance with the standard specifications. If less than 1% of the materials passed through the No. 200 sieve, then hydrometer analysis was not required.

A specified amount of materials was poured through the sieve apparatus. The weight of materials retained on each sieve was determined prior to calculating the percentage of materials passing through each sieve. The percentage of the materials retained on each sieve was obtained by dividing the weight of material retained on each sieve by the total weight of the sample. The amount of material that passed through each sieve was calculated by deducting the percentage retained on each sieve from 100%. The percent of materials that passed through each sieve was plotted against the sieve size on a semi-log graph. Figure 4.1 shows the grain size distribution curves of the RAP 1, RAP 2, RAP 3, RCCA 1, RCCA 2 and RCCA 3 materials. The coefficient of curvature ( $C_c$ ) and coefficient of uniformity ( $C_u$ ) were calculated from gradation curves and are shown in Table 4.1. Bulk specific gravity for coarse aggregate materials obtained from different sources was also determined in accordance with AASHTO T 85 guidelines. Maximum size of the aggregate was limited to 1 inch (25 mm) to ensure proper compaction and homogeneity of the test samples.

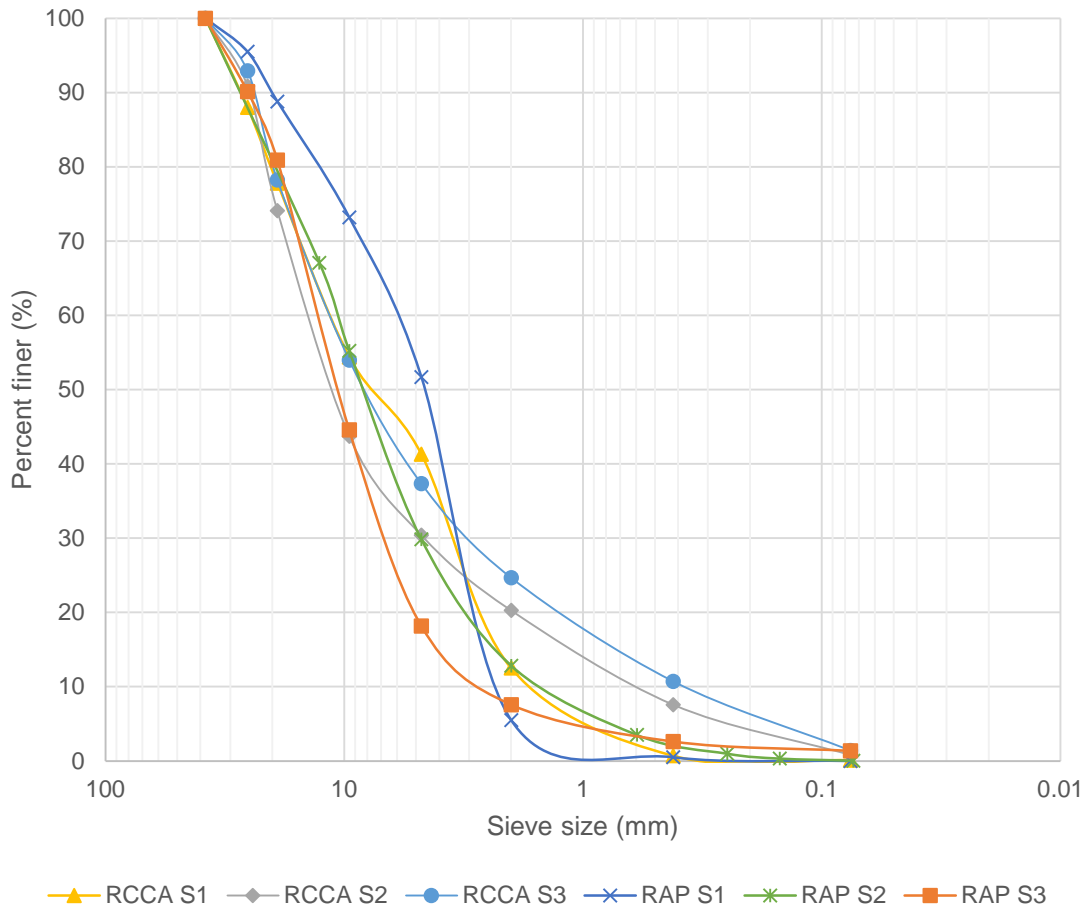


Figure 4.1 Particle size distribution of recycled base materials

Table 4.1 Material Properties

Parameters	RCCA 1	RCCA 2	RCCA 3	RAP 1	RAP 2	RAP 3
Coefficient of Curvature, $C_c$	0.60	2.42	2.03	0.93	1.21	1.17
Coefficient of Uniformity, $C_u$	6.67	26.89	32.43	2.29	6.97	4.67
Dry Specific Gravity	1.99	2	1.95	1.9	1.93	1.9

#### 4.3 Asphalt Content in RAP

RAP materials are covered with asphalt. The amount of asphalt content has a significant effect on the bonding of the RAP materials when used only as 100% RAP materials or in combination with RCCA and treated with cement. Asphalt content was determined by using the ignition method, as specified by Tex-236 F guidelines, in the TxDOT laboratory facility. The mean value of asphalt content for three different sources were 3.5%, 6.4%, and 4.7%. Test results are depicted in Table 4.2.

Table 4.2 Asphalt Content Test Results

Source	Material ID	Average Asphalt Content (%)
1	RAP 1	3.5
2	RAP 2	6.4
3	RAP 3	4.7

#### 4.4 Moisture-Density Tests

Optimum Moisture Content (OMC) is the moisture content at which compaction of a certain material yields its maximum dry density (MDD). In this study, OMC and MDD tests were conducted on each of the material combinations at different cement contents, following the Tex-113 E guidelines, as shown in Table 3.2. Compaction energy required for compaction is 13.25 ft-lb/in<sup>3</sup>. The molds were 6 inches in diameter and 8 inches in height. The compaction tests were performed on specimens of at least four different moisture contents, and the dry density was determined for different moisture contents. The obtained dry densities were plotted against the moisture contents, and the optimum moisture contents were determined from the peak of the trend

curve. The values obtained for different combinations of base materials are shown in Figure 4.2 to Figure 4.5.

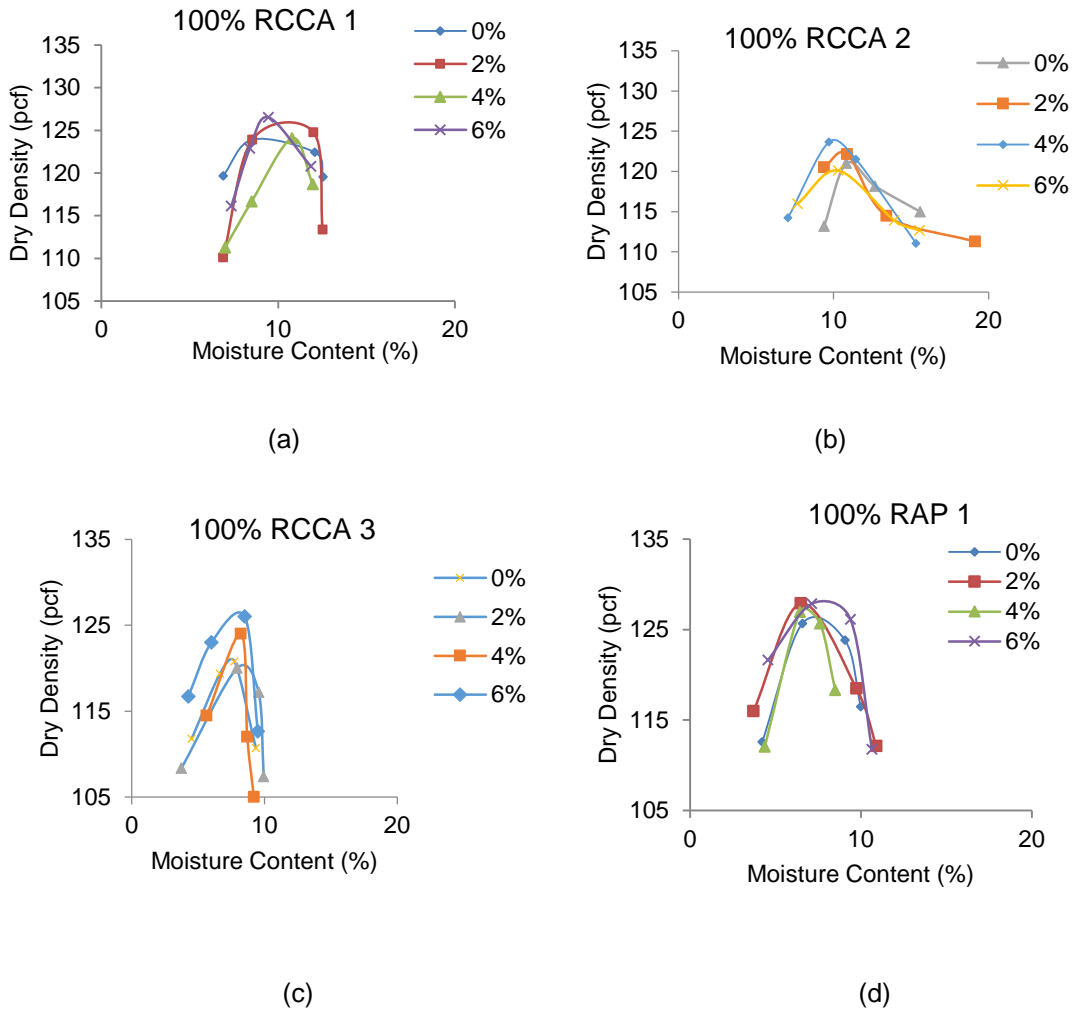
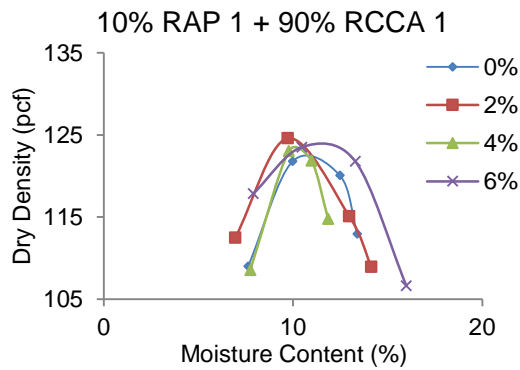
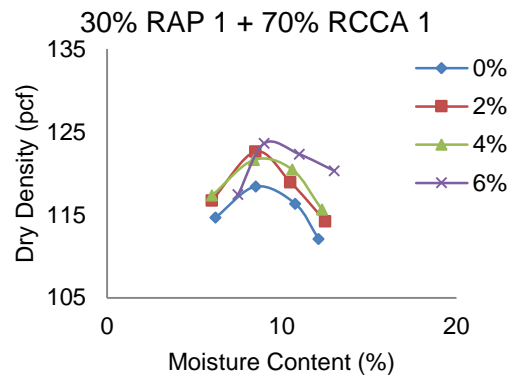


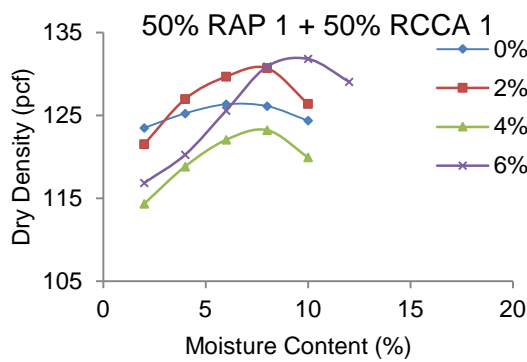
Figure 4.2 OMC and MDD determination of (a) 100% RCCA 1, (b) 100% RCCA 2, (c) 100% RCCA 3, and (d) 100% RAP 1 materials for 0, 2, 4, & 6% cement content



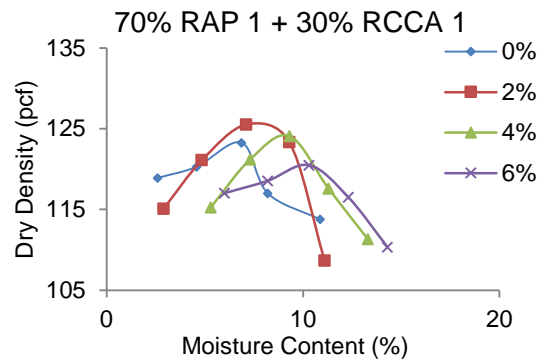
(a)



(b)



(c)



(d)

Figure 4.3 OMC and MDD determination of (a) 10% RAP 1-90% RCCA 1, (b) 30% RAP 1-70% RCCA 1, (c) 50% RAP 1-50% RCCA 1, (d) 70% RAP 1-30% RCCA 1 Materials for 0, 2, 4, & 6% cement content

The value of the optimum moisture content varied about 10%, with maximum dry density values ranging from 120-128 pcf. This indicates that the addition of RAP had no significant effect on the optimum moisture content or maximum dry density of the material mixes. Previous studies showed that similar gradation of RAP and RCCA materials yielded similar values of OMC and MDD (Faysal et. al., 2016). Guerrero (2004) reported that OMC and MDD of soil are highly effected

by particle size of the soil, especially the fines fraction. The RCCA and RAP materials used in this study had identical grain size distribution and low fines fractions, as shown in Figure 3.1. Test specimens for all of the laboratory tests were prepared at the optimum moisture content and maximum dry density obtained from the OMC and MDD tests.

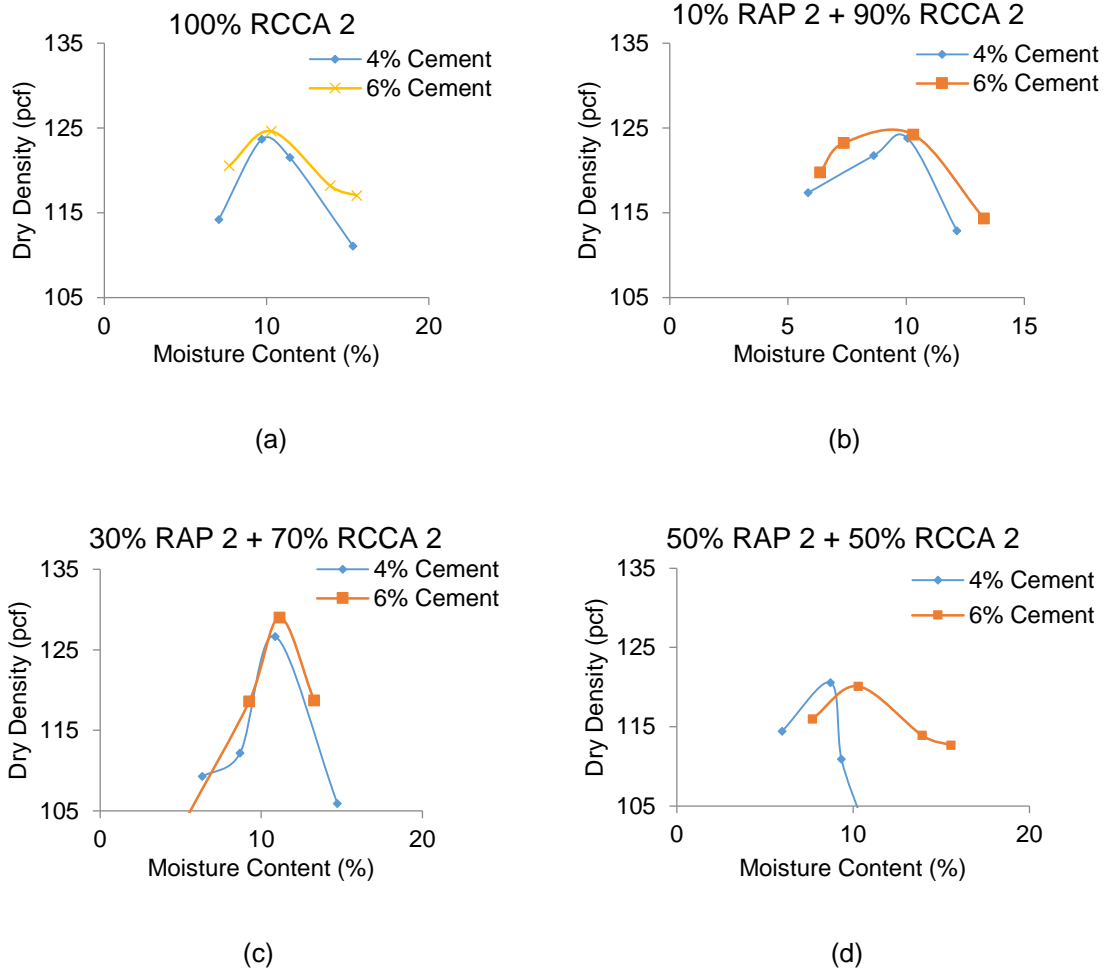


Figure 4.4 OMC and MDD determination of (a) 100% RCCA 2, (b) 10% RAP 2-90% RCCA 2, (c) 30% RAP 2-70% RCCA 2, (d) 50% RAP 2-50% RCCA 2 Materials for 4, & 6% cement content

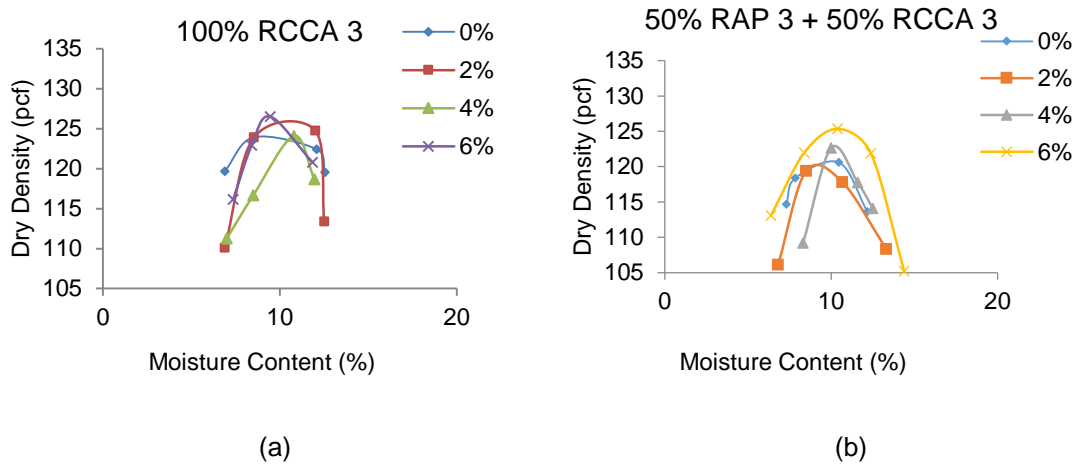


Figure 4.5 OMC and MDD determination of (a) 100% RCCA 3 (b) 50% RAP 3 +50% RCCA 3 Materials for 0, 2, 4, & 6% cement content

#### 4.5 Specimen Preparation

TxDOT guideline (Tex- 113 E) was followed for specimen preparation. The mold used to prepare the UCS samples was 6 in. (152.4 mm) in diameter and 8 in. (203.2 mm) in height; for the resilient modulus test, the mold height was 12 in. (254 mm). An automated mechanical compactor which met the TxDOT specifications was used for compacting. Prior to testing, the prepared specimens were kept in a moist room for seven days, in accordance with the soil-cement testing procedure (Tex- 120 E). The steps followed for the specimen preparation are shown in Figure 3.4.

#### 4.6 Unconfined Compressive Strength Test Results

The prepared 6 inch x 8 inch samples were tested in the compression testing machine in the UTA structures lab after seven days of curing. Three identical specimens were tested at different cement contents for each combination of material mixes obtained from three different sources. The average value of the three specimens was plotted in a figure to show the variation with change in cement content. All of the test results are included in the Appendix.

Lower standard deviation (SD) and coefficient of variation (COV) were observed at higher, rather than lower, cement content. This might have contributed to the better bonding matrix between the aggregate particles, which led to less variation in strength among different specimens.

Standard deviation and coefficient of variance increases with an increase in RAP content at a particular cement content. This trend was observed in all three sources of materials.

The results obtained from the tests are shown in Figure 4.6. As depicted in Figure 4.6, the unconfined compressive strength (UCS) of recycled base materials obtained from different sources decreased with an increase in the amount of RAP. The UCS decreased by about 12%, with a 50% to 70% increase in RAP content.

As per TxDOT design guidelines Item 276, "Cement Treatment (Plant Mixed)," for construction of pavement bases, the minimum unconfined compressive strength requirement is 300 psi. At 0% and 2% cement content, none of the combinations of the materials fulfilled the strength requirement. RCCA materials obtained from different sources met the requirement at 4% cement content. 100% RAP did not reach the 300 psi of compressive strength even at 6% cement content.

As depicted in Figure 4.6, Figure 4.7, and Figure 4.8, the compressive strength of the specimens increased significantly with inclusion of cement. 100% RCCA material met the requirement at 4% cement content, while 50% RAP + 50% RCCA combination of material met the requirement of 300 psi at 5% to 5.5% cement content. The test results signify that inclusion of RAP reduces strength.

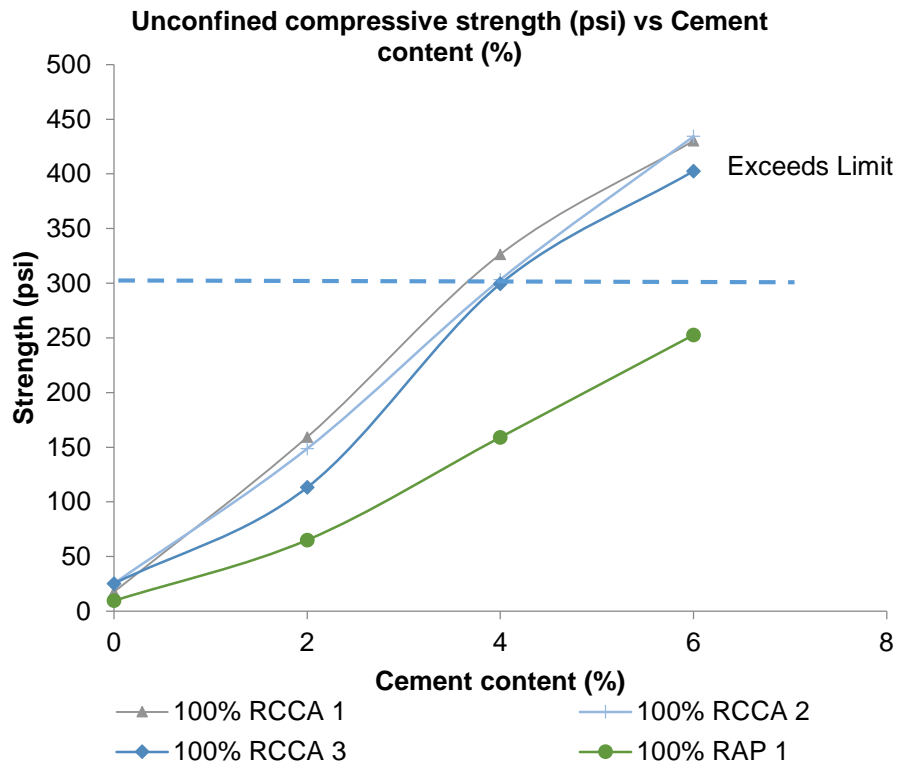


Figure 4.6 Unconfined compressive strength comparison

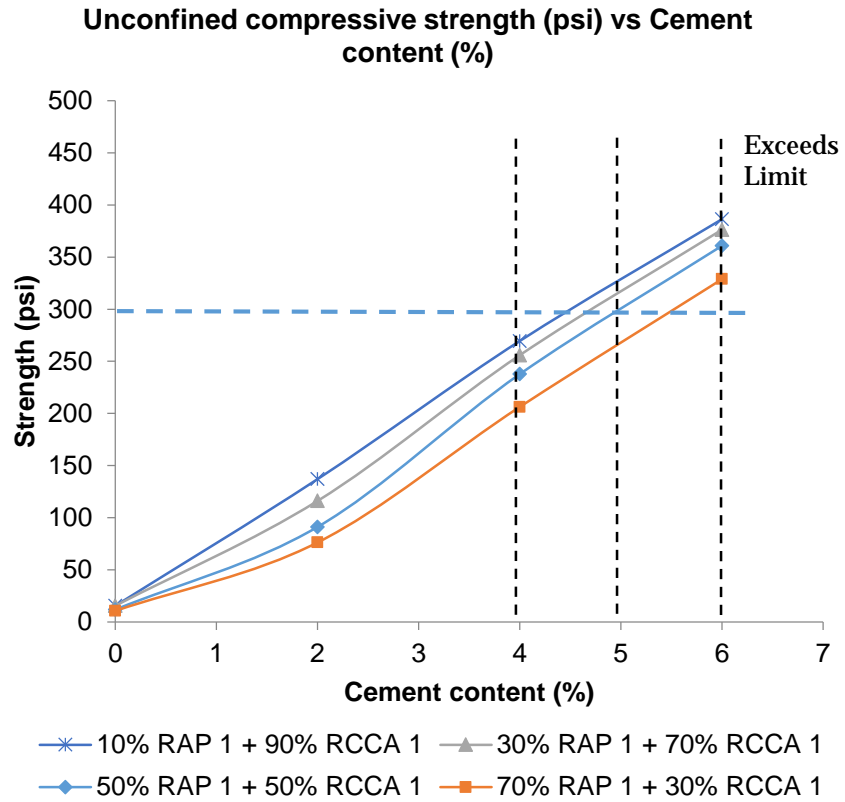


Figure 4.7 Comparison of UCS for RCCA and RAP mixes from Source 01

Table 4.3 Material Combination ID

Material Combination	ID
100% RCCA 2	M1
10% RAP 2 + 90% RCCA 2	M2
30% RAP 2 + 70% RCCA 2	M3
50% RAP 2 + 50% RCCA 2	M4

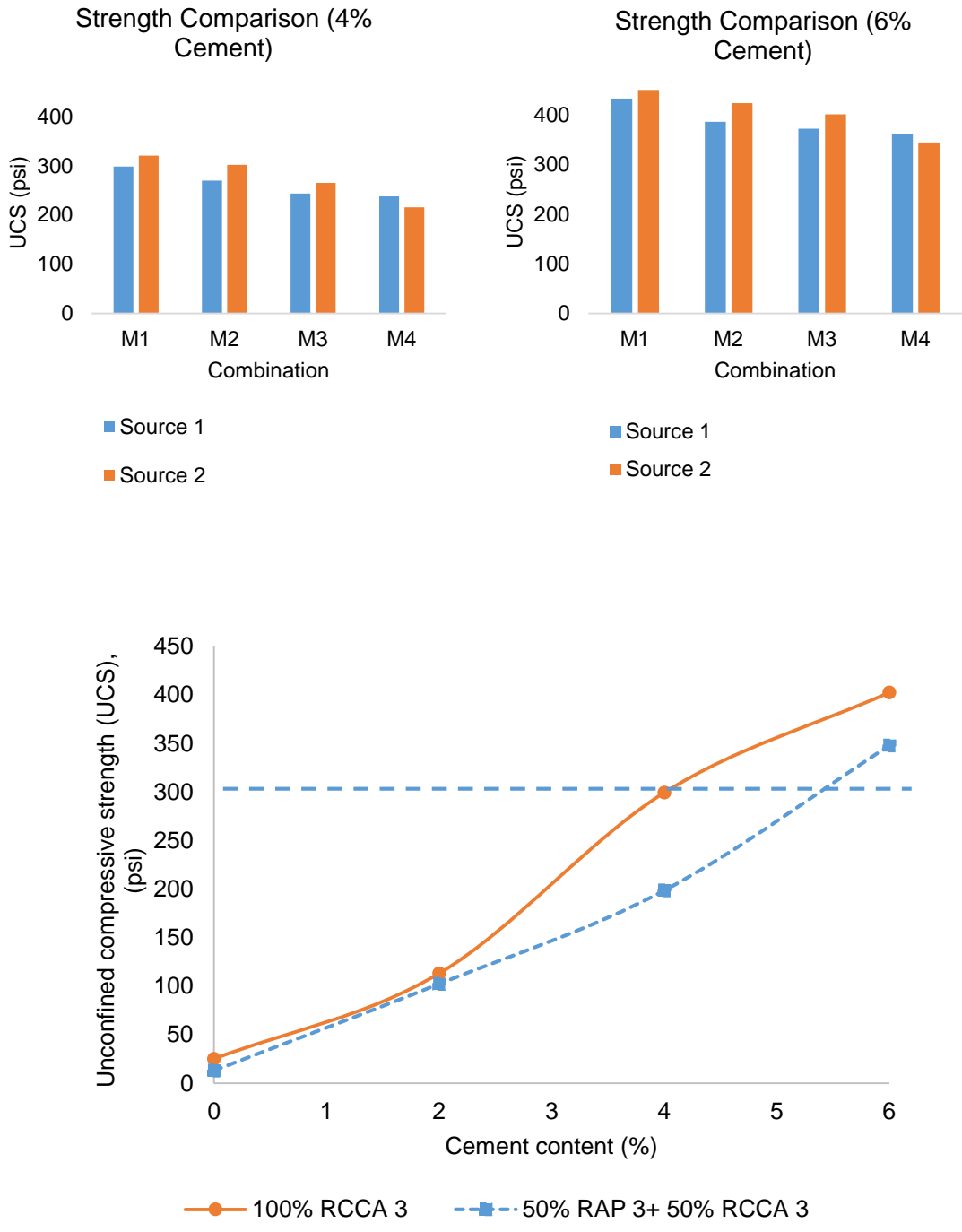


Figure 4.8 Comparison of UCS of different combinations of materials mixes from Source 03

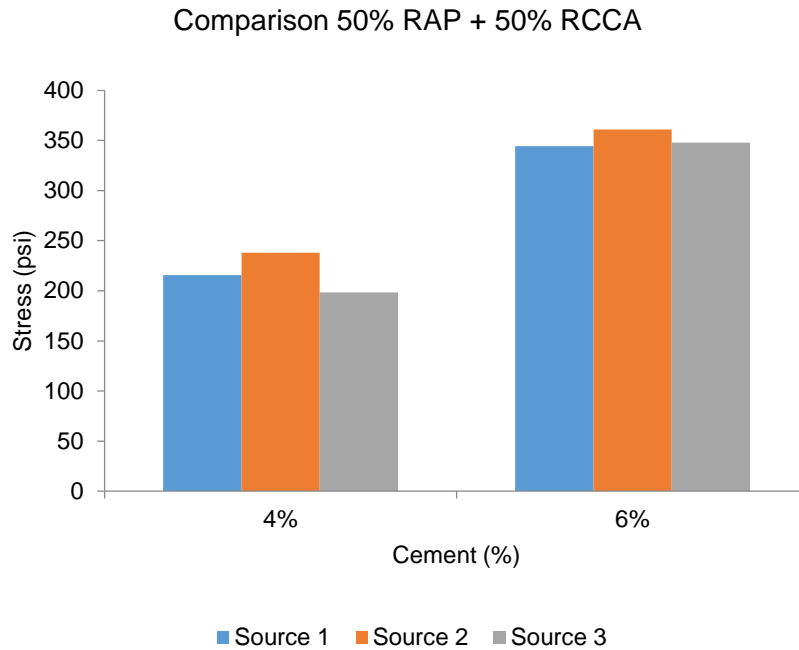
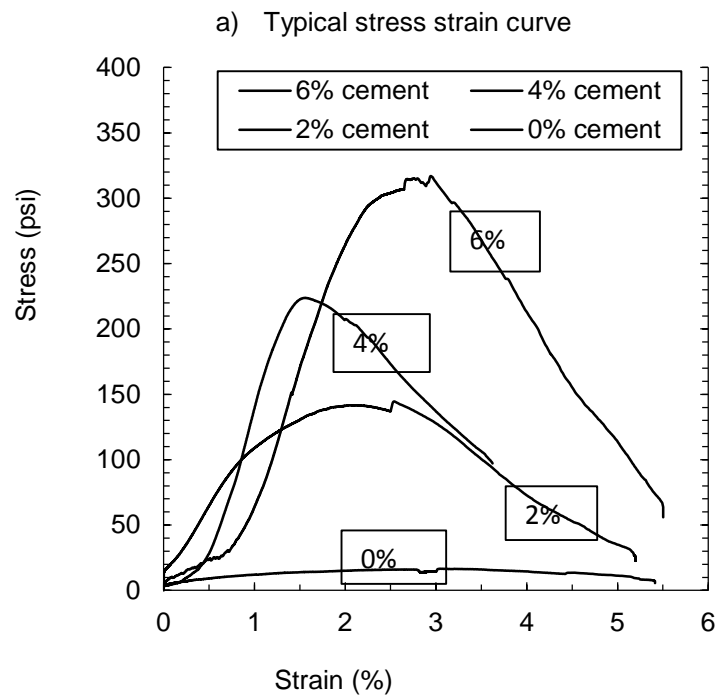
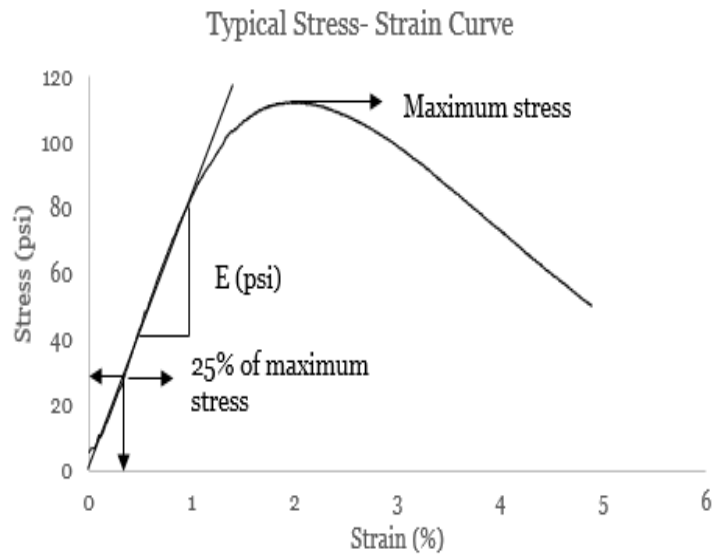


Figure 4.9 Comparison of UCS for 50% RAP + 50% RCCA combination

#### 4.7 Elastic Modulus (EM)

The modulus of elasticity of cement-stabilized RAP-RCCA blends was investigated by utilizing the strain-stress relationship obtained from the unconfined compressive strength tests. Modulus of elasticity (EM) was determined as the offset tangent modulus of the stress-strain curve. The value of elastic modulus was determined at 25% of peak/maximum stress to compare values of different combinations of recycled materials at different cement contents. A typical stress-strain curve found from the unconfined compressive strength test is presented in Figure 4.10, which indicates the non-brittle response of RAP-RCCA blends. Little variation of elastic modulus was observed for unbound mixes; whereas, inclusion of cement caused a dramatic increase of moduli values. For a fixed cement content, compressive strength tends to decrease with the increase of the RAP percentage.



b) Variation in EM with cement content

Figure 4.10 Stress-strain curves (Mahedi 2016)

The individual EM values of the three replicated tests of each combination of RAP and RCCA materials, with cement dosages from 0% to 6% at 2% intervals, are included in Appendix A.

Elastic modulus (EM) obtained from different combinations of RCCA and RAP materials at different cement contents were plotted against the corresponding UCS test results (Figure 4.11). The adjusted empirical correlation is a good estimate of elastic modulus from UCS of RCCA and RAP materials. The proposed model has a coefficient of determination ( $R^2$ ) of 0.91, which provides a good agreement with the test data. The proposed model is as follows:

$$EM_{(7 \text{ days})} = 88.89UCS_{(7 \text{ days})} + 4094.6$$

Where, EM = Elastic Modulus (psi) at 7 days and UCS = Unconfined Compressive Strength at 7 days.

Figure 4.10 shows a plot of elastic modulus (EM) for 100% RCCA and 100% RAP materials used at different cement contents. It was observed that 100% RCCA yielded higher values of EM than the 100% RAP materials at all cement contents. This shows that RCCA is a stronger aggregate than RAP. Elastic Modulus for different combinations of Source 1 RAP and RCCA materials was plotted against the cement content and is shown in Figure 4.12. It is evident that the addition of RAP has adverse effects on EM values. This effect is more significant at higher (4% and 6%) cement content than at lower (2%). Similar results are also seen for Source 3 material combinations (Figure 4.12). A drastic drop in EM values for Source 1 materials was observed for mixes containing 70% RAP at all cement contents (Figure 4.13).

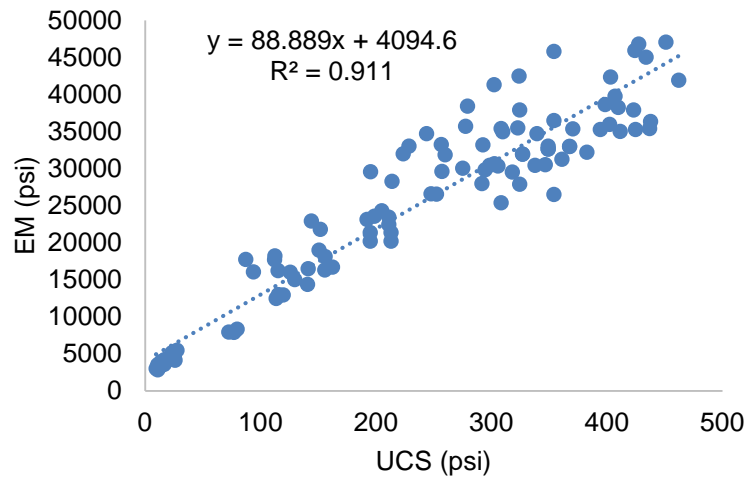


Figure 4.11 Statistical correlation between elastic modulus (EM) and unconfined compressive strength (UCS)

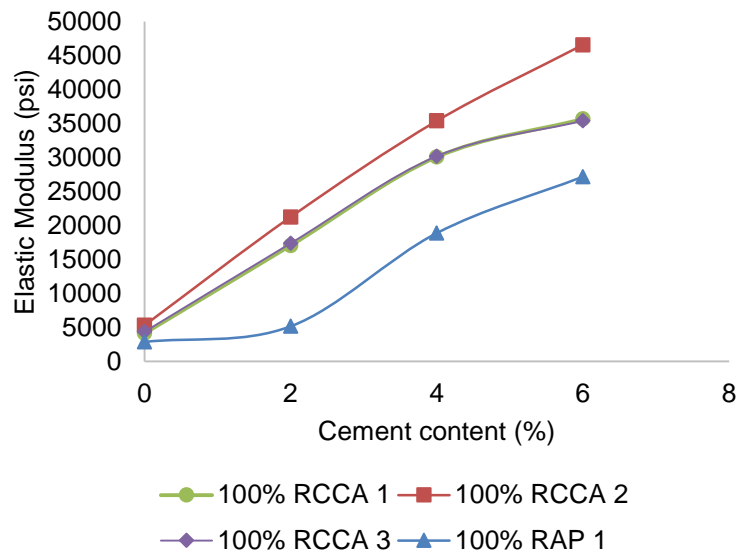


Figure 4.12 Comparison of EM for different combinations of materials

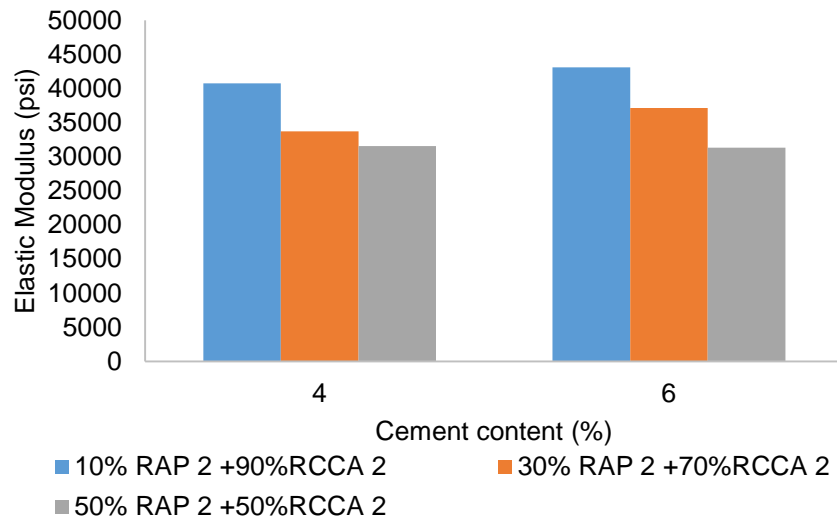


Figure 4.13 Comparison of EM for different combinations of materials at different cement contents

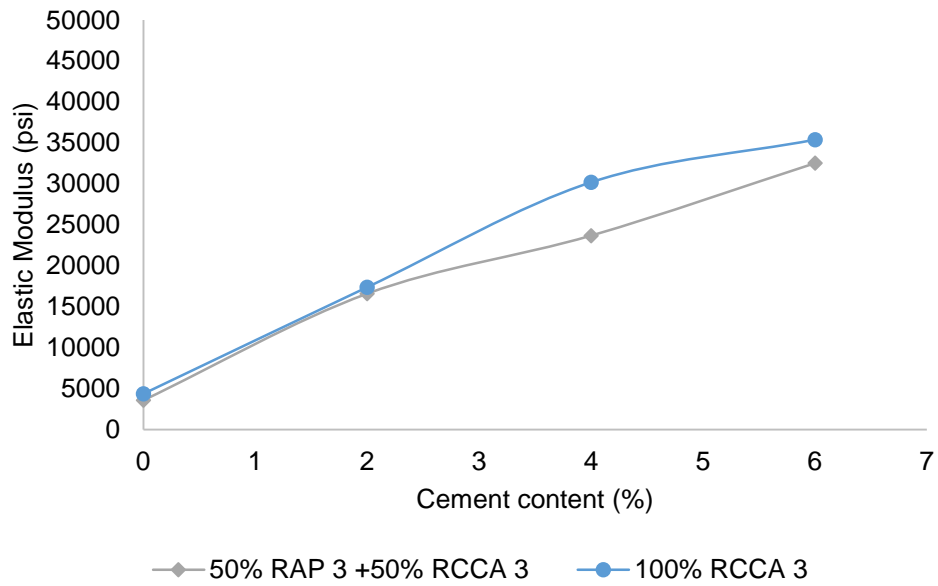


Figure 4.13 Comparison of EM for different combinations of materials at different cement contents

For Source 2 materials (Figure 4.13), the addition of 20% RAP reduced the EM values by about 21% at all cement contents. For all RAP 2 - RCCA 2 combinations, EM values increased by only 5 - 7% when cement content was raised from 4% to 6%

For all cases, an increase in cement content increased the value of the elastic modulus. However, this increase occurred in a more linear fashion for 100% RCCA materials than for 100% RAP materials (Figure 4.12). Similar results were observed for RCCA-RAP mixes, as shown in Figure 4.13. The addition of RAP resulted in a more non-linear relationship between EM and cement content. This can be attributed to the poor adhesion between cement and asphalt-coated RAP materials.

#### 4.8 Effect of Different Cement and RAP Contents

The addition of reclaimed asphalt pavement (RAP) tends to lower the unconfined compressive strength (UCS) and resilient modulus ( $M_r$ ) values of stabilized aggregate mixes (Faysal et. al., 2016a). According to the test results, the value of UCS and  $M_r$  decreases with an increase in RAP content. On the other hand, the inclusion of cement increases UCS and  $M_r$ .

##### 4.8.1 Combined Effects of Cement and RAP Content on UCS

The results obtained from the UCS tests for different combinations of materials were analyzed statistically, using the t-test, to compare and verify the significance of the effects of cement content and percentage of RAP on the strength properties. RCCA and RAP materials used in different mix combinations were obtained from different sources. For this reason, the t-test of unequal variances and groups of different combinations were analyzed to determine the effects. The values of UCS of different combinations at a particular cement content were used for comparison to conduct the statistical t-test. T-tests were performed using Microsoft Excel software. The statistical hypothesis testing utilizes p-values to determine the significance level of the test. The p-value used is usually 0.05 or 0.01. In this analysis, a p-value of 0.05 was used, which indicates that the chance of differences in average UCS occurring due to the increase in the RAP

content is less than 5% for these cement stabilized aggregates. The hypotheses used for this analyses are as follows:

Null Hypothesis,  $H_0: \mu_1 = \mu_2$  (signifies that the UCS for 100% RCCA 1 and 90% RCCA 1 +10% RAP 1 are same)

Alternative Hypothesis,  $H_1: \mu_1 \neq \mu_2$  (which shows that the UCS for 100% RCCA 1 and 90% RCCA 1+10% RAP 1 combination are different)

Where,  $\mu_1$  = mean of the UCS of 100% RCCA 1 aggregate treated with 4% cement and

$\mu_2$  = mean of the UCS of 90% RCCA 1 + 10% RAP 1 aggregate treated with 4% cement

The effect of RAP percentage in a combination can be explained if any significance difference is found in UCS. On the other hand, if no significant difference is found, the RAP content does not have any significant effect on UCS. Statistical analysis was conducted to determine the effect of cement content on resilient moduli of the aggregate specimens.

Null Hypothesis,  $H_0: \mu_1 = \mu_2$  (signifies that the UCS for 100% RCCA at 4% and 6% cement content are same)

Alternative Hypothesis,  $H_1: \mu_1 \neq \mu_2$  (which shows that the UCS for 90% RCCA+10% RAP at 4% and 6% cement content are different)

Where,  $\mu_1$  = mean of the UCS of 100% RCCA 1 aggregate treated with 4% cement and

$\mu_2$  = mean of the resilient modulus of 100% RCCA 1 aggregate treated with 6% cement content.

The effect of cement content in different combinations can be explained based on the significance level found from the statistical analyses. The results of the t-test analyses are included in Table 4.5, Table 4.6, and Table 4.7.

Table 4.4 T-Test Results for Effect of Cement Content on UCS (Source 1)

Source 1 Material Combination		Cement Content (%)	Factor	p-value	Significant
RCCA (%)	RAP (%)				
100	0	0 & 2	Cement Content	0.00030	Yes
90	10		Cement Content	0.00064	Yes
70	30		Cement Content	0.00034	Yes
50	50		Cement Content	0.0094	Yes
100	0	2 & 4	Cement Content	0.00008	Yes
90	10		Cement Content	0.00034	Yes
70	30		Cement Content	0.00092	Yes
50	50		Cement Content	0.00155	Yes
100	0	4 & 6	Cement Content	0.00207	Yes
90	10		Cement Content	0.00169	Yes
70	30		Cement Content	0.00005	Yes
50	50		Cement Content	0.00388	Yes

Table 4.5 T-Test Results for Effect of Cement Content on UCS (Source 2)

Source 2 Material Combination		Cement Content (%)	Factor	p-value	Significant
RCCA (%)	RAP (%)				
100	0	0 & 2	Cement Content	0.00009	Yes
90	10		Cement Content	0.00016	Yes
70	30		Cement Content	0.00035	Yes
50	50		Cement Content	N/A	Yes
100	0	2 & 4	Cement Content	0.00062	Yes
90	10		Cement Content	0.00715	Yes
70	30		Cement Content	0.00092	Yes
50	50		Cement Content	0.00155	Yes
100	0	4 & 6	Cement Content	0.00416	Yes
90	10		Cement Content	0.01557	Yes
70	30		Cement Content	0.00005	Yes
50	50		Cement Content	0.00387	Yes

Table 4.6 T-Test Results for Effect of Cement Content on UCS (Source 3)

Source 3 Material Combination		Cement Content (%)	Factor	p-value	Significant
RCCA (%)	RAP (%)				
100	0	0 & 2	Cement Content	0.00027	Yes
50	50		Cement Content	0.01679	Yes
100	0	2 & 4	Cement Content	0.00037	Yes
50	50		Cement Content	0.01776	Yes
100	0	4 & 6	Cement Content	0.00614	Yes
50	50		Cement Content	0.00111	Yes

It is evident that for all cement contents, 50-50% RAP - RCCA mixes have lower values of UCS than those developed for 100% RCCA mixes. The increase in UCS with an increase in cement content is statistically significant for all combinations of RAP and RCCA materials. Inclusion of cement improves the bonding matrix between aggregates and fine particles, which ensures better load transfer and provides higher strength. RCCA aggregates contain cementitious fine particles which create a bond with cement particles, resulting in higher compressive strength, with inclusion of cement content as high as 6%. 100% RCCA is a homogeneous mixture with cement and creates better interlocking between particles. On the other hand, the addition of RAP to the aggregate blend reduces the compressive strength because its particles are asphalt-coated, which develops a slip surface. The amount of fine particles in RAP aggregates is relatively less, as they are glued with the coated asphalt on the surface. For this reason, RAP particles create a weaker bond with cement than the RCCA particles.

Table 4.7 T-Test Results for Effect of RAP Content on UCS (Source 1)

Material Combination RCCA (%) – RAP (%)		Cement Content (%)	Factor	p-value	Significant
100-0	90-10	0	RAP Content	0.00147	Yes
90-10	70-30		RAP Content	0.05673	No
70-30	50-50		RAP Content	0.08911	No
50-50	30-70		RAP Content	0.42265	No
100-0	90-10	2	RAP Content	0.02183	Yes
90-10	70-30		RAP Content	0.06241	No
70-30	50-50		RAP Content	0.08859	No
50-50	30-70		RAP Content	0.22049	No
100-0	90-10	4	RAP Content	0.00497	Yes
90-10	70-30		RAP Content	0.01074	Yes
70-30	50-50		RAP Content	0.30024	No
50-50	30-70		RAP Content	0.19628	No
100-0	90-10	6	RAP Content	0.04593	No
90-10	70-30		RAP Content	0.21458	No
70-30	50-50		RAP Content	0.37736	No
50-50	30-70		RAP Content	0.00510	Yes

Table 4.8 T-Test Results for Effect of RAP Content on UCS (Source 2)

Material Combination RCCA (%) – RAP (%)		Cement Content (%)	Factor	p-value	Significant
100-0	90-10	0	RAP Content	0.00187	Yes
90-10	70-30		RAP Content	0.10894	No
70-30	50-50		RAP Content	N/A	No
100-0	90-10	2	RAP Content	0.02476	Yes
90-10	70-30		RAP Content	0.02345	Yes
70-30	50-50		RAP Content	0.08859	No
100-0	90-10	4	RAP Content	0.87841	No
90-10	70-30		RAP Content	0.15818	No
70-30	50-50		RAP Content	0.18328	No
100-0	90-10	6	RAP Content	0.6083	No
90-10	70-30		RAP Content	0.07094	No
70-30	50-50		RAP Content	0.00402	Yes

UCS decreases with an increase in RAP content in aggregate blends; however, statistical tests suggest that for most cases, the change in UCS is insignificant. For aggregate blends which contain more than 30% RAP materials, the minimum compressive strength requirement of 300 psi can only be reached at cement content that ranges from 5% to 6%. RAP materials obtained from Source 1 can be mixed as high as 70% with RCCA material. However, RAP materials obtained from Source 2 contained more than 6% asphalt content, which could not be blended with RCCA for percentage of RAP as high as 70%, even at 6% cement content. For 70% RAP + 30% RCCA blend, the minimum strength requirement can barely be fulfilled at 6% cement content. If RAP contains more than 6% asphalt, the blend of 70% RAP with 30% RCCA is not possible. The presence of fine particles in RCCA and cement content as high as 6% is not enough to neutralize the effect of asphalt coating over the RAP aggregates and develop sufficiently strong bonds between particles. Based on these facts, the percentage of RAP mixed in the RAP- RCCA blend was limited to 50%.

Table 4.9 T-Test Results for Effect of RAP Content on UCS (Source 3)

Material Combination RCCA (%) – RAP (%)		Cement Content (%)	Factor	p-value	Significant
100-0	50-50	0	RAP Content	0.00447	Yes
100-0	50-50	2	RAP Content	0.46343	No
100-0	50-50	4	RAP Content	0.000897	Yes
100-0	50-50	6	RAP Content	0.01134	Yes

#### 4.9 Resilient Modulus Test Results

The resilient modulus response of treated and untreated samples for different combinations is shown in Figure 4.16 to Figure 4.21. It was found that both the confining and deviator stresses have noteworthy effects on resilient modulus response. At higher confinements, samples become denser and hence stronger, which contributes to the increase of the resilient modulus. At a constant confining pressure, the resilient modulus increases with an increase of deviator stress, as the samples yield lower axial strain due to strain hardening, though the influence of deviator stress is less pronounced at higher confinements.

Moduli values also increased considerably with the increasing percentage of cement content at every confinement. It was found that RCCA materials are superior to RAP in terms of resilient modulus, yielding minimum values for mix 100% RAP and maximum for mix 100% RCCA.

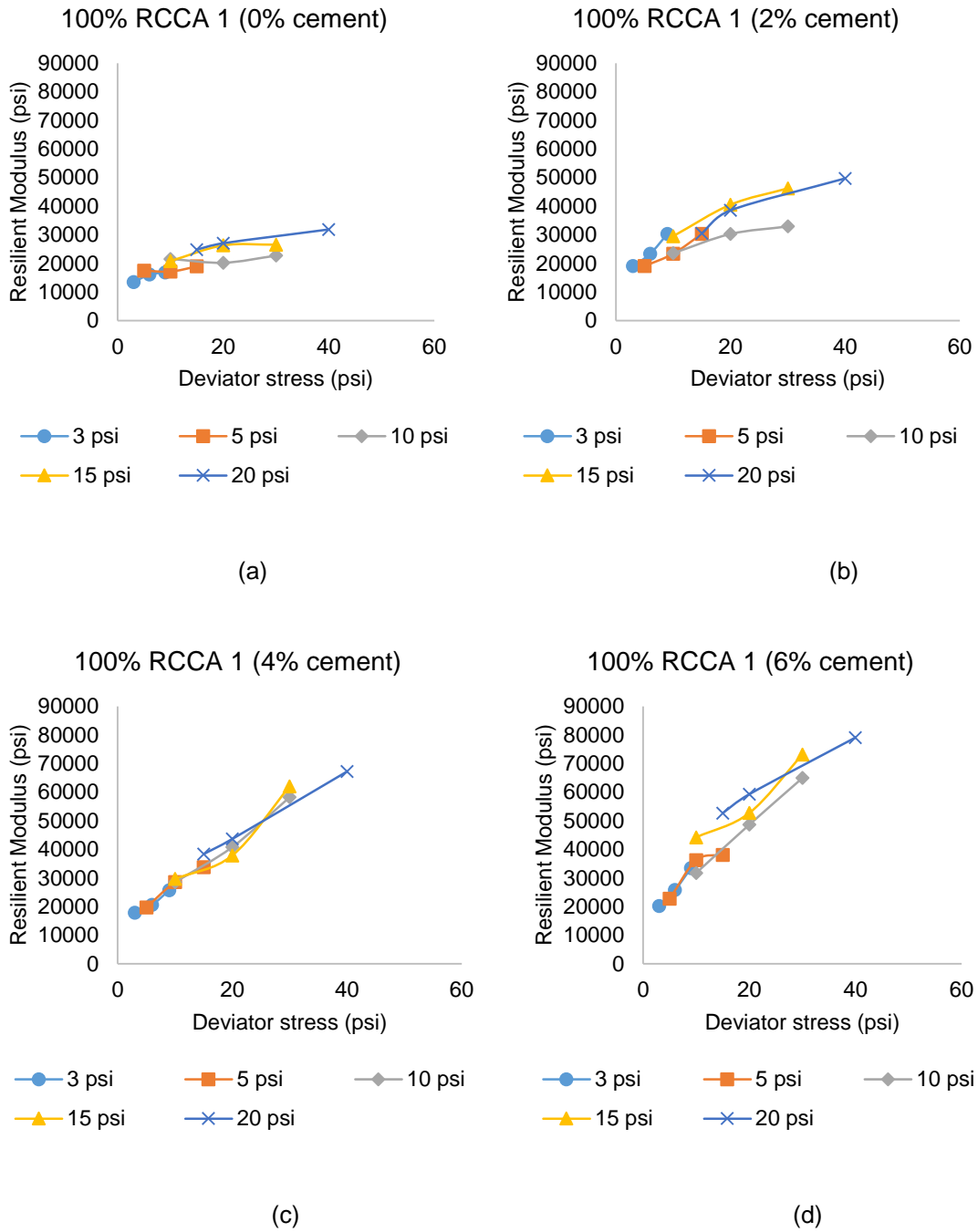
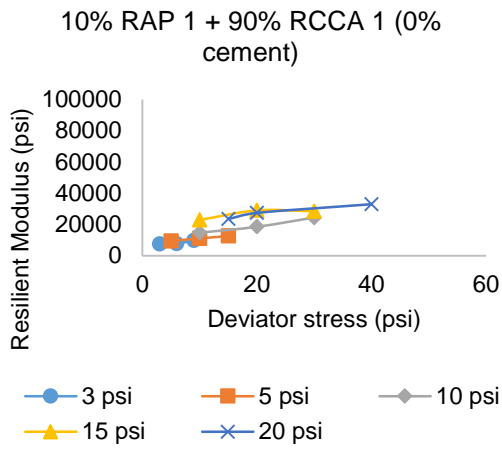
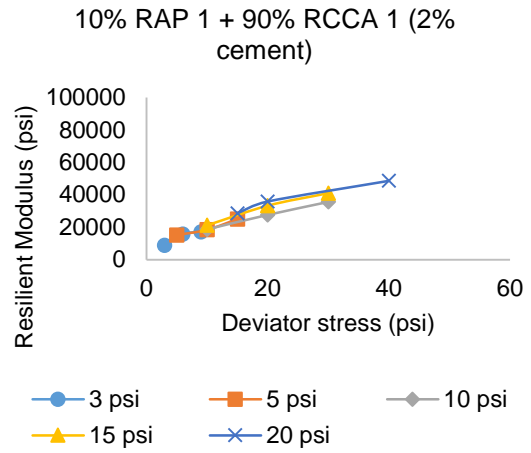


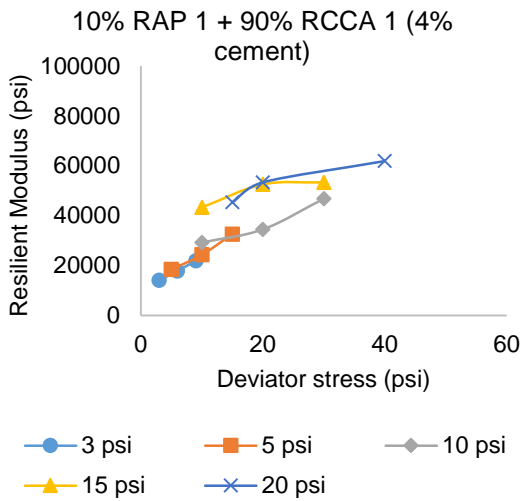
Figure 4.14 Comparison of resilient modulus test results for 100% RCCA 1 combination



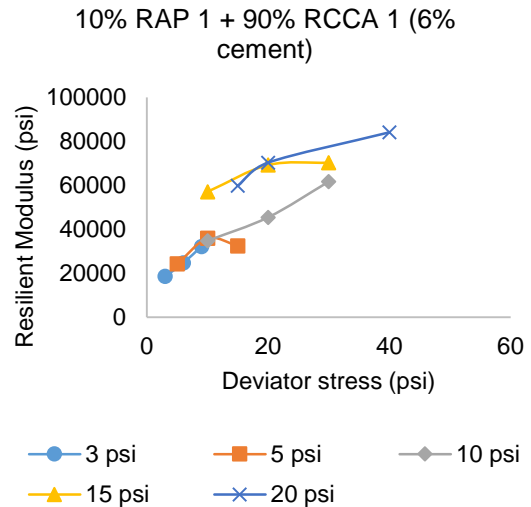
(a)



(b)

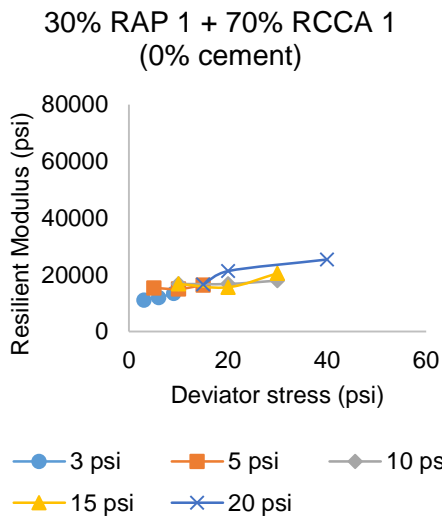


(c)

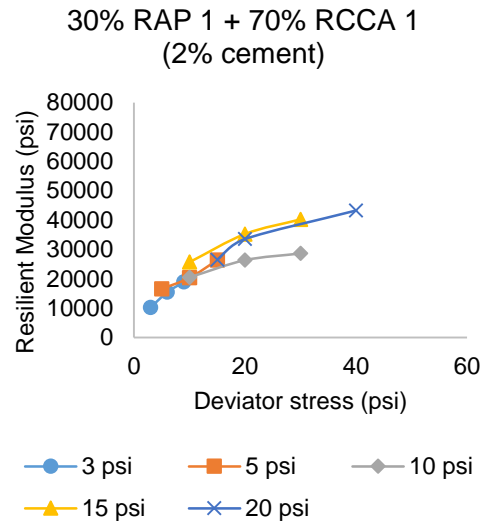


(d)

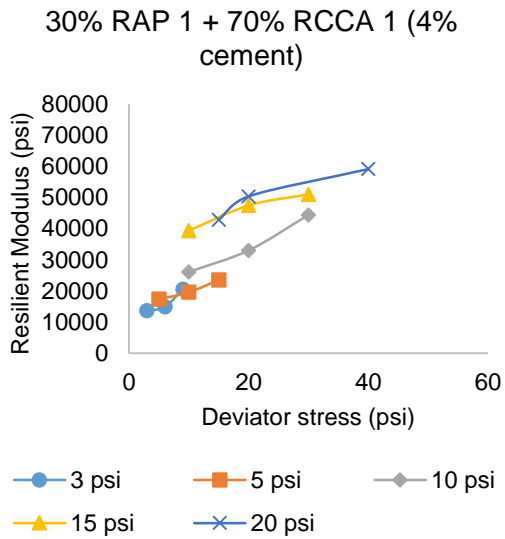
Figure 4.15 Comparison of resilient modulus test results for 10% RAP 1 + 90% RCCA 1 combination



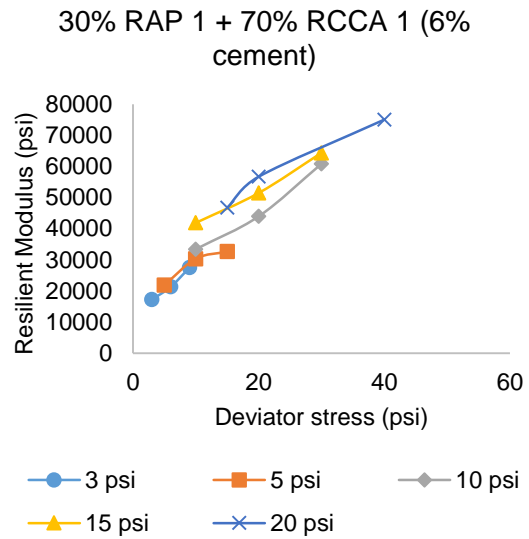
(a)



(b)

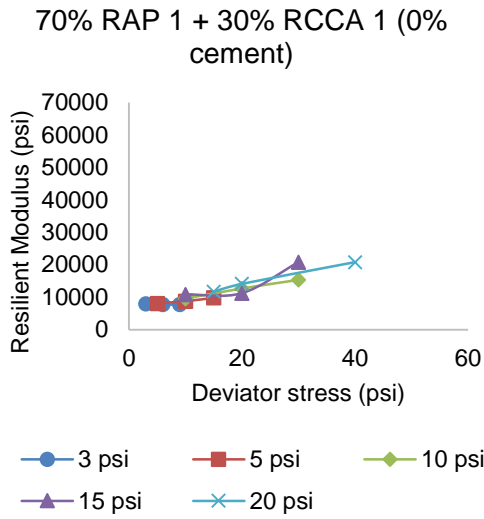


(c)

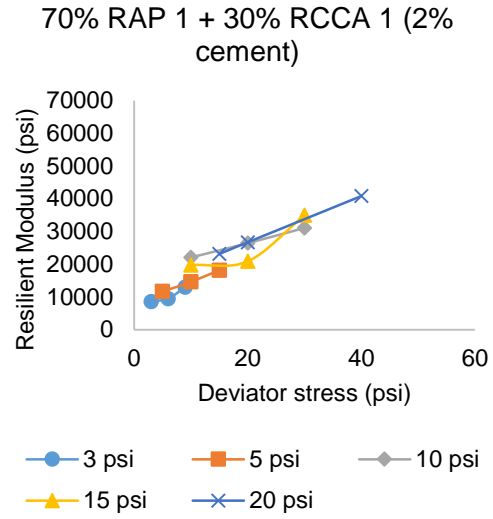


(d)

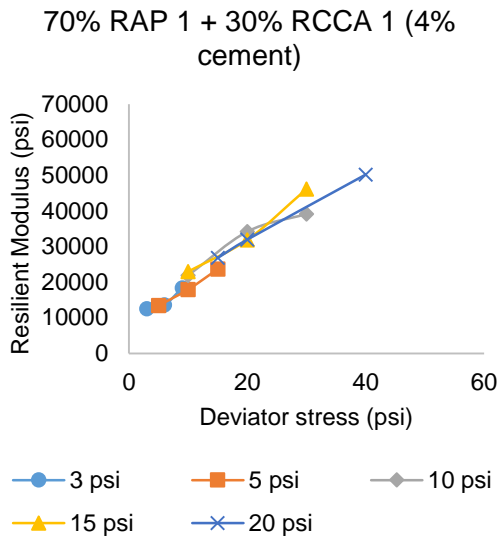
Figure 4.16 Comparison of resilient modulus test results for 30% RAP 1 + 70% RCCA 1 combination



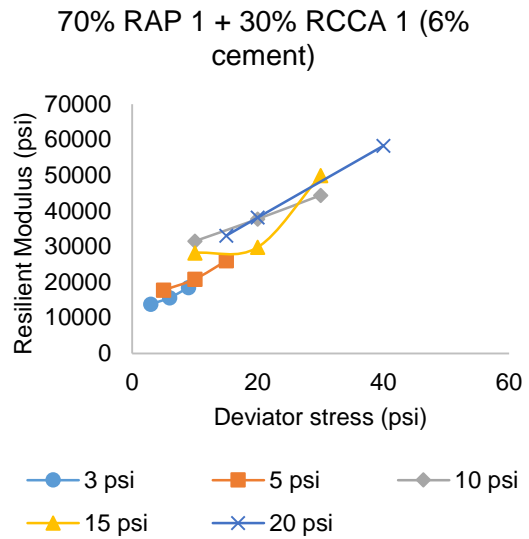
(a)



(b)

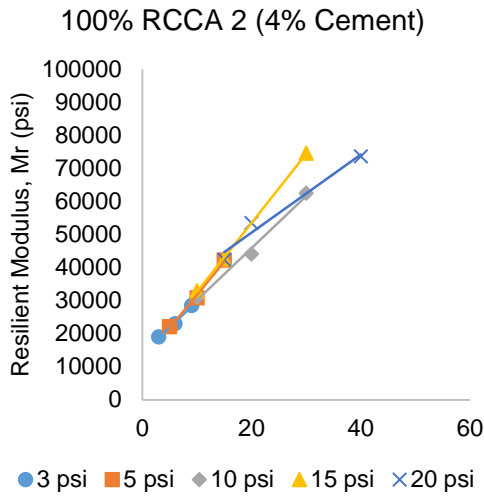


(c)

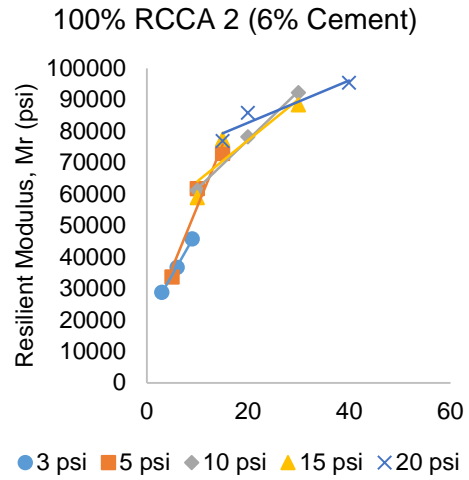


(d)

Figure 4.17 Comparison of resilient modulus test results for 70% RAP 1 + 30% RCCA 1 combination

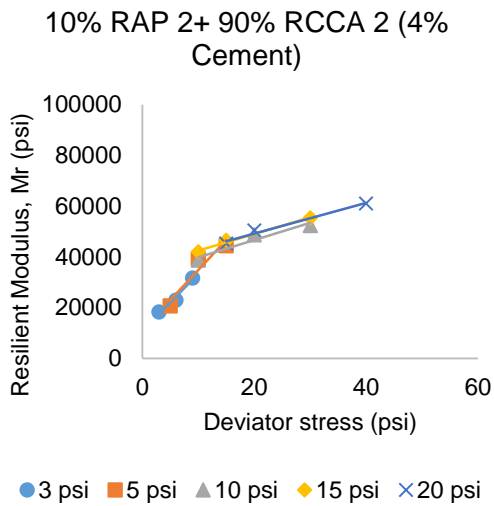


(a)

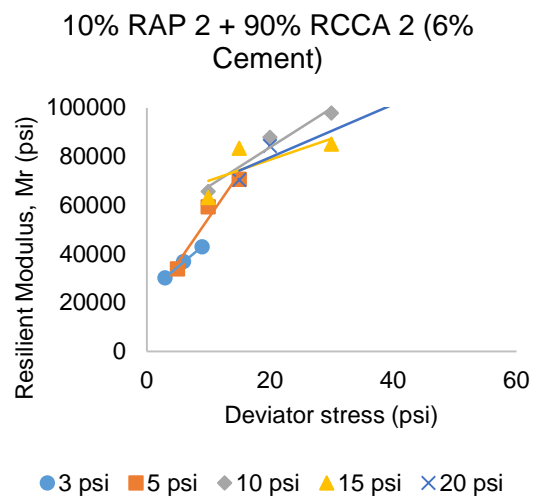


(b)

Figure 4.18 Comparison of resilient modulus test results for 100% RCCA 2 combination



(c)



(d)

Figure 4.19 Comparison of resilient modulus test results for 10% RAP 2 + 90%  
RCCA 2 combination

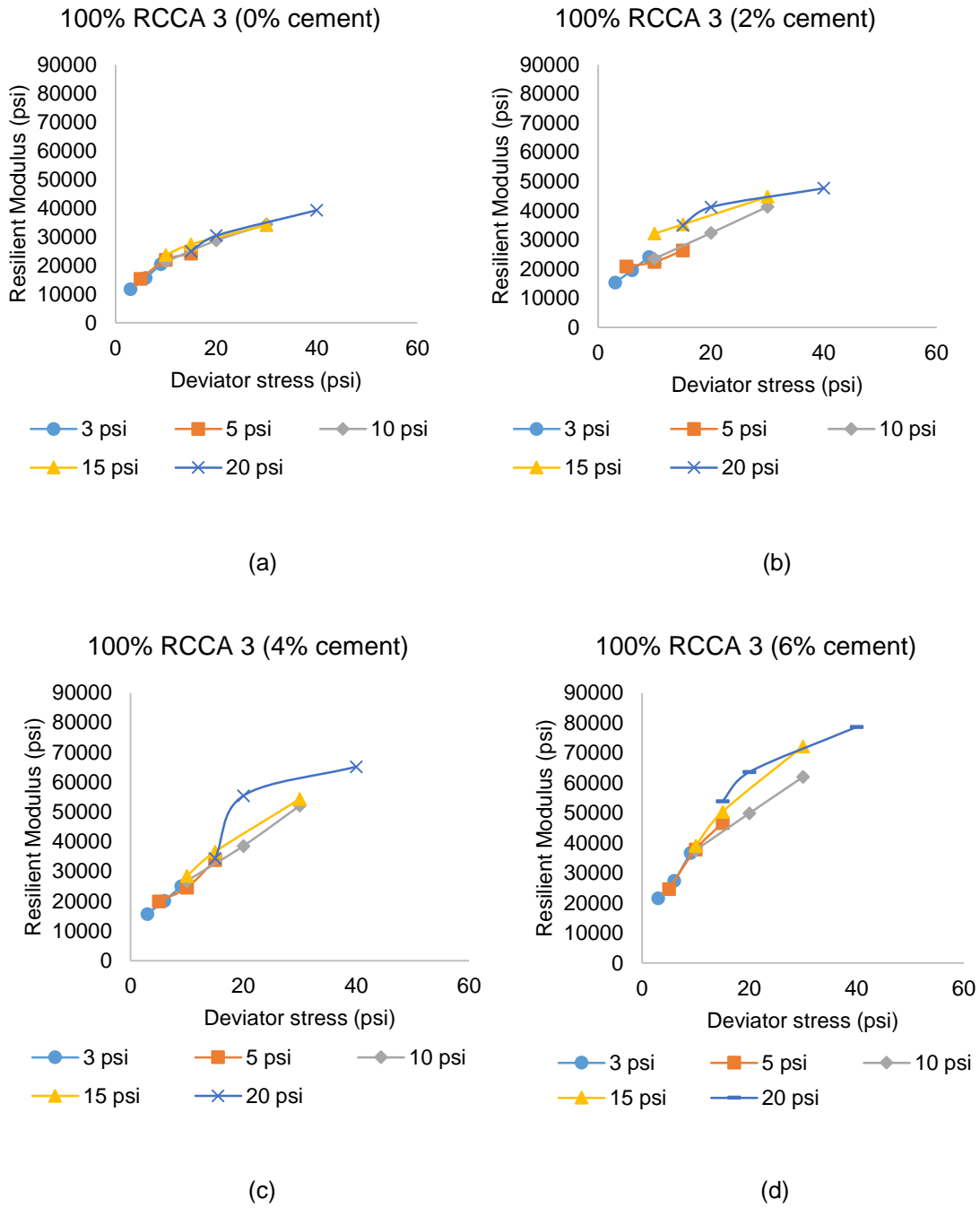


Figure 4.20 Comparison of resilient modulus test results for 100% RCCA 3 combination

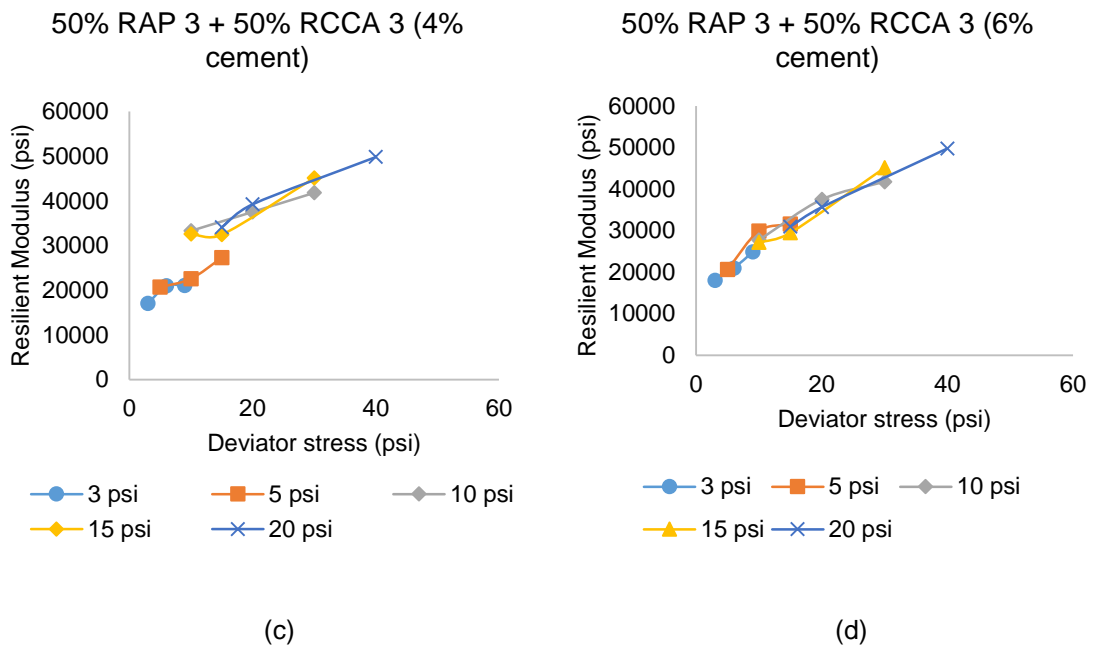
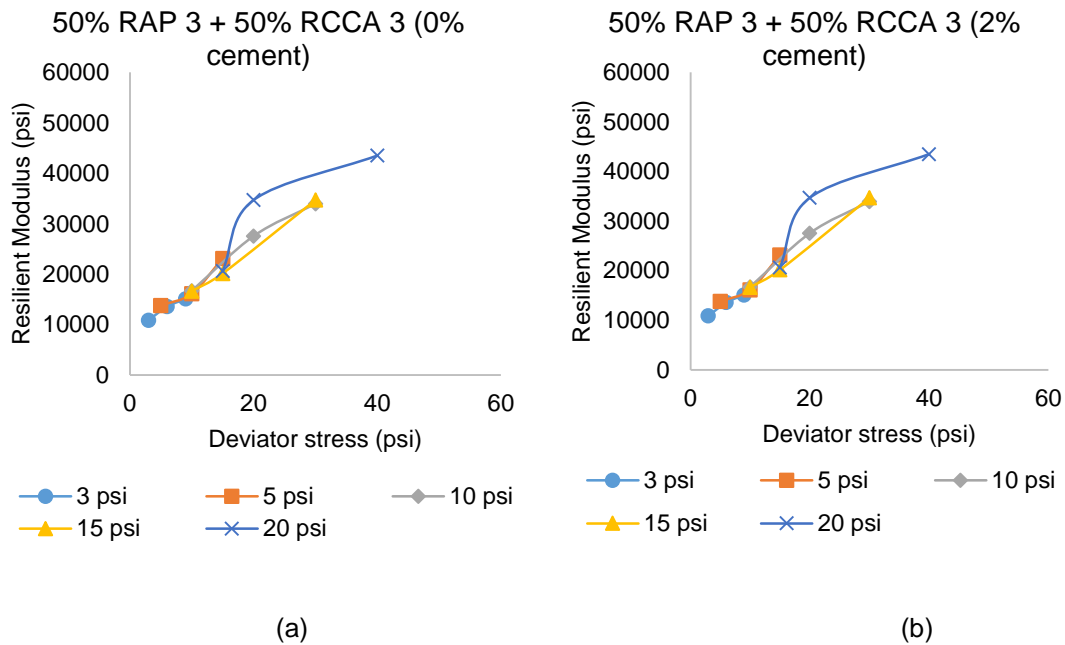


Figure 4.21 Comparison of resilient modulus test results for 50% RAP 3 + 50% RCCA 3 combination

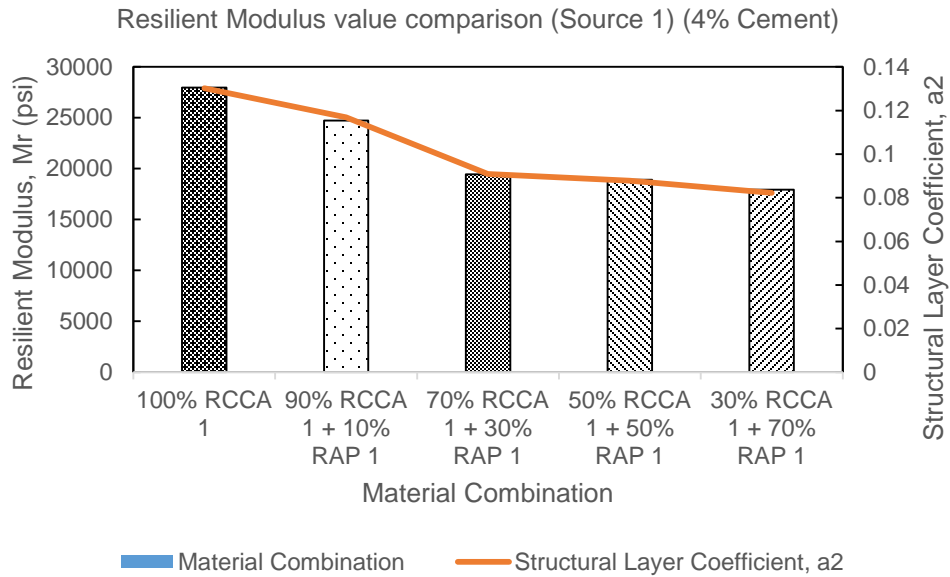


Figure 4.22 Resilient modulus value comparison (Source 1) (4% Cement)

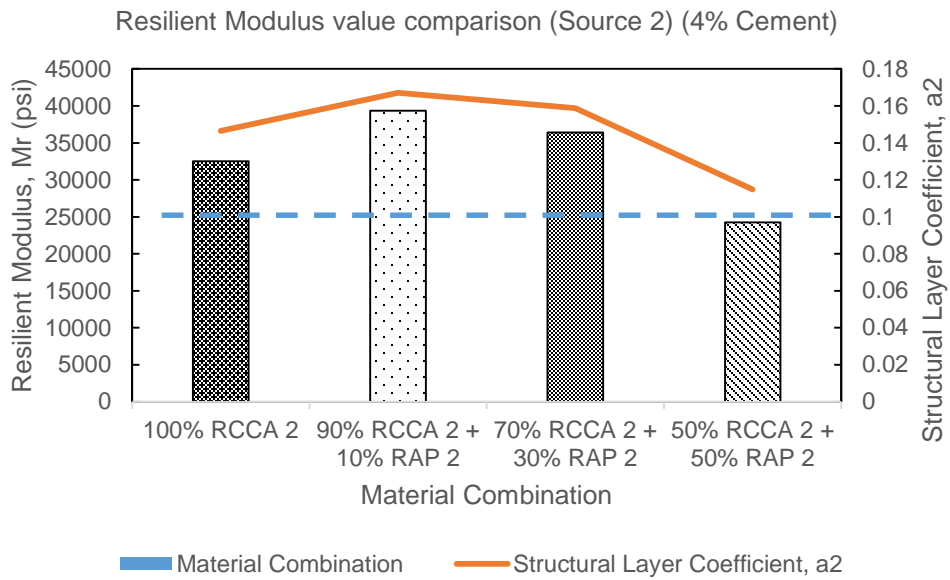


Figure 4.23 Resilient modulus value comparison (Source 2) (4% Cement)

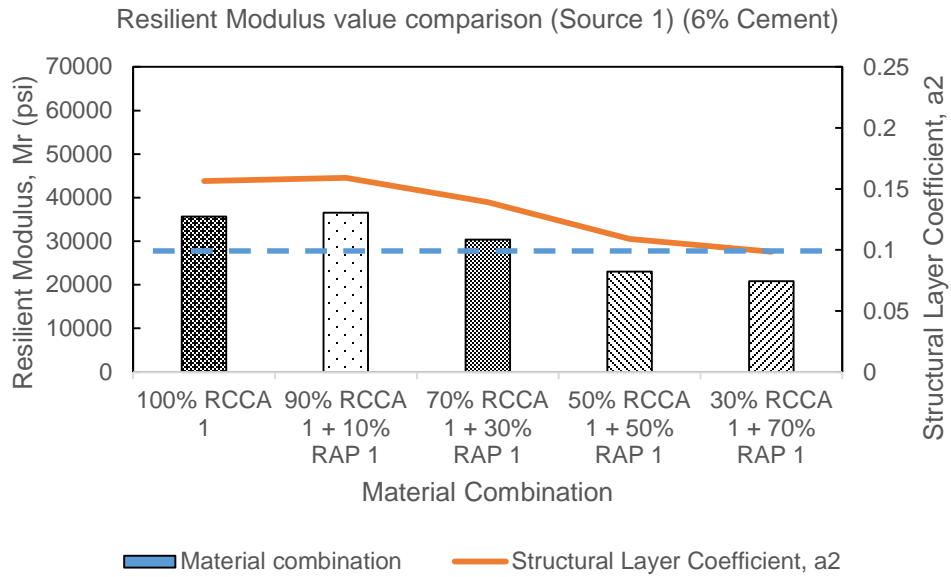


Figure 4.24 Resilient modulus value comparison (Source 1) (6% Cement)

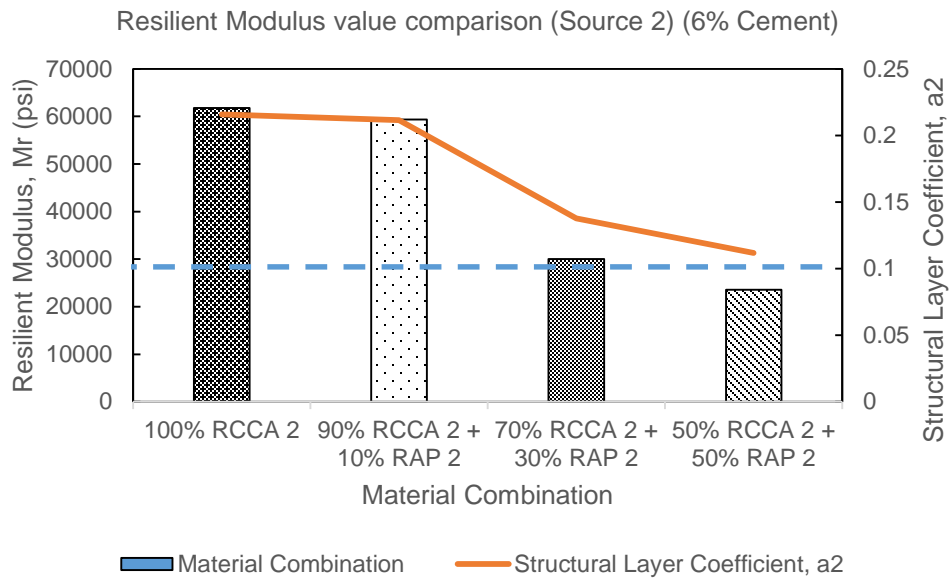


Figure 4.25 Resilient modulus value comparison (Source 2) (6% Cement)

#### 4.10 Effect of Cement Content on $M_r$

Resilient modulus of all material combinations used in this study showed a positive correlation with cement content. Figure 4.23 reflects that an addition of 2% cement, increased the resilient modulus values of 100% RCCA 3 mix by 9%, 28%, and 38%, respectively. On the contrary, for the same cement contents, the resilient modulus of the 50-50% RCCA 3-RAP 3 mix increased by 55%, 34%, and 5%, respectively. It can be inferred that additional cement stabilization effects the resilient modulus values at higher RAP content. A similar trend is also seen in Figure 4.25, where the  $k-\theta$  models of 50-50% RCCA 3-RAP 3 mix at 4% and 6% cement contents almost coincide with each other. This is due to the fact that RAP materials have asphalt-coated surfaces, which are not bound by cement as strongly as those of RCCA materials. Thus increasing the cement content from 4% to 6% does not have a significant effect on the 50-50% RCCA 3-RAP 3 mix.

#### 4.11 Effects of Stress Conditions on $M_r$

The sample specimens were subjected to different confining stresses, and each confining stress was subjected to three different deviator stresses, in accordance with AASHTO 2003 design guide. For a certain confining stress, the value of the resilient moduli increases with an increase in the deviator stress. It is evident that confining and deviator stresses have a significant influence on the resilient moduli of different combinations of aggregate specimens. Granular material is generally subjected to stress hardening with an increase in deviator stress and results in a higher resilient modulus (Buchanan 2007). Each cycle of deviatoric loading increases resilient moduli (Peng and Li 2004). According to the test results, the effect of deviator stress is more prominent in lower confining stress rather than in higher confining stress. At higher confining stress, the specimen becomes stronger and expands laterally, which reduces the effect of deviator stress on the increase in resilient moduli. Similar changes in strength were observed for both of the cement contents, for any combination of RCCA and RAP mixes, as shown in Figure 4.25.

#### 4.12 Effect of RAP content on $M_r$

For a particular cement content, the value of the resilient modulus decreases with an increase in RAP. RAP materials are relatively lightweight, as they have lower specific gravity (Table 4.1). RAP aggregates are coated with asphalt, which results in a slippery surface. However, the addition of 10% RAP to the RAP-RCCA mix at 6% cement content does not create any significance difference in  $M_r$ . The addition of 6% cement content might be able to neutralize the effect of surface asphalt on RAP materials. More than 10% RAP causes significant changes in the resilient modulus (Table 4.10, and Table 4.11).

#### 4.13 Statistical Analysis of Resilient Modulus Test Results

The results obtained from the resilient modulus tests for different combinations of materials were analyzed statistically, using the t-test, to compare and check the significance of effect of cement content and percentage of RAP on the stiffness properties. RCCA and RAP materials, used in different mix combinations, were obtained from same sources. For this reason, t-test results of paired groups of different combinations were analyzed to determine the effects, as shown in Table 4.10 and Table 4.11. The mean values of the resilient moduli of different combinations of test results were used for comparison to conduct the statistical t-test. T-tests were performed using Microsoft Excel software. The statistical hypothesis testing utilizes a p-value to determine the significance level of the test. The p-value usually used is 0.05 or 0.01. In this analysis, a p-value of 0.05 was used, which indicates that the differences in average resilient moduli occur due to an increase in RAP content of less than 5% for these cement-stabilized aggregates. The hypotheses used for these analyses are as follows:

Null Hypothesis,  $H_0: \mu_1 = \mu_2$  (signifies that the resilient modulus for 100% RCCA and 90% RCCA +10% RAP are same)

Alternative Hypothesis,  $H_1: \mu_1 \neq \mu_2$  (shows that the resilient modulus for 100% RCCA and 90% RCCA+10% RAP combination are different)

Where,  $\mu_1$  = mean of the resilient modulus of 100% RCCA aggregate treated with 4% cement and

$\mu_2$  = mean of the resilient modulus of 90% RCCA+ 10% RAP aggregate treated with 4% cement

The effect of RAP percentage in a combination can be explained if any significance difference is found in resilient modulus. Conversely, if no significant difference is found, the RAP content does not have any significant effect on resilient moduli. Statistical analysis was conducted to determine the effect of cement content on resilient moduli of the aggregate specimens.

Null Hypothesis,  $H_0: \mu_1 = \mu_2$  (signifies that the resilient modulus for 100% RCCA at 4% and 6% cement content are same)

Alternative Hypothesis,  $H_1: \mu_1 \neq \mu_2$  (which shows that the resilient modulus for 90% RCCA+10% RAP at 4% and 6% cement content are different)

Where,  $\mu_1$  = mean of the resilient modulus of 100% RCCA aggregate treated with 4% cement and

$\mu_2$  = mean of the resilient modulus of 90% RCCA+ 10% RAP aggregate treated with 4% cement

The effect of cement content in different combinations can be explained based on the significance level found from the statistical analyses. The results of the t-test analyses are included in Table 4.10, and Table 4.11.

Table 4.10 T-test Results for Effect of RAP Content (Source 3)

Material Combination		Cement Content (%)	Factor	p-value	Significant
RCCA (%) - RAP (%)					
100-0	90-10	4	RAP Content	0.003	Yes
90-10	70-30		RAP Content	0.045	Yes
70-30	50-50		RAP Content	0.02	Yes
100-0	90-10	6	RAP Content	0.13	No
90-10	70-30		RAP Content	1.36e-09	Yes
70-30	50-50		RAP Content	0.005	Yes

The results included in Table 4.10 and Table 4.11 indicate that there is a significant difference among the test results of aggregate specimens prepared in accordance with different combinations, except for the 100% RCCA and 10% RAP 3 + 90% RCCA 3 combination at 6% cement content. The addition of 10% RAP to RCCA does not have significance effect on the cementations characteristics of the RCCA at 6% cement content. There are significant differences between the resilient moduli for any combination of aggregate specimens at 4% and 6% cement content.

Table 4.11 T-Test Results for Effect of Cement Content (Source 3)

Material Combination		Cement Content (%)	Factor	p-value	Significant
RCCA (%)	RAP (%)				
100	0	4 & 6	Cement Content	6.96E-10	Yes
90	10		Cement Content	4.61E-08	Yes
70	30		Cement Content	0.00048	Yes
50	50		Cement Content	6.70E-05	Yes

#### 4.14 Statistical Modelling of $M_r$ , UCS, and EM Values

The resilient modulus test is labor intensive, expensive, and time consuming. For this reason, it is necessary to develop correlations of resilient modulus with other strength properties, such as unconfined compressive strength and elastic modulus values. Unconfined compressive strength (UCS), and elastic modulus (EM) are simple test procedures which can be conducted in less time.

The correlation is developed to predict or estimate the RM values of recycled aggregates with a reasonable degree of accuracy. A study conducted by Lotfi and Witczak (1985), to evaluate the value of UCS and  $M_r$  for base or sub-base materials, was used by the Maryland State Highway Administration. These results were used to develop semi-logarithmic regression models for the materials with correlation coefficients ranging from 0.842 to 0.905.

Regression models were developed in this study, correlating the  $M_r$  values with UCS and EM values obtained from the specimens cured for seven days. Regression models were developed corresponding to different confining and deviator stresses at 4% and 6% cement. The

strength and stiffness requirements were only fulfilled at 4% and 6% cement content, thus the models were developed for those specific cement contents.

#### 4.15 Prediction Models

Resilient modulus tests were conducted on three identical samples of each combination of RCCA and RAP materials stabilized at different cement contents. The coefficient of variation (COV) of the  $M_r$  values for all of them was found to be within 0.19% - 8.92%, which showed good repeatability of the performed tests. According to the AASHTO guidelines, resilient modulus test results need to be analyzed using different regression prediction models, such as bulk stress and deviatoric models, to evaluate the accuracy of the test results. One of them is the “k- $\theta$  model” proposed by Moosazehd and Witczak (1981).

$$M_r = k_1 \theta^{k_2} \quad (1)$$

Where  $k_1$  and  $k_2$  are model parameters and  $\theta$  is the bulk stress expressed as a combination of confining ( $\sigma_c$ ) and deviator stresses ( $\sigma_d$ ) in the form  $3\sigma_c + \sigma_d$ . The other model used in this study is the improved three-parameter model (Puppala et. al., 1997).

$$M_r = k_3 \sigma_c^{k_4} \sigma_d^{k_5} \quad (2)$$

Where  $k_3$ ,  $k_4$  and  $k_5$  are model parameters.

Linear statistical regression analysis was conducted to determine  $k_1$ ,  $k_2$ ,  $k_3$ ,  $k_4$ , and  $k_5$ . The model parameters, along with the calculated statistical parameters, are presented in Table 4.12 to Table 4.14.

The k- $\theta$  model parameter  $\log k_1$  indicates magnitudes, while  $k_2$  indicates the non-linear nature of the stress dependency (Potturi 2006). The three-parameter model  $\log k_3$  indicates the magnitude of the resilient moduli, while  $k_4$ , and  $k_5$  represent the non-linear nature of the stress

dependency. The trend of  $\log k_1$ ,  $k_2$ ,  $\log k_3$ ,  $k_4$ ,  $k_5$  were difficult to explain with respect to the amount of RAP mixed in different combinations and with added cement.

Table 4.12 Statistical Parameters Obtained from Prediction Model for RCCA and RAP Materials  
Obtained from Source 1 (0% and 2% cement content)

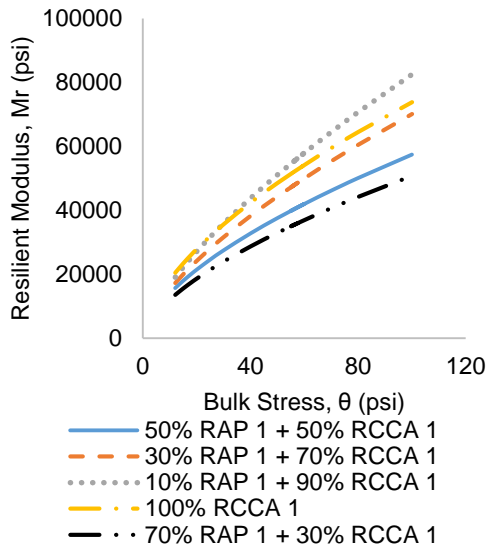
Cement Content (%)	Material Combination	$\log k_1$	$k_2$	$R^2$	$\log k_3$	$k_4$	$k_5$	$R^2$
0	100      0	3.78	0.34	0.92	3.95	0.20	0.16	0.93
	90        10	3.00	0.76	0.97	3.46	0.46	0.29	0.94
	70        30	3.27	0.76	0.91	3.75	0.17	0.28	0.92
	50        50	3.24	0.75	0.86	3.81	0.17	0.37	0.94
	30        70	3.30	0.65	0.89	3.60	0.16	0.53	0.94
2	100      0	3.61	0.53	0.86	3.87	0.17	0.37	0.94
	90        10	3.41	0.76	0.97	3.85	0.47	0.30	0.95
	70        30	3.27	0.76	0.95	3.75	0.47	0.28	0.96
	50        50	3.24	0.75	0.86	3.81	0.17	0.37	0.94
	30        70	3.30	0.65	0.89	3.60	0.16	0.53	0.94

The value of  $R^2 > 0.8$  for almost all cases, with one or two exceptions, signifying good correlation with the statistical regression analysis. The three-parameter model had higher values of  $R^2$  than the two-parameter model, in all cases. This is because the three-parameter model

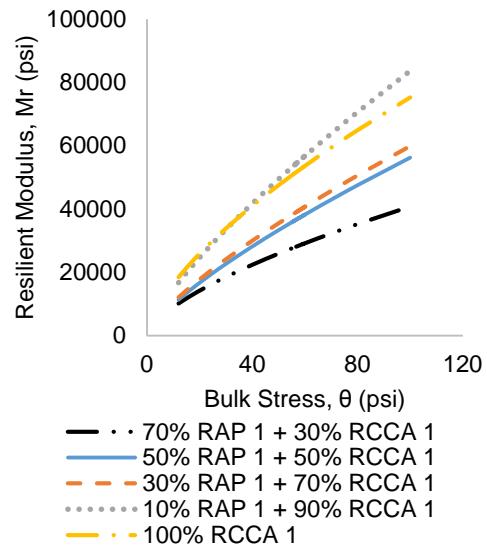
considers the individual effects of confining and deviator stresses on resilient modulus in contrast to the k- $\theta$  model that considers only a combined bulk stress.

Table 4.13 Statistical Parameters Obtained from Prediction Model for RCCA and RAP Materials  
Obtained from Source 1 (0% and 2% cement content)

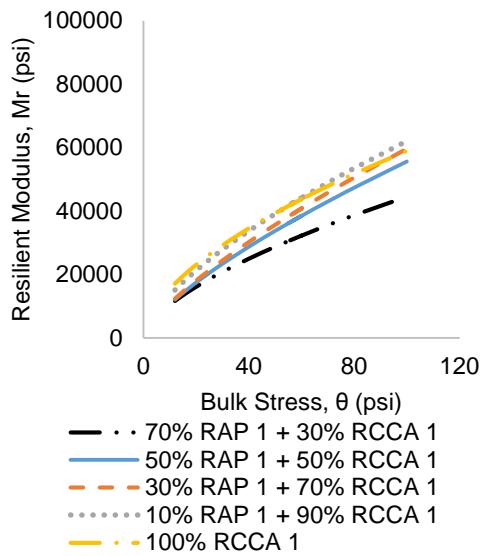
Cement Content (%)	Material Combination		log k <sub>1</sub>	k <sub>2</sub>	R <sup>2</sup>	log k <sub>3</sub>	k <sub>4</sub>	k <sub>5</sub>	R <sup>2</sup>
	RCCA (%)	RAP (%)							
4	100	0	3.60	0.58	0.79	3.828	0.014	0.621	0.96
	90	10	3.46	0.67	0.96	3.855	0.374	0.296	0.96
	70	30	3.29	0.74	0.97	3.750	0.468	0.282	0.97
	50	50	3.30	0.72	0.96	3.726	0.387	0.332	0.96
	30	70	3.38	0.63	0.83	3.653	0.079	0.593	0.96
6	100	0	3.96	0.60	0.86	3.96	0.15	0.47	0.96
	90	10	3.54	0.69	0.93	3.95	0.39	0.28	0.92
	70	30	3.52	0.66	0.93	3.75	0.47	0.28	0.96
	50	50	3.54	0.61	0.77	3.75	0.00	0.67	0.92
	30	70	3.46	0.62	0.88	3.74	0.15	0.51	0.93



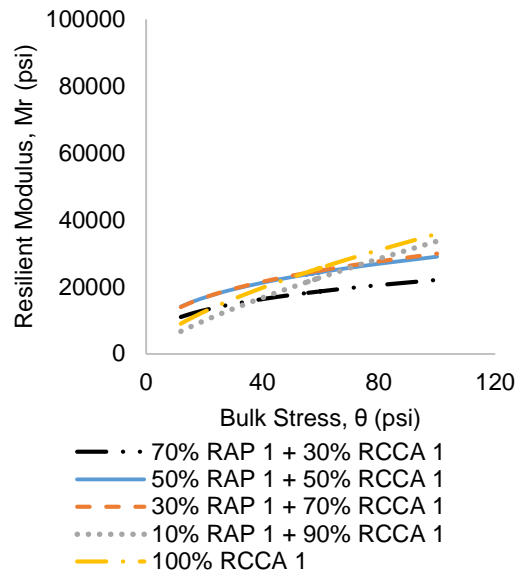
(a)



(b)



(c)



(d)

Figure 4.26 Two-parameter model ( $k$ - $\theta$ ) for different RAP 1-RCCA 1 (Source 1) combinations stabilized at (a) 6 %, (b) 4%, (c) 2% and (d) 0% cement content.

Table 4.14 Statistical Parameters Obtained from Prediction Model for RCCA and RAP Materials  
Obtained from Source 2

Cement Content (%)	Material Combination		log $k_1$	$k_2$	$R^2$	log $k_3$	$k_4$	$k_5$	$R^2$	C.O.V (%)
	RCCA	RAP								
	(%)	(%)								
4	100	0	2.82	0.59	0.91	0.55	0.19	0.41	0.97	1.2-12.91
	90	10	2.71	0.49	0.92	0.50	0.23	0.25	0.95	0.94-9.39
	70	30	1.45	0.39	0.92	1.55	0.17	0.28	0.96	0.71-7.20
	50	50	2.66	0.47	0.91	0.45	0.18	0.31	0.95	0.86-8.47
6	100	0	2.91	0.47	0.93	0.71	0.21	0.26	0.98	0.83-5.88
	90	10	1.57	0.44	0.94	0.69	0.07	0.39	0.96	0.78-3.65
	70	30	2.88	0.65	0.91	0.58	0.23	0.40	0.96	1.06-11.09
	50	50	2.72	0.46	0.91	0.52	0.23	0.24	0.93	2.79-10.37

Table 4.12, and Table 4.13 show the statistical parameters calculated for the prediction models of Source 1 RCCA and RAP materials. The simpler  $k$ - $\theta$  model (two-parameter model) for these materials was plotted as shown in Figure 4.26. It was observed that the increase of RAP by 10% had no significant effect on the resilient modulus ( $M_r$ ). A further increase in RAP content decreased  $M_r$  at all cement contents. This effect of RAP content was more pronounced in higher cement contents (4% and 6%) than in lower ones. Prediction models for the un-stabilized Source 1 materials (Figure 4.22d) yielded resilient modulus values to about half of those stabilized at 2% cement content.

The  $k$ - $\theta$  models for the Source 2 materials (RAP 2 and RCCA 2) are shown in Figure 4.27. At 6% cement content, it was seen that addition of RAP by 30% has minimal effects on  $M_r$ . An further addition of 20% RAP reduces the  $M_r$  values by about 50%.

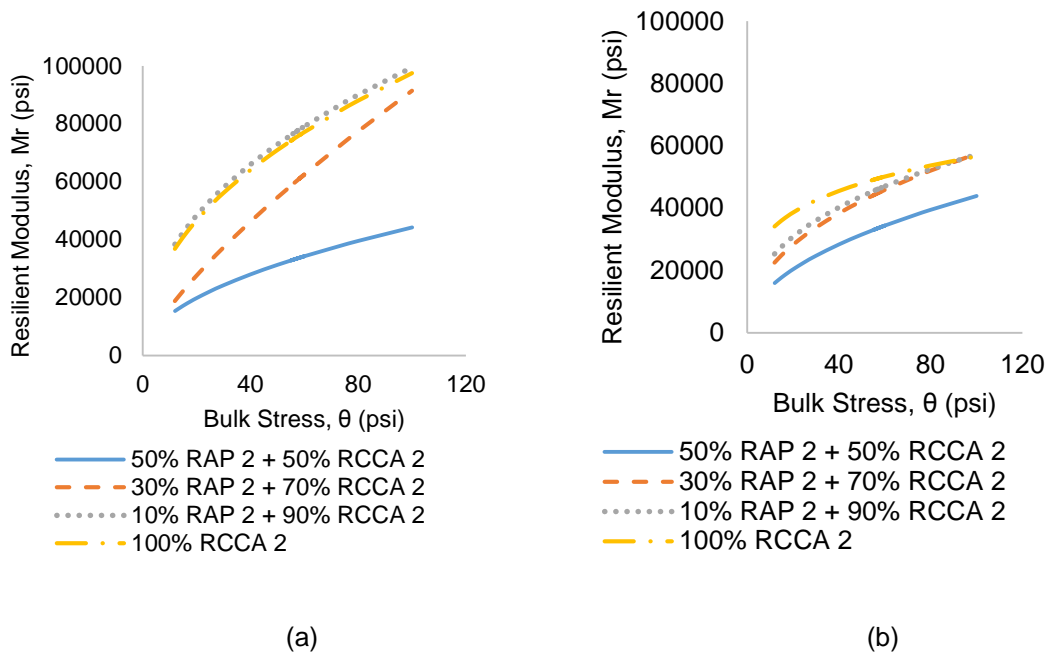


Figure 4.27 Two-parameter model ( $k$ - $\theta$ ) for different RAP 2-RCCA 2 (Source 2) combinations stabilized at (a) 6 % and (b) 4% cement content

For Source 3 (Figure 4.28), the addition of reclaimed asphalt pavement (RAP) tends to lower the resilient modulus values of stabilized aggregate mix (Faysal et. al., 2016). Similar results were obtained in this study. It is evident that at all cement contents, the  $k$ - $\theta$  models developed for the 50-50% RCCA-RAP mix predicted lower values of  $M_r$  than those developed for 100% RCCA mix. Also from Figure 4.26, it is seen that on an average, a pure RCCA mix has a resilient modulus about 25% higher than a RAP-RCA mix; the difference increases to 40% at 6% cement content.

Table 4.15 Statistical Parameters Obtained from Prediction Model for RCCA and RAP Materials  
Obtained from Source 3

Cement Content (%)	Material Combination		log $k_1$	$k_2$	$R^2$	log $k_3$	$k_4$	$k_5$	$R^2$	C.O.V (%)
	RCCA	RAP								
	(%)	(%)								
0	100	0	3.69	0.43	0.82	3.87	0.03	0.44	0.98	3.72- 8.92
	50	50	3.11	0.68	0.81	3.61	0.20	0.45	0.9	2.82- 7.64
2	100	0	3.68	0.49	0.90	3.94	0.19	0.32	0.95	1.25- 4.53
	50	50	3.29	0.64	0.86	3.63	0.20	0.46	0.95	2.33- 6.67
4	100	0	3.51	0.63	0.81	3.81	0.12	0.53	0.96	3.72- 8.92
	50	50	3.90	0.37	0.80	4.04	0.03	0.37	0.97	1.89- 5.54
6	100	0	3.78	0.54	0.83	4.05	0.12	0.53	0.97	0.19- 5.82
	50	50	3.88	0.39	0.82	4.05	0.06	0.36	0.95	4.46- 8.33

For most of the cases, the value of coefficient of determination ( $R^2$ ) decreased with the increase in RAP content in the material combinations. This might have contributed to the increasing heterogeneity due to the addition of RAP content. This bulk stress most practically represents the stress conditions in flexible pavement base layers (Cetin 2010). It has also been mentioned in AASHTO design guidelines that most aggregate base courses that are designed for bulk stress values must be limited to 30 psi (AASHTO 2003).

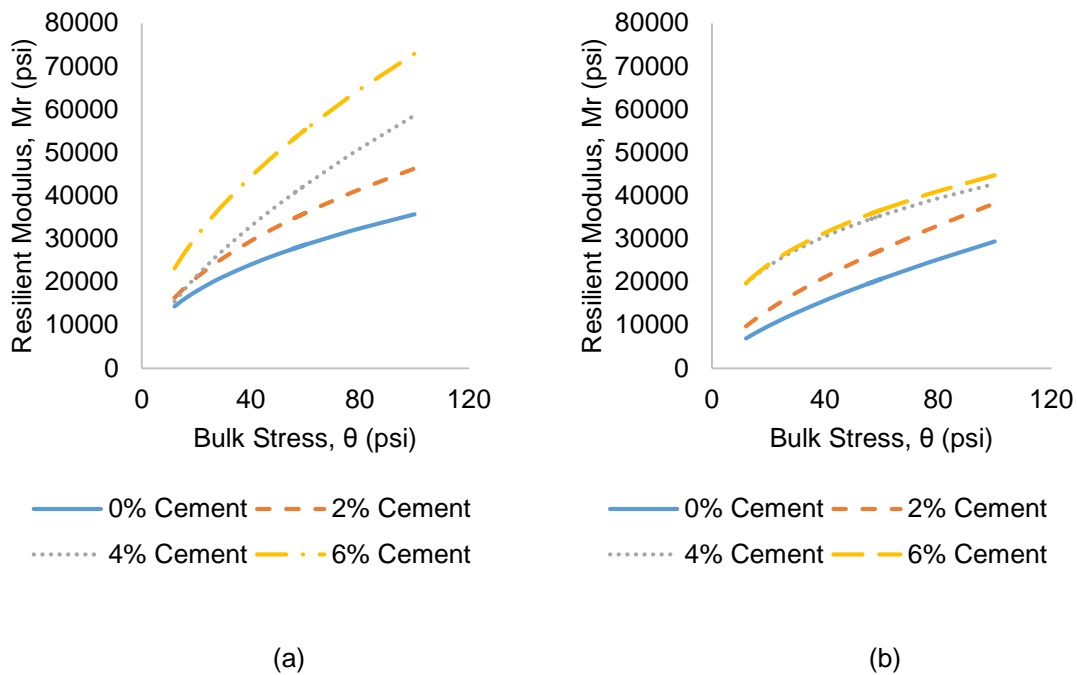


Figure 4.28 Two-parameter model ( $k-\theta$ ) for fitting resilient modulus of (a) 100 % RCCA 3 and (b) 50-50% RCCA 3 – RAP 3 from Source 3

#### 4.16 Asphalt Content

RAP materials are covered with asphalt. The amount of asphalt content might have an effect on the performance of RAP materials on the base layer of pavement. Asphalt content was determined in the TxDOT laboratory by using the ignition method, as specified by Tex-236 F guidelines. Test results are included in Table 4.1.

#### 4.17 Effect of Asphalt Content

RAP materials reduce strength when they are mixed in different proportions with RCCA. RAP aggregates are coated with asphalt, which hinders the cementation process. It is necessary to determine the effect of asphalt on the strength and stiffness properties of different mixes so that it can be used in blending it with RCCA. According to the previous discussion, the maximum amount of RAP which can be mixed with RCCA is 50%. The RAP materials obtained from source

3 contained 4.4% of asphalt, which was mixed with different amounts of asphalt so that, on an average, it had an asphalt content of 6.5% and 8.4%. The RAP materials are identified in Table 4.16. The RAP sample was collected, mixed at different asphalt contents, and mixed with RCCA at different cement contents, as shown in Table 4.17. These different blends of RAP materials were mixed with RCCA. Samples were prepared for a combination of 50% RAP and 50% RCCA, and were treated with different cement dosages. Notations for different mixes are included in Table 4.17. Prepared specimens were subjected to unconfined compressive strength (UCS), split tensile strength (STS), and resilient modulus ( $M_r$ ) laboratory tests.

Table 4.16 RAP Materials Containing Different Asphalt Contents

Asphalt Content (%)	Materials ID
4.4	RAP 3a
6.5	RAP 3b
8.4	RAP 3c

Table 4.17 Notation for Different Mixes

Material Combination	Cement Content (%)	Mix ID
50% RAP 3a + 50% RCCA 3	4	Mix 1
50% RAP 3a + 50% RCCA 3	6	Mix 2
50% RAP 3b + 50% RCCA 3	4	Mix 3
50% RAP 3b + 50% RCCA 3	6	Mix 4
50% RAP 3c + 50% RCCA 3	4	Mix 5
50% RAP 3c + 50% RCCA 3	6	Mix 6

#### 4.17.1 Particle Size Distribution

RAP materials obtained from Source 3, which contained 4.4% asphalt, were subjected to quantitative determination of the distribution of the particle sizes in accordance with TEX 110E guideline for standard test method for particle-size analysis of soils. Additional asphalt was added to the two different batches of Source 3 materials, and the final asphalt contents were found to be 6.5% and 8.4%. Those two batches were denoted as RAP 3b and RAP 3c.

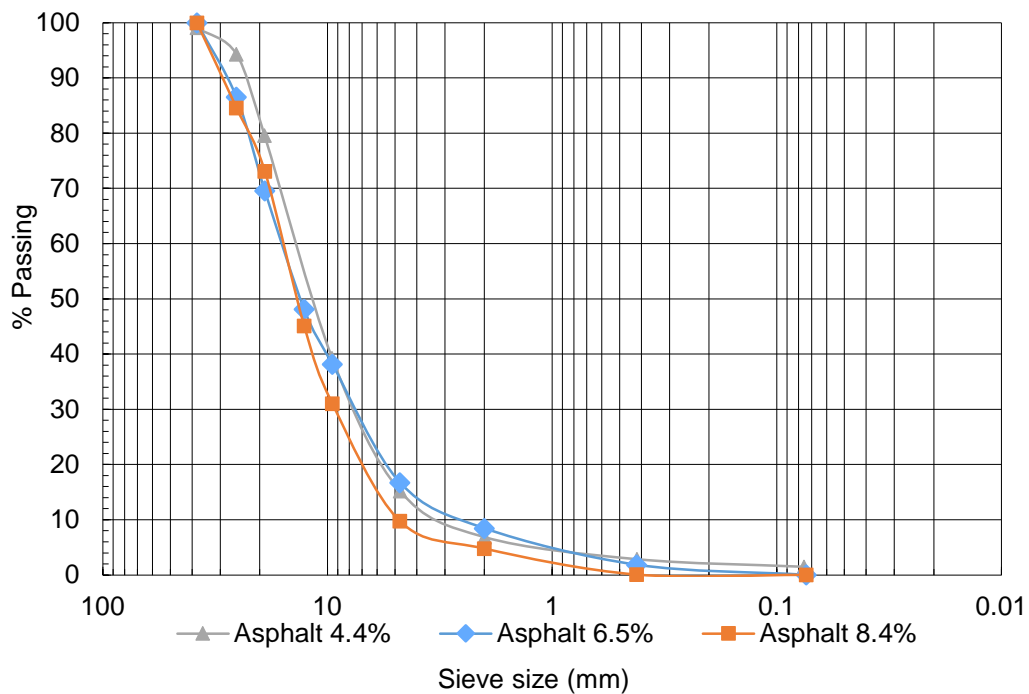


Figure 4.29 Particle size analysis of RAP materials containing different asphalt contents

According to the test results, the particle size distribution curve shifts to the left side with inclusion of asphalt with RAP materials, which indicates the increased particle size. This might have occurred because of the agglomeration of the fine particles on the surface of the relatively coarser materials during asphalt mixing. According to the USCS (Unified Soil Classification System) guidelines, if more than 50% of the material is larger than what will pass through a No.

200 sieve, then the aggregates are classified as coarse-grained soils. The amount of materials larger than that was 98.50% for RAP 3a, and the amount of soil retained for RAP 3b and RAP 3c within the No. 200 sieve was 100% for both of the cases. Test results indicated there was an approximate 1 to 1.5% reduction in fine particles.

Table 4.18 Particle Size Distribution Results Description

Type	D <sub>10</sub> (mm)	D <sub>30</sub> (mm)	D <sub>60</sub> (mm)	D <sub>max</sub> (mm)	C <sub>u</sub>	C <sub>c</sub>
RAP 3a	3	7	14	37.58	4.67	1.17
RAP 3b	2.7	7.7	10.7	37.58	3.96	2.05
RAP 3c	5	9.5	10.7	37.58	2.14	1.69

Coefficient of curvature (C<sub>c</sub>) and coefficient of uniformity (C<sub>u</sub>) obtained for RAP 3a are 1.17 and 4.67 conformed to the criteria of  $1 < C_c < 3$  and  $C_u > 4$  and can be designated as well-graded gravel (GW). On the other hand, according to the USCS classification, with the addition of asphalt binder it becomes poorly-graded aggregates, which might have occurred because of the increase in particle size.

#### 4.17.2 Strength Tests

##### 4.17.2.1 Unconfined Compressive Strength (UCS)

The specimens of 6"x 8" size were tested in the universal testing machine in the UTA structures lab after seven days of curing period. The test results were used to determine the UCS. The peak value obtained from the stress-strain plot represents the UCS value of the particular specimen. Three identical specimens were tested for each cement content of 50% RAP and 50% RCCA combination. The average value of the three specimens was taken to get the representative value of UCS. UCS test results are included in the following table.

Table 4.19 Unconfined Compressive Strength Results for 50% RAP 3a + 50% RCCA 3 (Asphalt  
4.4%)

Cement Content (%)	Sample ID	Load on Specimen (lb.)	Stress (psi)	Mean Strength (psi)	SD	COV (%)
0	1	376	13	13.06	0.72	5.53
	2	385	14			
	3	346	12			
2	1	3554	126	102.29	20.59	20.13
	2	2652	94			
	3	2466	87			
4	1	5795	199	198.56	6.45	3.25
	2	4581	192			
	3	6458	205			
6	1	10392	358	348.03	10.54	3.03
	2	9236	337			
	3	9865	349			

Table 4.20 Unconfined Compressive Strength Results for 50% RAP 3b + 50% RCCA 3 (Asphalt  
6.5%)

Cement Content (%)	Sample ID	Load on Specimen (lb.)	Stress (psi)	Mean Strength (psi)	SD	COV (%)
2	1	3079	108.95	107.82	2.47	2.29
	2	3095	109.52			
	3	2967	104.99			
4	1	5556	196.60	190.33	7.18	3.77
	2	4859	182.50			
	3	5423	191.90			
6	1	8378	296.46	289.86	6.18	2.13
	2	8032	284.22			
	3	8164	288.89			

Table 4.21 Unconfined Compressive Strength Results for 50% RAP 3c + 50% RCCA 3 (Asphalt 8.4%)

Cement Content (%)	Sample ID	Load on Specimen (lb.)	Stress (psi)	Mean Strength (psi)	SD	COV (%)
4	1	4527	160.19	163.91	8.64	5.27
	2	4911	173.78			
	3	4458	157.75			
6	1	7265	257.08	254.80	8.15	3.20
	2	7392	261.57			
	3	6945	245.75			

Tests results indicated that higher coefficients of variation (COV) were observed at lower cement contents, which might have occurred because of the relatively weaker bonding matrix between aggregates.

Unconfined compressive strength (UCS) decreased with an increase in asphalt content of the same RAP obtained from Source 3, as shown in Figure 4.68. Asphalt inclusion makes the surface of the RAP particles slippery by providing an extra thick layer of asphalt on the surface of aggregates.

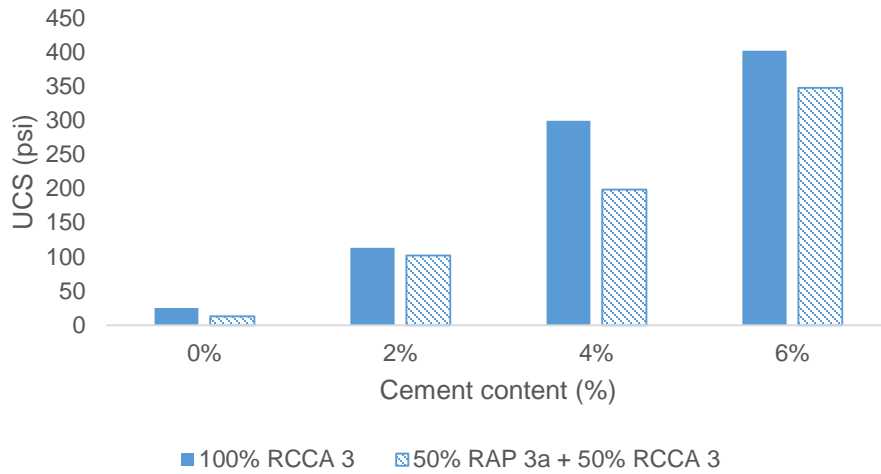


Figure 4.30 Decrease in UCS with the inclusion of RAP

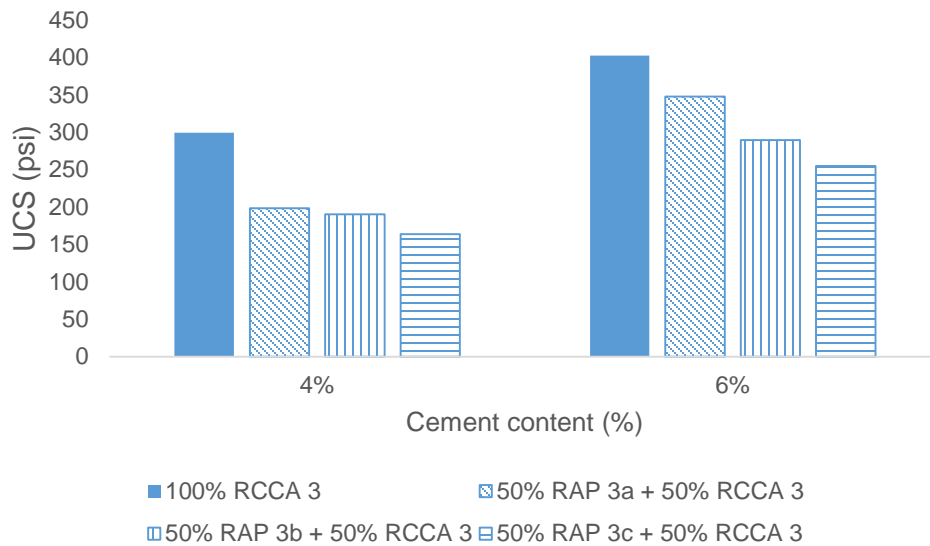


Figure 4.31 Decrease in UCS with additional asphalt on RAP

UCS values for the 50% RAP+50% RCCA combination at 4% cement content were 198, 190, and 160 psi for RAP materials containing 4.4%, 6.5%, and 8.4% asphalt, respectively. UCS values decreased by 18% with the addition of 4% asphalt at 4% cement content. UCS values for the 50% RAP+50% RCCA combination at 6% cement content were 348, 290, and 255 psi for RAP

materials containing 4.4%, 6.5%, and 8.4% asphalt, respectively. The UCS value decreased by 27% with the addition of 4% asphalt at 6% cement content.

#### 4.17.2.2 Split Tensile Strength

The split tensile strength (STS) tests were conducted as per ASTM C496-96 procedure for cylindrical concrete specimens. The cylindrical specimen was 12 inches long and 6 inches wide. The tests were conducted on the specimen after seven days of curing. Splitting tensile strength is generally greater than direct tensile strength and lower than flexural strength (modulus of rupture) (ASTM C496-96). STS was used to evaluate the shear resistance provided by concrete. Test results obtained for different combinations of materials are depicted in

Table 4.22 Split Tensile Strength for 100% RCCA 3

Cement Content (%)	Sample ID	Load on Specimen (lb.)	Stress (psi)	Mean Strength (psi)	SD	COV (%)
0	1	398	3.52	3.69	0.18	4.94
	2	415	3.67			
	3	439	3.88			
2	1	1931	17.07	18.56	1.37	7.40
	2	2130	18.83			
	3	2237	19.78			
4	1	3179	28.11	27.67	1.85	6.68
	2	2900	25.64			
	3	3309	29.26			
6	1	3759	33.24	34.60	1.55	4.47
	2	4103	36.28			
	3	3876	34.27			

The test results varied from 3.69 psi to 34.6 psi for 100% RCCA 3 and from 1.19 to 30.94 psi for 50% RAP 3+ 50% RCCA 3 mixtures, with the variation in cement content from 0% to 6%. The value of split tensile strength increased with an increase in cement content, which signifies

the effect of better interlocking behavior of the material matrix with inclusion of cement dosage.

The inclusion of RAP reduced both UCS and STS of the prepared specimens.

Table 4.23 Split Tensile Strength for 50% RAP 3a + 50% RCCA 3 (4.4% Asphalt)

Cement Content (%)	Sample ID	Load on Specimen (lb.)	Stress (psi)	Mean Strength (psi)	SD	COV (%)
0	1	134	1.18	1.19	0.10	8.18
	2	146	1.29			
	3	124	1.09			
2	1	1621	14.33	15.15	0.71	4.67
	2	1752	15.49			
	3	1766	15.61			
4	1	2379	21.03	20.02	1.27	6.34
	2	2103	18.59			
	3	2309	20.41			
6	1	3540	31.30	30.94	0.84	2.73
	2	3390	29.97			
	3	3567	31.53			

The increase in unconfined compressive strength was much higher than the splitting tensile strength, which might have occurred because the interlocking matrix contributed more to the compressive strength than to the tensile strength. A similar trend was found in the study conducted by Ghafoori et al., in 1995. Unconfined compressive strength and splitting tensile strength decreased with an increase in RAP content from 0% to 50% for a particular cement content, which was also found in previous studies conducted by Faysal et al. in 2017.

Katman et al (2012) stated that the inclusion of asphalt in the RAP increases the tensile strength of the specimen; the results of the tests conducted in this research confirm that statement. 100% RCCA samples had higher tensile strength than the 50% RAP 3a +50% RCCA 3. However, with an increase in asphalt content from 4.4% to 8.4%, the value of tensile strength increased by

33.33% for 50-50 combinations at 4% cement content and by 25% for 50-50 combinations at 6% cement content. The rate of increase in tensile strength was higher in 4% cement than in 6% cement content. Relatively higher cement content results in more brittle behavior, which reduces the tensile strength. Tensile strength of the 50 – 50 combination at 8.4% asphalt content was about 15% more than the tensile strength of 100% RCCA 3 materials, which indicates the improved ductile behavior of the 50% RAP 3c+ 50% RCCA 3 combination. On the other hand, UCS reduces with increase in asphalt content and does not meet the minimum compressive strength requirement of 300 psi. The ratio of STS to UCS varied from 8% to 15% for both of the material combinations.

Table 4.24 Split Tensile Strength for 50% RAP 3b + 50% RCCA 3 (6.5% Asphalt)

Cement Content (%)	Sample ID	Load on Specimen (lb.)	Stress (psi)	Mean Strength (psi)	SD	COV (%)
2	1	2431	21.49	25.03	4.05	16.18
	2	3330	29.44			
	3	2730	24.14			
4	1	3179	28.11	26.93	1.06	3.94
	2	2947	26.06			
	3	3010	26.61			
6	1	3954	34.96	36.74	1.93	5.26
	2	4388	38.80			
	3	4125	36.47			

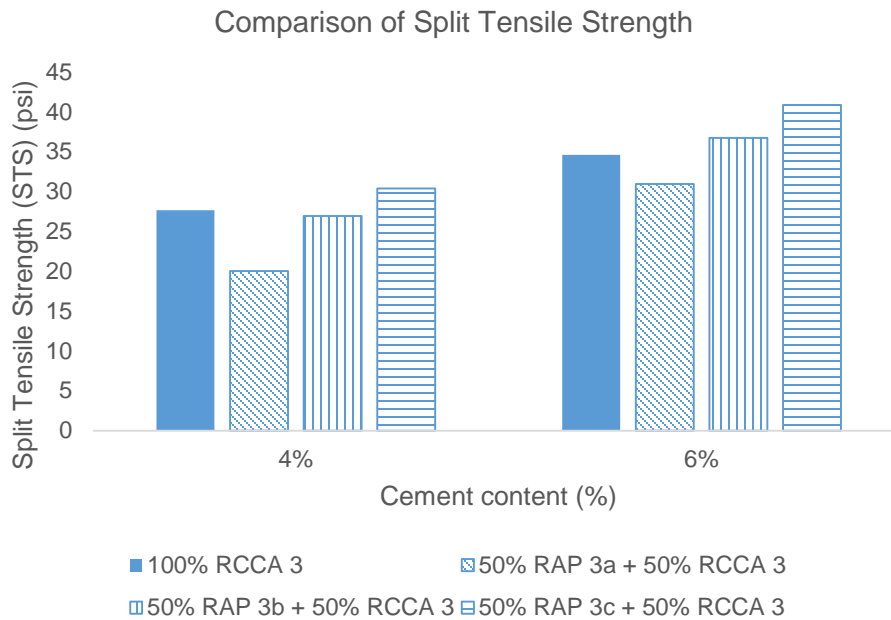


Figure 4.32 Comparison of split tensile strength

#### 4.17.2.3 Comparison between UCS and STS

The value of STS usually remains within 10% to 15% of UCS for concrete cylinder specimens (Anoglu et al. 2006). The value of STS stays within 10% to 20% of UCS for cement-treated base materials (Anagnos et al. 1970). Figure 4.71 shows that both UCS and STS increased with an increase in cement content from 4% to 6%. However, the increase in UCS was comparatively higher than the increase of the STS, which resulted in a lower ratio of STS/UCS. This indicates that excess cement increases brittle behavior. RAP materials containing higher amounts of asphalt had higher split tensile strength than compressive strength, which resulted in a higher value of STS/UCS ratio.

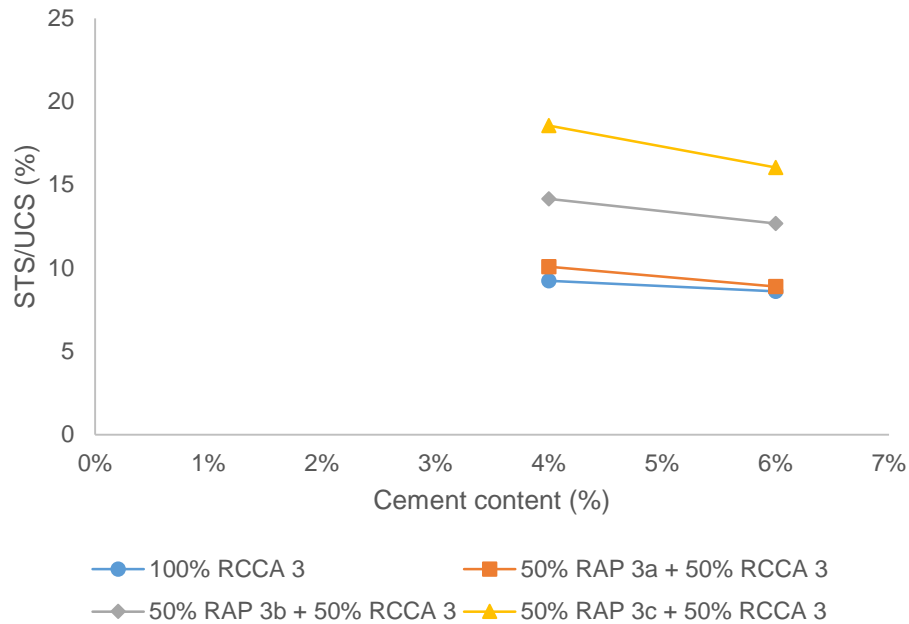


Figure 4.33 Comparison between SCS/UCS at different cement contents

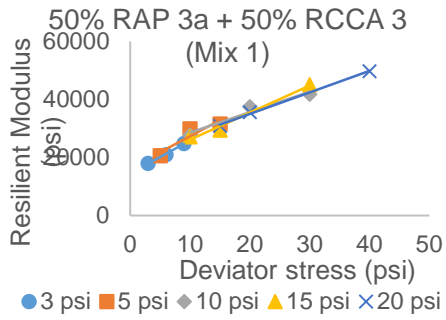
#### 4.17.3 Resilient Modulus

Resilient modulus ( $M_r$ ) tests were conducted in accordance with the AASHTO 2003 guidelines.  $M_r$  values decreased with an increase in asphalt binder at a particular cement content. RAP materials, which contain a high amount of asphalt binder, have a thick asphalt film around the aggregate particles, which creates a matrix that is softer than the matrix created by materials which contain a thinner asphalt film. A soft asphalt binder might have caused the stress concentration that resulted in micro-cracking within the concrete matrix (Huang et al. 2005). This might have contributed to the reduction in resilient modulus with inclusion of asphalt binder at a particular cement content.

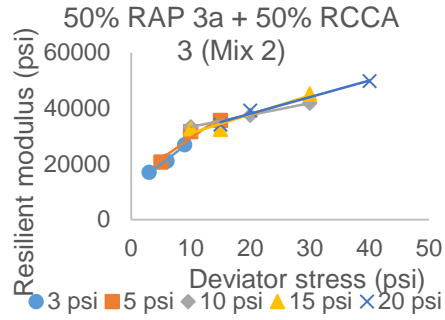
The value of resilient modulus decreased about 13% from Mix 1 to Mix 3, and about 7% from Mix 3 to Mix 5. For the mixtures with 6% cement, the resilient modulus decreased about 15% from Mix 2 to Mix 4 and about 8% from Mix 4 to Mix 6. On the other hand, the resilient

modulus increased with an increase in cement content. There was an approximate 10% increase from Mix 1 to Mix 2, 13% increase from Mix 3 to Mix 4, and 12% increase from Mix 5 to Mix 6. The inclusion of cement improves the internal bonding matrix between asphalt-coated aggregate particles and crushed concrete aggregate particles.

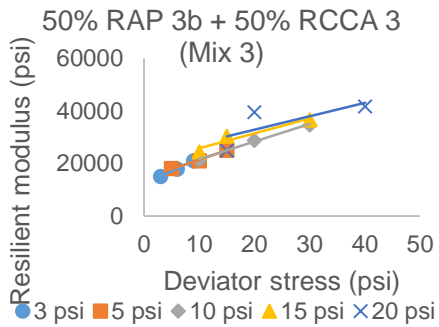
Resilient modulus results were fitted to the two-parameter k- $\theta$  model and three parameter model to verify the accuracy of the test results. According to the AASHTO test procedure requirements, the obtained resilient modulus data was used to develop prediction models. One of them was the “k- $\theta$  model” proposed by Moosazedh and Witczak (1981):  $M_r = k_1 \theta^{k_2}$ , where  $k_1$  and  $k_2$  are model parameters and  $\theta$  is the bulk stress expressed as a combination of confining ( $\sigma_c$ ) and deviator stresses ( $\sigma_d$ ) in the form  $3\sigma_c + \sigma_d$ . . Another model used in this study was the improved three-parameter model (Puppala et. al., 1996):  $M_r = k_3 \sigma_c^{k_4} \sigma_d^{k_5}$ , where  $k_3$ ,  $k_4$  and  $k_5$  are model parameters (Salah et al. 2017).



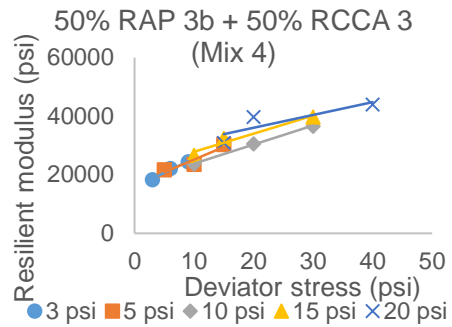
(a)



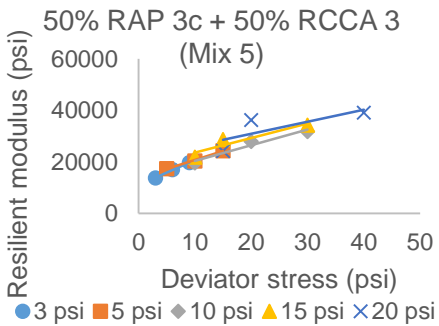
(b)



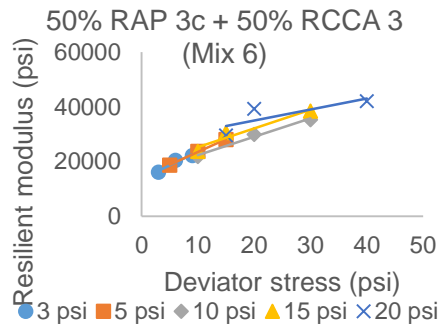
(c)



(d)



(e)



(f)

Figure 4.34 Comparison of resilient modulus ( $M_r$ ) at different combinations

The k- $\theta$  model parameter  $\log k_1$  indicates magnitudes, while  $k_2$  indicates the non-linear nature of the stress dependency (Potturi 2006). The three-parameter model, parameter  $\log k_3$ , indicates the magnitude of the resilient moduli, while  $k_4$ , and  $k_5$  represent the non-linear nature of the stress dependency. The trends of  $\log k_1$ ,  $k_2$ ,  $\log k_3$ ,  $k_4$ , and  $k_5$  were difficult to explain with respect to the amount of RAP mixed in different combinations and with added cement.

Table 4.25 Model Parameters

Mix ID	k- $\theta$ Model			Three parameter model			
	$\log k_1$	$k_2$	$R^2$	$\log k_3$	$k_4$	$k_5$	$R^2$
Mix 1	3.82	0.41	0.81	3.61	0.10	0.63	0.94
Mix 2	3.73	0.46	0.95	4.01	0.00	0.42	0.97
Mix 3	3.71	0.44	0.82	3.89	0.10	0.37	0.92
Mix 4	3.87	0.37	0.81	4.04	0.08	0.30	0.93
Mix 5	3.70	0.42	0.81	3.89	0.10	0.35	0.94
Mix 6	3.79	0.40	0.80	3.97	0.08	0.35	0.94

The value of  $R^2 > 0.8$ , with one or two exceptions, signified good correlation with the statistical regression analysis. The three-parameter model had higher values of  $R^2$  than the two-parameter model for all cases. This is because the three-parameter model considers the individual effects of confining and deviator stresses on resilient modulus, in contrast to the k- $\theta$  model that considers only a combined bulk stress. In , the resilient modulus values obtained from statistical k- $\theta$  model for different combinations of materials are plotted.

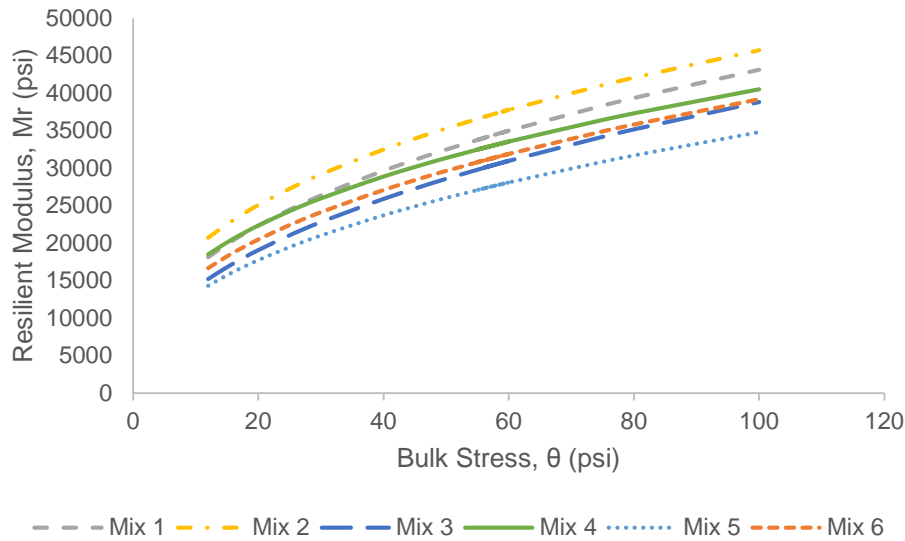


Figure 4.35 Changes in resilient modulus at different asphalt contents

#### 4.17.4 Test Results Analysis

The presence of fine particles in the aggregates has a significant effect on the strength of the materials. The higher the finer aggregate content is, the higher the compressive strength seems to be (Yuan et al. 2012). Finer content varies from 1% to 6%, which is relatively higher (Yuan et al. 2012). Previous studies suggested that the value of CBR increases with an increase in the percentage of fine particles, and CBR values increase approximately 1% with an increase of 1% fine particles for the applied compaction energy of 17.52 lb-ft/ft<sup>3</sup> (Babic et al. 2000). According to the test results, the amount of fines passing through a No. 200 sieves tended to be zero with the inclusion of asphalt binder to the RAP, which might have contributed to the lower compressive strength and resilient modulus for the material combinations which contained more asphalt.

Moreover, additional asphalt binder on the surface of the particles results in a weaker bond between the particles. The thicker the asphalt layer, the weaker the bonding matrix between the particles, which allows the particles to slip when subjected to loading. However, additional

asphalt increases the tensile strength, but at the same time, it reduces the compressive strength and resilient modulus.

Materials in the base layer are subjected to both tension and compression under traffic load; therefore, it is vital for them to fulfill the tension and compression requirements. Usually, the tensile strength is about 10% to 15% of the compressive strength. According to the test results, the tensile strength varied from 9% to 18% of the compressive strength.

The asphalt content of 6% or more did not meet the strength requirement of 300 psi. At 4% cement content, the 50% RAP 3 + 50% RCCA 3 material combination had strength less than 300 psi.

#### Summary:

- Increase in asphalt content reduces the effectiveness of cement as a binder material. Based on the test results, RAP materials which contain 6.5% asphalt cannot be molded at 0% cement content, and RAP materials with 8.4% asphalt binder cannot be molded at 0% or 2% cement content.
- Adding 2% of asphalt binder to the RAP in increments reduces the compressive strength by 10% to 15% with each increment.
- Resilient modulus decreases by 8% to 13% with each increment of 2% asphalt binder added to the RAP.
- Split tensile strength increases with an increase in asphalt binder to the RAP.
- For all of the combinations of the materials, tensile strength is approximately 8% to 19% of compressive strength.

#### 4.18 Effects of Wet and Dry Cycles

The pavement base layer is the most important layer for distributing the traffic load on the subgrade. Variations in climatic conditions affect the pavement performance, and consecutive wetting and drying actions are emphasized in AASHTO (2005). Recycled base materials are weaker than the natural limestone aggregates, which led to the evaluation of the long term durability of recycled materials. Different numbers of wetting and drying cycles were applied to the prepared specimens, after which they were subjected to resilient modulus tests.

Table 4.26 Experimental Program for Resilient Modulus ( $M_r$ ) Tests

Material	Cement Content (%)	Mix ID	Tests	Test Samples					Control Samples					
				Wetting-drying (WD) cycles					Aging (days)					
				0	4	8	16	30	7	15	25	40	70	
50% RAP 3 +	4%	MIX 4	$M_r$	√	√	√	√	√	√	√	√	√	√	√
50% RCCA 3	6%	MIX 6	$M_r$	√	√	√	√	√	√	√	√	√	√	√

The effects of successive wetting-drying (W-D) cycles on strength properties of cement-stabilized RCCA-RAP mix materials were investigated in this study. Due to the lack of standard procedures for wetting-drying of stabilized base materials, experimental methods reported by researchers (Khoury and Zaman, 2002; and Faysal et al. 2017) were adopted for this study. RCCA and RAP materials mixed in 50%-50% proportions and stabilized with 4% (MIX 4) and 6% (MIX 6) cement content were used for this purpose. For each of these material combinations, three control samples and three test samples were prepared, cured for seven days, and then tested for resilient modulus according to AASHTO T 307-99 test procedures. The test samples were then subjected to wetting-drying (W-D) cycles. Each W-D cycle consisted of drying the sample in the oven (71°C/160°F) for 24 hours, followed by submerging it in potable water for 24 hours. For this study, the 0, 4, 8, 16, and 30 W-D cycles were considered. After completing a specified number

of cycles, the samples were used for tests for resilient modulus ( $M_r$ ). The control samples were cured by following the conventional process. After curing for 15, 25, 40, and 70 days, the samples were tested again for  $M_r$ . In this study each sample was subjected to multiple resilient modulus tests after specific times. This approach was considered reasonable since resilient modulus tests involve very low levels of strain (Khoury and Zaman, 2007).

Environmental tests were conducted on the test samples prepared from the RCCA-RAP material mix, as shown in Table 4.27. The samples were subjected to 0, 4, 8, 16, and 30 W-D cycles. At the end of the cycles, the samples were soaked in deionized water for 24 hours, and leachate samples were collected. Environmental tests such as total suspended solids (TSS), total dissolved solids (TDS), chemical oxygen demand (COD), turbidity, and pH tests were conducted on the collected leachate samples according to the ASTM standard methods. TSS and TDS tests were conducted for filterable and non-filterable matter in water. A glass fiber filter paper of 1.5 $\mu$ m nominal pore size was used to filter the leachate samples. The solid materials retained on the filter paper are called total suspended solids (TSS); filtrate is called total dissolved solids (TDS).

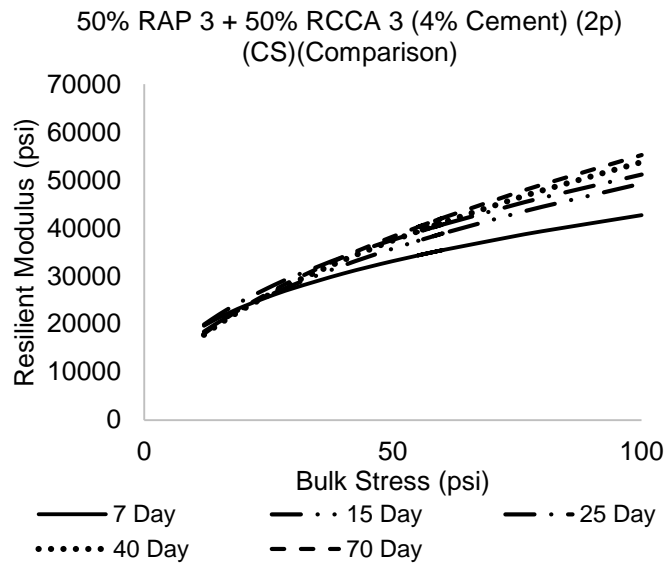
Table 4.27 Environmental Tests Program

Material	Cement content (%)	Mix ID	Environmental Tests	Test Samples				
				Wetting-drying (WD) cycles				
				0	4	8	16	30
50% RAP 3 + 50% RCCA 3	4	MIX 4	COD	√	√	√	√	√
			TDS	√	√	√	√	√
			TSS	√	√	√	√	√
			Turbidity	√	√	√	√	√
			pH	√	√	√	√	√
	6	MIX 6	COD	√	√	√	√	√
			TDS	√	√	√	√	√
			TSS	√	√	√	√	√
			Turbidity	√	√	√	√	√
			pH	√	√	√	√	√

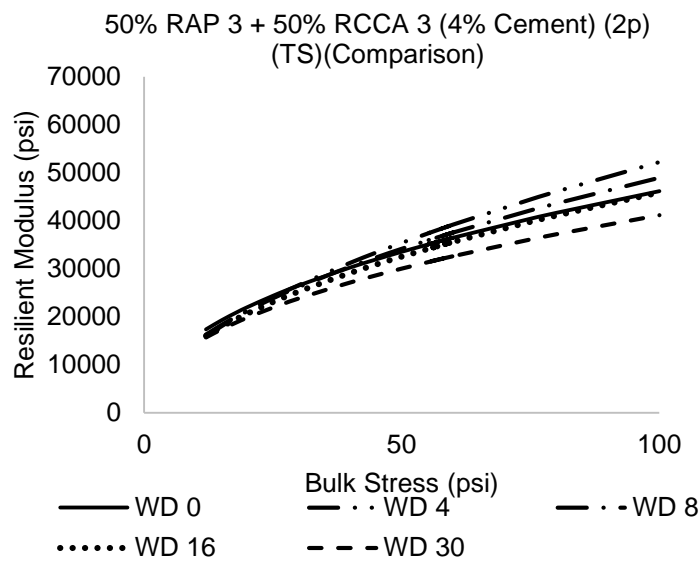
#### 4.18.1 Resilient Modulus Test Results

##### 4.18.1.1 Data Analysis and Model Fitting

Two separate sets of control and tests samples were prepared for MIX 4 and MIX 6. Each set consisted of three identical samples, on which resilient modulus tests were conducted. For all of the cases, the coefficient of variation (COV) of the  $M_r$  values was found to be within 0.15% - 8.63%, which showed good repeatability of the performed tests. According to AASHTO test procedure requirements, the obtained resilient modulus data was used to develop prediction models. One of them was the “k- $\theta$  model” proposed by Moosazedh and Witczak (1981):  $M_r = k_1\theta^{k_2}$ , where  $k_1$  and  $k_2$  are model parameters and  $\theta$  is the bulk stress expressed as a combination of confining ( $\sigma_c$ ) and deviator stresses ( $\sigma_d$ ) in the form  $3\sigma_c + \sigma_d$ . Figure 4.36 and Figure 4.37 show the k- $\theta$  models developed for the control and test samples of MIX 4 and MIX 6. The improved three-parameter model was also used in this study (Puppala et. al., 1996):  $M_r = k_3\sigma_c^{k_4}\sigma_d^{k_5}$ , where  $k_3$ ,  $k_4$  and  $k_5$  are model parameters. Statistical analysis was conducted to examine the accuracy of these models. The model parameters, along with the calculated statistical parameters, are presented in Table 4.28 and Table 4.29.

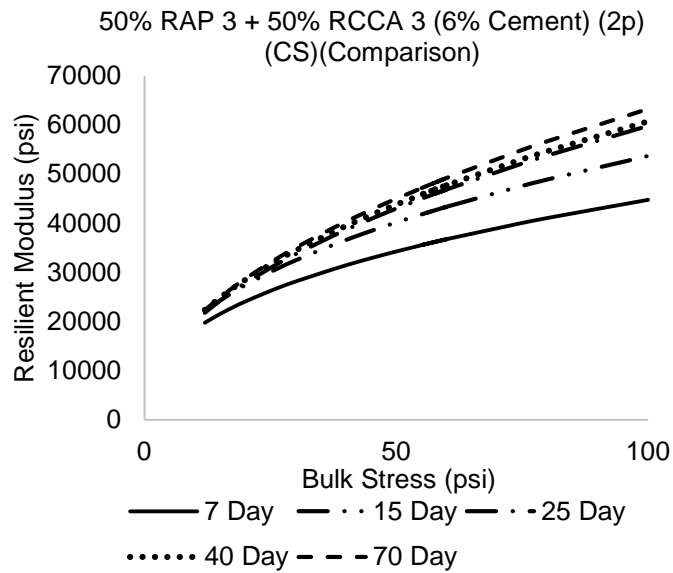


(a)

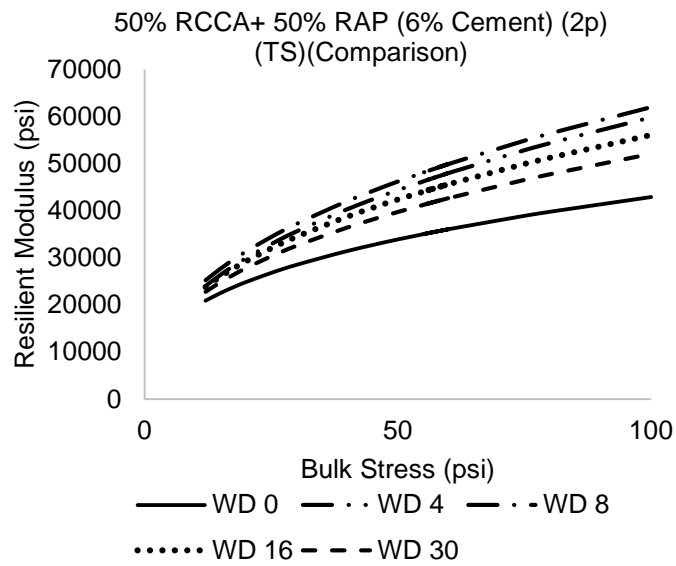


(b)

Figure 4.36 Graphical plot of k- $\theta$  or 2p models developed for (a) Control samples (CS) and (b) Test samples (TS) of MIX 4 materials



(a)



(b)

Figure 4.37 Graphical plot of  $k-\theta$  or  $2p$  models developed for (a) Control samples (CS) and (b) Test samples (TS) of MIX 6 materials

Table 4.28 Model Parameters for MIX 4

		Two Parameter Model			Three Parameter Model			
		k <sub>1</sub>	k <sub>2</sub>	R <sup>2</sup>	k <sub>3</sub>	k <sub>4</sub>	k <sub>5</sub>	R <sup>2</sup>
Number of W-D Cycles	0	5528.7	0.46	0.83	11074	0.04	0.41	0.89
	4	3956.8	0.56	0.92	7866.7	0.24	0.34	0.95
	8	4487	0.52	0.94	8874.5	0.28	0.24	0.95
	16	4669.4	0.49	0.91	9788.2	0.39	0.11	0.91
	30	5088	0.45	0.91	10384	0.40	0.03	0.91
Curing	7 day	7918.2	0.37	0.82	11074	0.03	0.37	0.97
	15 day	5814.8	0.46	0.83	9218.9	0.08	0.41	0.94
	25 day	6575.6	0.44	0.97	11825	0.24	0.20	0.98
	40 day	4861.7	0.52	0.95	9581.8	0.28	0.25	0.96
	70 day	4797.4	0.53	0.94	9294.5	0.24	0.30	0.96

Table 4.29 Model Parameters for MIX 6

		Two-Parameter Model			Three-Parameter Model			
		k <sub>1</sub>	k <sub>2</sub>	R <sup>2</sup>	k <sub>3</sub>	k <sub>4</sub>	k <sub>5</sub>	R <sup>2</sup>
W-D Cycles	0	9006	0.34	0.82	12482.5	0.041	0.32	0.97
	4	8249.41	0.43	0.84	13021	0.08	0.38	0.97
	8	8816.9	0.42	0.90	14379.7	0.12	0.32	0.96
	16	8764.35	0.40	0.89	14162.8	0.14	0.27	0.96
	30	8646	0.39	0.94	14427.4	0.20	0.19	0.96
Curing	7 day	7587.86	0.39	0.82	11096	0.06	0.36	0.95
	15 day	7828	0.42	0.82	11863	0.10	0.35	0.93
	25 day	6664.81	0.48	0.87	10810.1	0.10	0.41	0.97
	40 day	6939.94	0.47	0.85	11072.5	0.08	0.42	0.96
	70 day	6581	0.49	0.81	10302	0.09	0.46	0.96

4.18.1.2 Effects of Aging

The two-parameter k-θ model developed for the control samples of MIX 6 is plotted in Figure 4.37(a). With an increase in curing time, the resilient modulus (M<sub>r</sub>) curves for the samples shifted, resulting in higher values of resilient modulus. The M<sub>r</sub> values increased by about 30% after 25 days of curing, beyond which the curves of 40 and 70 days almost coincided with each other. This indicates that the MIX 6 material gains almost all of its stiffness within the first 25 days.

Plots for the MIX 4 material, as shown in Figure 4.36(a), reflect similar trends. In this case, the  $M_r$  values increased to about 20% at the end of 25 days.

Table 4.30 Model Parameters for MIX 6

		Two-Parameter Model			Three-Parameter Model			
		$k_1$	$k_2$	$R^2$	$k_3$	$k_4$	$k_5$	$R^2$
W-D Cycles	0	9006	0.34	0.82	12482.5	0.041	0.32	0.97
	4	8249.41	0.43	0.84	13021	0.08	0.38	0.97
	8	8816.9	0.42	0.90	14379.7	0.12	0.32	0.96
	16	8764.35	0.40	0.89	14162.8	0.14	0.27	0.96
	30	8646	0.39	0.94	14427.4	0.20	0.19	0.96
Curing	7 day	7587.86	0.39	0.82	11096	0.06	0.36	0.95
	15 day	7828	0.42	0.82	11863	0.10	0.35	0.93
	25 day	6664.81	0.48	0.87	10810.1	0.10	0.41	0.97
	40 day	6939.94	0.47	0.85	11072.5	0.08	0.42	0.96
	70 day	6581	0.49	0.81	10302	0.09	0.46	0.96

#### 4.18.1.3 Effects of Wet-Dry Cycles

The test samples of both MIX 4 and MIX 6 materials were first cured for seven days and then subjected to wet-dry (W-D) cycles. Resilient modulus ( $M_r$ ) tests were conducted on the samples after 0, 4, 8, 16, and 30 W-D cycles. The  $k$ - $\theta$  models developed for the test samples of MIX 6 are plotted in Figure 4.37(b). It was observed that  $r$  increased by about 42% after 8 W-D cycles. This is because moisture intrusion resulting from the first 8 W-D cycles contributed towards cement hydration, rather than weakening the materials. This induced higher stiffness properties, which increased resilient modulus. Additional wet-dry cycles caused a reduction in  $M_r$  values. A cumulative drop of about 21% in resilient modulus was observed from 8 to 30 W-D cycles.

MIX 4 materials exhibited a comparatively weaker response to the wet-dry cycles. Values of resilient modulus were found to increase by 16% at the end of 4 W-D cycles (Figure 4.36(b)). A further increase in W-D cycles caused a decrease in  $M_r$  values.

At the end of 30 W-D cycles, the  $M_r$  of the test samples was found to be about 11% lower than the 7-day cured value. This can be attributed to the fact that repeated wetting-drying processes have adverse effects on binding properties of cement (Khoury and Zaman, 2007).

#### 4.19 Environmental Tests

##### 4.19.1 *Chemical Oxygen Demand (COD)*

The amount of oxygen required by water-borne organic and inorganic matter for oxidation by a strong chemical oxidant such as dichromate solution is designated as chemical oxygen demand (COD). The COD test is an indirect method of determining the organic pollutants in water, especially surface and waste water. Potassium dichromate solution is used as an indicator of the organic substances in the solution. The reduction in dichromate solution indicates the amount of oxygen that can be consumed by the impurities in water (ASTM 2011). The value of COD is typically used to monitor and control the inorganic and organic oxygen-consuming pollutants in water (ASTM 2012).

##### 4.19.1.1 *Effect of Combinations of Materials on COD*

According to the test results shown in Figure 4.38, the value of COD decreased with an increase in cement content. The amount of traceable fine particles in the leachate also decreased with an increase in cement content. The value of COD decreased by 41% with inclusion of cement content from 0% to 6% in the RCCA materials. The amount of COD decreased by 33.33% with inclusion of cement content from 2% to 6% in mixed materials. Hence, the value of COD increases with the inclusion of RAP materials, which contributes to RAP materials being relatively weaker and degrading more than 100% RCCA materials (Faysal et al. 2016a). The value of COD obtained was less than 120 mg/L, which complies with EPA guidelines.

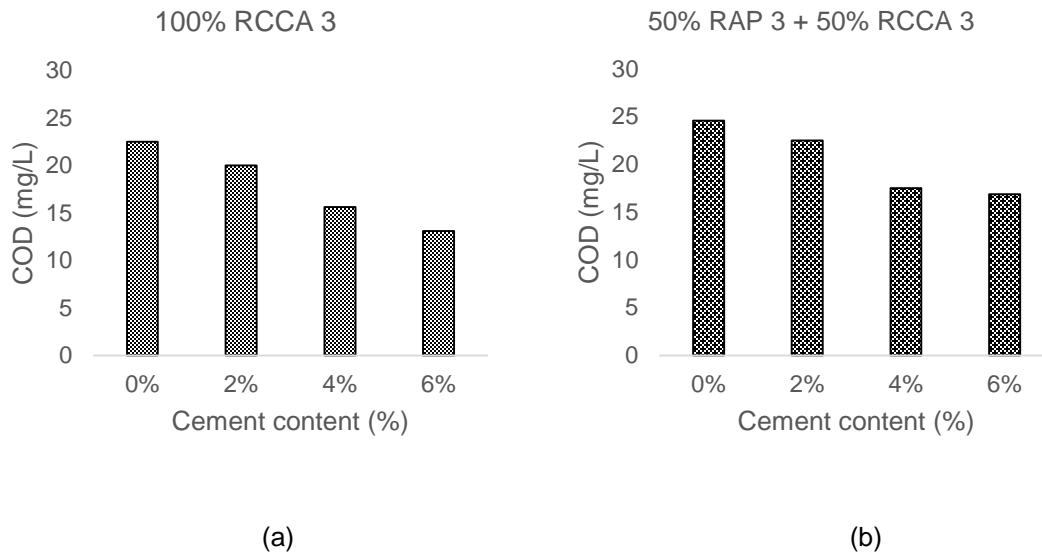


Figure 4.38 Chemical Oxygen Demand (COD) test results (a) 100% RCCA 3, and (b) 50% RAP 3 + 50% RCCA 3

#### 4.19.1.2 Effects of Wet-Dry Cycles on COD

The COD concentration in the water samples was determined by using the Spectronic 20D+ model spectrometer. Changes in COD with different numbers of wet and dry cycles is shown in Figure 4.39. Test results indicated that the value of COD increased up to 4 wet-dry cycles, and COD decreased from 4 to 8 wet-dry cycles. MIX 4 samples released a higher concentration of chemicals when subjected to 4 wet-dry cycles, after which there was a reduction in the released chemical compounds. The amount of chemical compounds released into the leachate for MIX 6 samples up to 4 wet-dry cycles was higher than that of 4 to 8 wet-dry cycles, which might have occurred because of the reduction in the rate of hydration. The value of COD obtained for MIX 4 samples was less than the MIX 6 samples, indicating that specimens stabilized with higher cement content release more chemical compound in the leachate.

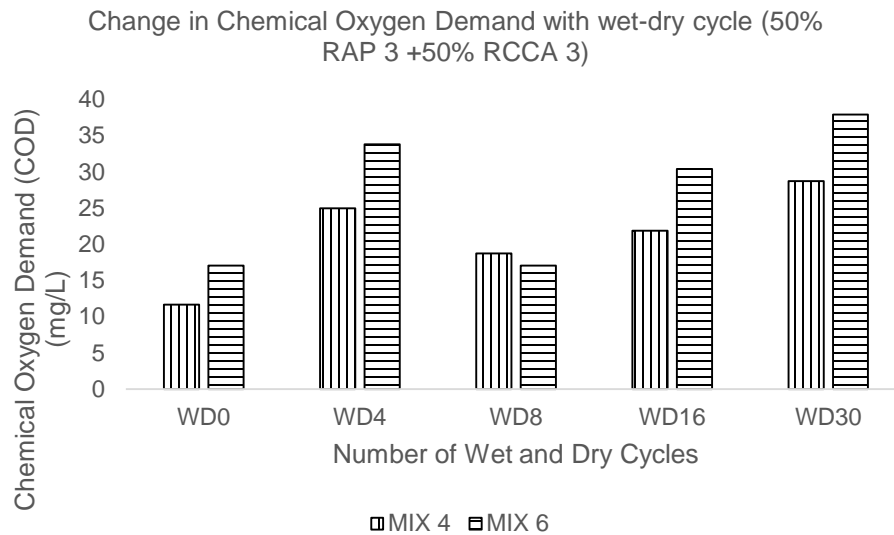


Figure 4.39 Change in chemical oxygen demand (COD) with wetting-drying cycles

The value of resilient modulus decreases with an increase in the number of W-D cycles. Khoury and Zaman (2007) reported that this reduction in strength is due to the adverse effects of repeated wetting-drying processes on binding properties of cement. The value of resilient modulus decreased after the completion of 8 W-D cycles for the specimens stabilized with 4% and 6% cement. The decrease in the resilient modulus shows the degradation of the specimens, which led to the increased value of the COD. From 8 to 30 wet-dry cycles, the value of COD increased by 1.5 and 2.2 times for MIX 4 and MIX 6 samples, respectively. The value of COD obtained was less than 120 mg/L, which is within the EPA guidelines.

#### 4.19.2 Total Suspended Solids (TSS)

Total suspended solids (TSS), also known as non-filterable matter, is an important parameter for determining the impurities in raw water, wastewater, and in streams. A TSS test was conducted in accordance with ASTM D5907-13 standard method for non-filterable matter.

#### 4.19.2.1 Effect of Different Combinations of Materials on TSS

Inclusion of RAP content reduces the unconfined compressive strength (Faysal et al 2016) and might have contributed to the higher amount of suspended solids in the leachate. According to the EPA guidelines, the value of TSS should be less than 100mg/L (EPA 2005). TSS test results indicated that the values were well within the limit for all combinations of the materials (Figure 4.40).

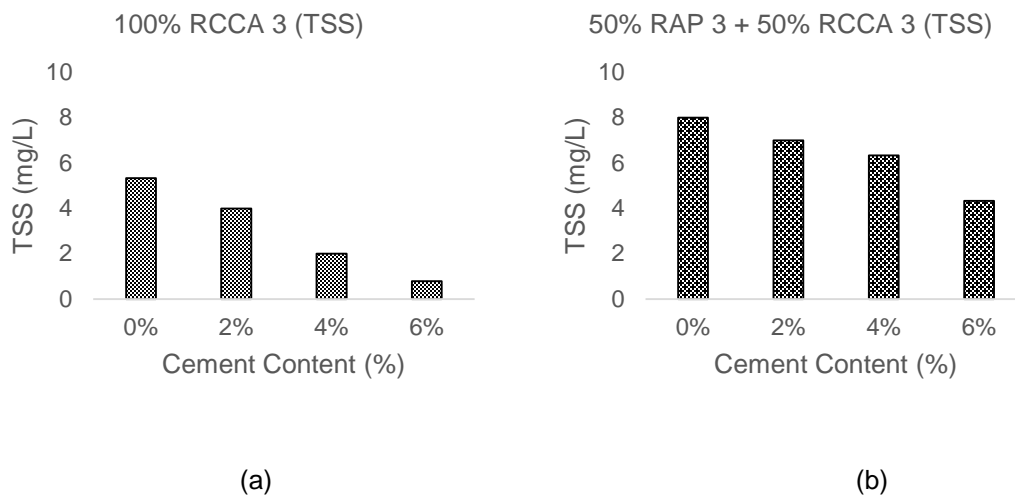


Figure 4.40 Total suspended solids (TSS) test results (a) 100% RCCA 3, and (b) 50% RAP 3 + 50% RCCA 3

#### 4.19.2.2 Effects of Wet-dry Cycles on TSS

TSS test results showed that the value of TSS in leachate samples decreased by 80% and 83% for MIX 4 and MIX 6, respectively, with the increase in the number of wet and dry cycles from 0 to 30. This might have occurred because of the improved interparticle bond and well-developed matrix due to hydration of cementitious materials within the specimens. According to the test results, the value of TSS was higher for the leachate samples obtained for MIX 4 than for MIX 6. This may be because the 4% cement content was weaker than the prepared specimens at 6% cement content, as shown in Figure 4.41.

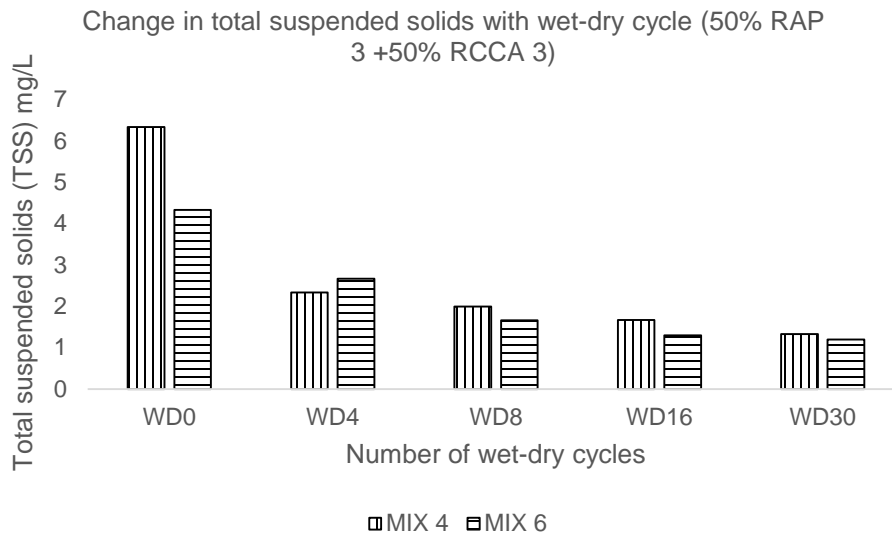


Figure 4.41 Change in total suspended solids (TSS) with wetting-drying cycles

#### 4.19.3 Total Dissolved Solids (TDS)

Total dissolved solids (TDS) or filterable parameter is one of the important parameters for the treatment of raw water, wastewater, and for monitoring streams. TDS tests were performed in accordance with the ASTM D5907-13 standard method for filterable matter (ASTM). Filtrate was obtained after passing the leachate through the glass fiber filter paper of 1.5  $\mu\text{m}$  nominal pore size. Dissolved solids represent the amount of cementitious materials washed out from the specimen due to its reaction with water (Faysal et al. 2017).

##### 4.19.3.1 Effect of Different Combinations of Materials on TDS

The value of TSS reduces with the inclusion of a higher cement dosage, which is quite contrary to the trend obtained for TDS. Dissolved solids represent the amount of cementitious material washed out from the specimen due to its reaction with water. Variations in TDS readings with change in cement content and RAP content are included in Figure 4.42. The amount of TDS in leachate was higher for 6% cement content, and it reduced with decreasing cement content.

The value of TDS should be less than 500mg/L as per EPA guidelines (EPA 2005), and the test results complied with the limit.

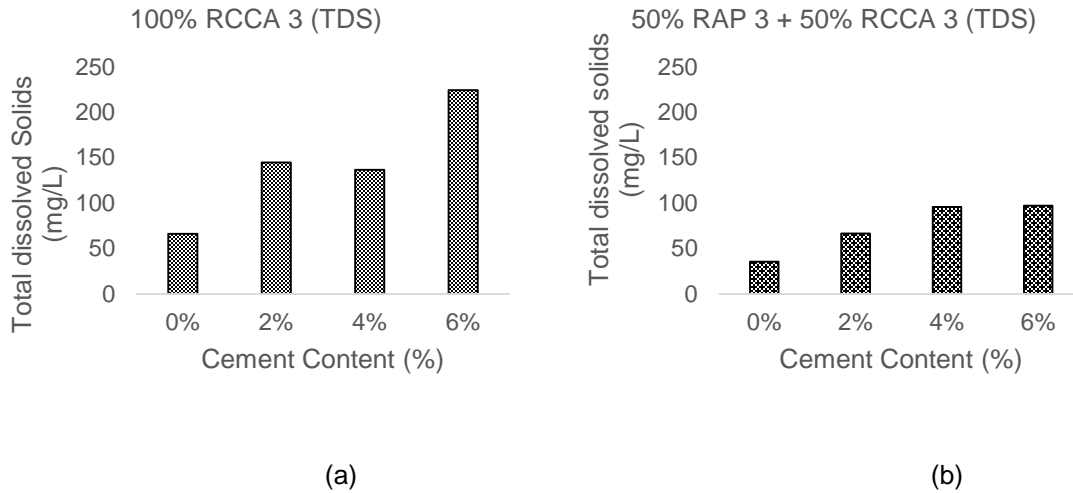


Figure 4.42 Total dissolved solids (TDS) test results (a) 100% RCCA 3, and (b) 50% RAP 3 + 50% RCCA 3

#### 4.19.3.2 Effect of Wet-Dry Cycles on TDS

TDS tests were conducted on the collected leachate samples after 0, 4, 8, 16, and 30 wet and dry cycles. The value of TDS changed with the cement content and number of wet and dry cycles (Figure 4.43). The lower cement content resulted in a value of TDS that was lower than that of the specimens containing a higher cement content. TDS values obtained at different cycles followed a trend similar to COD. TDS values increased with an increase in wet-dry cycles up to 4; after that, they reduced after completion of 8 wet-dry cycles. During the first 4 wet-dry cycles, the value of TDS increased due to the rapid hydration process. The value of TDS increased 75% and 83% for MIX 4 and MIX 6 samples, respectively, with the increase in WD cycles from 8 to 30 cycles. The increased value of TDS denotes the degradation of strength of specimens, which complies with the trend obtained from the resilient modulus test results at different numbers of wet

and dry cycles. TDS test results were well within the limit of 500 mg/L as per EPA guidelines (EPA 2005).

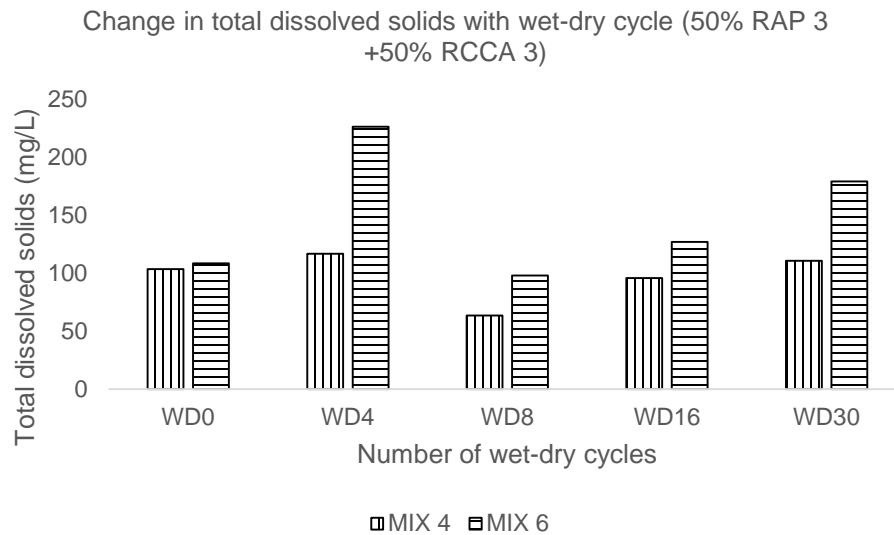


Figure 4.43 Change in total dissolved solids (TDS) with wetting-drying cycles

#### 4.19.4 Turbidity

Turbidity is a parameter employed to determine the amount of suspended matter, such as soil particles, different types of organic and inorganic matter, and microorganisms present in water. Turbidity was measured using a HACH 2100P portable turbidimeter that operates on the nephelometric principle of turbidity measurement in Nephelometric Turbidity Unit (NTU). This equipment measures the optical property of water, such as the amount of light scattered and absorbed while passing through the water sample.

##### 4.19.4.1 Effects of Different Combinations of Materials on Turbidity

The variations in turbidity test results, due to different combinations of cement-stabilized materials, are included in Figure 4.44. It can be inferred that the value of turbidity decreases with

increase in cement content. The maximum value of turbidity was 1NTU, which satisfies the EPA guidelines.

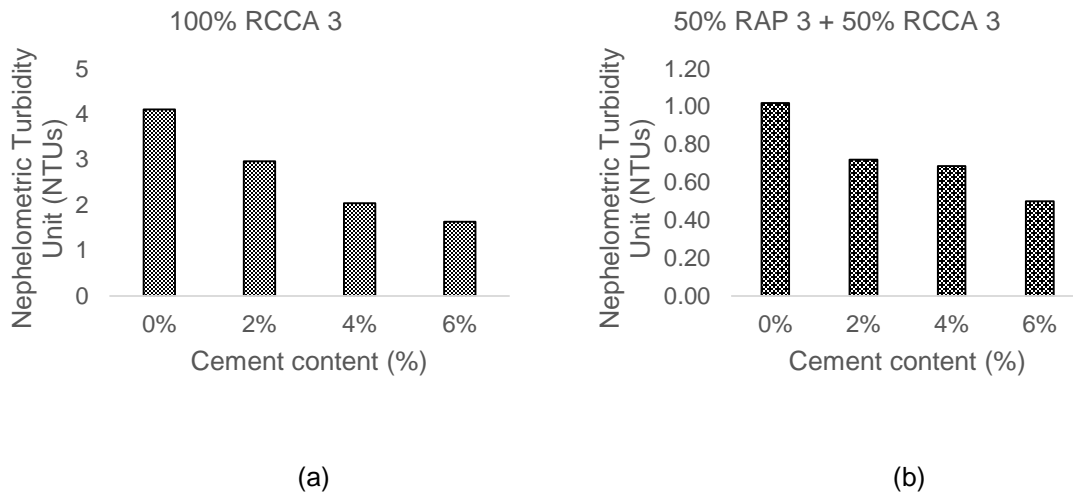


Figure 4.44 Turbidity test results (a) 100% RCCA 3, and (b) 50% RAP 3 + 50% RCCA 3

#### 4.19.4.2 Effect of Wet-Dry Cycles on Turbidity

Turbidity tests were conducted on the collected leachate samples after 0, 4, 8, 16, and 30 wet and dry cycles. The value of turbidity changed with the cement content and number of wet and dry cycles (Figure 4.45). The lower cement content resulted in a higher value of turbidity than the specimens which contain higher cement content. Turbidity test results were well within the limit of 5 NTU as per EPA guidelines (EPA 2005).

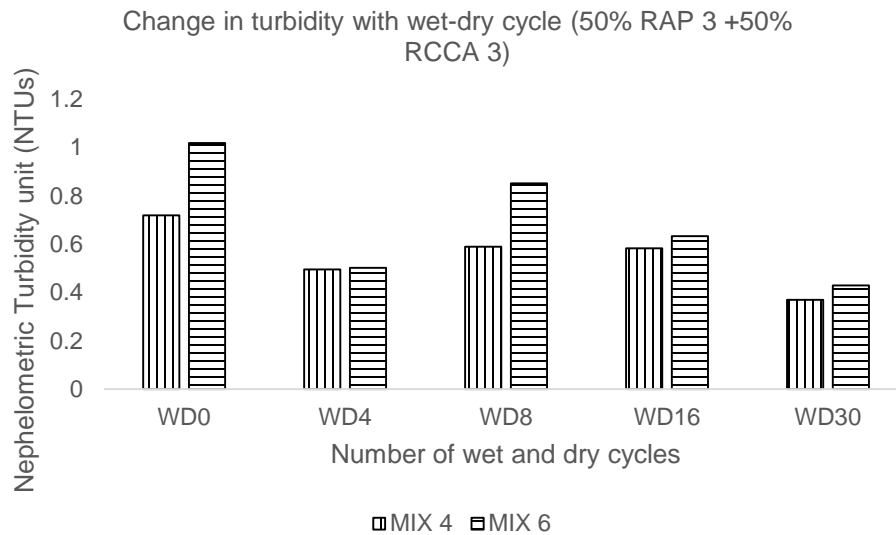


Figure 4.45 Change in turbidity with wetting-drying cycles

#### 4.19.5 pH

pH is the measure of the acidity or alkalinity of water or leachate samples. A pH test was performed in accordance with ASTM D1287. The value of pH ranges from 0 to 14. pH values from 0 to 7 indicate acidic property, whereas values ranging from 7 to 14 indicate alkaline properties. The value of pH was determined by using a dual channel pH conductivity meter.

##### 4.19.5.1 Effect of Different Combinations of Materials on pH

The pH test results were obtained by inserting the probe of the pH meter into the solution of deionized water that the specimens had soaked in for 24 hours, following the seven-day curing period. The value of pH increased with an increase in cement content in the prepared specimens. This might have occurred because of the hydration reaction that took place between the water and calcium carbonate to form soluble calcium hydroxide (Faysal et al. 2017). Test results are shown in Figure 4.46. The alkaline chemical compound in the solution affected the value of pH by increasing the alkalinity of the solution, as evidenced by the test results. pH tests were conducted on the solution after only seven days of curing period, which was not sufficient time for the total

completion of the hydration reaction (Hoyos et al. 2011). The value of pH is expected to decrease in cement-treated specimens cured for longer period of time, and the inclusion of RAP 3 content in RCCA 3 materials has quite a significant effect on pH readings. The value of pH decreased with inclusion of RAP 3 materials in the combinations (Figure 4.46). RAP material consists of asphalt, which contains carboxylic acid and reduces the value of pH (Curtis 1992). The value of pH should be within the range of 6 to 9 as per EPA guidelines for storm water sampling (EPA 2005). Test results obtained for 100% RCCA 3 did not fall within the range of EPA guidelines for storm water sampling. However, it is worth noting that cement-treated RCCA 3 material used as a base layer is not expected to be in direct contact with runoff water; therefore, it would not affect the potable water. Consequently, the pH value obtained from the specimen soaked in water might be a conservative estimation (Hoyos et al. 2011).

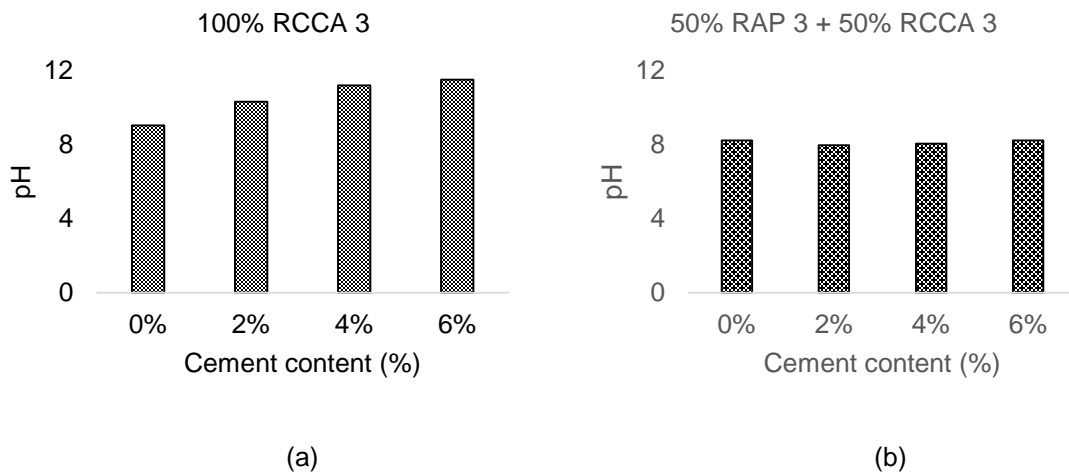


Figure 4.46 Turbidity test results (a) 100% RCCA 3, and (b) 50% RAP 3 + 50% RCCA 3

#### 4.19.5.2 Effects of Wet-Dry Cycles on pH

pH tests were conducted on the collected leachate samples after 0, 4, 8, 16, and 30 wet and dry cycles. The value of pH changed with the cement content and number of wet and dry cycles (Figure 4.47). The pH value of MIX 6, which contained 6% cement, had a higher value of

pH than MIX 4, which contained 4% cement content. The pH value dropped until the completion of 8 wetting-drying cycles, then resilient modulus test results showed that the  $M_r$  values decreased after 8 wetting-drying cycles, indicating the weakening of the tested specimens, which released alkali chemical constituents into the solution and increased the pH.

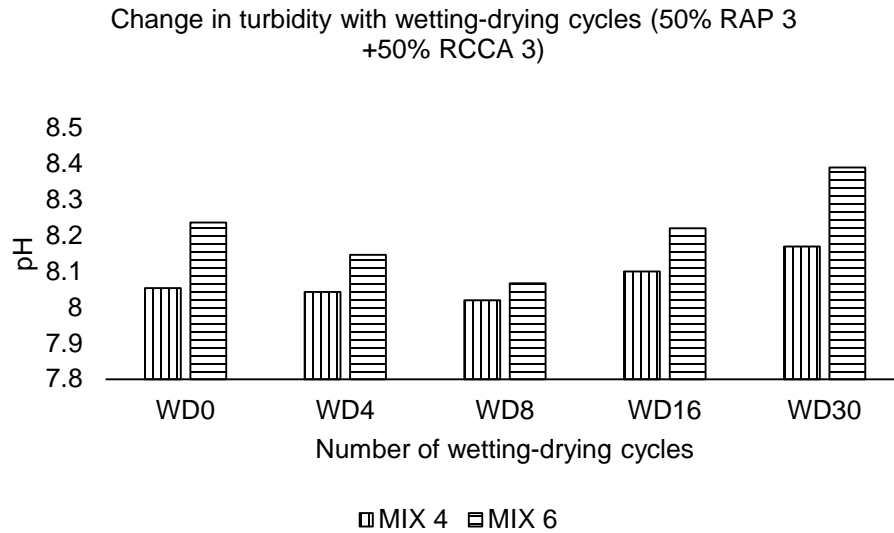


Figure 4.47 Change in pH with wetting-drying cycles

#### 4.20 Summary

The objective of this chapter was to determine the effects, on the strength and stiffness properties, of mixing RAP materials with RCCA at different cement contents. Different amounts of asphalt were added to RAP materials obtained from a particular source, and the strength and stiffness properties were determined. Durability was determined by applying different numbers of wetting-drying cycles to the prepared specimens. The vulnerability of these materials to different environmental conditions was also determined.

## Chapter 5

### Regression Model

#### 5.1 Introduction

Resilient modulus ( $M_r$ ) is one of the most important parameters for design of pavement structures. However, the resilient modulus test is expensive, time consuming, and labor intensive. Consequently, it is necessary to determine the value of resilient modulus by using other strength properties, which can be obtained from tests that are easier to administer. Lotfi and Witczak (1985) evaluated the  $M_r$  and UCS values of five cement-treated base/ subbase materials used by the Maryland State Highway Administration, and correlated the  $M_r$  and UCS values to develop semi-logarithmic regression models for the materials with correlation coefficients ranging from 0.842 to 0.905. Another study, conducted by Pandey in 1996, developed correlations of  $M_r$  with UCS and EM values. The  $M_r$  values used for developing the correlation corresponded to bulk stress of 30 and 50 psi. However, the model developed for  $M_r$  was fixed at higher bulk stress, such as 30 psi and 50 psi, due to higher variability of  $M_r$  at lower bulk stresses.

In this study, four parameters, cement content, unconfined compressive strength (UCS), elastic modulus (EM), and bulk stress ( $\theta$ ), were used to develop a statistical model. A multiple linear regression (MLR) model was developed to correlate the resilient modulus ( $M_r$ ) with bulk stress ( $\theta$ ), cement content, unconfined compressive strength (UCS), and elastic modulus (EM). Multiple linear regression (MLR) analyses were conducted using statistical analysis software R Studio (2016), and model assumptions were verified. The analysis procedure is illustrated in Figure 5.1.

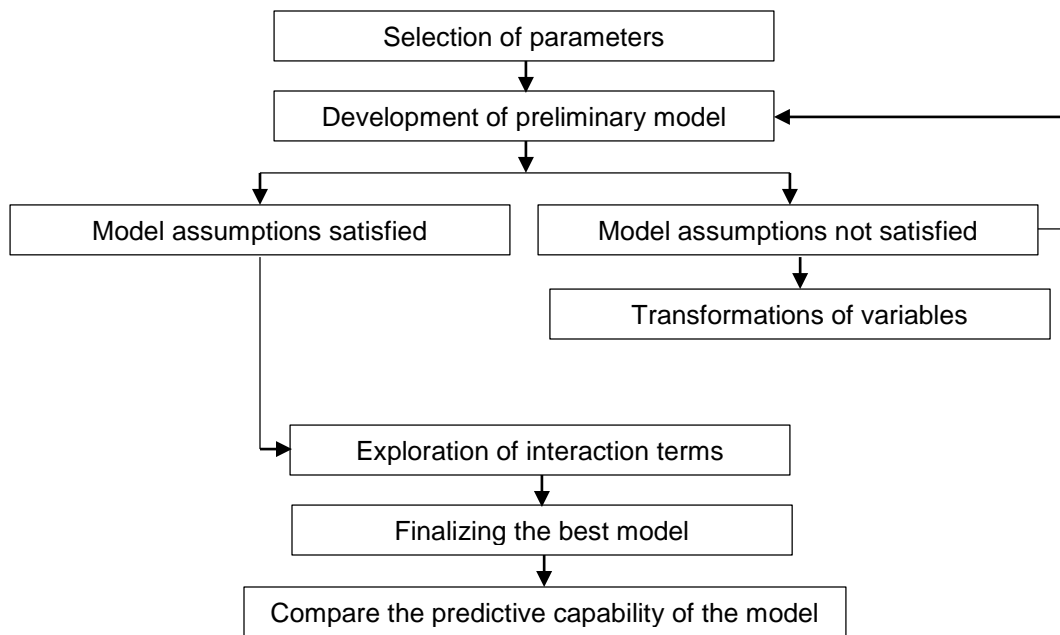


Figure 5.1 MLR model development using R Studio

## 5.2 Parameters Selection for MLR Model

The predictor variables of a MLR model should not be correlated among themselves (Kutner et al. 2005). However, predictors cannot always be controlled in real life scenarios, and correlation among themselves does exist. The problem of interrelation among predictor variables is designated as multicollinearity. If a strong correlation exists among predictors, the answer obtained depends highly on the predictors in the model. Change in expected results for unit change in a predictor variable may be inappropriate in this situation. Multicollinearity may pose three setbacks in a MLR model, such as: a) reducing the coefficient of regression b) difficulty in determining the importance of the variables, and c) increasing the variance (Stevens, 1995).

The strength parameters such as UCS and EM are correlated with each other because they are obtained from same test data. According to the test results in this study, UCS and EM increased with an increase in cement content. The value of the resilient modulus depends on the bulk stress ( $\theta$ ) which can be validated by the  $k$ - $\theta$  model discussed in previous chapter.

The objective of this study is to develop a MLR model to correlate resilient modulus ( $M_r$ ) of recycled base materials with bulk stress ( $\theta$ ), cement content, unconfined compressive strength, and elastic modulus so that resilient modulus test data can be obtained from an unconfined compressive strength test, rather than the resilient modulus test, which is more difficult to perform.

### 5.3 Multiple Linear Regression Analysis

This section includes a detailed description of the multiple linear regression analysis. Based on the lab test results, a MLR equation was developed to predict the resilient modulus of recycled base materials as a function of bulk stress ( $\theta$ ), cement content (CC), unconfined compressive strength (UCS), and elastic modulus (EM).

#### 5.3.1 Correlation Analysis

##### 5.3.1.1 Response vs. Predictor Plots

The response variable was plotted against each of the predictor variables, as shown in the following figures. The units used for all of the parameters are in psi. The relationship between  $M_r$  and BS seems to be curved, and the error variance increased with an increase in bulk stress (Figure 5.2).  $M_r$  increased with cement content (Figure 5.3).  $M_r$  and UCS showed a curvilinear relationship (Figure 5.4), and a similar trend was observed for  $M_r$  and EM.

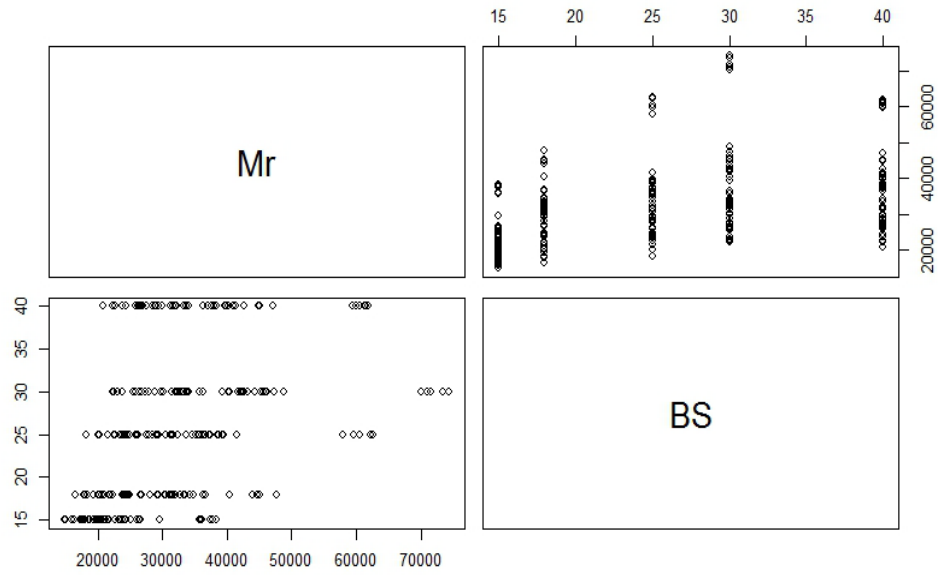


Figure 5.2 The correlation of resilient modulus ( $M_r$ ) with bulk stress (BS) (units are in psi)

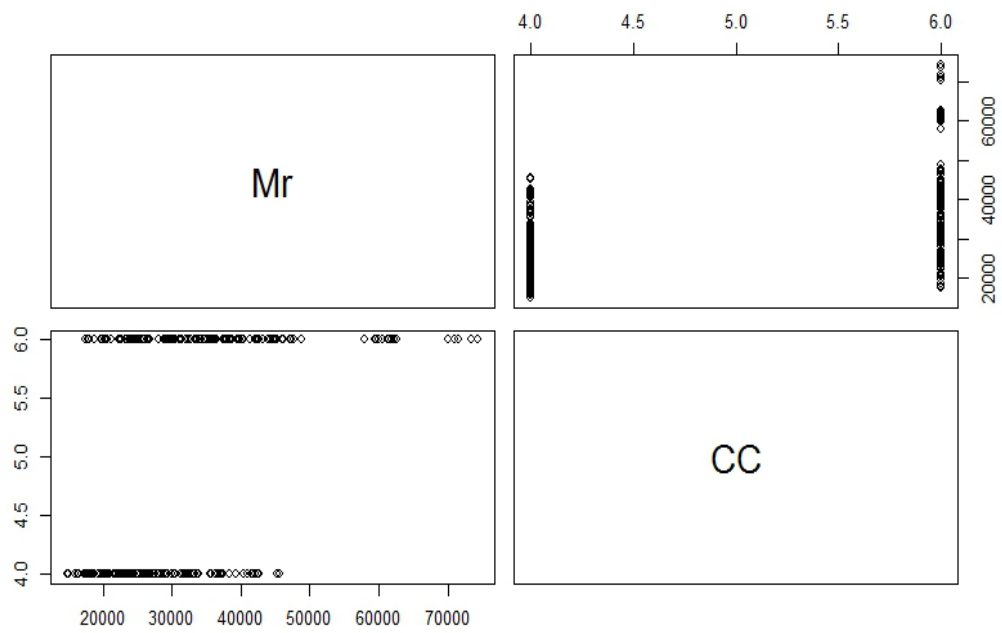


Figure 5.3 The correlation of resilient modulus ( $M_r$ ) (psi) with cement content (CC)

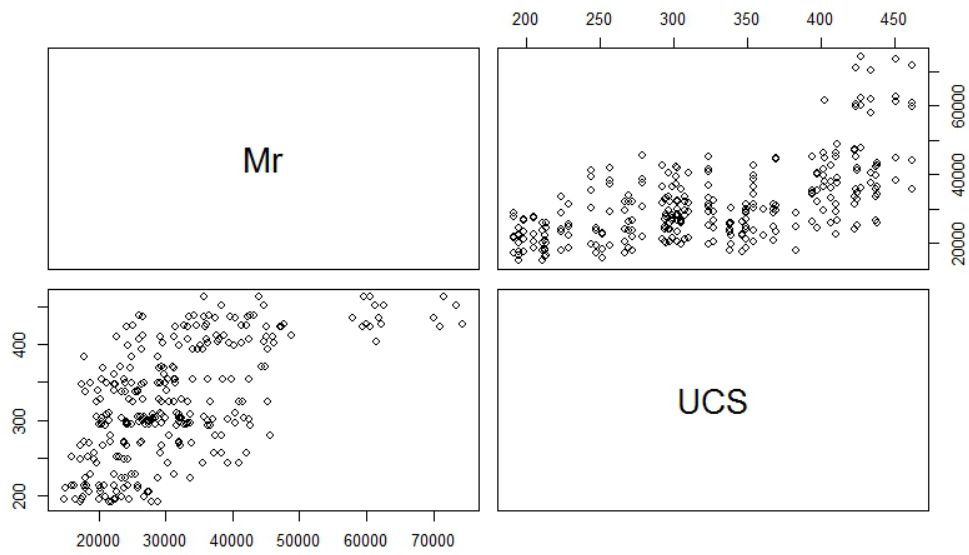


Figure 5.4 The correlation of resilient modulus ( $M_r$ ) (psi) with unconfined compressive strength (UCS)

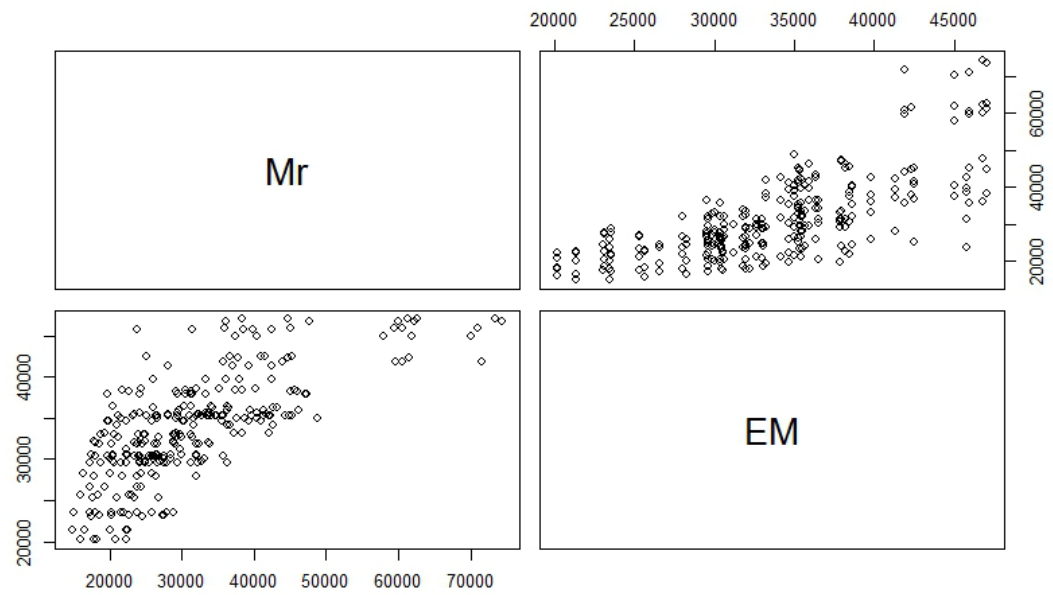


Figure 5.5 The correlation of resilient modulus ( $M_r$ ) (psi) with elastic modulus (EM) (psi)

### 5.3.1.2 Predictor vs. Predictor Plots

The predictor vs. predictor plots help us determine the multicollinearity between predictor variables. According to the predicting plot, bulk stress (BS) does not pose any correlation with cement content (CC), unconfined compressive strength (UCS), or elastic modulus (EM). An unconfined compressive strength test was performed without any confinement. BS showed no correlations with CC, UCS, and EM. On the other hand, cement content showed a substantial relationship with UCS and EM, and UCS and EM showed a strong correlation.

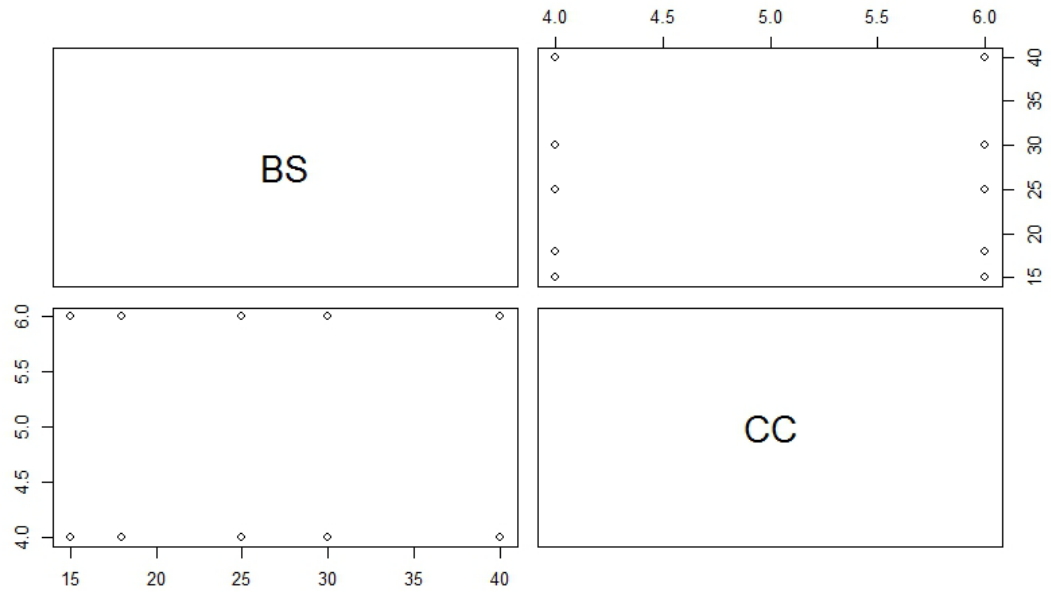


Figure 5.6 The correlation between bulk stress (BS) (psi) and cement content (CC)

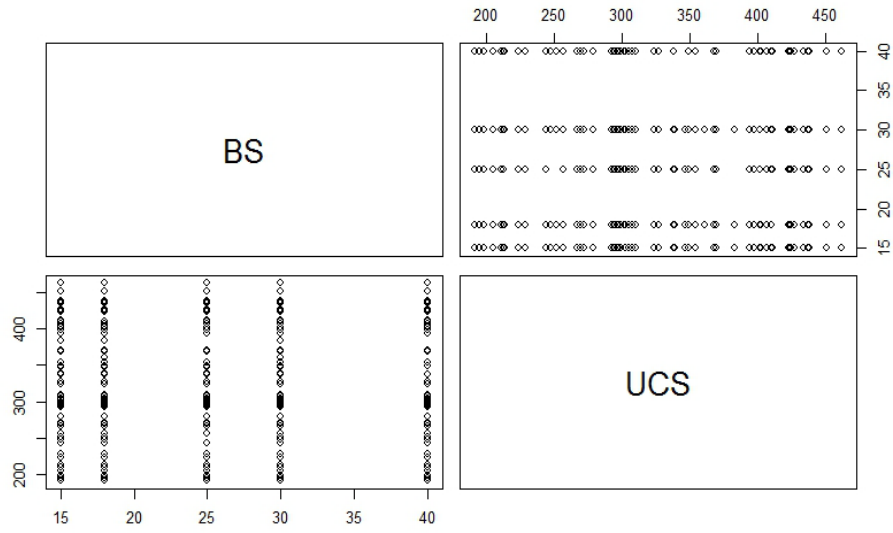


Figure 5.7 The correlation between bulk stress (BS) (psi) and unconfined compressive strength (UCS) (psi)

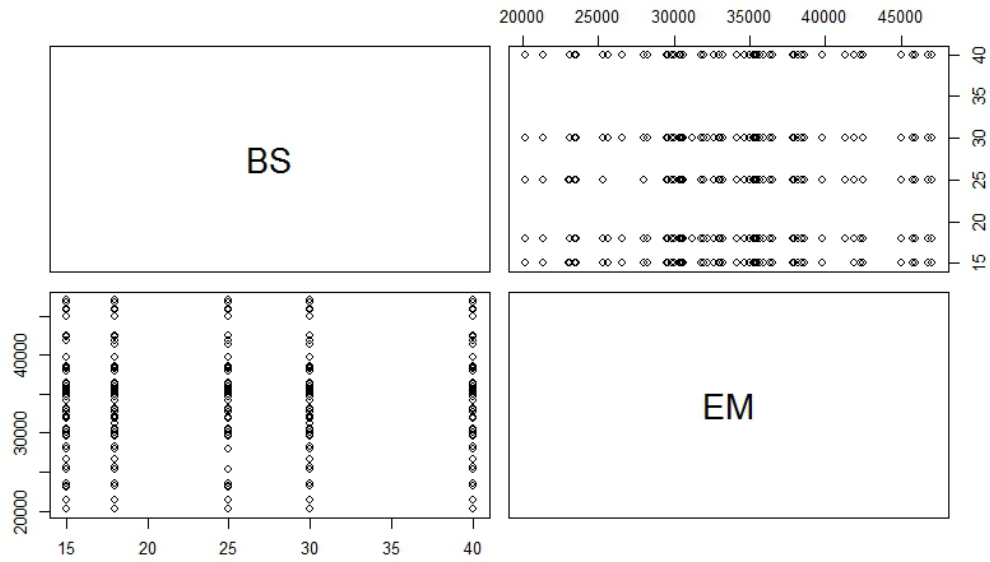


Figure 5.8 The correlation between bulk stress (BS) (psi) and elastic modulus (EM) (psi)

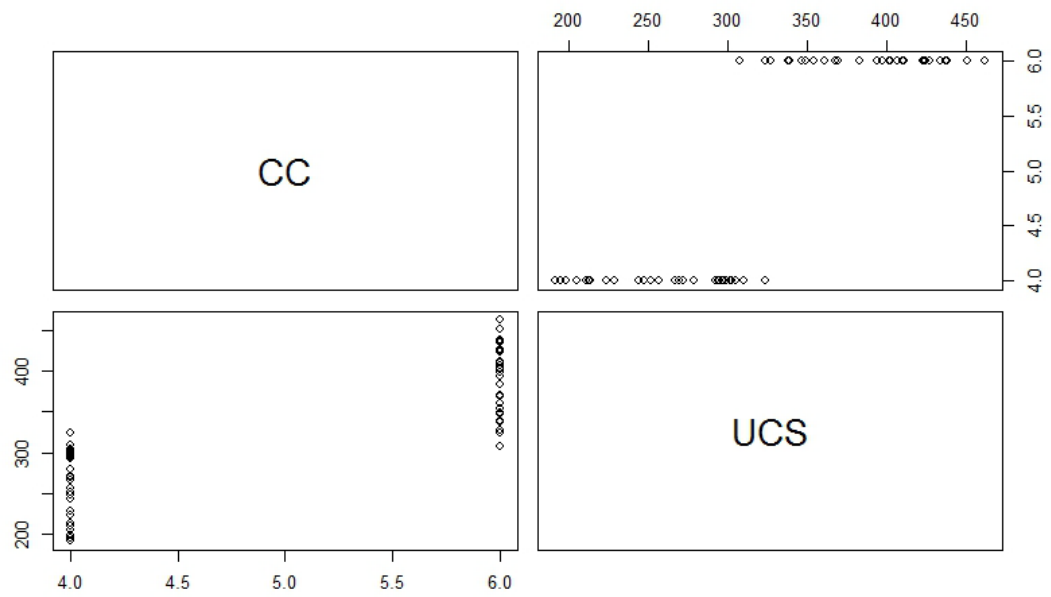


Figure 5.9 The correlation between bulk stress (BS) (psi) and elastic modulus (EM) (psi)

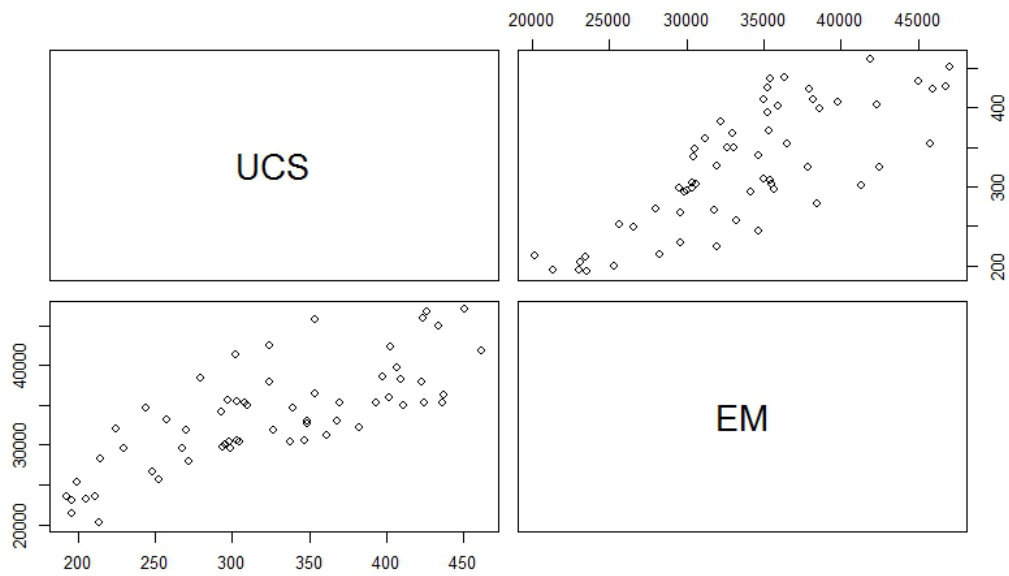


Figure 5.10 The correlation between unconfined compressive strength (UCS) (psi) and elastic modulus (EM) (psi)

Table 5.1 Correlation:  $M_r$ , BS, CC, UCS, EM

Parameters	$M_r$	BS	CC	UCS	EM
$M_r$	1.00	0.43	0.40	0.61	<b>0.72</b>
BS	0.43	1.00	0.00	0.00	0.02
CC	0.40	0.00	1.00	<b>0.84</b>	0.57
UCS	0.61	0.00	<b>0.84</b>	1.00	<b>0.77</b>
EM	<b>0.72</b>	0.00	0.57	<b>0.77</b>	1.00

Table 5.1 shows correlations among different responses and dependent variables. Cement content appears to be strongly correlated ( $r = 0.84$ ) with UCS, and UCS and EM are strongly correlated ( $r = 0.77$ ) with EM. BS is not correlated with any other predictors. The value of  $r > 0.7$  for two of the predictor variables, which suggests that multicollinearity exists within the model.

### 5.3.2 Development of Preliminary Model

A preliminary multiple linear regression model was developed, correlating resilient modulus ( $M_r$ ) with bulk stress (BS), cement content (CC), unconfined compressive strength (UCS), and elastic modulus (EM). It can be represented as:

$$M_r = \beta_0 + \beta_1 BS + \beta_2 CC + \beta_3 UCS + \beta_4 EM + \epsilon_i$$

Where, BS = bulk stress (psi), CC = cement content (%), UCS = unconfined compressive strength (psi), EM = elastic modulus (psi),  $\beta_0$ ,  $\beta_1$ ,  $\beta_2$ ,  $\beta_3$ , and  $\beta_4$  are regression parameters, and  $\epsilon_i$  is random error.

The physical meaning of regression parameters can be expressed as the variation in mean response  $E[Y]$  per unit increase of a predictor variable when all other independent variables in the regression model remain constant. The regression parameters were estimated by

minimizing the sum of squared errors for the sample. The predictor variables are quantitative in nature.

R Studio software was used to conduct the regression analyses and observe the relationship among the variables. The analysis of variance (ANOVA) was obtained from the software, and a summary of ANOVA is included in Table 5.2.

Table 5.2 ANOVA Summary

	Df	Sum Sq	Mean Sq	F value	Pr(>F)	VIF
BS	1	6.57E+09	6569181949	175.26	2.20E-16	1.002
CC	1	6.01E+09	6009632162	160.33	2.20E-16	3.491
UCS	1	8.95E+09	8952434395	238.84	2.20E-16	5.855
EM	1	4.19E+09	4190708259	111.8	2.20E-16	2.623
Intercept						0
Residuals	277	1.04E+10	37482663			

Table 5.3 Regression Parameters

Parameters	Coefficients
Intercept	-20950.94
BS	527.94
CC	-2442.91
UCS	54.62
EM	0.99

The preliminary fitted MLR equation can be presented as follows:

$$M_r = -20950.94 + 527.94BS + -2442.91CC + 54.62UCS + 0.99EM$$

Where, BS = bulk stress (psi), CC = cement content (%), UCS = unconfined compressive strength (psi), EM = elastic modulus (psi).

The appropriateness of the model should be verified for the data under consideration. The intended MLR model should be justified in terms of constant error variance, normality of error terms, outliers, and multicollinearity among the predictor variables (Stevens, 1995; Kutner et al. 2005, Huda, 2011, Kibria, 2014). The assumptions of the preliminary fitted model were verified, using graphical plots and statistical tests.

### 5.3.3 *Verification of Preliminary Model*

Multiple linear regression (MLR) models must satisfy the following assumptions:

1. The response should be linear functions of predictors.
2. Residuals should have constant variance.
3. Residuals are normally distributed.
4. Residuals are not auto-correlated.

## 5.4 MLR Model Form

Residuals vs predictor variables and residuals vs fitted values plots are generally used to identify the applicability of linear regression for a data set. The appropriate situation for the applicability of a linear regression model is when the residuals are located within a horizontal band centered on a horizontal axis. The points in the residuals vs predictors have to be scattered, and there is no systematic trend of the points. If any curvature is found in the plots, then the linear regression model is not appropriate, and a quadratic term is needed in the model. According to Figure 5.11 and Figure 5.12, residuals vs bulk stress and residuals vs cement content plot did not show any specific curvature. However, residuals vs UCS and residuals vs EM showed a curvilinear shape around the horizontal axis (Figure 5.13, and Figure 5.14). Although specific curves were not identified from diagnostic plots, transformation of the predictor variables might be required to increase the scatter in the residuals.

According to Figure 5.15, the residual vs fitted value plot also showed a curvilinear relationship. This suggests that the transformation of response might be required to increase the scatter in the residuals.

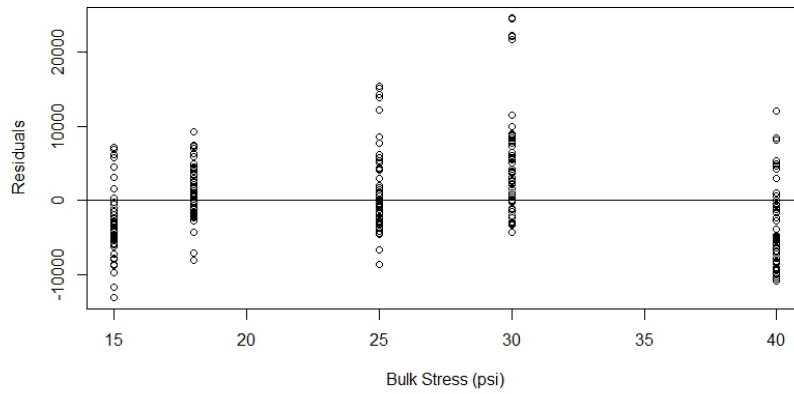


Figure 5.11 Residuals vs bulk stress (BS) (psi) plot

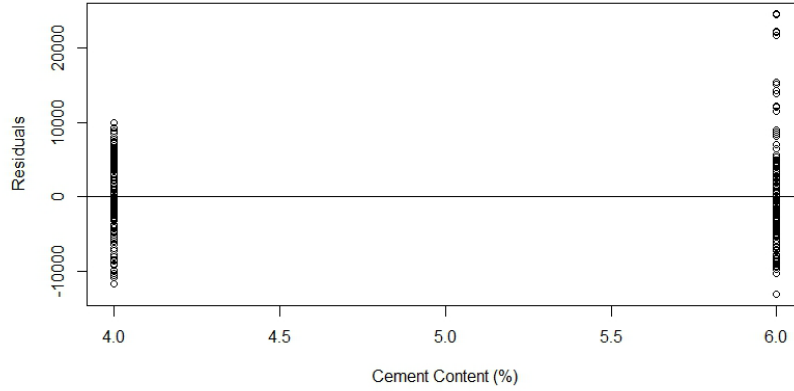


Figure 5.12 Residuals vs cement content (CC) (%) plot

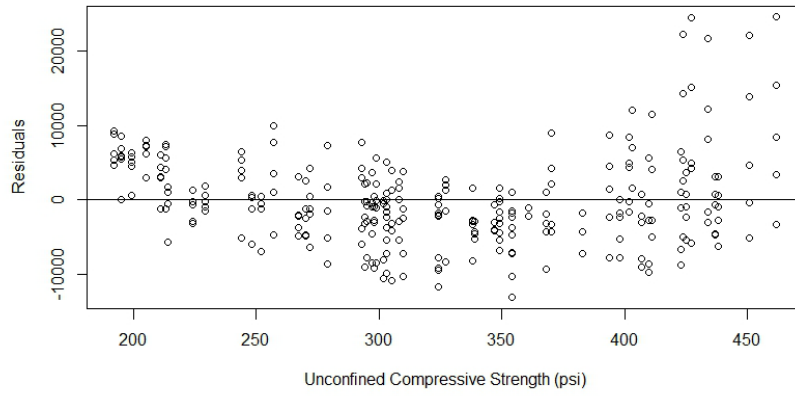


Figure 5.13 Residuals vs unconfined compressive strength (UCS) (psi)

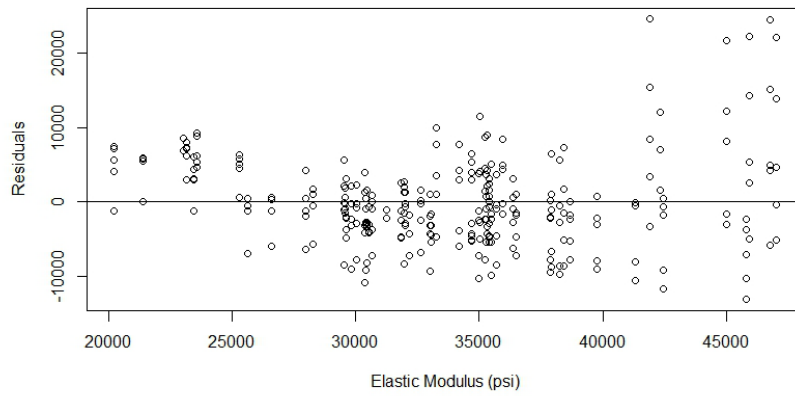


Figure 5.14 Residuals vs elastic modulus (EM) (psi)

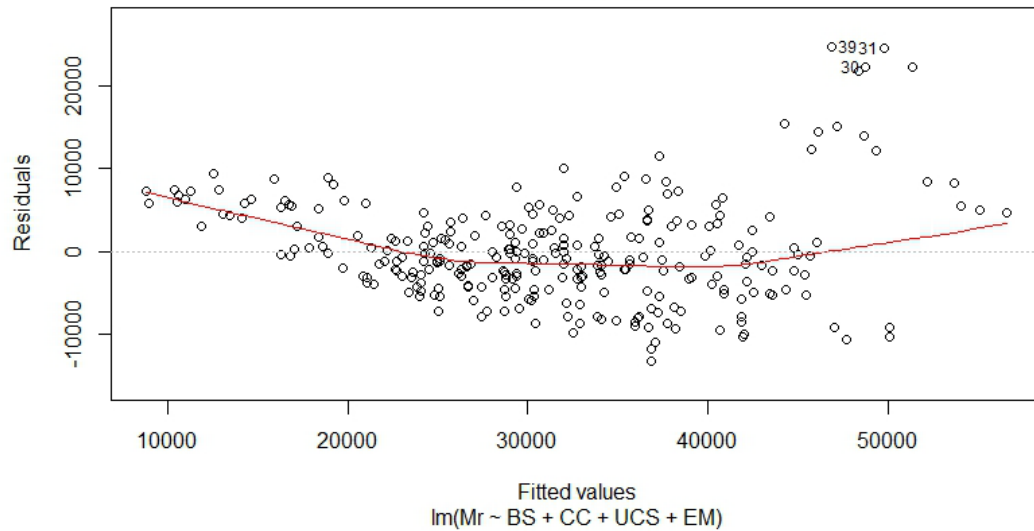


Figure 5.15 Residuals vs fitted ( $\hat{y}$ ) value plot

#### 5.4.1.1 Constant Error Variance

The constant error variance assumption of a MLR model can be evaluated by utilizing residuals vs fitted value graphical plots. If the residuals are scattered and do not follow any specific trend, then the error variance can be designated as a constant error variance. The presence of a funnel shape in the residual plots indicates non-constant variance. The residuals were plotted against the predicted value ( $\hat{y}$ ) for the current data set, which is shown in Figure 5.15. It can be seen that the residuals were not scattered around the horizontal axis, depicting the non-constant error variance of the MLR model. This also suggests the transformation of the response variable.

#### 5.4.1.2 Normality

The normality of the error in the MLR model can be determined from a normal probability plot. A moderately linear plot indicates that the error distribution is normal. The normal probability plot for the current analysis is shown in Figure 5.16.

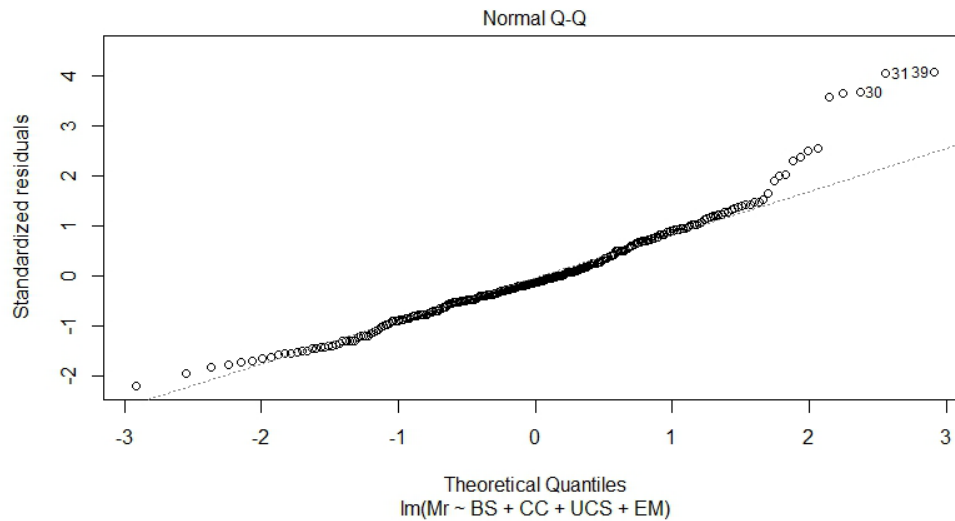


Figure 5.16 Normal probability plot

The graphical plot showed that it has a long tail at the right and a short tail at the left side. Therefore, the errors of the model are not normally distributed. The normality of the preliminary model was further verified, using the modified-Levene test, to check the constant variances.

#### 5.4.1.3 Outliers and Influence

Outliers are known as an extreme observation in a data set. They can create major problems in the least square method by pulling the fitted line disproportionately towards the outlying observation (Kutner et al. 2005). The presence of outliers in an MLR model can be checked, using residual plots and statistical tests.

The potential outliers in the current model were diagnosed by using leverage values and the Bonferroni outlier test. The influences of outliers were determined by DFFITS, DFBETAS, and Cook's distance. Leverage values, studentized deleted residuals, DFFITS, DFBETAS, and Cook's distance were obtained from the R Studio output. The R Studio output for the diagnostic of outliers is attached in Appendix A.

## X Outlier

*DFFITS*: DFFITS stands for difference in fits for observation. The guideline is to flag the absolute values of DFFITS greater than 1, as an influential outlier for a small-to-medium data set. It was observed that the absolute DFFITS values were always less than 1 for the current data set.

*DFBETAS*: This measures the impact of an observation on a particular predictor. The guideline is to flag absolute DFBETAS that are greater than 1 in a medium-to-large dataset. None of the observations were higher than 1.

*Cook's Distance*: The influence of any observation on predicted values is determined by using Cook's distance. The guideline to flag if  $D_i > F(p, n-p)$ . Here,  $F(p, n-p) = F_{0.05}(5, 277) = 2.21$ . Cook's distance ( $D_i$ ) was less than the value obtained from F statistics for all of the current dataset. If  $D_i$  is greater than 0.5, then the  $i^{\text{th}}$  data point is worthy of further investigation, as it may be influential. However, none of the Cook's distances were greater than 0.5. Therefore, none of the observations were flagged as influential.

### 5.4.1.4 Multicollinearity

The variance inflation factor (VIF) is a measure of multicollinearity among the predictor variables. VIF quantifies how much the variance is inflated. If the value of VIF is greater than 1.0, multicollinearity occurs among the predictor variables. According to the guidelines, the model with an individual VIF greater than 5 is an indication of the presence of multicollinearity. The VIFs of the predictor variables are included in Table 5.4.

Table 5.4 Variance Inflation Factor (VIF)

Variables	BS	CC	UCS	EM
VIF	1	3.491	5.855	2.623

#### 5.4.2 Transformation of Variables and Check for MLR Assumptions

The current MLR model does not satisfy the normality and constant error variance assumptions, and the residual vs predictor variable plot also depicted a curvature problem. For this reason, transformation of variables was applied to eliminate these issues. The power of the transformation of response variable was -0.545, which was determined from the R Studio output, using the Box-Cox plot method (). The predictor variable BS was -1.12, so the BS parameter was transformed into  $BS' = -1.12$ . Hence, the transformed model was as follows:

$$M_r' = \beta_0 + \beta_1 BS' + \beta_2 CC + \beta_3 UCS + \beta_4 EM + \varepsilon_i$$

Where,  $BS' = BS^{-1.12}$  and  $M_r' = M_r^{-0.545}$

The transformed parameter was checked for adequacy, using the residual vs fitted plot, as shown in . It was observed that the residuals were scattered around the horizontal axis. After transformation, the assumption of the linear model was satisfied.

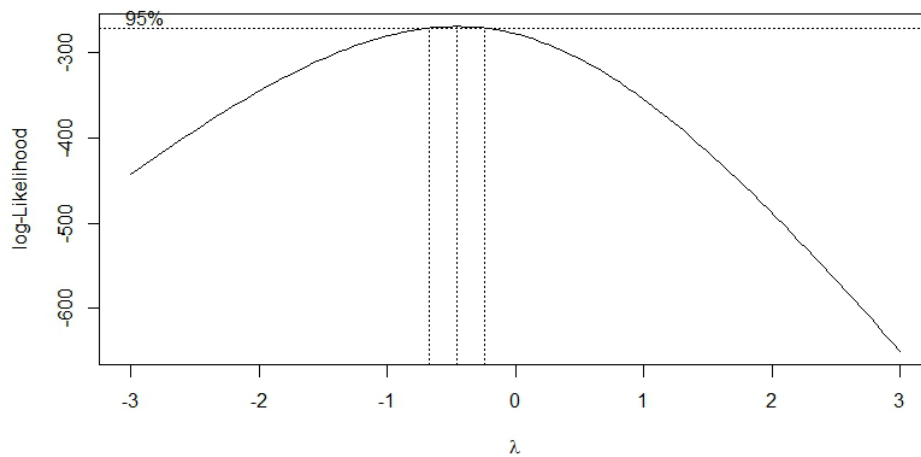


Figure 5.17 Box-Cox plot for transformation of response variable ( $\lambda = 0.545$ )

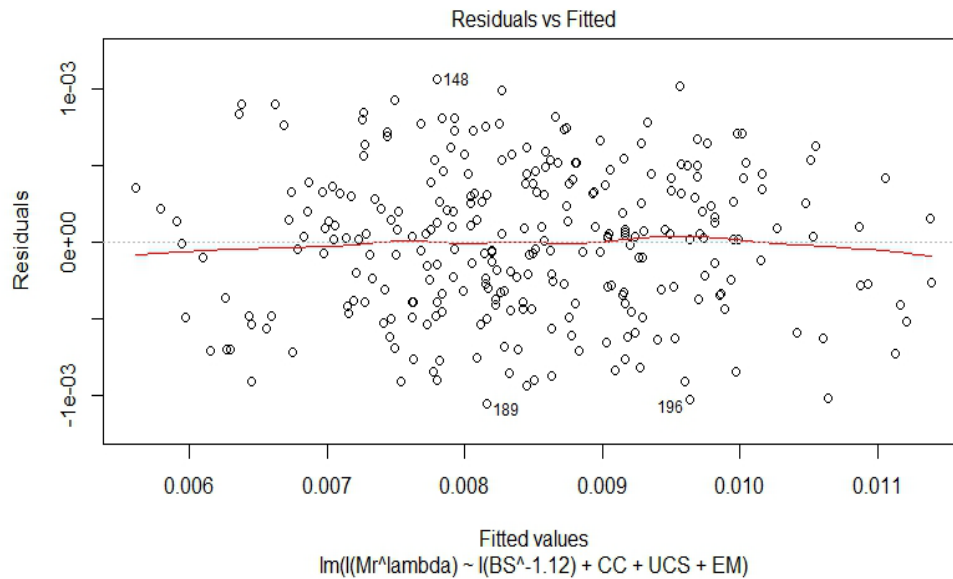


Figure 5.18 Residual vs fitted plot

The model was checked for constant error variance, using residual vs predicted plot, and no specific shape was found in the plot (Figure 5.18). No funnel shape was observed in the residual vs fitted plot after transformation. Therefore, non-constant variance was not found in the transformed model.

The normality plot of the transformed model, based on the R Studio output, is shown in Figure 5.19. The residual vs theoretical quantiles plot was mostly linear. Normality was tested at 0.05 level of significance, using the Shapiro-Wilk normality test in R Studio, and output suggests a p value of 0.0121, which is larger than  $\alpha = 0.01$ . So, we failed to reject the null hypothesis, and normality was ok at  $\alpha = 0.01$ .

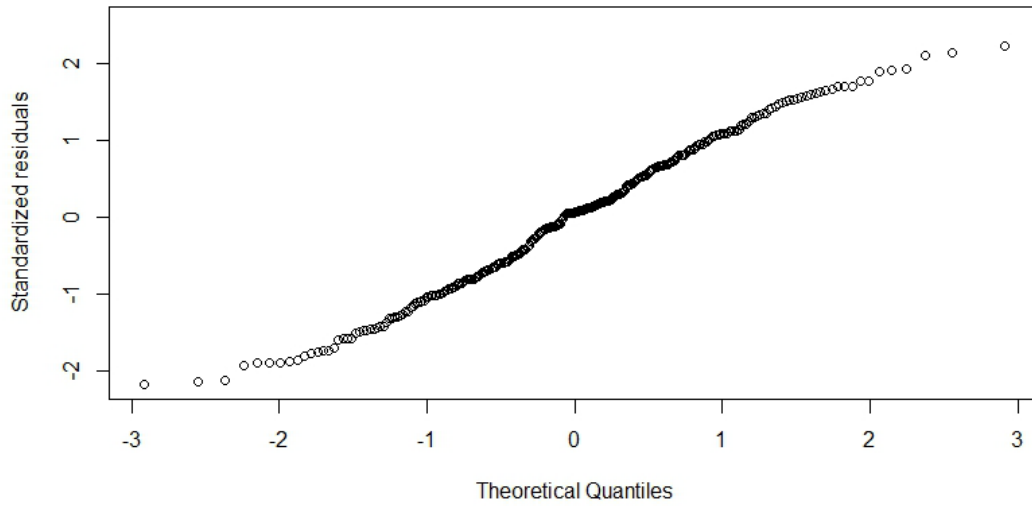


Figure 5.19 Residual vs theoretical quantiles plot after transformation

#### 5.4.2.1 *Outlier Test for Transformed Model*

Outliers were checked, using leverage values and the Bonferroni outlier test. The observed maximum distance was 0.0016, which is less than 0.035 ( $2p/n = 0.035$ ). As a result, no observation was flagged as X-outlier after transformation of the model. According to the Bonferroni outlier test, the value of  $t_{\max} = 2.245 < 2.58[t(1 - \alpha/2n; n - p - 1)]$ . Therefore, no observation was identified as Y-outlier. Based on the R Studio output for DFFITS, DFBETAS, and Cook's distance, it was concluded that none of the outlying observations influenced the transformed model.

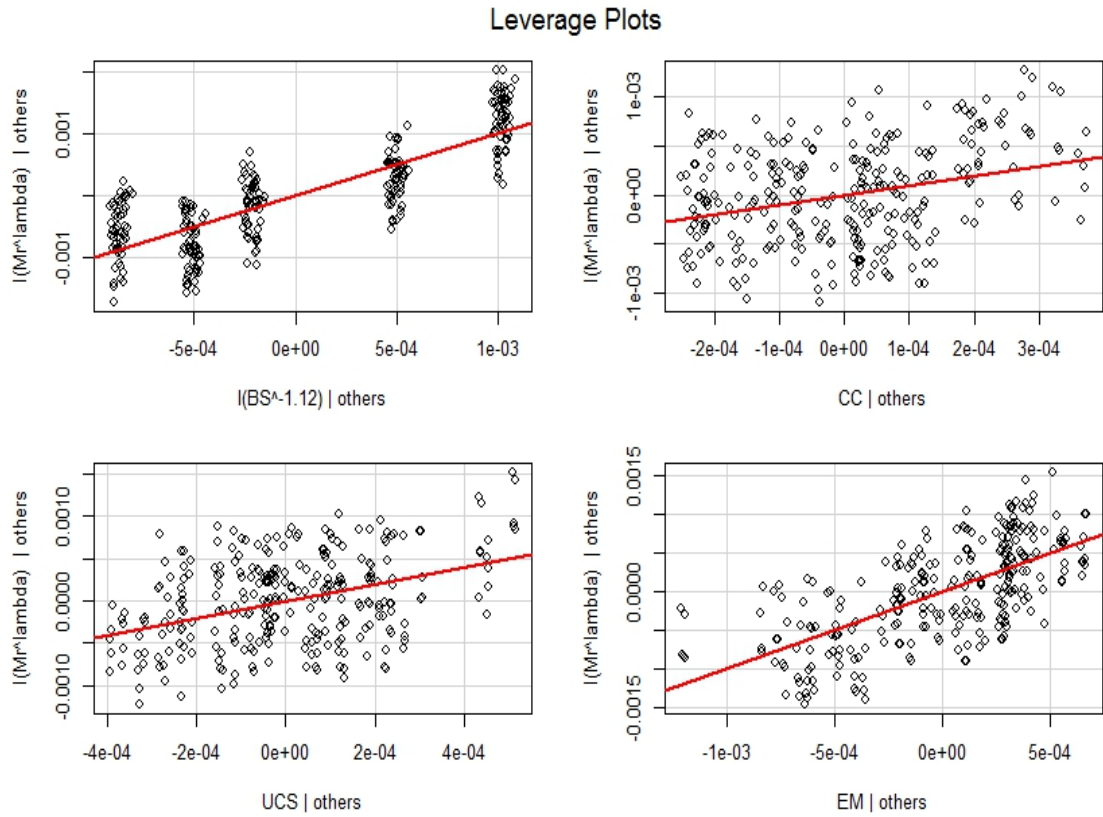


Figure 5.20 Leverage plot of transformed model

#### 5.4.2.2 ANOVA Transformed Model

The transformed model incorporates resilient modulus ( $M_r$ ) with bulk stress (BS), cement content (CC), unconfined compressive strength (UCS), and elastic modulus (EM). The transformed model is as follows:

$$M_r' = 1.10E-02 + 5.88E-02BS' + 2.90E-04CC - 6.56E-06UCS - 1.09E-07EM$$

Where,  $BS' = BS^{-1.12}$  and  $M_r' = M_r^{-0.545}$

If the value of unconfined compressive strength (UCS) and elastic modulus (EM) become zero, the value of resilient modulus is supposed to be zero. Therefore, the model did not include the condition of  $UCS = EM = 0$ , and the intercept “1.10E-02” has practically no meaning as a

separate term in model.  $\beta_1 = 5.88E-02$  BS' indicates the increase in the mean response of  $M_r'$  by 5.88E-02 psi for per-unit increase in bulk stress when other predictors remain constant. Similarly,  $\beta_1 = 2.90E-04$  presents that an increase in cement content increases the value of  $M_r'$  for per-unit increase in CC. However, it is supposed to have a decreasing effect, which might not have been reflected in the model because of the decrease in resilient modulus at a particular cement content, with an increase in the RAP content in the material combination. Inclusion of cement content renders a misleading representation of its actual effects.  $\beta_2 = -6.56E-06$  presents decrease in mean response of  $M_r'$  by  $-6.56E-06$  for per-unit increase in UCS.  $\beta_3 = -1.09E-07$  presents decrease in mean response of  $M_r'$  by  $-1.09E-07$  for per-unit increase in EM. The ANOVA analysis obtained from R Studio output is included in Table 5.5.

Table 5.5 Parameter Estimates of the Initial Transformed Model

Variables	Estimate	Std. Error	t value	Pr(> t )	VIF
(Intercept)	1.10E-02	1.99E-04	55.153	<0.001	0
I(BS <sup>1.12</sup> )	5.88E-02	2.47E-03	23.857	<0.001	1
CC	2.90E-04	5.38E-05	5.4	<0.001	3.4901
UCS	-6.56E-06	9.15E-07	-7.169	<0.001	5.8549
EM	-1.09E-07	7.37E-09	-14.721	<0.001	2.6231

Analysis of Variance (ANOVA)			
Residual Std. Error	0.0004831	Degrees of Freedom (DOF)	277
R <sup>2</sup>	0.856	R <sup>2</sup> <sub>adjusted</sub>	0.854
F - Statistic (DOF=4)	410.3	p value from F - statistics	<0.001

The coefficient of regression of the model was 85.6%. Therefore, the model explained 85.6% of the variation in resilient modulus (psi) in response to bulk stress, cement content, unconfined compressive strength, and elastic modulus. The p value obtained for each predictor was less than 0.001, which indicates that the predictors in the model were significant at 0.01 level

of significance. The P value from F statistics was less than  $<0.001$ , which indicates that a regression relationship existed between the response variable and the predictor variables.

#### *5.4.3 Final Model Selection*

Best subset method, stepwise regression, and backward elimination methods were used to analyze the potential best model and relative influences of the predictor variables.

##### *5.4.3.1 Best Subset Selection*

The best subset method determines the best models, based on the  $R^2$ ,  $R_{\text{adjusted}}^2$ , Mallows's  $C_p$  and Akaike's information criteria (AIC). A good model must have higher  $R^2$ , and  $R_{\text{adjusted}}^2$ , and lower  $C_p$ , and must meet the Akaike's information criteria (AIC). The summary of results is represented in Table 5.6.

Table 5.6 Summary of best Subset Selection Method

Parameters in Model				C <sub>p</sub>	AIC
BS	CC	UCS	EM		
-	-	-	√	187.60	-3974.6
-	-	√	-	323.06	-3901.6
√	-	-	-	509.98	-3839.8
-	√	-	-	532.72	-3811.6
√	-	-	√	23.18	-4163.9
√	-	√	-	148.66	9878.6
-	-	√	√	181.95	-3978.3
-	√	-	√	189.31	-3972.8
-	√	√	-	282.77	-3856.6
√	√	-	-	351.65	-3825.7
√	-	√	√	<b>15.86</b>	-4868.2
√	√	-	√	25.18	-4161.9
√	√	√	-	114.80	-4140.3
-	√	√	√	167.74	-3988.4
√	√	√	√	<b>5.00</b>	-4936.84

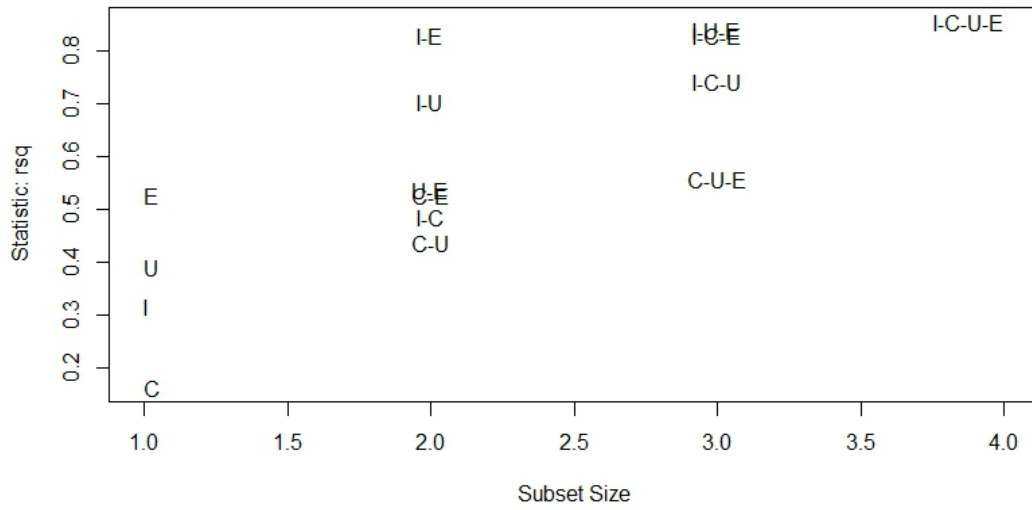


Figure 5.21 Value of  $R^2$  for different subsets of variables

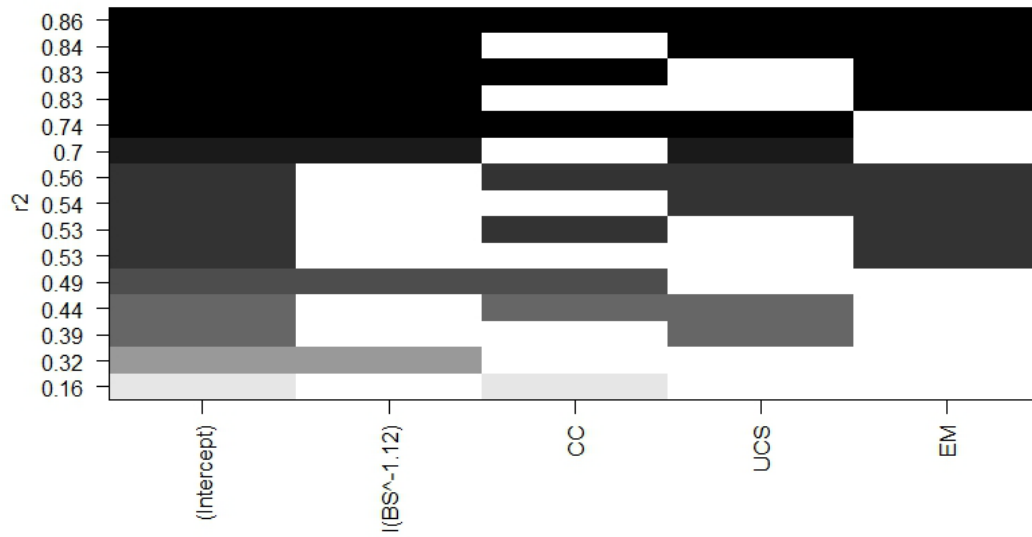


Figure 5.22 Value of  $R^2$  for different subsets of variables

#### 5.4.3.2 Backward Elimination

The backward elimination process begins by including all of the variables in the model; after that, it incrementally removes the insignificant variables. The analyses continue until no insignificant variable remains in the model. However, in this analysis, all of the predicted variables are significant at 0.01 significance level.

#### 5.4.3.3 Stepwise Regression

The stepwise regression method can be used to obtain better models by considering forward and backward elimination. This method includes the most statistically significant variable at first, and regression analysis is carried out. Each new step includes another variable to the previous model, and the procedure is repeated. The final output from R Studio depicts the final model, which shows all of the predictor variables included initially.

However, this model has higher  $R_{\text{adjusted}}^2 = 0.86$  and lowest  $C_p = 5$ , predictor variables that show a higher variance inflation factor (VIF), as shown in Table 5.5. The predictor variable CC is also misleading regarding the changes in the model, which is why the predictor variable cement content (CC) was removed from the model. So the final model is as follows:

$$M_r' = \beta_0 + \beta_1 BS' + \beta_2 UCS + \beta_3 EM$$

Where,  $BS' = BS^{-x}$  and  $M_r' = M_r^{-\lambda}$ , BS = bulk stress (psi), UCS = unconfined compressive strength (psi), EM = elastic modulus (psi).

#### 5.4.4 Transformation of Variables for Final Model

The Box-Cox method was utilized to obtain the value of  $\lambda$ . The value of  $\lambda = 0.465$  in accordance with the output from R Studio software. The R Studio output is shown in . The predictor variable BS was also transformed into  $BS' = BS^{-1.12}$  to increase scatter in the residual plot. Hence, the transformed model is as follows:

$$M_r' = \beta_0 + \beta_1 BS' + \beta_2 UCS + \beta_3 EM$$

Where,  $BS' = BS^{-1.12}$  and  $Mr' = Mr^{-0.465}$ ,  $BS$  = bulk stress (psi),  $UCS$  = unconfined compressive strength (psi),  $EM$  = elastic modulus (psi).

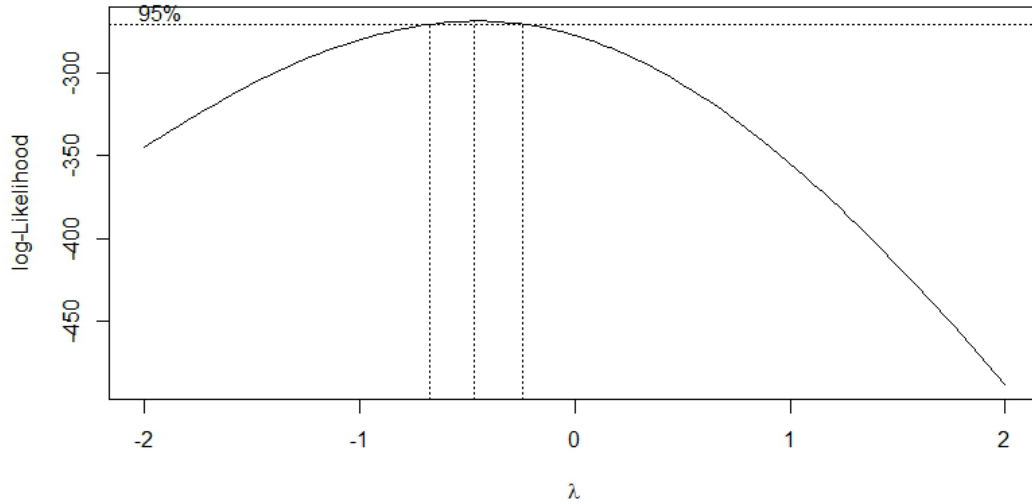


Figure 5.23 Box-Cox plot to obtain transformation of dependent variable

The transformed model was checked, using the diagnostic plots shown in Figure 5.24, Figure 5.25, and Figure 5.26. The residuals were scattered around the horizontal axis and did not follow any specific trend. Therefore, the transformed model satisfies the assumption of linear model.

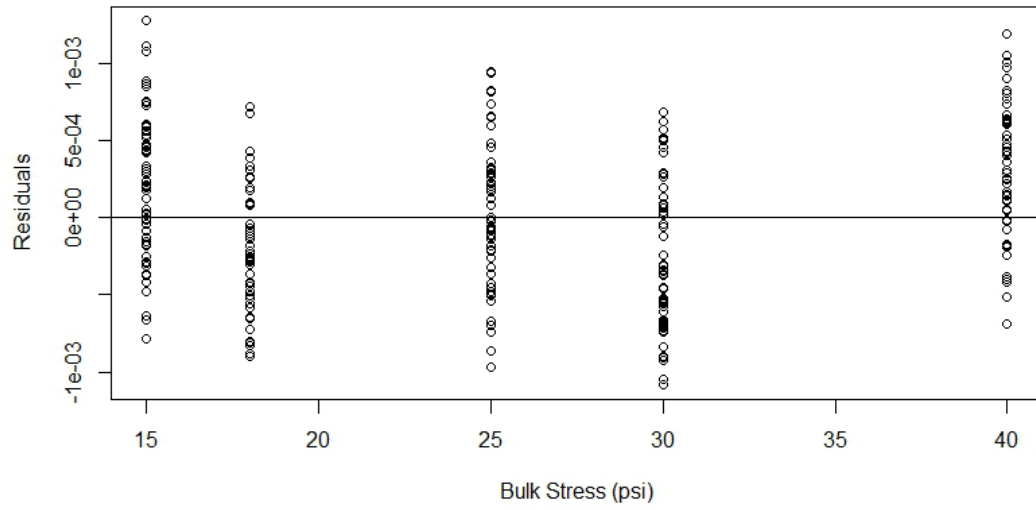


Figure 5.24 Residuals vs bulk stress (BS) (psi) plot

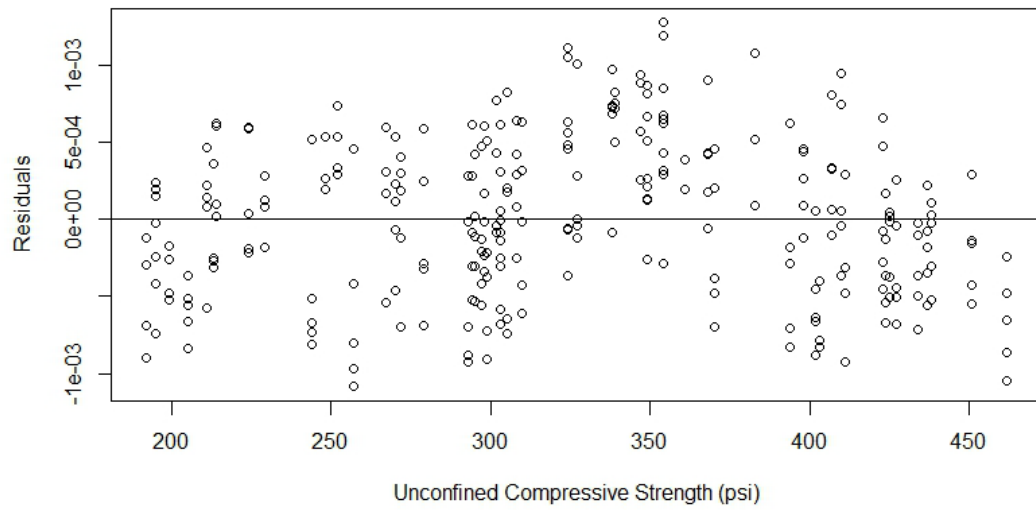


Figure 5.25 Residuals vs unconfined compressive strength (UCS) (psi) plot

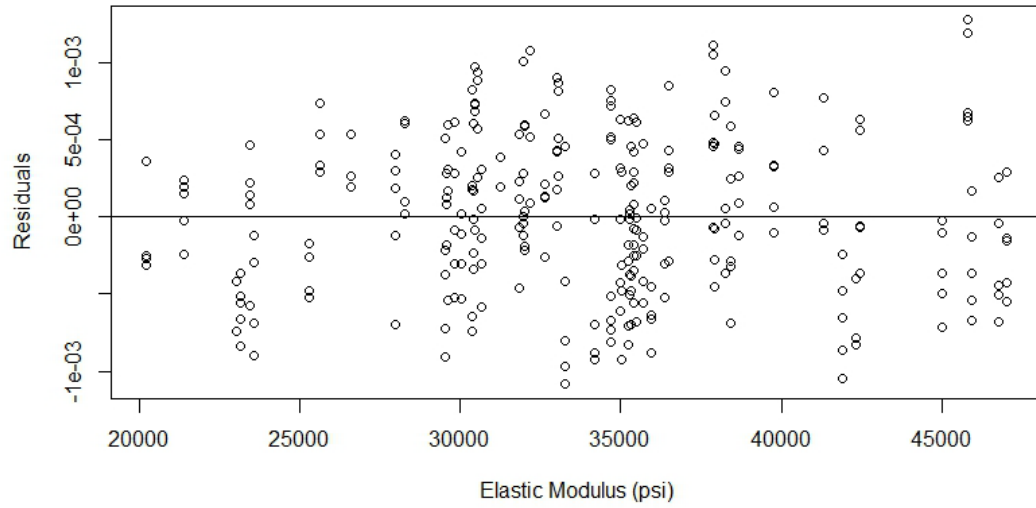


Figure 5.26 Residuals vs elastic modulus (EM) (psi) plot

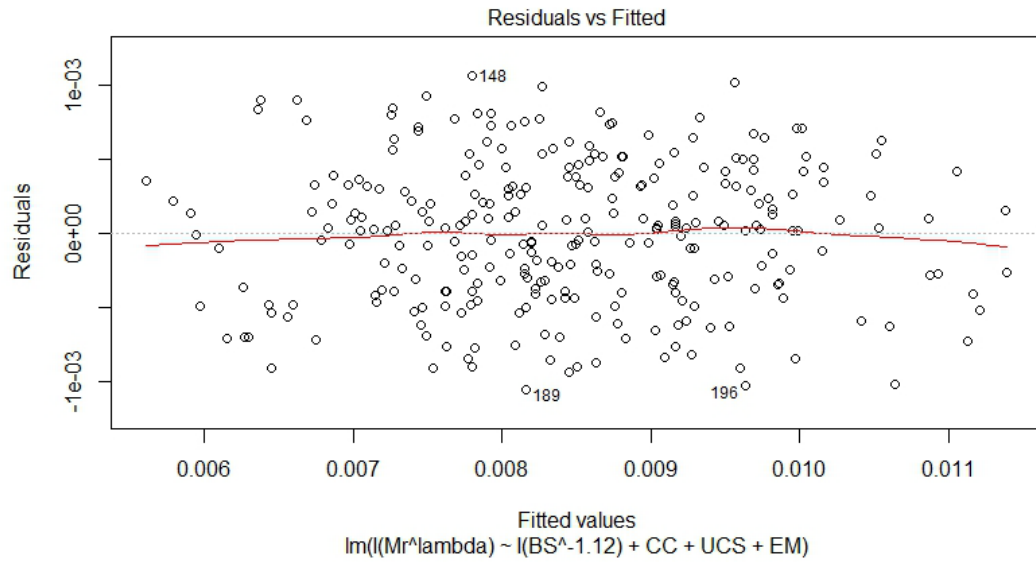


Figure 5.27 Residuals vs fitted value plot

Constant error variance in the model was diagnosed, using the residual vs fitted value plot, as shown in Figure 5.27. The plot depicts that the values are scattered around the horizontal axis.

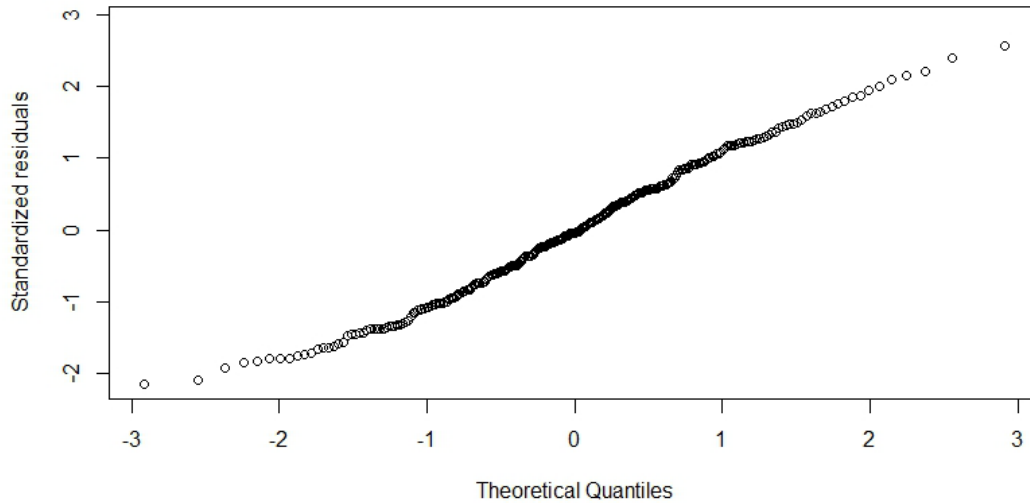


Figure 5.28 Normal probability plot for transformed model.

The normality plot, based on the R Studio output, is shown in Figure 5.28. The residual vs theoretical quantiles plot was mostly linear. Normality was tested at 0.05 level of significance. The normality was tested, using the Shapiro-Wilk normality test in R Studio, and output suggested a p value of 0.03032, which is larger than  $\alpha = 0.01$ . So we failed to reject the null hypothesis, and normality was ok at  $\alpha = 0.01$ .

The Breusch-Pagan test method was also used to check the constant error variance. With a p-value of 0.12, which is greater than 0.01, we failed to reject the null hypothesis that variance of residuals is constant, and therefore, residuals are homoscedastic.

Non-constant Error Variance Test	
Chi-square	2.43873
Df	1
P	0.118372

#### 5.4.4.1 *Outlier Test of the Transformed Model*

Outliers were checked, using leverage values and the Bonferroni outlier test. The observed maximum distance was 0.0016, which is less than 0.0284 ( $2p/n = 0.035$ ). As a result no observation was flagged as X-outlier after transformation of the model. According to the Bonferroni outlier test, the largest absolute studentized residual had a p value of 0.009, which is less than 0.05 at 95% confidence interval. As a result no observation was identified as outlier.

Based on the R Studio output for DFFITS, DFBETAS, and Cook's distance, it was concluded that none of the outlying observations had influence on the transformed model.

#### 5.4.4.2 *ANOVA of Transformed Model*

The transformed model incorporates resilient modulus ( $M_r$ ) with bulk stress (BS), unconfined compressive strength (UCS), and elastic modulus (EM). The transformed model is as follows:

$$M_r' = 1.15E-02 + 5.92E-02BS' - 2.82E-06UCS - 1.17E-07EM$$

Where,  $BS' = BS^{-1.12}$  and  $M_r' = M_r^{-0.465}$

If the value of unconfined compressive strength (UCS) and elastic modulus (EM) become zero, the value of the resilient modulus is also supposed to be zero. Therefore, the model did not include the condition of  $UCS = EM = 0$ , and the intercept "1.15E-02" has practically no meaning as a separate term in the model.  $\beta_1 = 5.92E-02$  indicates the increase in the mean response of  $M_r'$  by 5.92E-02 psi for per-unit increase in bulk stress when other predictors remain constant. Similarly,  $\beta_2 = -2.82E-06$  presents a decrease in mean response of  $M_r'$  by  $-2.82E-06$  for per-unit

increase in UCS.  $\beta_3 = -1.17E-07$  presents a decrease in the mean response of  $M_r'$  by  $-1.17E-07$  for per-unit increase in EM. The ANOVA analysis obtained from the R Studio output is included in Table 5.7.

Table 5.7 Estimation of Parameters of Final Model

Parameters	Df	Sum Sq	Mean Sq	F value	Pr(>F)
$I(BS^{-1.12})$	1	1.40E-04	1.40E-04	543.18	<0.001
UCS	1	1.75E-04	1.75E-04	680.69	<0.001
EM	1	6.17E-05	6.17E-05	239.91	<0.001
Residuals	278	7.15E-05	2.57E-07		

Residual Std. Error	0.000507	Degrees of Freedom (DOF)	277
$R^2$	0.8404	$R^2_{\text{adjusted}}$	0.84
F - Statistic (DOF=4)	487.9	p value	<0.001

The coefficient of regression of the model was 84.04%. Therefore, the model explained 84.04% of the variation in resilient modulus (psi) in response to bulk stress, unconfined compressive strength, and elastic modulus. The p value obtained for each predictor was less than 0.001, which indicates that the predictors in the model were significant at 0.01 level of significance. P values from the F statistics were less than <0.001, which indicates that a regression relationship exists between the response variables and the predictors variables.

#### 5.4.5 Simplification of Final Model

The model was then simplified into the model shown below. The predictor variable BS was transformed into  $M_r' = M_r^{-0.5}$ , and  $BS' = BS^{-1}$  to increase scatter in the residual plot. Hence, the transformed model is as follows:

$$M_r' = \beta_0 + \beta_1 BS' + \beta_2 UCS + \beta_3 EM$$

Where,  $BS' = BS^{-1}$  and  $Mr' = Mr^{-0.5}$ ,  $BS$  = bulk stress (psi),  $UCS$  = unconfined compressive strength (psi),  $EM$  = elastic modulus (psi).

The transformed model was verified by using the diagnostic plots, as shown in Figure 5.29, , and Figure 5.31. The residuals were scattered around the horizontal axis and did not follow any specific trend. Therefore, the transformed model satisfies the assumption of the linear model.

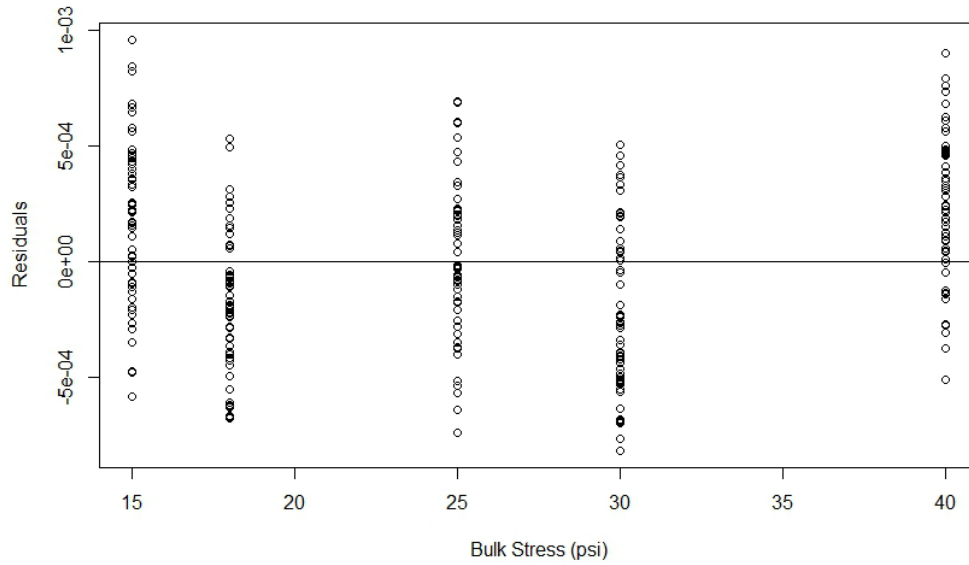


Figure 5.29 Residuals vs bulk stress (BS) (psi) plot

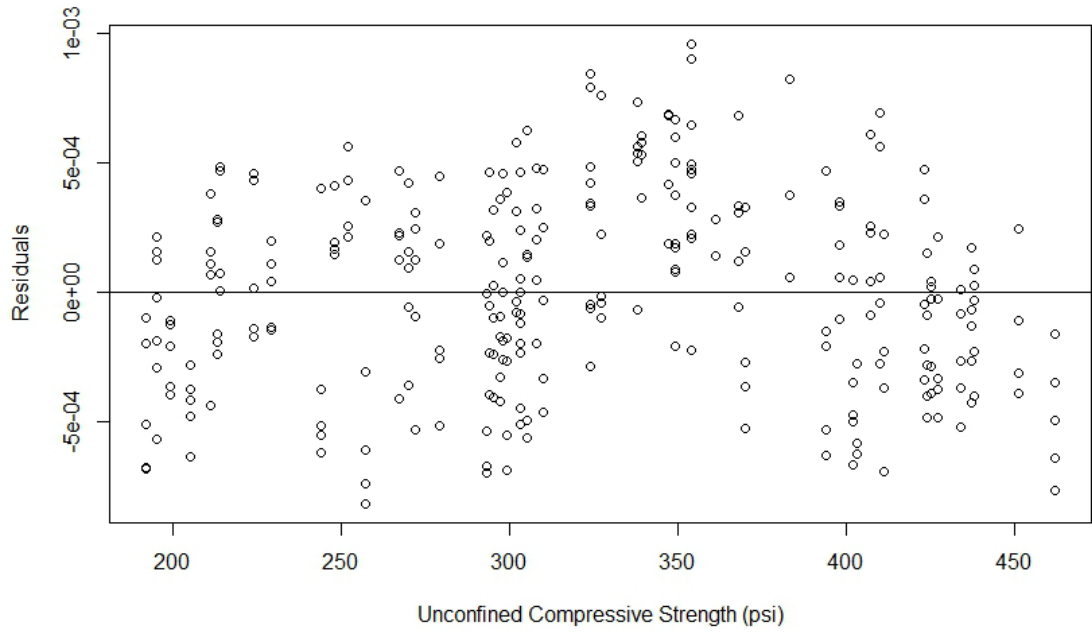


Figure 5.30 Residuals vs unconfined compressive strength (UCS) (psi) plot

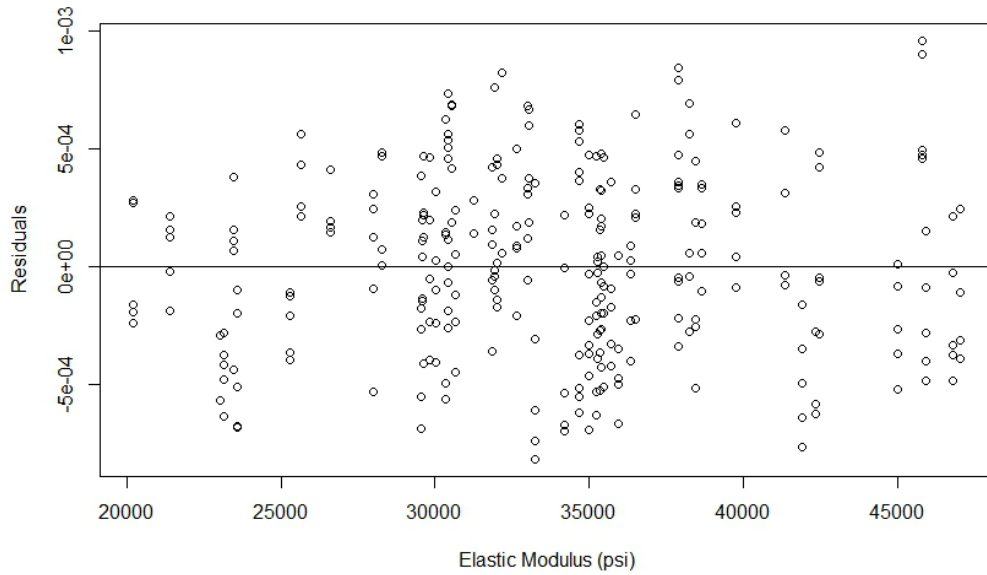


Figure 5.31 Residuals vs elastic modulus (EM) (psi) plot

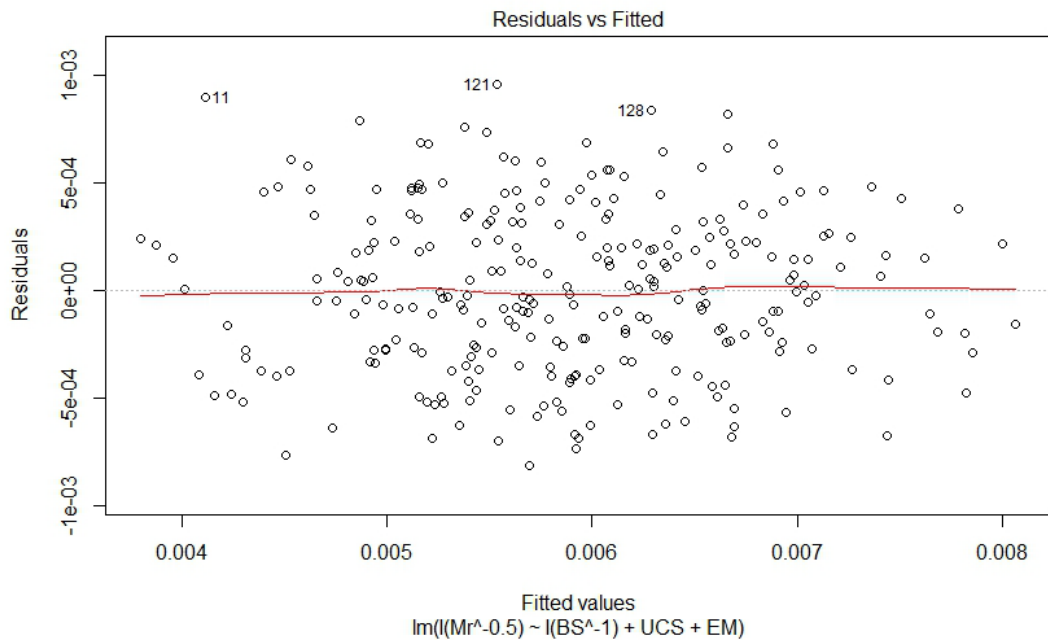


Figure 5.32 Residuals vs fitted value plot

Constant error variance in the model was diagnosed by using the residual vs fitted value plot, as shown in Figure 5.32. The plot depicts that the values were scattered around the horizontal axis.

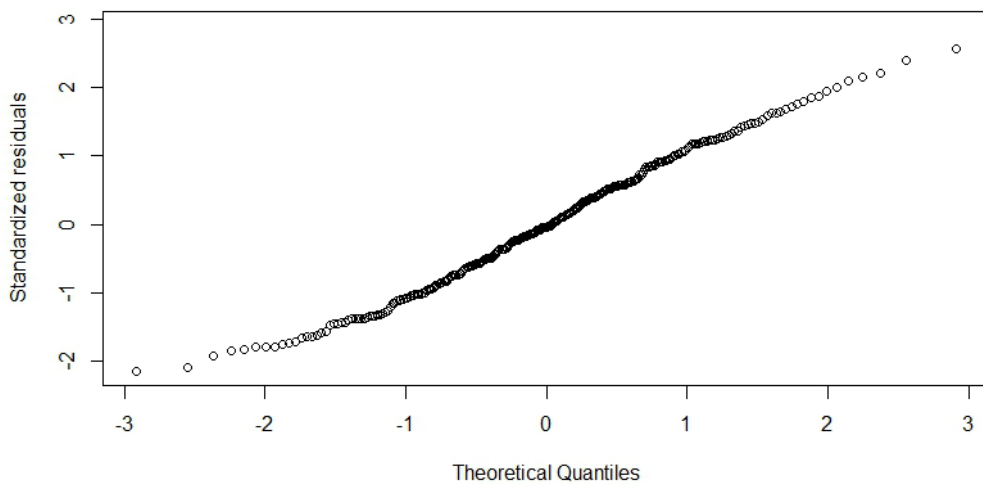


Figure 5.33 Normal probability plot for transformed model

The normality plot of the transformed model is shown in Figure 5.33, based on the R Studio output. The residual vs theoretical quantiles plot was mostly linear. Normality was tested at 0.05 level of significance, using the Shapiro-Wilk normality test in R Studio. The output suggested a p value of 0.0266, which is larger than  $\alpha = 0.01$ . So we failed to reject the null hypothesis, and normality was ok at  $\alpha = 0.01$ .

The Breusch-Pagan test method was also used to check the constant error variance. With a p-value of 0.12 which is greater than 0.01, we failed to reject the null hypothesis that variance of residuals is constant and therefore, residuals are homoscedastic.

Non-constant Error Variance Test	
Chi-square	2.43873
Df	1
p	0.12

#### 5.4.5.1 *Outlier Test of the Transformed Model*

Outliers were checked, using leverage values and the Bonferroni outlier test. The observed maximum distance was 0.0016, which is less than 0.0284 ( $2p/n = 0.035$ ). As a result no observation was flagged as X-outlier after transformation of the model. According to the Bonferroni outlier test, the largest absolute studentized residual had a p value of 0.009, which is less than 0.05 at 95% confidence interval. As a result no observation was identified as outlier.

Based on the R Studio output for DFFITS, DFBETAS, and Cook's distance, it was found that none of the outlying observations had influence on the transformed model.

#### 5.4.5.2 ANOVA of Transformed Model

The transformed model incorporates resilient modulus ( $M_r$ ) with bulk stress (BS), unconfined compressive strength (UCS), and elastic modulus (EM).  $M_r$  values range from 14807 psi to 74319 psi, UCS values range between 192 psi and 462 psi, BS values range between 15 psi and 40 psi, and EM ranges from 20220 psi to 47034 psi. The transformed model is as follows:

$$M_r' = 8.01E-03 + 3.41E-02BS' - 2.11E-06UCS - 8.74E-08EM$$

Where,  $BS' = BS^{-1}$  and  $M_r' = M_r^{-0.5}$

If the value of unconfined compressive strength (UCS) and elastic modulus (EM) become zero, the value of resilient modulus is also supposed to be zero. Therefore, the model did not include the condition of  $UCS = EM = 0$ , and the intercept “8.01E-03” has practically no meaning as a separate term in the model.  $\beta_1 = 3.41E-02$  indicates the increase in the mean response of  $M_r'$  by 5.92E-02 psi for per-unit increase in bulk stress when other predictors remain constant. Similarly,  $\beta_2 = -2.11E-06$  presents a decrease in the mean response of  $M_r'$  by  $-2.11E-06$  for per-unit increase in UCS.  $\beta_3 = -8.74E-08$  presents a decrease in the mean response of  $M_r'$  by  $-1.17E-07$  for per-unit increase in EM. The ANOVA analysis obtained from the R Studio output is included in Table 5.8.

Table 5.8 Estimation of Parameters of Final Model

Parameters	Df	Sum Sq	Mean Sq	F value	Pr(>F)
I(BS <sup>-1</sup> )	1	7.78E-05	7.78E-05	533.8	<0.001
UCS	1	9.77E-05	9.77E-05	670.74	<0.001
EM	1	3.44E-05	3.44E-05	236.04	<0.001
Residuals	278	4.05E-05	1.46E-07		

Residual Std. Error	0.000382	Degrees of Freedom (DOF)	278
R <sup>2</sup>	0.8382	R <sup>2</sup> <sub>adjusted</sub>	0.8365
F - Statistic (DOF=4)	487.9	p value	<0.001

The coefficient of regression of the model was 83.82%. Therefore, the model explained 83.82% of the variation in resilient modulus (psi) in response to bulk stress, unconfined compressive strength, and elastic modulus. The p value obtained for each predictor was less than 0.001, which indicates that the predictors in the model were significant at 0.01 level of significance. The P values from the F statistics were less than <0.001, which indicates that a regression relationship exists between response variable and predictors variables.

#### 5.5 Comparison of Actual Test Data with Model Predicted Data

The experimental results of 50% RAP 3 + 50% RCCA 3 material combinations at different asphalt contents were used to evaluate the predictive capacity of the developed multiple linear regression model for resilient modulus ( $M_r$ ) value of recycled materials. The resilient modulus ( $M_r$ ) values were used for different combinations of materials and cement contents at 15 psi, 18 psi, 25 psi, and 30 psi bulk stresses. According to Figure 5.34, the developed model can predict 87% of the variation in resilient modulus at different combinations.

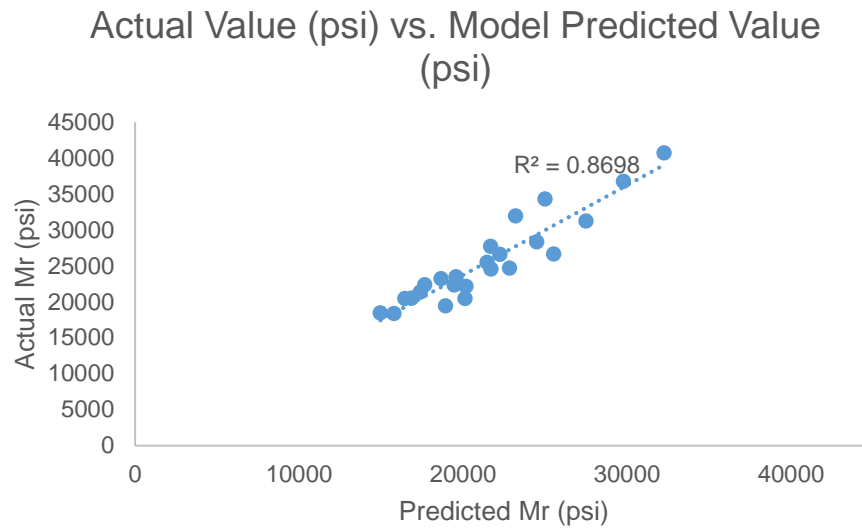


Figure 5.34 Model validation using test data

#### 5.6 Development of Design Chart

Design charts were developed using the multiple linear regression models that were developed by utilizing the unconfined compressive strength (UCS), elastic modulus (EM) and resilient modulus ( $M_r$ ) test results. The values of the structural layer coefficient ( $a_2$ ) for the corresponding resilient modulus ( $M_r$ ) were determined using the following equation (AASHTO 2003):

$$a_2 = 0.249 \times \log M_r - 0.977$$

Where,  $M_r$  = Resilient modulus (psi).

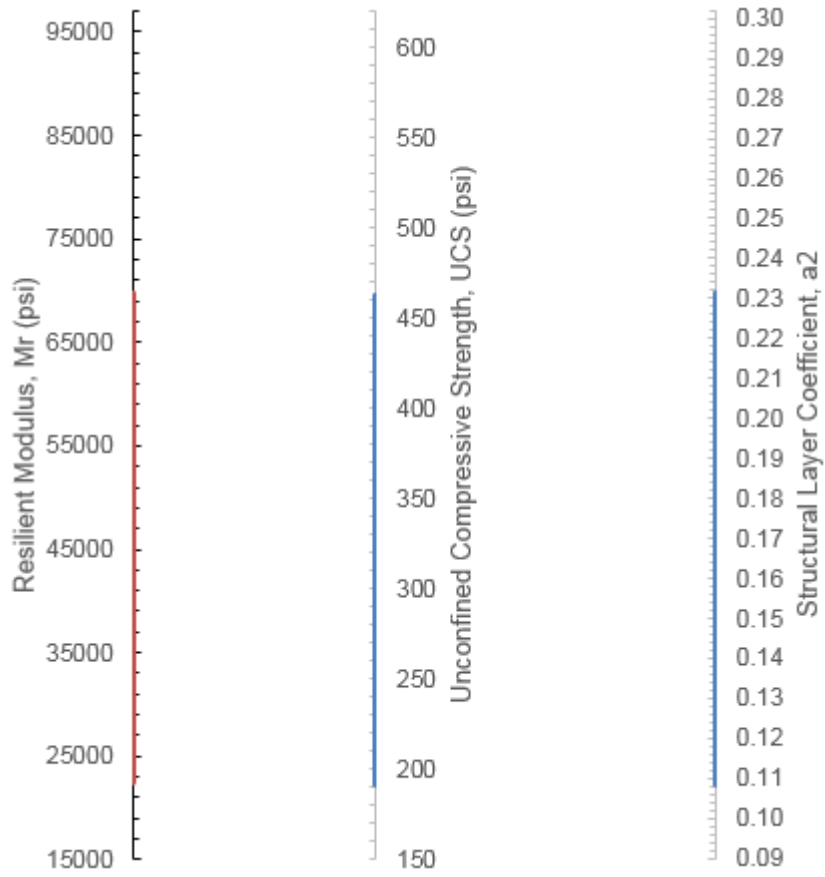


Figure 5.35 Design chart ( $\sigma_c = 10$  psi,  $\sigma_d = 10$  psi,  $\theta = 40$  psi)

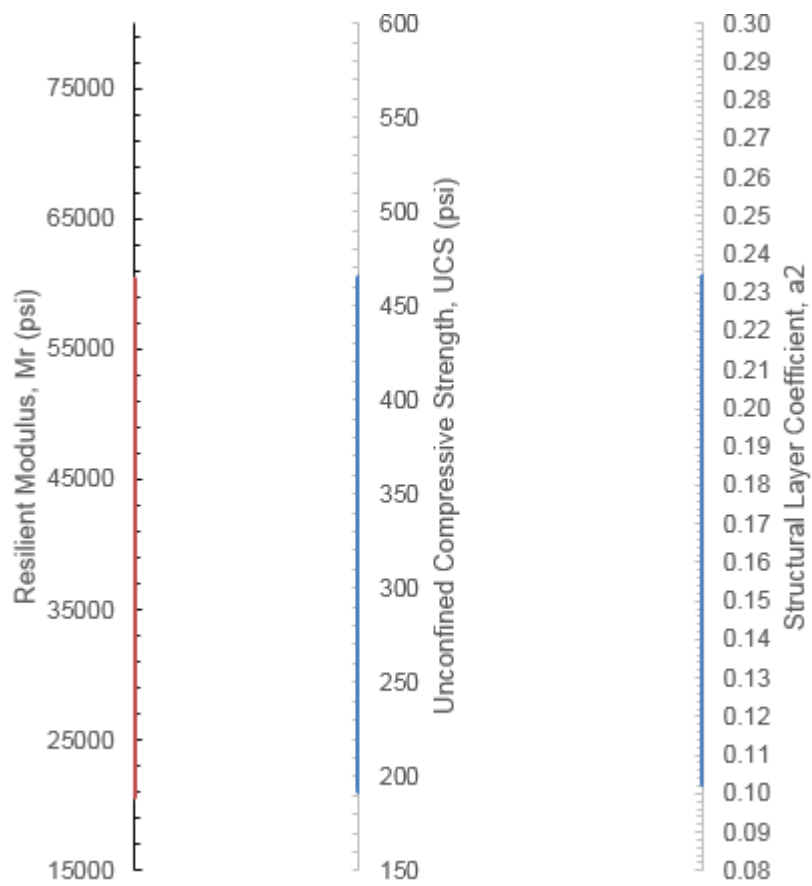


Figure 5.36 Design chart ( $\sigma_c = 5$  psi,  $\sigma_d = 15$  psi,  $\theta = 30$  psi)

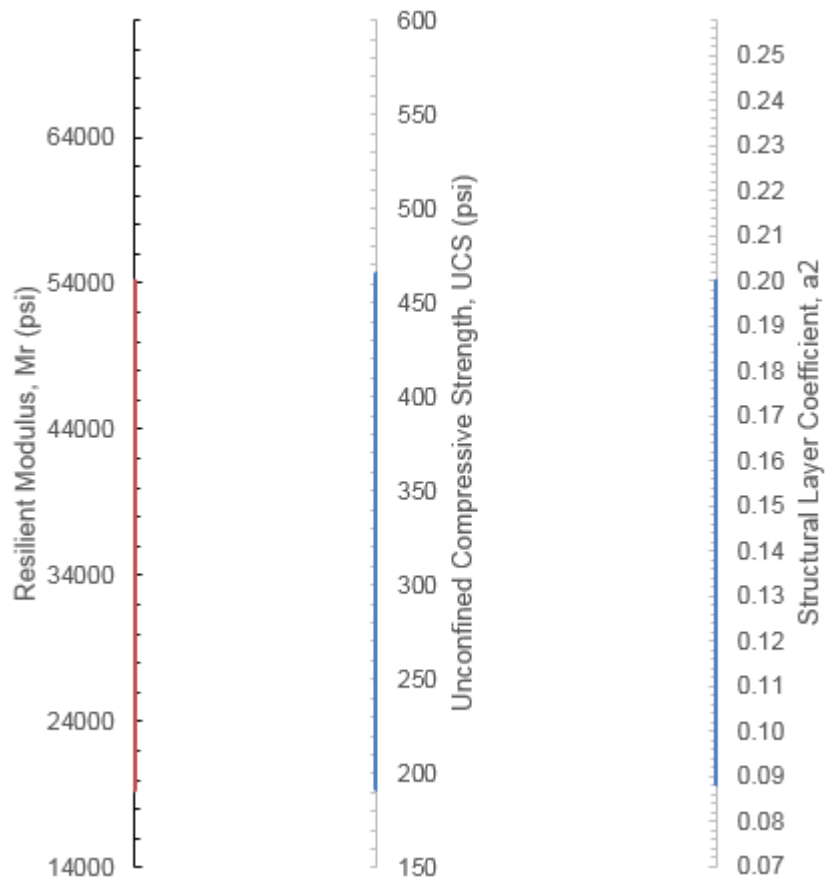


Figure 5.37 Design chart ( $\sigma_c = 5$  psi,  $\sigma_d = 10$  psi,  $\theta = 25$  psi)

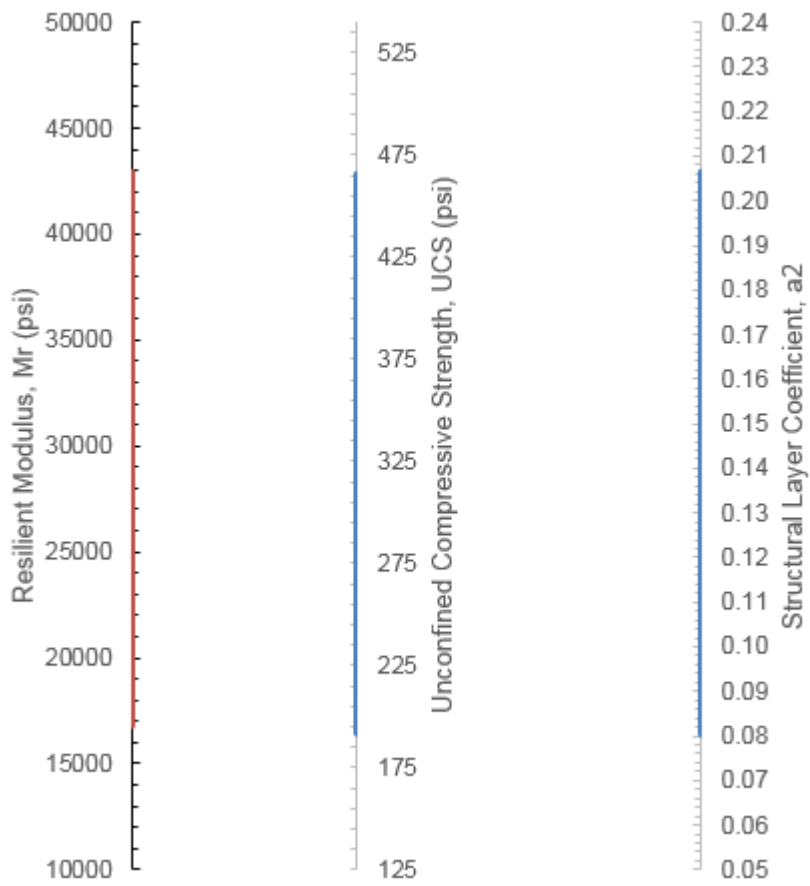


Figure 5.38 Design chart ( $\sigma_c = 3$  psi,  $\sigma_d = 9$  psi,  $\theta = 18$  psi)

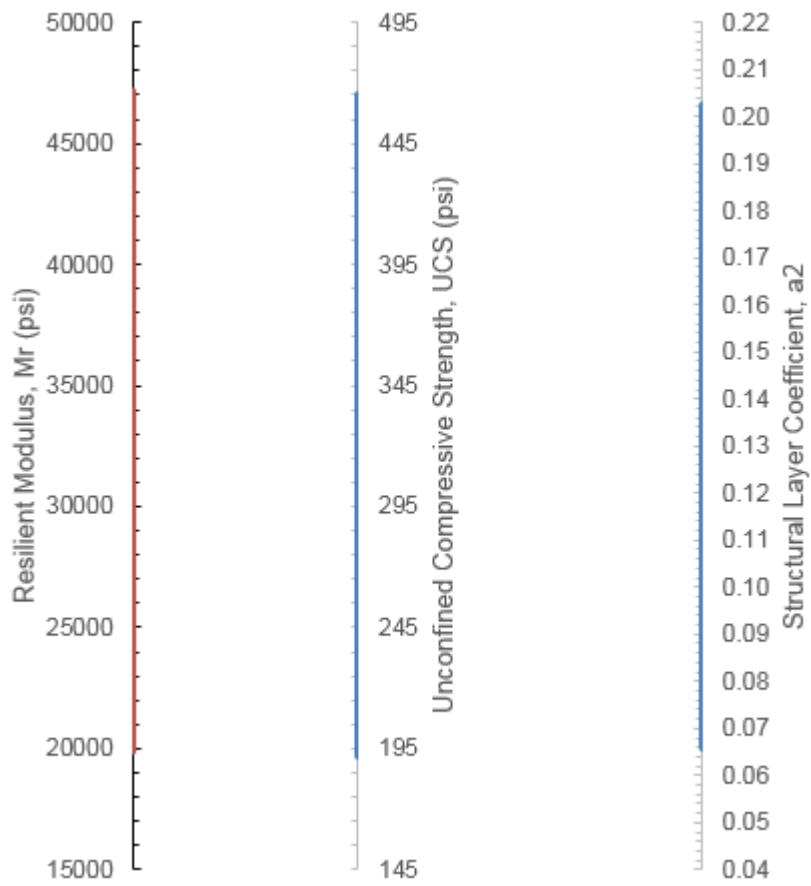


Figure 5.39 Design chart ( $\sigma_c = 3$  psi,  $\sigma_d = 6$  psi,  $\theta = 15$  psi)

## Chapter 6

### Conclusion and Future Recommendations

#### 6.1 Introduction

Recycled crushed concrete aggregate (RCCA) and reclaimed asphalt pavement (RAP) are the most available recycled materials and might be used as an alternative to natural virgin aggregates. They usually have variable properties, because they are obtained from different sources. However, limited study has been conducted to determine the area-specific guidelines for use of these materials as base layer for flexible pavement. The available universal design guidelines were developed by the American Association of State Highway and Transportation Officials (AASHTO 2003) for natural aggregate, but they do not pertain to area-specific recycled materials. Therefore, it was necessary to conduct a study on the recycled flex base materials available in North Texas, in order to evaluate their applicability to the base layer of pavement. The overall objective of this study was to develop a correlation between the resilient modulus and different strength properties of RAP and RCCA materials. An experimental program was developed to determine the resilient modulus ( $M_r$ ), bulk stress (BS), unconfined compressive strength (UCS), and elastic modulus (EM). Thereafter, the MLR model was developed to correlate the resilient modulus ( $M_r$ ) with bulk stress (BS), unconfined compressive strength (UCS), and elastic modulus (EM). An environmental testing program was also undertaken to evaluate the effects of these materials on the environment. Test results revealed that recycled materials are relatively weaker than natural aggregates. For this reason, durability tests were also conducted on the prepared specimens to find the weakest combination of the RAP and RCCA materials.

#### 6.2 Summary and Conclusions

A summary of the conducted research test results is as follows:

1. RCCA and RAP materials were collected from TxDOT-specified sources to ensure the quality of the recycled materials which are usually used for construction.

2. The physical properties of RCCA and RAP materials, such as particle size gradation, LA abrasion values, specific gravity, and dry-density were determined, and the effect of these materials on the strength and stiffness properties were evaluated.
3. Different combinations of RAP and RCCA materials' strength and stiffness properties were evaluated for untreated and cement-treated conditions.
4. The value of strength obtained at 0% and 2% cement content for different combinations of RAP and RCCA materials did not meet the criteria of minimum unconfined compressive strength of 300 psi.
5. 100% RCCA material met the minimum strength criteria of 300 psi at 4% cement content. The maximum amount of RAP that can be added into the mix with RCCA is 50%. A combination of 50% RAP and 50% RCCA materials reached the unconfined compressive strength of 300 psi at 5% to 6% cement content. A combination of 70% RAP and 30% RCCA materials fulfilled the minimum strength requirement of 300 psi at 6% cement content. However, RCAA materials mixed with RAP that contained more than 6% asphalt could not be molded into the specimens, even at 6% cement content. For this reason, the amount of RAP was fixed at 50% within the combination.
6. Resilient modulus ( $M_r$ ) reduced with inclusion of RAP mixed with RCCA materials. The value of the resilient modulus decreased by 50% with inclusion of 50% RAP at any cement content. However, according to our test results, inclusion of 10% RAP does not have any significant effect of resilient modulus at 6% cement content.
7. According to previous studies, the maximum bulk stress that can be achieved in the field is 30 psi. For this reason, the value used to compare the resilient modulus was limited to a bulk stress of 30 psi. The structural layer coefficient for the base layer of flexible pavement has to be more than 0.1, which can only be achieved for a maximum RAP content of 50% combined with RCCA, and must be treated with a cement content ranging from 4% to 6%.

8. The value of unconfined compressive strength and resilient modulus increases with an increase in cement content.
9. The effect of asphalt content was determined by using a combination of 50% RAP + 50% RCCA at 4% and 6% cement content. Asphalt was added to the RAP to evaluate the effect of asphalt on unconfined compressive strength, split tensile strength, and the resilient modulus. An increase in the asphalt content reduced both compressive strength and resilient modulus. However, additional asphalt also increased the split tensile strength, due to its viscous properties.
10. Based on the test results, a 4.4% to 6.4% increase in asphalt content hinders the bonding process between aggregates, making it impossible to prepare a specimen at 0% cement content. For asphalt content of 8.4%, a specimen could not be prepared at 0% and 2% cement content for a combination of 50% RAP + 50% RCCA. Nor could specimens be prepared for a 50% RAP + 50% RCCA combination when asphalt content was more than 6%, even at 6% cement content, irrespective of particle gradation.
11. A 50% RAP + 50% RCCA material combination yielded the lowest strength, yet it fulfilled the compressive strength requirement and structural coefficient ( $a_2$ ). For this reason, 50% RAP + 50% RCCA material combinations at 4% and 6% cement content were subjected to durability tests. Durability for this combination of materials was evaluated by applying different numbers of wetting and drying cycles. According to the test results, 50% RAP + 50% RCCA materials combinations treated with 6% cement have a structural coefficient of 0.11, even after 30 wet-dry cycles. On the other hand, the same combination of materials treated with 4% cement content have a structural layer coefficient of less than 0.1 after 30 wetting-drying cycles.
12. The environmental effects of using untreated or cement-treated recycled materials were evaluated. Environmental tests were conducted on the leachate collected after 24 hours of curing. Environmental tests included chemical oxygen demand (COD), total suspended

solids (TSS), total dissolved solids (TDS), turbidity, and pH. Test results were well within the range of EPA guidelines for storm water sampling.

13. Similar environmental tests were also conducted to evaluate leachate quality after specimens were subjected to a certain number of wetting-drying cycles, such as 0, 4, 8, 16, and 30 cycles. Test results obtained from different environmental tests were well below the permissible value given in EPA guidelines for storm water sampling.

14. An MLR model was developed to determine the value of the resilient modulus ( $M_r$ ) for different combinations of recycled materials treated at 4% and 6% cement, using the value of unconfined compressive strength (UCS), elastic modulus (EM), and bulk stress (BS).

The final model is as follows:

$$M_r' = 8.01E-03 + 3.41E-02BS' - 2.11E-06UCS - 8.74E-08EM$$

Where,  $BS' = BS^{-1}$  and  $M_r' = M_r^{-0.5}$

The coefficient of regression of the model was 83.82%. Therefore, the model explained 83.82% of the variation in resilient modulus (psi) in response to bulk stress, unconfined compressive strength, and elastic modulus.

15. Different combinations of recycled materials at 0% and 2% cement content did not fulfill the strength requirement of 300 psi. However, these combinations of materials can be used when the strength requirement is low, such as for a sub-base layer.

### 6.3 Recommendations for Future Study

1. The current study was conducted using cement as the stabilizer agent. However, fly ash can be used for future studies as an alternative stabilizer.
2. The effects of asphalt might be neutralized by using sand. A future study can incorporate sand to neutralize the effects of asphalt.

3. The MLR model was developed and verified using laboratory testing results. A future study might incorporate a field test section, where the resilient modulus can be obtained by using a falling weight deflectometer (FWD). The field test data might be used to evaluate the model and add additional factors, as required.
4. The current study was conducted only for the recycled materials available in the North Texas region. A similar study could be conducted on the recycled materials available throughout a larger region to make a comprehensive design chart for the entire state.

APPENDIX A  
Statistical Modelling

Table A1 Input Dataset for R Studio

Observation	M <sub>r</sub>	BS	CC	UCS	EM
1	41253	40	6	425	35267
2	42594	40	6	438	36354
3	39684	40	6	437	35386
4	61250	40	6	451	47034
5	59479	40	6	424	45927
6	60035	40	6	427	46785
7	34072	40	6	394	35247
8	41312	40	6	402	35946
9	37623	40	6	411	35006
10	40130	40	6	398	38652
11	39826	40	6	354	45782
12	37927	40	6	407	39756
13	61900	40	6	434	45000
14	60570	40	6	462	41909
15	61458	40	6	403	42333
16	31913	40	6	308	35386
17	36244	40	6	354	36487
18	31247	40	6	324	37895
19	44912	40	6	370	35333
20	47082	40	6	423	37909
21	45110	40	6	410	38235
22	25831	40	6	338	30437
23	28915	40	6	368	32992
24	26552	40	6	327	31948
25	30010	40	6	349	32645
26	41997	30	6	425	35267
27	43181	30	6	438	36354
28	42219	30	6	437	35386
29	73463	30	6	451	47034
30	71021	30	6	424	45927
31	74319	30	6	427	46785
32	45250	30	6	394	35247
33	46092	30	6	402	35946
34	48768	30	6	411	35006
35	40229	30	6	398	38652

Table A1 Continued					
36	42448	30	6	354	45782
37	42467	30	6	407	39756
38	70127	30	6	434	45000
39	71489	30	6	462	41909
40	33664	30	6	308	35386
41	34095	30	6	354	36487
42	33256	30	6	324	37895
43	44324	30	6	370	35333
44	47214	30	6	423	37909
45	46034	30	6	410	38235
46	30099	30	6	339	34687
47	28732	30	6	383	32188
48	29829	30	6	361	31256
49	26332	30	6	347	30526
50	25390	30	6	338	30437
51	28787	30	6	349	33042
52	29794	30	6	368	32992
53	32299	30	6	327	31948
54	31367	30	6	349	32645
55	34690	25	6	425	35267
56	36445	25	6	438	36354
57	35742	25	6	437	35386
58	62597	25	6	451	47034
59	60508	25	6	424	45927
60	62260	25	6	427	46785
61	35446	25	6	394	35247
62	39492	25	6	402	35946
63	38772	25	6	411	35006
64	35128	25	6	398	38652
65	38493	25	6	354	45782
66	36046	25	6	407	39756
67	58003	25	6	434	45000
68	59648	25	6	462	41909
69	29401	25	6	308	35386
70	31203	25	6	354	36487
71	30561	25	6	324	37895
72	29401	25	6	370	35333

Table A1 Continued					
73	31435	25	6	423	37909
74	29154	25	6	410	38235
75	25773	25	6	339	34687
76	22545	25	6	347	30526
77	23412	25	6	338	30437
78	24822	25	6	349	33042
79	31293	25	6	368	32992
80	28986	25	6	327	31948
81	29120	25	6	349	32645
82	32642	18	6	425	35267
83	34278	18	6	438	36354
84	33540	18	6	437	35386
85	44658	18	6	451	47034
86	44968	18	6	424	45927
87	47651	18	6	427	46785
88	34756	18	6	394	35247
89	36332	18	6	402	35946
90	32079	18	6	398	38652
91	31340	18	6	354	45782
92	33258	18	6	407	39756
93	40473	18	6	434	45000
94	43897	18	6	462	41909
95	44723	18	6	403	42333
96	28135	18	6	308	35386
97	30305	18	6	354	36487
98	29282	18	6	324	37895
99	31128	18	6	370	35333
100	33315	18	6	423	37909
101	31282	18	6	410	38235
102	22354	18	6	339	34687
103	24900	18	6	383	32188
104	22323	18	6	361	31256
105	22342	18	6	347	30526
106	23954	18	6	338	30437
107	23913	18	6	349	33042
108	24689	18	6	368	32992
109	24568	18	6	327	31948

Table A1 Continued					
110	26810	18	6	349	32645
111	24995	15	6	425	35267
112	25972	15	6	438	36354
113	26560	15	6	437	35386
114	38303	15	6	451	47034
115	35819	15	6	424	45927
116	36064	15	6	427	46785
117	26343	15	6	394	35247
118	29530	15	6	402	35946
119	26627	15	6	411	35006
120	24415	15	6	398	38652
121	23722	15	6	354	45782
122	25961	15	6	407	39756
123	37448	15	6	434	45000
124	35678	15	6	462	41909
125	37698	15	6	403	42333
126	21237	15	6	308	35386
127	20458	15	6	354	36487
128	19678	15	6	324	37895
129	23158	15	6	370	35333
130	24150	15	6	423	37909
131	22678	15	6	410	38235
132	19772	15	6	339	34687
133	17845	15	6	383	32188
134	17464	15	6	347	30526
135	17914	15	6	338	30437
136	18648	15	6	349	33042
137	20653	15	6	368	32992
138	20281	15	6	327	31948
139	21224	15	6	349	32645
140	29938	40	4	303	30652
141	27461	40	4	299	29547
142	28416	40	4	295	30028
143	33377	40	4	297	35690
144	32082	40	4	303	35480
145	31604	40	4	310	34985
146	26908	40	4	294	29835

Table A1 Continued					
147	27508	40	4	298	30415
148	26110	40	4	305	30348
149	26458	40	4	272	27986
150	29364	40	4	267	29615
151	31895	40	4	270	31842
152	38421	40	4	279	38438
153	37103	40	4	302	41328
154	40858	40	4	324	42462
155	20849	40	4	213	20220
156	23842	40	4	211	23457
157	22250	40	4	195	21387
158	40969	40	4	244	34687
159	36289	40	4	293	34188
160	38357	40	4	257	33256
161	24348	40	4	214	28265
162	24241	40	4	248	26589
163	22604	40	4	252	25635
164	33658	40	4	224	32000
165	31240	40	4	229	29588
166	26821	40	4	199	25314
167	28886	40	4	192	23586
168	27510	40	4	205	23147
169	31973	30	4	303	30652
170	36352	30	4	299	29547
171	33163	30	4	295	30028
172	40349	30	4	297	35690
173	41746	30	4	303	35480
174	40456	30	4	310	34985
175	32822	30	4	294	29835
176	31926	30	4	298	30415
177	35748	30	4	305	30348
178	31936	30	4	272	27986
179	32108	30	4	267	29615
180	33853	30	4	270	31842
181	45658	30	4	279	38438
182	42388	30	4	302	41328
183	45217	30	4	324	42462

Table A1 Continued					
184	22352	30	4	213	20220
185	25918	30	4	211	23457
186	22441	30	4	195	21387
187	39262	30	4	244	34687
188	42681	30	4	293	34188
189	41996	30	4	257	33256
190	25768	30	4	214	28265
191	23727	30	4	248	26589
192	23050	30	4	252	25635
193	28787	30	4	224	32000
194	25390	30	4	229	29588
195	26734	30	4	199	25314
196	27818	30	4	192	23586
197	27256	30	4	205	23147
198	28409	25	4	303	30652
199	27959	25	4	299	29547
200	27508	25	4	295	30028
201	33578	25	4	297	35690
202	32445	25	4	303	35480
203	31532	25	4	310	34985
204	24838	25	4	294	29835
205	26013	25	4	298	30415
206	25893	25	4	305	30348
207	23821	25	4	272	27986
208	24132	25	4	267	29615
209	26205	25	4	270	31842
210	37404	25	4	279	38438
211	39250	25	4	302	41328
212	41421	25	4	324	42462
213	18135	25	4	213	20220
214	20201	25	4	211	23457
215	20006	25	4	195	21387
216	35463	25	4	244	34687
217	36568	25	4	293	34188
218	37178	25	4	257	33256
219	24545	25	4	195	23042
220	23412	25	4	224	32000

Table A1 Continued					
221	24822	25	4	229	29588
222	23425	25	4	199	25314
223	21575	25	4	192	23586
224	22718	25	4	205	23147
225	26530	18	4	303	30652
226	26523	18	4	299	29547
227	24275	18	4	295	30028
228	29398	18	4	297	35690
229	28085	18	4	303	35480
230	29122	18	4	310	34985
231	24111	18	4	294	29835
232	24177	18	4	298	30415
233	26761	18	4	305	30348
234	21704	18	4	272	27986
235	20514	18	4	267	29615
236	23719	18	4	270	31842
237	30455	18	4	279	38438
238	28090	18	4	302	41328
239	36663	18	4	324	42462
240	17807	18	4	213	20220
241	17895	18	4	211	23457
242	16529	18	4	195	21387
243	30374	18	4	244	34687
244	31564	18	4	293	34188
245	29265	18	4	257	33256
246	20099	18	4	214	28265
247	19266	18	4	248	26589
248	18339	18	4	252	25635
249	23954	18	4	224	32000
250	22342	18	4	229	29588
251	20960	18	4	199	25314
252	21880	18	4	192	23586
253	20231	18	4	205	23147
254	20321	15	4	303	30652
255	21615	15	4	299	29547
256	20044	15	4	295	30028
257	24075	15	4	297	35690

Table A1 Continued					
258	23361	15	4	303	35480
259	21507	15	4	310	34985
260	20390	15	4	294	29835
261	20445	15	4	298	30415
262	19647	15	4	305	30348
263	17730	15	4	272	27986
264	17320	15	4	267	29615
265	18514	15	4	270	31842
266	21754	15	4	279	38438
267	25117	15	4	324	42462
268	15992	15	4	213	20220
269	14984	15	4	211	23457
270	14807	15	4	195	21387
271	19632	15	4	244	34687
272	21034	15	4	293	34188
273	19348	15	4	257	33256
274	16255	15	4	214	28265
275	17309	15	4	248	26589
276	15849	15	4	252	25635
277	17464	15	4	195	23042
278	17914	15	4	224	32000
279	18648	15	4	229	29588
280	17570	15	4	199	25314
281	17230	15	4	192	23586
282	18506	15	4	205	23147

Table A2 R Studio Output for Checking Outliers

Observation	Cook's Distance	DFFITS	DFBETAS				
			(Intercept)	$I(BS^{-1.12})$	CC	UCS	EM
1	2.37E-04	0.0344	0.0087	-0.0177	-0.0058	0.0210	-0.0187
2	9.35E-04	0.0683	0.0161	-0.0333	-0.0177	0.0459	-0.0353
3	2.62E-03	0.1144	0.0313	-0.0536	-0.0296	0.0792	-0.0662
4	2.84E-03	0.1191	-0.0357	-0.0547	-0.0181	0.0167	0.0499
5	3.87E-04	0.0439	-0.0164	-0.0216	0.0033	-0.0052	0.0244
6	1.12E-03	0.0747	-0.0293	-0.0350	0.0046	-0.0099	0.0442
7	4.27E-03	0.1462	0.0207	-0.0923	0.0230	0.0388	-0.0511
8	1.01E-05	0.0071	0.0010	-0.0044	0.0006	0.0023	-0.0024
9	1.51E-03	0.0867	0.0195	-0.0490	-0.0038	0.0427	-0.0430
10	1.79E-03	0.0944	-0.0079	-0.0625	0.0202	0.0048	0.0036
11	3.35E-02	0.4115	-0.1976	-0.1468	0.2179	-0.2927	0.3300
12	7.06E-03	0.1885	-0.0214	-0.1214	0.0245	0.0190	0.0161
13	8.64E-07	-0.0021	0.0006	0.0011	0.0001	-0.0002	-0.0008
14	2.12E-04	-0.0325	-0.0009	0.0154	0.0118	-0.0197	0.0053
15	3.33E-03	-0.1291	0.0387	0.0756	-0.0297	0.0218	-0.0549
16	1.97E-03	0.0990	-0.0228	-0.0440	0.0802	-0.0740	0.0373
17	7.04E-04	0.0592	-0.0092	-0.0358	0.0373	-0.0259	0.0121
18	1.37E-02	0.2624	-0.0798	-0.1192	0.1971	-0.1950	0.1306
19	3.35E-03	-0.1295	-0.0008	0.0848	-0.0590	0.0153	0.0125
20	2.85E-05	-0.0119	-0.0012	0.0070	0.0013	-0.0056	0.0035
21	2.16E-05	0.0104	0.0002	-0.0066	0.0005	0.0029	-0.0015
22	1.06E-02	0.2305	0.0355	-0.1272	0.1342	-0.0408	-0.0743
23	8.52E-03	0.2070	0.0323	-0.1278	0.0803	0.0094	-0.0731
24	1.02E-02	0.2269	0.0027	-0.1233	0.1627	-0.0958	-0.0149
25	3.34E-03	0.1292	0.0101	-0.0775	0.0742	-0.0264	-0.0260
26	1.55E-03	-0.0880	-0.0168	0.0295	0.0170	-0.0594	0.0522
27	7.09E-04	-0.0594	-0.0103	0.0186	0.0171	-0.0436	0.0332
28	1.12E-03	-0.0746	-0.0162	0.0223	0.0213	-0.0560	0.0464
29	4.58E-03	-0.1513	0.0612	0.0428	0.0257	-0.0232	-0.0691
30	8.12E-03	-0.2019	0.0996	0.0624	-0.0150	0.0259	-0.1235
31	9.15E-03	-0.2144	0.1085	0.0624	-0.0129	0.0304	-0.1383
32	5.55E-03	-0.1670	-0.0087	0.0728	-0.0290	-0.0519	0.0667
33	4.67E-03	-0.1530	-0.0067	0.0655	-0.0131	-0.0588	0.0595
34	1.06E-02	-0.2317	-0.0359	0.0872	0.0132	-0.1287	0.1278
35	5.06E-06	0.0050	-0.0011	-0.0023	0.0012	0.0003	0.0003
36	4.10E-03	0.1431	-0.0802	-0.0311	0.0785	-0.1061	0.1203
37	4.83E-06	0.0049	-0.0012	-0.0022	0.0007	0.0006	0.0005
38	7.21E-03	-0.1902	0.0781	0.0626	0.0107	-0.0158	-0.0843
39	1.50E-02	-0.2753	0.0144	0.0819	0.1101	-0.1815	0.0478
40	2.13E-03	-0.1032	0.0328	0.0296	-0.0888	0.0823	-0.0420

41	7.14E-05	0.0189	-0.0053	-0.0078	0.0134	-0.0094	0.0045
42	3.72E-04	0.0431	-0.0173	-0.0126	0.0345	-0.0343	0.0232
43	6.22E-03	-0.1770	0.0196	0.0814	-0.0932	0.0240	0.0191
44	1.93E-03	-0.0983	-0.0013	0.0385	0.0126	-0.0526	0.0323
45	1.33E-03	-0.0814	0.0079	0.0357	-0.0041	-0.0264	0.0130
46	8.38E-04	0.0646	-0.0138	-0.0250	0.0508	-0.0351	0.0095
47	2.70E-03	0.1163	0.0236	-0.0446	0.0228	0.0404	-0.0713
48	4.78E-05	0.0154	0.0023	-0.0061	0.0067	0.0013	-0.0079
49	2.12E-03	0.1028	0.0126	-0.0390	0.0571	-0.0073	-0.0452
50	3.25E-03	0.1275	0.0102	-0.0475	0.0817	-0.0249	-0.0451
51	1.13E-03	0.0750	-0.0033	-0.0311	0.0498	-0.0201	-0.0130
52	9.54E-04	0.0690	0.0050	-0.0294	0.0302	0.0038	-0.0276
53	2.32E-03	-0.1077	0.0083	0.0393	-0.0849	0.0502	0.0074
54	4.14E-05	-0.0144	0.0002	0.0059	-0.0093	0.0033	0.0032
55	4.62E-05	0.0152	0.0019	-0.0023	-0.0032	0.0108	-0.0094
56	1.16E-04	0.0240	0.0027	-0.0033	-0.0073	0.0184	-0.0139
57	3.07E-05	0.0124	0.0020	-0.0017	-0.0037	0.0097	-0.0079
58	2.32E-03	-0.1075	0.0524	0.0121	0.0195	-0.0173	-0.0512
59	4.84E-03	-0.1557	0.0917	0.0198	-0.0112	0.0205	-0.0999
60	4.82E-03	-0.1554	0.0925	0.0183	-0.0089	0.0226	-0.1045
61	4.21E-04	-0.0458	0.0020	0.0096	-0.0083	-0.0156	0.0197
62	1.90E-03	-0.0974	0.0050	0.0197	-0.0083	-0.0408	0.0406
63	2.37E-03	-0.1089	-0.0087	0.0191	0.0073	-0.0645	0.0634
64	2.74E-04	0.0369	-0.0131	-0.0080	0.0096	0.0027	0.0023
65	4.76E-03	0.1542	-0.0959	-0.0141	0.0858	-0.1165	0.1326
66	6.05E-04	0.0549	-0.0209	-0.0112	0.0082	0.0074	0.0067
67	3.06E-03	-0.1237	0.0630	0.0169	0.0080	-0.0110	-0.0579
68	8.59E-03	-0.2077	0.0259	0.0257	0.0874	-0.1426	0.0368
69	1.40E-04	-0.0264	0.0103	0.0036	-0.0234	0.0217	-0.0112
70	1.24E-04	0.0248	-0.0099	-0.0049	0.0189	-0.0132	0.0065
71	4.74E-04	0.0486	-0.0233	-0.0066	0.0401	-0.0400	0.0272
72	7.64E-04	0.0618	-0.0140	-0.0139	0.0352	-0.0090	-0.0070
73	4.78E-03	0.1549	-0.0120	-0.0275	-0.0223	0.0890	-0.0538
74	6.65E-03	0.1833	-0.0385	-0.0374	0.0085	0.0652	-0.0311
75	3.82E-03	0.1384	-0.0434	-0.0259	0.1149	-0.0798	0.0223
76	7.07E-03	0.1885	0.0091	-0.0354	0.1100	-0.0139	-0.0873
77	3.53E-03	0.1329	0.0006	-0.0246	0.0894	-0.0272	-0.0493
78	3.80E-03	0.1381	-0.0193	-0.0282	0.0977	-0.0395	-0.0251
79	3.06E-04	-0.0391	0.0007	0.0082	-0.0182	-0.0024	0.0167
80	1.00E-03	-0.0707	0.0113	0.0127	-0.0585	0.0347	0.0048
81	4.78E-05	-0.0154	0.0016	0.0031	-0.0106	0.0038	0.0036
82	2.99E-03	-0.1223	0.0067	-0.0383	0.0261	-0.0839	0.0717
83	3.03E-03	-0.1229	0.0071	-0.0368	0.0378	-0.0913	0.0676

Table A2 Continued							
84	3.90E-03	-0.1396	0.0005	-0.0395	0.0424	-0.1060	0.0857
85	9.06E-05	-0.0212	0.0133	-0.0066	0.0039	-0.0034	-0.0098
86	2.53E-03	-0.1124	0.0822	-0.0368	-0.0062	0.0137	-0.0696
87	3.95E-03	-0.1405	0.1027	-0.0439	-0.0059	0.0190	-0.0915
88	7.04E-03	-0.1884	0.0505	-0.0757	-0.0287	-0.0611	0.0737
89	7.74E-03	-0.1976	0.0537	-0.0790	-0.0124	-0.0786	0.0749
90	2.53E-04	-0.0355	0.0202	-0.0157	-0.0078	-0.0026	-0.0024
91	5.85E-03	0.1709	-0.1241	0.0373	0.0916	-0.1261	0.1450
92	1.52E-04	-0.0275	0.0161	-0.0119	-0.0033	-0.0036	-0.0034
93	8.85E-05	-0.0210	0.0139	-0.0073	0.0016	-0.0019	-0.0095
94	4.59E-03	-0.1515	0.0427	-0.0468	0.0630	-0.1003	0.0245
95	8.96E-03	-0.2126	0.1575	-0.0826	-0.0491	0.0387	-0.1069
96	9.12E-03	-0.2138	0.1123	-0.0525	-0.1829	0.1715	-0.0901
97	2.49E-03	-0.1116	0.0659	-0.0418	-0.0784	0.0556	-0.0288
98	3.51E-03	-0.1323	0.0814	-0.0345	-0.1048	0.1056	-0.0732
99	3.12E-03	-0.1251	0.0563	-0.0523	-0.0641	0.0163	0.0117
100	6.19E-04	-0.0555	0.0155	-0.0210	0.0084	-0.0303	0.0176
101	2.16E-05	-0.0104	0.0044	-0.0044	-0.0003	-0.0035	0.0015
102	2.84E-03	0.1192	-0.0593	0.0405	0.0930	-0.0652	0.0195
103	1.08E-05	0.0073	-0.0005	0.0025	0.0013	0.0026	-0.0045
104	8.08E-04	0.0635	-0.0079	0.0213	0.0268	0.0059	-0.0323
105	8.77E-05	0.0209	-0.0030	0.0067	0.0115	-0.0014	-0.0091
106	1.20E-03	-0.0773	0.0140	-0.0240	-0.0492	0.0149	0.0270
107	5.40E-05	0.0164	-0.0057	0.0059	0.0108	-0.0044	-0.0027
108	2.94E-05	0.0121	-0.0028	0.0046	0.0051	0.0008	-0.0048
109	1.38E-03	-0.0831	0.0280	-0.0255	-0.0653	0.0390	0.0048
110	2.24E-03	-0.1058	0.0328	-0.0377	-0.0677	0.0242	0.0228
111	2.12E-04	0.0325	-0.0052	0.0184	-0.0063	0.0194	-0.0164
112	4.84E-04	0.0491	-0.0077	0.0267	-0.0137	0.0322	-0.0235
113	9.46E-05	-0.0217	0.0023	-0.0113	0.0060	-0.0147	0.0117
114	1.66E-04	-0.0287	0.0188	-0.0156	0.0049	-0.0041	-0.0119
115	4.64E-04	-0.0481	0.0358	-0.0275	-0.0019	0.0049	-0.0261
116	7.35E-05	-0.0191	0.0143	-0.0105	-0.0006	0.0022	-0.0111
117	1.54E-03	-0.0876	0.0306	-0.0593	-0.0098	-0.0231	0.0270
118	6.35E-03	-0.1784	0.0629	-0.1200	-0.0072	-0.0579	0.0534
119	1.44E-03	-0.0848	0.0189	-0.0520	0.0064	-0.0409	0.0384
120	2.02E-03	0.1005	-0.0587	0.0718	0.0162	0.0060	0.0061
121	4.33E-02	0.4683	-0.3546	0.1943	0.2313	-0.3211	0.3724
122	1.35E-03	0.0821	-0.0493	0.0577	0.0069	0.0087	0.0085
123	2.31E-03	-0.1073	0.0731	-0.0640	0.0078	-0.0085	-0.0421
124	2.43E-03	-0.1102	0.0389	-0.0604	0.0411	-0.0644	0.0151
125	1.20E-02	-0.2462	0.1811	-0.1605	-0.0444	0.0361	-0.1033
126	9.33E-05	0.0216	-0.0123	0.0103	0.0166	-0.0156	0.0083

Table A2 Continued							
127	6.67E-03	0.1829	-0.1124	0.1185	0.1038	-0.0743	0.0399
128	1.72E-02	0.2942	-0.1920	0.1454	0.2076	-0.2107	0.1479
129	7.16E-05	0.0189	-0.0093	0.0131	0.0075	-0.0019	-0.0013
130	4.49E-03	0.1499	-0.0535	0.0965	-0.0202	0.0681	-0.0383
131	7.86E-03	0.1987	-0.0943	0.1377	0.0019	0.0536	-0.0217
132	4.67E-03	0.1529	-0.0828	0.0930	0.0991	-0.0701	0.0220
133	1.88E-02	0.3086	-0.0557	0.1868	0.0439	0.0952	-0.1578
134	9.48E-03	0.2182	-0.0528	0.1281	0.1003	-0.0118	-0.0803
135	5.19E-03	0.1611	-0.0440	0.0929	0.0867	-0.0263	-0.0475
136	7.37E-03	0.1923	-0.0795	0.1225	0.1028	-0.0419	-0.0247
137	1.54E-03	0.0878	-0.0284	0.0573	0.0296	0.0049	-0.0278
138	7.04E-06	0.0059	-0.0024	0.0034	0.0040	-0.0024	-0.0003
139	1.51E-05	0.0087	-0.0033	0.0055	0.0045	-0.0016	-0.0015
140	4.68E-03	0.1531	0.1175	-0.0837	-0.1002	0.0848	-0.0537
141	8.98E-03	0.2124	0.1710	-0.1147	-0.1333	0.1211	-0.0917
142	5.81E-03	0.1707	0.1359	-0.0971	-0.1033	0.0862	-0.0615
143	5.87E-03	0.1716	0.0745	-0.0970	-0.0845	0.0169	0.0500
144	9.40E-03	0.2176	0.1035	-0.1220	-0.1220	0.0441	0.0449
145	1.10E-02	0.2356	0.1260	-0.1296	-0.1505	0.0795	0.0185
146	9.94E-03	0.2237	0.1796	-0.1272	-0.1338	0.1130	-0.0834
147	1.01E-02	0.2250	0.1756	-0.1269	-0.1405	0.1161	-0.0767
148	1.94E-02	0.3134	0.2427	-0.1666	-0.2081	0.1843	-0.1230
149	3.88E-03	0.1394	0.1200	-0.0848	-0.0592	0.0481	-0.0558
150	8.05E-04	0.0634	0.0494	-0.0415	-0.0222	0.0093	-0.0101
151	5.03E-04	0.0501	0.0315	-0.0327	-0.0163	0.0000	0.0054
152	2.11E-03	0.1027	0.0132	-0.0481	-0.0189	-0.0329	0.0682
153	2.18E-02	0.3315	0.0188	-0.1363	-0.0998	-0.0667	0.2264
154	2.04E-02	0.3208	0.0260	-0.1258	-0.1432	-0.0075	0.1929
155	2.78E-03	0.1177	0.0972	-0.0565	0.0051	0.0062	-0.0683
156	1.25E-04	0.0249	0.0186	-0.0137	0.0036	-0.0049	-0.0075
157	7.07E-05	0.0188	0.0134	-0.0093	0.0044	-0.0044	-0.0065
158	5.40E-03	-0.1645	-0.0331	0.0834	-0.0112	0.0884	-0.0999
159	2.81E-04	0.0374	0.0203	-0.0224	-0.0191	0.0062	0.0059
160	1.96E-03	-0.0989	-0.0404	0.0593	0.0109	0.0313	-0.0402
161	4.61E-03	0.1519	0.0736	-0.0856	0.0360	-0.0794	0.0307
162	4.57E-03	0.1514	0.1279	-0.0947	-0.0280	0.0138	-0.0510
163	9.79E-03	0.2220	0.1961	-0.1315	-0.0541	0.0488	-0.1045
164	1.37E-03	-0.0828	-0.0226	0.0428	-0.0171	0.0510	-0.0413
165	6.92E-04	-0.0588	-0.0298	0.0353	-0.0069	0.0259	-0.0135
166	1.51E-03	-0.0868	-0.0487	0.0463	-0.0263	0.0416	-0.0005
167	1.37E-02	-0.2628	-0.1582	0.1342	-0.0834	0.1127	0.0292
168	6.36E-03	-0.1784	-0.1280	0.0955	-0.0346	0.0444	0.0491
169	6.13E-05	-0.0175	-0.0133	0.0061	0.0129	-0.0109	0.0068

170	6.20E-03	-0.1764	-0.1412	0.0613	0.1246	-0.1125	0.0840
171	1.23E-03	-0.0783	-0.0623	0.0291	0.0541	-0.0449	0.0315
172	1.70E-03	-0.0921	-0.0355	0.0334	0.0519	-0.0105	-0.0308
173	2.70E-03	-0.1163	-0.0503	0.0417	0.0744	-0.0268	-0.0276
174	1.82E-03	-0.0954	-0.0475	0.0334	0.0691	-0.0364	-0.0088
175	1.15E-03	-0.0759	-0.0610	0.0282	0.0518	-0.0434	0.0315
176	1.77E-04	-0.0297	-0.0231	0.0109	0.0211	-0.0173	0.0113
177	3.39E-03	-0.1301	-0.0995	0.0443	0.0969	-0.0853	0.0561
178	3.12E-03	-0.1249	-0.1098	0.0509	0.0620	-0.0499	0.0569
179	1.51E-03	-0.0870	-0.0693	0.0392	0.0368	-0.0153	0.0159
180	1.08E-03	-0.0735	-0.0455	0.0327	0.0289	-0.0002	-0.0097
181	6.66E-03	-0.1827	-0.0101	0.0525	0.0375	0.0632	-0.1323
182	1.98E-04	0.0314	-0.0004	-0.0077	-0.0102	-0.0067	0.0229
183	5.77E-04	0.0536	0.0008	-0.0123	-0.0256	-0.0012	0.0343
184	2.23E-03	-0.1054	-0.0860	0.0329	-0.0043	-0.0062	0.0658
185	5.54E-03	-0.1666	-0.1229	0.0607	-0.0258	0.0362	0.0553
186	2.17E-03	-0.1040	-0.0723	0.0337	-0.0257	0.0266	0.0386
187	8.72E-03	-0.2094	-0.0275	0.0671	-0.0142	0.1232	-0.1406
188	5.74E-03	-0.1699	-0.0866	0.0666	0.1010	-0.0327	-0.0318
189	1.10E-02	-0.2366	-0.0847	0.0937	0.0318	0.0851	-0.1115
190	4.76E-05	-0.0154	-0.0069	0.0057	-0.0040	0.0090	-0.0036
191	1.03E-03	0.0716	0.0620	-0.0305	-0.0160	0.0077	-0.0276
192	1.57E-03	0.0886	0.0799	-0.0352	-0.0253	0.0224	-0.0471
193	2.18E-05	-0.0104	-0.0022	0.0035	-0.0023	0.0071	-0.0058
194	6.14E-04	0.0553	0.0262	-0.0222	0.0070	-0.0277	0.0148
195	5.99E-03	-0.1733	-0.0919	0.0608	-0.0570	0.0915	-0.0018
196	1.79E-02	-0.3011	-0.1729	0.1007	-0.1028	0.1409	0.0355
197	1.24E-02	-0.2499	-0.1759	0.0884	-0.0520	0.0684	0.0750
198	9.39E-05	0.0216	0.0155	-0.0032	-0.0170	0.0143	-0.0088
199	7.86E-07	0.0020	0.0015	-0.0003	-0.0015	0.0013	-0.0010
200	1.01E-04	0.0224	0.0169	-0.0035	-0.0166	0.0137	-0.0095
201	1.50E-05	-0.0086	-0.0027	0.0012	0.0052	-0.0011	-0.0031
202	1.11E-04	0.0235	0.0087	-0.0033	-0.0161	0.0058	0.0060
203	4.46E-04	0.0471	0.0207	-0.0065	-0.0364	0.0191	0.0048
204	2.49E-03	0.1115	0.0853	-0.0176	-0.0818	0.0682	-0.0488
205	1.58E-03	0.0888	0.0653	-0.0137	-0.0677	0.0552	-0.0354
206	2.46E-03	0.1108	0.0801	-0.0157	-0.0875	0.0766	-0.0499
207	9.10E-04	0.0674	0.0572	-0.0122	-0.0366	0.0292	-0.0327
208	1.14E-03	0.0754	0.0576	-0.0152	-0.0356	0.0148	-0.0148
209	7.19E-04	0.0599	0.0339	-0.0116	-0.0263	0.0004	0.0090
210	9.81E-04	-0.0699	0.0010	0.0077	0.0153	0.0250	-0.0528
211	6.47E-05	0.0179	-0.0014	-0.0016	-0.0061	-0.0039	0.0135
212	4.79E-04	0.0489	-0.0021	-0.0039	-0.0241	-0.0011	0.0322

Table A2 Continued							
213	2.21E-03	0.1051	0.0822	-0.0155	0.0039	0.0066	-0.0680
214	3.62E-04	0.0425	0.0297	-0.0072	0.0067	-0.0097	-0.0147
215	2.24E-04	-0.0334	-0.0219	0.0051	-0.0085	0.0089	0.0128
216	6.73E-03	-0.1838	-0.0111	0.0242	-0.0120	0.1128	-0.1299
217	2.43E-03	-0.1103	-0.0495	0.0177	0.0712	-0.0230	-0.0227
218	7.51E-03	-0.1947	-0.0558	0.0327	0.0295	0.0748	-0.0994
219	1.08E-02	-0.2334	-0.1363	0.0370	-0.0721	0.0952	0.0497
220	3.71E-03	0.1362	0.0194	-0.0194	0.0308	-0.0966	0.0797
221	1.57E-05	0.0088	0.0036	-0.0016	0.0011	-0.0047	0.0026
222	1.86E-03	-0.0964	-0.0463	0.0156	-0.0328	0.0535	-0.0014
223	9.02E-04	-0.0671	-0.0354	0.0105	-0.0236	0.0328	0.0080
224	2.54E-03	-0.1127	-0.0748	0.0187	-0.0240	0.0323	0.0352
225	1.54E-03	-0.0878	-0.0421	-0.0326	0.0662	-0.0547	0.0326
226	3.23E-03	-0.1272	-0.0671	-0.0460	0.0919	-0.0815	0.0586
227	1.05E-04	-0.0229	-0.0115	-0.0088	0.0162	-0.0132	0.0088
228	7.14E-04	-0.0597	-0.0054	-0.0240	0.0344	-0.0071	-0.0204
229	3.08E-05	-0.0124	-0.0017	-0.0049	0.0081	-0.0029	-0.0031
230	5.08E-04	-0.0503	-0.0106	-0.0196	0.0369	-0.0192	-0.0053
231	1.02E-04	-0.0226	-0.0115	-0.0087	0.0158	-0.0130	0.0090
232	2.88E-06	-0.0038	-0.0018	-0.0015	0.0028	-0.0022	0.0014
233	2.23E-03	-0.1056	-0.0522	-0.0379	0.0801	-0.0693	0.0438
234	5.19E-06	0.0051	0.0029	0.0021	-0.0026	0.0021	-0.0022
235	1.45E-03	0.0852	0.0383	0.0390	-0.0381	0.0157	-0.0141
236	1.16E-05	0.0076	0.0020	0.0035	-0.0032	0.0001	0.0011
237	7.59E-04	-0.0615	0.0109	-0.0201	0.0136	0.0206	-0.0446
238	8.03E-03	0.2005	-0.0433	0.0589	-0.0675	-0.0409	0.1463
239	6.26E-04	-0.0558	0.0100	-0.0159	0.0271	0.0010	-0.0357
240	1.51E-03	-0.0868	-0.0523	-0.0237	-0.0021	-0.0056	0.0539
241	1.90E-05	0.0097	0.0047	0.0032	0.0013	-0.0021	-0.0031
242	1.99E-04	0.0315	0.0149	0.0090	0.0073	-0.0080	-0.0115
243	1.08E-02	-0.2329	0.0279	-0.0793	-0.0113	0.1346	-0.1581
244	5.12E-03	-0.1603	-0.0310	-0.0683	0.0975	-0.0315	-0.0319
245	5.86E-03	-0.1716	-0.0082	-0.0714	0.0268	0.0599	-0.0826
246	6.95E-06	0.0059	0.0010	0.0021	0.0014	-0.0034	0.0015
247	6.53E-04	0.0571	0.0315	0.0236	-0.0142	0.0067	-0.0212
248	1.96E-03	0.0989	0.0603	0.0379	-0.0307	0.0259	-0.0515
249	1.27E-03	-0.0796	0.0035	-0.0268	-0.0160	0.0533	-0.0450
250	4.81E-04	-0.0490	-0.0083	-0.0195	-0.0051	0.0242	-0.0139
251	5.10E-03	-0.1598	-0.0444	-0.0517	-0.0499	0.0842	-0.0037
252	1.71E-02	-0.2946	-0.0997	-0.0886	-0.0964	0.1378	0.0316
253	5.67E-03	-0.1686	-0.0768	-0.0539	-0.0322	0.0457	0.0492
254	1.59E-03	0.0891	0.0252	0.0558	-0.0572	0.0469	-0.0272
255	3.52E-04	-0.0419	-0.0137	-0.0258	0.0259	-0.0228	0.0160

Table A2 Continued							
256	9.66E-04	0.0694	0.0204	0.0448	-0.0414	0.0333	-0.0217
257	3.53E-05	0.0133	-0.0006	0.0087	-0.0064	0.0013	0.0038
258	6.46E-04	0.0567	-0.0004	0.0370	-0.0310	0.0111	0.0119
259	5.50E-03	0.1659	0.0091	0.1066	-0.1028	0.0532	0.0154
260	2.88E-04	0.0379	0.0114	0.0244	-0.0224	0.0182	-0.0123
261	7.45E-04	0.0609	0.0172	0.0391	-0.0374	0.0298	-0.0180
262	3.62E-03	0.1345	0.0408	0.0822	-0.0877	0.0753	-0.0466
263	3.16E-03	0.1256	0.0414	0.0847	-0.0541	0.0418	-0.0439
264	6.87E-03	0.1857	0.0392	0.1341	-0.0666	0.0272	-0.0227
265	5.70E-03	0.1690	0.0119	0.1226	-0.0563	0.0021	0.0205
266	1.08E-02	0.2331	-0.0607	0.1315	-0.0468	-0.0678	0.1491
267	1.99E-02	0.3161	-0.0801	0.1577	-0.1409	-0.0044	0.1842
268	1.67E-03	-0.0912	-0.0395	-0.0471	-0.0012	-0.0055	0.0500
269	3.41E-03	0.1305	0.0381	0.0775	0.0140	-0.0234	-0.0352
270	5.76E-04	0.0536	0.0166	0.0285	0.0106	-0.0119	-0.0170
271	5.42E-03	0.1647	-0.0354	0.0968	0.0055	-0.0815	0.0971
272	3.23E-03	0.1271	0.0034	0.0869	-0.0636	0.0206	0.0212
273	4.00E-03	0.1414	-0.0128	0.0958	-0.0193	-0.0395	0.0560
274	5.20E-03	0.1613	0.0033	0.1003	0.0308	-0.0781	0.0343
275	1.01E-03	0.0710	0.0219	0.0485	-0.0149	0.0069	-0.0207
276	6.54E-03	0.1811	0.0678	0.1177	-0.0480	0.0396	-0.0764
277	5.78E-03	-0.1700	-0.0391	-0.0946	-0.0408	0.0573	0.0283
278	5.65E-03	0.1681	-0.0254	0.0988	0.0276	-0.0963	0.0826
279	1.49E-04	0.0273	0.0003	0.0181	0.0020	-0.0109	0.0065
280	1.50E-03	-0.0865	-0.0107	-0.0503	-0.0225	0.0390	-0.0022
281	3.69E-03	-0.1358	-0.0252	-0.0751	-0.0376	0.0551	0.0120
282	1.05E-02	-0.2295	-0.0635	-0.1329	-0.0357	0.0528	0.0563

## References

1. American Association of State Highway, & Transportation Officials. (1993). *AASHTO Guide for Design of Pavement Structures, 1993* (Vol. 1). AASHTO.
2. AASHTO T307-99 (2003), "Standard Method of Test for Determining the Resilient Modulus of Soils and Aggregate Materials." American Association of State Highway and Transportation Officials, Washington, D.C.
3. AASHTO, T308-10 (2010). Standard method of test for determining the asphalt binder content of hot mix asphalt (HMA) by the ignition method. Washington DC, USA: American Association of State Highway and Transportation Officials.
4. Allen, J. J. (1977). *The effects of non-constant lateral pressures on the resilient response of granular materials*. University Microfilms.
5. Anagnos, J. N., & Kennedy, T. W. (1972). *Practical method of conducting the indirect tensile test* (No. 98-10 Res Report). Center for Highway Research University of Texas at Austin.
6. Arioglu, N., Girgin, Z. C., & Arioglu, E. (2006). Evaluation of ratio between splitting tensile strength and compressive strength for concretes up to 120 MPa and its application in strength criterion. *ACI Materials Journal*, 103(1), 18-24.
7. ASTM. (2011). *Standard test method for pH of engine coolants and anti-rusts*, ASTM D1287-11. West Conshohocken, PA.
8. ASTM. (2012). *Standard test methods for chemical oxygen demand (dichromate oxygen demand) of water*, ASTM D1252. West Conshohocken, PA.
9. ASTM. (2013). *Standard test methods for filterable matter (total dissolved solids) and non-filterable matter (Total suspended solids) in water*, ASTM D5907-13. West Conshohocken, PA.

10. ASTM. "Annual book of standards, volume 04.08, soil and rock." West Conshohocken, PA.
11. Babić, B., Prager, A., & Rukavina, T. (2000). Effect of fine particles on some characteristics of granular base courses. *Materials and structures*, 33(7), 419-424.
12. Barksdale, R. D. (1972, September). Laboratory evaluation of rutting in base course materials. In *Presented at the Third International Conference on the Structural Design of Asphalt Pavements, Grosvenor House, Park Lane, London, England, Sept. 11-15, 1972*. (Vol. 1, No. Proceeding).
13. Barskale, R. D., & Itani, S. Y. (1989). Influence of aggregate shape on base behavior. *Transportation Research Record*, (1227).
14. Bosquez, J. (2009). "A comprehensive study of recycled concrete aggregates as a drainable base layer for pavements." *University of Texas at Arlington, Arlington, TX*.
15. Brand, A. (2012). Fractionated reclaimed asphalt pavement as a coarse aggregate replacement in a ternary blended concrete pavement.
16. Buchanan, S. (2007). Resilient Modulus: What, Why, and How. *Vulcan Materials Company*.
17. Cetin, B., Aydilek, A. H., & Guney, Y. (2010). Stabilization of recycled base materials with high carbon fly ash. *Resources, Conservation and Recycling*, 54(11), 878-892.
18. Chen, D., Chen, D. H., Laguros, J. G., & Zaman, M. M. (1995). Characterization of base/subbase materials under repetitive loading. *Journal of testing and evaluation*, 23(3), 180-188.
19. Chesner, W. H., Collins, R. J., & MacKay, M. H. (1998). User guidelines for waste and by-product materials in pavement construction (No. FHWA-RD-97-148).

20. Chong, D., Wang, Y., Guo, H., and Lu, Y. (2013). "Volatile Organic Compounds Generated in Asphalt Pavement Construction and Their Health Effects on Workers." *J. Const. Eng. and Management*. 140(2), 04013051.
21. Copeland, A. (2011). *Reclaimed asphalt pavement in asphalt mixtures: state of the practice* (No. FHWA-HRT-11-021).
22. Croney, P., & Croney, D. (1997). *The Design and Performance of Road Pavement*.
23. Curtis, C. W. (1992). "Investigation of Asphalt-Aggregate Interaction in Asphalt Pavements." *American Chemical Society, Fuel*. 37, 1292-1297.
24. Dawson, A. R., Thom, N. H., & Paute, J. L. (1996). Mechanical characteristics of unbound granular materials as a function of condition. *Gomes Correia, Balkema, Rotterdam*, 35-44.
25. EPA. (2005). *Benchmarks for storm-water sampling*, Business Environmental Resource Center, City of Sacramento, California.
26. Euch Khay, S. E., Euch Ben Said, S. E., Loulizi, A., & Neji, J. (2014). Laboratory Investigation of Cement-Treated Reclaimed Asphalt Pavement Material. *Journal of Materials in Civil Engineering*, 27(6), 04014192.
27. Faysal, M., Mahedi, M., Hossain, M.S., Aramoon, A., and Thian, B., Khan, M.A. and Khan, M. S. (2016). Determination of Structural Coefficient of Different Combinations of Cement Treated / Untreated Recycled Base Material. In *Geotechnical and Structural Engineering Congress 2016* (pp. 1198-1208).
28. Faysal, M., Mahedi, M., Aramoon, A., Thian, B., Hossain, M. S., & Khan, M. S. (2016). Strength Characterization of Untreated and Cement-Treated Recycled Flex-Base Materials. *Geotechnical and Structural Engineering Congress 2016*. 1233-1244.

29. Faysal, M., Hossain, S., Salah, S. B., Khan, M. S., & Flores, C. M. (2017). Characterization of Strength and Long-Term Durability of Recycled Flex Base Materials. In *Transportation Research Board 96th Annual Meeting* (No. 17-04301).
30. Faysal, M., Hossain, M. S., Salah, S. B., Bhattacharjee, S., Thian, B., & Khan, M. S. Characterization of the Geo-Environmental Properties of Untreated or Cement Treated Recycled Base Materials in Pavement Base Layer Applications. *Geotechnical Frontiers 2017*, 415-423.
31. Gautam, B., Yuan, D., Abdallah, I., and Nazarian, S. (2009). Guidelines for using local material for roadway base and subbase. Research Report 0-5562-1, Center for Transportation Infrastructure Systems, The University of Texas at El Paso, El Paso, TX.
32. George, K. P. "Prediction of resilient modulus from soil index properties." (2004).
33. George, K. P., & Uddin, W. (1994). In Situ and Laboratory Characterization of Nonlinear Pavement Layer Moduli. In *Nondestructive Testing of Pavements and Backcalculation of Moduli: Second Volume*. ASTM International.
34. Ghafoori, N., and S. Dutta. Pavement Thickness Design for No-Fines Concrete Parking Lots. *Journal of Transportation Engineering*, Vol. 121, No. 6, 1995, pp. 476-484.
35. Gnanendran, C. T., & Woodburn, L. J. (2003). Recycled Aggregate for Pavement Construction and the Influence of Stabilization. *Publication of: ARRB Transport Research, Limited*.
36. Grilli, A., Bocci, E., & Graziani, A. (2013). Influence of reclaimed asphalt content on the mechanical behaviour of cement-treated mixtures. *Road Materials and Pavement Design*, 14(3), 666-678.

37. Guerrero, A. M. A. (2004). Effects of the Soil Properties on the Maximum Dry Density Obtained from the Standard Proctor Test (Doctoral dissertation, University of Central Florida Orlando, Florida).
38. Guthrie, W. S., Sebesta, S., & Scullion, T. (2002). *Selecting optimum cement contents for stabilizing aggregate base materials* (No. FHWA/TX-05/7-4920-2.). Texas Transportation Institute, Texas A & M University System.
39. Guthrie, S.W., Cooley, D., and Eggett, D.L., 2007, "Effects of Reclaimed Asphalt Pavement on Mechanical Properties of Base Materials," J. Transp. Res. Board, No. 2005, pp. 44-52.
40. Hansen, K. R., & Copeland, A. (2013). Annual asphalt pavement industry survey on recycled materials and warm-mix asphalt usage: 2009–2012 (No. IS-138).
41. Hicks, R. G., & Monismith, C. L. (1971). Factors influencing the resilient response of granular materials. *Highway research record*, (345).
42. Hossain, M. S. (2008). *Characterization of subgrade resilient modulus for Virginia soils and its correlation with the results of other soil tests* (No. VTRC 09-R4).
43. Hossain, M. S., & Kim, W. S. (2014). *Estimation of Subgrade Resilient Modulus Using the Unconfined Compression Test* (No. FHWA/VCTIR 15-R12)
44. Hoyos, L. R., Puppala, A. J., and Ordonez, C. O. (2011). "Characterization of cement-fiber-treated reclaimed asphalt pavement aggregates: Preliminary investigation." *Journal of Materials in Civil Engineering* 23.7 (2011): 977-989.
45. Huang, Y., Bird, R.N., Heidrich, O. (2007). A review of the use of recycled solid waste materials in asphalt pavements. *Resources, Conservation and Recycling*, Vol. 52, No. 1, pp 58-73.

46. Janoo, V., Berg, R. L., Simonsen, E., & Harrison, A. (1994). Seasonal changes in moisture content in airport and highway pavements. In *Symposium and Workshop on Time Domain Reflectometry in Environmental, Infrastructure, and Mining Applications*, Evanston, IL (pp. 357-362).
47. Jones, D., Wu, R., & Louw, S. (2014). Full-Depth Recycling Study: Test Track Construction and First Level Analysis of Phase 1 HVS and Laboratory Testing.
48. Kandhal, P. and Mallick, R.B. (1997). Pavement Recycling Guidelines for State and Local Governments—Participant's Reference Book, Report No. FHWA-SA-98-042, Federal Highway Administration, Washington, DC.
49. Kelly, T. D., Matos, G. R., Buckingham, D. A., DiFrancesco, C. A., Porter, K. E., Berry, C., Goonan, T., and Sznoppek, J. (2010). "Historical statistics for mineral and material commodities in the United States." US Geological Survey data series. 140.
50. Khoury, N., & Zaman, M. (2002). Effect of wet-dry cycles on resilient modulus of class C coal fly ash-stabilized aggregate base. *Transportation Research Record: Journal of the Transportation Research Board*, (1787), 13-21.
51. Khoury, N., & Zaman, M. (2005). Durability effects on flexural behavior of fly ash stabilized limestone aggregate. *Journal of Testing and Evaluation*, 34(3), 1-9.
52. Khoury, N., & Zaman, M. M. (2007). Durability of stabilized base courses subjected to wet-dry cycles. *International Journal of Pavement Engineering*, 8(4), 265-276.
53. Kibria, G. (2014). Evaluation of physio-mechanical properties of clayey soils using electrical resistivity imaging technique.
54. Kim, S., Byron, T., and Sholar, G. A. "Evaluation of use of high percentage of re-claimed asphalt pavement (RAP) for Superpave mixtures." *FDOT/SMO/07-507* (2007).

55. Kolas, S. (1996). Mechanical properties of cement-treated mixtures of milled bituminous concrete and crushed aggregates. *Materials and Structures*, 29(7), 411-417.
56. Kutner, M.H., Nachtsheim, C. J., Neter, J. and Li, W. (2005). "Applied linear statistical model." *5th ed., McGraw Hill Inc., NY*.
57. Lee, W., Bohra, N. C., Altschaeffl, A. G., & White, T. D. (1997). Resilient modulus of cohesive soils. *Journal of Geotechnical and Geoenvironmental Engineering*, 123(2), 131-136.
58. Lekarp, F., Isacsson, U., & Dawson, A. (2000). State of the art. I: Resilient response of unbound aggregates. *Journal of transportation engineering*, 126(1), 66-75
59. Li, P., & Liu, J. (2010). Characterization of asphalt treated base course material. *University of Alaska*.
60. Lim, S., & Zollinger, D. (2003). Estimation of the compressive strength and modulus of elasticity of cement-treated aggregate base materials. *Transportation Research Record: Journal of the Transportation Research Board*, (1837), 30-38.
61. Lotfi, H. A., & Witczak, M. W. (1985). Dynamic characterization of cement-treated base and subbase materials. *Transportation Research Record*, (1031).
62. Mahedi, M. (2016). Potential applicability of stress wave velocity method on pavement base materials as a non-destructive testing technique.
63. Mahedi, M., Hossain, M. S., Faysal, M., Sadik, M., & Ahmed, A. (2017). Prediction of Strength and Stiffness Properties of Recycled Pavement Base Materials Using Non-Destructive Impact Echo Test.
64. Mahedi, M., Hossain, M. S., Faysal, M., Khan, M. S., Mahedi, M., Hossain, M. S., & Khan, M. S. (2017). Potential Applicability of Impact Echo Method on Pavement Base Materials

- as A Non-Destructive Testing Technique. In *Proceedings, 96th Annual Meeting, Transportation Research Board, Washington, DC.*
65. Masad, E. (2003). *The development of a computer controlled image analysis system for measuring aggregate shape properties* (No. NCHRP-IDEA Project 77)
  66. Minnesota Department of Transportation (2007). *Pavement Design Manual.*
  67. Moossazadeh, J., & Witczak, M. W. (1981). Prediction of subgrade moduli for soil that exhibits nonlinear behavior. *Transportation Research Record*, (810).
  68. Naidu, G., & Adishesu, S. (2011). Influence of coarse aggregate shape factors on bituminous mixtures. In *International Journal of Engineering Research and Applications (IJERA).*
  69. Nazarian, S., Pezo, R., Melarkode, S., & Picornell, M. (1996). Testing methodology for resilient modulus of base materials. *Transportation Research Record: Journal of the Transportation Research Board*, (1547), 46-52
  70. Naidu, G., & Adishesu, S. (2011). Influence of coarse aggregate shape factors on bituminous mixtures. In *International Journal of Engineering Research and Applications (IJERA).*
  71. Ordonez, C. A. (2006). *Characterization of cemented and fiber-reinforced RAP aggregate materials for base/sub-base applications.* The University of Texas at Arlington.
  72. Padgett, T. H. and Stanley, M. T. (1996). Performance of construction features incorporating recycled materials. North Carolina Department of Transportation, Division of Highways, Raleigh, NC 27611.

73. Pandey, K. K. (1996). Evaluation of resilient moduli and layer coefficients of a coal ash stabilized marginal aggregate base for AASHTO flexible pavement design (Doctoral dissertation, University of Oklahoma).
74. *Pavement Surface Layers*. Charlottesville, Virginia: Virginia Transportation Research Council.
75. Potturi, A. K. (2006). *Evaluation of resilient modulus of cement and cement-fiber treated reclaimed asphalt pavement (RAP) aggregates using repeated load triaxial test*. MS Thesis, University of Texas at Arlington.
76. Puppala, A., Mohammad, L., & Allen, A. (1996). Engineering behavior of lime-treated Louisiana subgrade soil. *Transportation Research Record: Journal of the Transportation Research Board*, (1546), 24-31.
77. Puppala, A. J., Hoyos, L. R., & Potturi, A. K. (2011). Resilient moduli response of moderately cement-treated reclaimed asphalt pavement aggregates. *Journal of Materials in Civil Engineering*, 23(7), 990-998.
78. R Studio (2012). R Studio: Integrated development environment for R (Version 1.0.136) [Computer software]. Boston, MA. Retrieved October, 2016.
79. Rada, G., & Witczak, M. W. (1981). *Comprehensive evaluation of laboratory resilient moduli results for granular material* (No. 810).
80. Richardson, B. J. E., & Jordan, D. O. (1994). "Use of recycled concrete as a road pavement material within Australia." In 17th ARRB Conf., Gold Coast, Queensland, 15-19 August 1994; Proc., Volume 17, Part 3.
81. Rodway, L. E. (1979). Void spacing in exposed concrete flat-work. *Concrete International*, 1(02), 83-89.

82. Salah, S. B. (2016). Performance of cement treated recycled aggregates under wetting-drying cycles.
83. Salah, S. B., Hossain, S., Faysal, M., Khan, M. S., and Flores, C. M. (2017). Effect of Wetting-Drying Cycle on Durability of Cement-Stabilized Recycled Pavement Base Aggregates. Accepted for publication in GeoMEast 2017 proceedings, Sharm-El-Sheikh, Egypt.
84. Saride, S., Puppala, A. J., & Williammee, R. (2010). Civil Engineers Ground Improvement 163 February 2010 Issue G11. *Sta*, 717(715), 00.
85. Sherwood, P. (1995). *Alternate Materials in Road Construction: A Guide to the Use of Recycled and Secondary Aggregates*, 1995.
86. Specifications, U. F. G. (2010). *Concrete Pavement for Airfields and Other Heavy-Duty Pavements*. UFGS 32-13-11. Construction Criteria Base, National Institute of Building Sciences, Washington, DC.
87. Smith, W. S., & Nair, K. (1973). *Development of procedures for characterization of untreated granular base course and asphalt-treated base course materials* (No. FHWA-RD-74-61 Final Rpt.).
88. Stevens, J. (1996). "Applied multivariate statistics for the social sciences." Lawrence Erlbaum Associates, Inc., New Jersey.
89. Sukumaran, B., Kyatham, V., Shah, A., & Sheth, D. (2002, May). Suitability of using California bearing ratio test to predict resilient modulus. In *Proceedings: Federal Aviation Administration Airport Technology Transfer Conference, (May 2002)*.
90. Taha, R., Ali, G., Basma, A., and Al-Turk, O. (1999). "Evaluation of reclaimed asphalt pavement aggregate in road bases and subbases." *Transportation Research Record*

- 1652, 1, 7th Int. Conf. on Low Volume Roads, Transportation Research Board, National Research Council, Washington, D.C., 264–269.
91. Taha, R, Al-Harthy, A., Al-Shamsi, K., and Al-Zubeidi, M. (2002). “Cement stabilization of reclaimed asphalt pavement aggregate for road bases and subbases.” *J. Materials in Civil Eng.*, 14(3), 239-245.
  92. Texas Department of Transportation. (1999). *Determining the Specific Gravity of soils.* Tex-108-E, Austin, TX.
  93. Texas Department of Transportation. (1999). *Particle size analysis of soils.* Tex-110-E, Austin, TX.
  94. Texas Department of Transportation (1999). *Laboratory compaction characteristics and moisture- density relationship of base materials.* Tex-113-E, Austin, TX.
  95. Texas Department of Transportation (1999). *Soil-cement testing procedure.* Tex-120-E, Austin, TX.
  96. Texas Department of Transportation. (2016). *Tex-236-F: Test Procedure for determining asphalt paving mixtures by the ignition method.* Austin, Texas: Texas Department of Transportation.
  97. Texas Department of Transportation. (2007). *Tex-421-A: Test procedure for splitting tensile strength of cylindrical concrete specimen.* Austin, Texas: Texas Department of Transportation.
  98. Thom, N.H. and Brown, S. F. (1988). “The Effect of Grading and Density on the Mechanical Properties of a Crushed Dolomitic Limestone,” *Proceedings of the 14th ARRB Conference, Part 7.* 1988, pp. 94-100.

99. Thompson, M. R., & Barenberg, E. J. (1989). Calibrated Mechanistic Structural Analysis Procedures for Pavements: Phase - I Final Report *NCHRP Project*, 1-26.
100. Thompson, M. R., & Robnett, Q. L. (1976). *Resilient properties of subgrade soils* (No. FHWA-IL-UI-160 Final Rpt.).
101. Thompson, M. R., & Nauman, D. (1993). *Rutting rate analyses of the AASHO road test flexible pavements* (No. 1384).
102. Transportation Applications of Recycled Concrete Aggregate—FHWA. (2004). "State of the Practice National Review." U.S. Department of Transportation Federal Highway Administration, Washington, DC, USA, 2004; pp. 1-47.
103. Uzan, J. (1985). Characterization of granular material. *Transportation Research Record*, (1022).
104. Wilburn, D. R. and Goonam T. G. (1998). Aggregates from Natural and Recycled Sources: Economic Assessments for Construction Applications-A Materials Flow Analysis. U. S. Geological Survey Circular, 1176
105. Witczak, M. W. (2003). NCHRP 1-28A: Harmonized test method for laboratory determination of resilient modulus for flexible pavement design. Final Report. TRB, National Research Council, Washington, DC.
106. Weyers, R. E., Williamson, G. S., Mokarem, D. W., Lane, D. S., & Cady, P. D. (2005). *WHRP 06-07 Final Report - Testing Methods to Determine Long Term Durability of Wisconsin Aggregate Resources*. Wisconsin Highway Research Program.
107. Won, M. (2001). Effects of Coarse Aggregate on Concrete Pavement Performance. *9th Annual ICAR Symposium*. Austin, Texas: International Center for Aggregates Research.

108. Yuan, D., Nazarian, S., Hoyos, L., & Puppala, A. (2011). Evaluation and mix design of cement-treated base materials with high content of reclaimed asphalt pavement. *Transportation Research Record: Journal of the Transportation Research Board*, (2212), 110-119.

### Biographical Information

Mohammad Faysal was born in Dhaka, Bangladesh on September 17, 1988. He graduated with a Bachelor of Science in Civil Engineering from Bangladesh University of Engineering and Technology in April 2012. He began his career as an Assistant Project Engineer with Ventura Properties Limited, Dhaka in May 2012, then took a position as an Assistant Engineer for Axis Design Consultants Ltd, Dhaka in October 2012. He served there as a structural engineer until July 2013. The author joined the University of Texas at Arlington in fall 2013 for graduate studies as a PhD student. He had the opportunity to work as a graduate research assistant under the supervision of Dr. Sahadat Hossain. The author's research interests include strength properties of pavement materials, subgrade materials, slope stability analysis and remediation, and non-destructive testing.